NUREG/CR-4251
PNL-5461
Vol. 2

Mitigative Techniques for Ground-Water Contamination Associated With Severe Nuclear Accidents

Case Study Analysis of Hydrologic Characterization and Mitigative Schemes

Prepared by P. L. Oberlander, R. L. Skaggs, J. M. Shafer

Pacific Northwest Laboratory
Operated by
Battelle Memorial Institute

Prepared for
U.S. Nuclear Regulatory Commission

NUREG/CR-4251
PNL-5461
Vol. 2

Mitigative Techniques for Ground-Water Contamination Associated With Severe Nuclear Accidents

Case Study Analysis of Hydrologic Characterization and Mitigative Schemes

Manuscript Completed: May 1985
Date Published: August 1985

Prepared by
P. L. Oberlander, R. L. Skaggs, J. M. Shafer

Pacific Northwest Laboratory
Richland, WA 99352

T. J. Nicholson, NRC Project Manager

Prepared for
Division of Radiation Programs and Earth Sciences
Office of Nuclear Regulatory Research
U.S. Nuclear Regulatory Commission
Washington, D.C. 20555
NRC FIN B2454

PREFACE

ORGANIZATION OF THE REPORT

This report is divided into two volumes. Volume 1, "Mitigative Techniques for Ground-Water Contamination Associated with Severe Nuclear Accidents: Analysis of Generic Site Conditions," examines generalized aspects of a nuclear core melt accident. The contents of Volume 1 are:

Executive Summary of Volumes 1 and 2

Section 1 - presents a overview of the study including: purpose of study, study objectives, and the scope of the study with associated limitations.

Section 2 - discusses the major types of severe commercial nuclear power reactor accidents considered for this study. Section 2 includes a discussion of radionuclide release mechanisms and rates expected following a reactor core melt accident.

Section 3 - describes the generic hydrogeologic classification scheme and presents the definition of each generic classification. Ground-water flow parameters (e.g., hydraulic conductivity, effective prorosity, etc.) and contaminant transport parameters (e.g., longitudinal dispersion, retardation, etc.) are discussed.

Section 4 - identifies the various ground-water contaminant mitigation techniques and strategies that may be applicable to ground-water contamination resulting from a severe accident.

Section 5 - presents the results of the evaluation of the radionuclide flux for each generic hydrogeologic classification with an assessment of appropriate mitigation measures.

Volume 2, "Mitigative Techniques for Ground-Water Contamination Associated with Severe Nuclear Accidents: Case Study Analysis of Hydrologic Characteristics and Interdictive Schemes," considers the site-specific aspects of selected hydrogeologic environments and individual mitigative techniques. Three case studies are presented to examine mitigative techniques in greater detail than is possible in the generic analysis. Volume 2 contains:

Section 6 - discusses the geologic and hydrologic conditions at the South Texas Plant. Included are simulations of premitigative contaminant migration, mitigative benefits of a cut-off wall and injection wells.

Section 7 - continues the discussion of the South Texas Plant in greater detail. Emphasis is placed on near-field simulations, design considerations and performance assessment.

Section 8 - presents an analysis of the special features of plant configuration and hydrologic characterization of a fractured anisotropic unit.

Section 9 - discusses the primary findings of the study and includes suggestions for further research.

Section 10 - presents the summary of conclusions.

Appendix A - presents a glossary of geotechnical terms used in this report.

Appendix B - provides a generalized guide to site characterization and code selection.

Appendix C - provides a description of the TRANS ground-water flow code.

Appendix D - gives a list supplemental references on contaminant mitigation.

PURPOSE

The case studies highlight the hydrogeologic methodologies required to characterize a site for analysis and the selection of a preferred mitigative scheme. The determination of an appropriate method to interdict ground-water contamination and design engineering structures can only be made at the case study level of analysis. General information is included on topical subjects for the convenience of the reader and to serve as a reference guide to further information. The case studies also demonstrate the conceptual model development that supports the accident scenario(s) and the use of selected mathematical models.

Furthermore, the case studies serve as a validation of the conclusions reached in the generic hydrogeological analysis. The case study results (e.g., maximum contaminant discharge flux and feasible mitigative techniques) are compared to generic based conclusions reached in Volume 1.

The components of each case study are designed to start with the information gained from the generic anlaysis and follow an iterative process of collecting more information and developing more sophisticated conceptual and numerical models. This process is outlined in Volume 1, Figure 1.5-2. In the event of a severe accident the process would be continued until either the analysis indicated that no contaminant interdiction was necessary or that the mitigative scheme in place would be an effective safeguard of environmental concerns.

Case Study Objectives

The case studies are conducted with two concurrent objectives. First, to consider to the greatest possible extent the effects of various contrasting geologic environments on selection of mitigative techniques. And secondly, to emphasize within each case study a separate component of the site characterization process such as, hydrologic description, model selection, code development, and cost effectiveness in contaminant interdiction. The core elements of the three case studies are given in Table I.

TABLE I. Overview of Case Study Content

Case Study No.	Name	Topics of Concentration
One	South Texas Plant	Unconsolidated hydrologic unit, hydrogeologic characterization, evaluation of mitigative methods.
Two	South Texas Plant	Performance assessment, cost effectiveness, mitigative scheme selection.
Three	Marble Hill Indiana	Consolidated fractured hydrologic unit, anisotropic flow field, plant structures

Selection of Sites For Case Study Analysis

The two locations chosen for case study analysis were selected from many sites that fulfilled the hydrogeologic requirements. The availablility and content of the geotechnical data bases were the overriding considerations in site selection. The South Texas Plant and Marble Hill Nuclear Generating Station have no known site or plant characteristics that would make these reactors prone to a severe nuclear accident.

English units of measure are used in Volume 2 so that this document is compatible with existing site documents (e.g., Final Saftey Analysis Reports and U.S. Geological Survey Reports, etc).

CONTENTS

6.0 CASE STUDY NO. 1

6.1 INTRODUCTION

Chapter 5.0 presents the results of pre-mitigative severe accident radionuclide release and transport analyses for each of the six generic site classifications. In addition, a set of matrices is provided which relate the feasibility of implementing selected mitigative techniques for each of the sites to composite hydrogeologic characteristics and technology constraints. The overall purpose of Chapter 5.0 is to provide a screening tool to determine the relative likelihood of significant radionuclide discharges at a given site by generic classification and to identify a preliminary set of feasible mitigative alternatives for further consideration. Clearly, determination of the "best" mitigative action(s) (in terms of technical feasibility, performance, maintenance requirements, service life and costs) requires a detailed evaluation of pre- and post-mitigative radionuclide transport through the ground-water system to potentially accessible environments. The South Texas Plant[a] (STP) case study described in this chapter is representative of the general methodology for performing such an evaluation. Emphasis is focused on the characterization and evaluation of ground-water flow and contaminant transport phenomena important to the South Texas Plant. The intent of this initial case study is to discuss some of the methods, procedures, and analyses necessary to determine the impact of various mitigative strategies on the ground-water flow regime of a specific site. Subsequent case studies will be more heavily involved with issues related to power plant configuration and more comprehensive mitigation performance tradeoff analysis.

6.1.1 Case Study Objectives

The primary objective of STP Case Study No. 1 is to demonstrate a general approach for hydrogeologic characterization and ground-water flow analysis for leading to site-specific evaluation of mitigative techniques. In addition, the case study is designed to:

- quantitatively assess achievable mitigation as a function of site hydrogeology, accident scenario and basic mitigative technique design characteristics proposed for the STP site, and
- numerically and graphically illustrate the spatial effects of selected mitigative techniques on ground-water potentials, flow velocities and travel times.

6.1.2 Relationship of Case Study No. 1 to Generic Classification - Mitigation Matrix

The hydrogeologic conditions underlying the STP site are representative of the porous unconsolidated silicate classification which is described in

(a) The South Texas Plant was selected solely because of adequate data availability. The case study is strictly hypothetical and is intended only to demonstrate certain analytical procedures.

Chapter 3.0 and discussed further in Section 5.6. Relative to the other generic hydrogeologic classifications, the porous unconsolidated silicate sites have high hydraulic conductivity, high effective porosity, low hydraulic gradient and slightly greater than average distances (compared to other power plant sites) to surface water. In general these characteristics apply to the STP site. Given this correlation between the STP site and the porous unconsolidated silicate classification, the matrix presented in Table 5.6.2-1 serves as a useful guide for preliminary selection of mitigative techniques for more indepth evaluation. In turn, the results of the case study will provide quantitative verification of the matrix.

6.1.3 General Methodology for Evaluation of Mitigative Alternatives

The recommended methodology for the evaluation of selected techniques for mitigation of possible ground-water contamination due to severe accidents at nuclear power plants consists of four main steps:

Step 1. Survey of regional ground-water hydrogeologic characteristics and regional flow analysis to determine local boundary conditions.

Step 2. Pre-mitigative local ground-water flow and transport analysis.

Step 3. Performance evaluation of feasible mitigative techniques based on ground-water and contaminant transport simulation.

Step 4. Sensitivity analyses of contaminant transport to hydrogeologic parameters.

This overall approach is intended to be universally applicable to most nuclear power plant sites. The appropriate means would be selected for analyzing ground-water flow and contaminant transport phenomena, dependent on site-specific conditions such as the geologic medium (e.g., porous sandstone, porous unconsolidated silicate, etc.), proximity to water users, and accident scenario. The computational requirements could range from simplified analytical representations to more sophisticated finite-difference or finite-element modeling depending on site conditions, data availability, and compatibility of computational approach with the objective of assessing the feasibility of mitigative alternatives.

A survey of regional ground-water flow characteristics is conducted in order to establish the general hydrogeologic conditions relevant to the study site. The regional ground-water flow analysis, using appropriate ground-water analytical and/or numerical modeling techniques provides the necessary data for determination of appropriate boundary conditions for the local analysis. The local flow and transport analyses are also performed by employing appropriate modeling techniques. As noted above, the techniques employed will be largely a function of the geologic medium hydraulic properties, data availability and the ability of the technique to determine the performance of particular mitigative

method. Generally, the primary measure of relative performance for the mitigative strategies will be contaminant flux at the location of the nearest downgradient surface water body or other accessible environment. Consideration should also be given to the contaminant flux at accessible off-site hydrologic units which may be used for water supply. Without some level of ground-water modeling of site-specific characteristics it would be virtually impossible to recommend, with confidence, an appropriate mitigative strategy.

The local flow and transport analyses are first applied to a pre-mitigative accident scenario to determine the baseline contaminant migration. These results provide the basis for subsequent trade-off analyses of the effectiveness of various mitigation approaches. Parametric studies are typically performed to determine possible limits of the effectiveness (i.e., performance) of a mitigative strategy in relation to both uncertainties in hydrogeologic parameters (e.g., hydraulic conductivity) and changes in major design characteristics of individual mitigative strategies (e.g., slurry walls).

The engineering interpretation of case study results will lead to consideration of performance related factors pertinent to the choice of mitigative alternatives. These factors include construction considerations, cost, durability, and the impact on water table elevations in the immediate vicinity of the plant. The durability issue is particularly important in light of the extended period of acceptable performance that may be required of the selected mitigative strategy. Durability considerations, which are dependent on the configuration of the mitigative strategy, may range from long-term effects of grout exposure to the hydrologic environment to mechanical equipment deterioration (e.g., pumps for well injection).

6.1.4 Case Study No. 1 Approach and Limitations

The approach taken for the STP case study is consistent with the general methodology described in Section 6.1.3. Specifically, a regional hydrogeologic analysis to determine local boundary conditions and a local flow and transport analysis are conducted using the TRANS ground-water flow and transport code developed by the Illinois Water Survey Division (Prickett et al. 1981). The criteria followed in the evaluation and selection of TRANS are discussed in Section 6.4.

For the remainder of this section, the term "model" is used to define a numerical computer code (e.g., TRANS) in conjunction with the data set or the site being studied (STP). In applying a code such as TRANS it is important to realize that a "model", as defined, is a simplification of the real world. However, when properly developed and validated a site specific model does approximate the attributes of the real ground-water system that are important to the objectives of the study. While not a perfect indicator of observed contaminant movement, a hydrologic flow and transport model can provide reconnaissance level (or better) understanding of the transport phenomena for the purpose of evaluating the effectiveness of various mitigative alternatives.

The primary limitation of the STP case study is that, due to the demonstrative nature and scope of this study, only previously published data are

used. If required data are sparse or unavailable, hypothesized data are generated based on the best information available and engineering judgment. In reality a field program would be conducted to provide a sufficient level of data to properly characterize the hydrogeologic properties of the site.

Other limitations of the case study relate to representing the STP aquifer system as a two-dimensional (horizontal) flow system and assuming steady-state simulation of water movement. Use of a two-dimensional model assumes vertically averaged flow and transport over the total aquifer thickness. It also assumes instantaneous mixing in the vertical. In terms of evaluating mitigative alternatives, injection and withdrawal wells and low permeability barriers are assumed to fully penetrate the aquifer. Further, it is assumed that no contaminant leakage occurs between the bottom of impermeable barriers and the aquifer bottom. Though these assumptions represent simplifications of the actual STP flow system, they do not detract significantly from the ability to realistically evaluate mitigative alternatives at the STP.

6.2 DEFINITION OF CASE STUDY NO. 1

6.2.1 Geographical Location and Physical Setting

The STP is situated in south-central Matagorda County, Texas approximately 4.9 km due west of the Colorado River. The STP is located on the Texas Gulf Coastal Plain approximately 17 km inland from Matagorda Bay and 24 km inland from the Gulf of Mexico. Figure 6.2.1-1 shows the site location within the State of Texas. The STP site is influenced by the coastal hydrometeorologic regime and tidal effects of the Gulf of Mexico. In summary, these influences result in (Houston Power and Light 1978):

1. high gross natural evapotranspiration rates,
2. high annual rainfall volumes and hourly intensities,
3. high winds,
4. tropical cyclones,
5. high ambient air temperatures,
6. high natural river water temperatures,
7. moisture-laden warm air masses, and
8. brackish surface water.

The geomorphology of Matagorda County (and the STP site) is typical of a slightly eroded coastal plain. The area is characterized by low relief, abandoned river valleys, marshes, and offshore barrier bars. The surface of the STP site is a depositional plain of the last ice age (Hammond 1969).

The STP site is within the humid subtropical region of Texas, and receives average annual precipitation on the order of 100 cm. Rainfall is normally well distributed on an annual basis with maximum rainfall usually occurring in

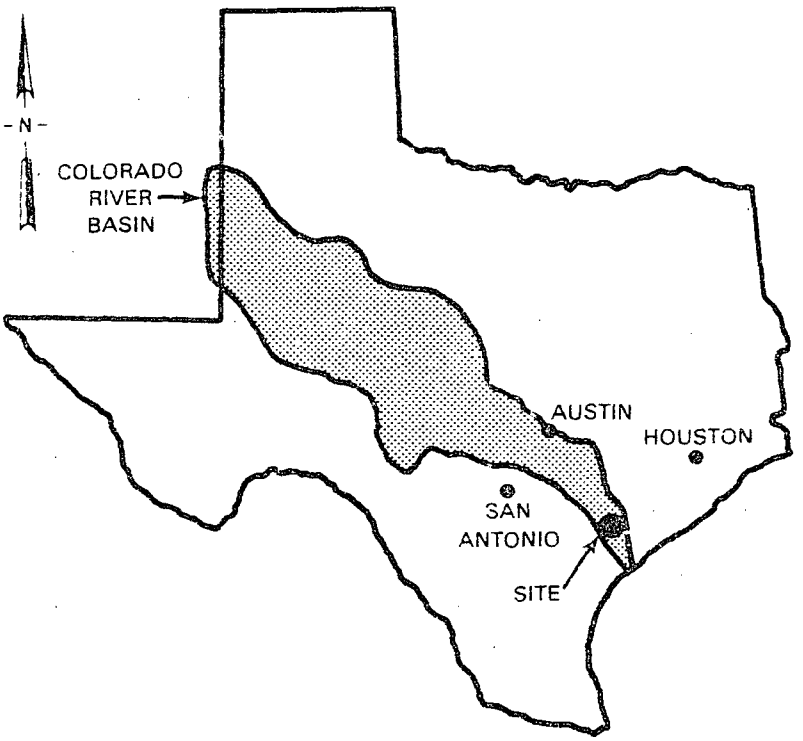

FIGURE 6.2.1-1. STP Site Location Map

September and minimum rainfall occurring in March (Hammond 1969). The area experiences long, hot summers with temperatures exceeding 32°C (90°F) for about 100 days each year. During the winter, cold fronts occasionally move down from the north which mix with the warm air lying over the Gulf of Mexico and produce cloudy, mild, but drizzly weather. Spring experiences mild days, brisk winds and frequent showers. Strong southeast winds begin in March but diminish in April and May and give way to pleasant sea breezes by mid-June. During late June, July and early August, the sea breeze greatly subsides and occasionally fails completely. The area is subject to tropical disturbances during summer and fall with potentially destructive winds. Thunderstorms are frequent but hail is infrequent and tornadoes are rare (NOAA 1980).

6.2.2 Reactor Design and Plant Configuration

The STP is composed of two units each having identical pressurized water reactors (PWR). The two units are roughly 180 m apart and use certain shared facilities including the cooling reservoir, spillway and blowdown facilities, and essential cooling pond. The reactor core-rated thermal power is 3,800 Mwt. High pressure light water serves as the coolant, neutron moderator, reflector, and solvent for the neutron absorber (Houston Power and Light 1978). The reactor containment building has a diameter of approximately 45 m

with a concrete basemat roughly 5.5 m thick. The containment is designed to withstand the internal pressure buildup following a loss of coolant accident.

Figure 6.2.2-1 shows the plant area (i.e., containment buildings, etc.) in relation to other station features. The plant grade is at 8.5 m MSL. The cooling reservoir is located south of the plant area and covers approximately 2800 ha or a little over half of the site property. The impoundment is supplied by water diverted from the Colorado River. The essential cooling pond, located east of the station, is intended to provide cooling water for safe shutdown of the plant. The essential cooling pond is an offstream impoundment which, under normal conditions is supplied with water from the cooling reservoir but has a backup well with 2000 ℓ/min pumping capacity (Houston Power and Light 1978). The essential cooling pond covers nearly 19 ha.

Offsite utility service could be important in considering the types of mitigative techniques that may be implementable. There are eight 345 kV transmission circuits from the STP 345 kV switchyard to the interconnecting grids of the STP owners. The transmission system provides reliable offsite power services any time power is unavailable from the station.

6.2.3 Definition of Accident Scenario

6.2.3.1 Severe Power Plant Accident

The South Texas Plant is a PWR incorporating a double loop for removal of heat from the reactor core. In a postulated severe accident, insufficient heat is removed from the reactor and the core materials overheat to the point of melting. The molten nuclear fuel and supporting materials could contain sufficient heat to melt through the reactor vessel and drop onto the floor of the containment building. The hot core materials would then thermally decompose and melt the concrete containment basemat (USNRC 1975).

The basemat structure could be penetrated (i.e., melted through) by the core melt mass or severely fractured allowing radioactive debris to enter the geologic materials below the power plant. Once the core debris containing nuclear fuel, steel, and liquified geomaterials entered the substratum, cooling would initiate solidification. The decay heat of the radionuclides in the debris would contain enough energy to prevent ground-water contact for about one year (Niemczyk et al. 1981). Ground water flowing through and around the core debris would leach radionuclides from the core melt mass and begin transporting contaminant away from the site. A more complete description of accident sequences and contaminant release is contained in Chapter 2.

In addition to core debris, the cooling water and water used in emergency spray systems could collect in the containment building sump. This water, referred to as "sump water", would become contaminated in the accident process and could be released into the geologic units beneath the plant due to basemat failure. The STP is capable of producing both types of contaminant releases in a severe accident.

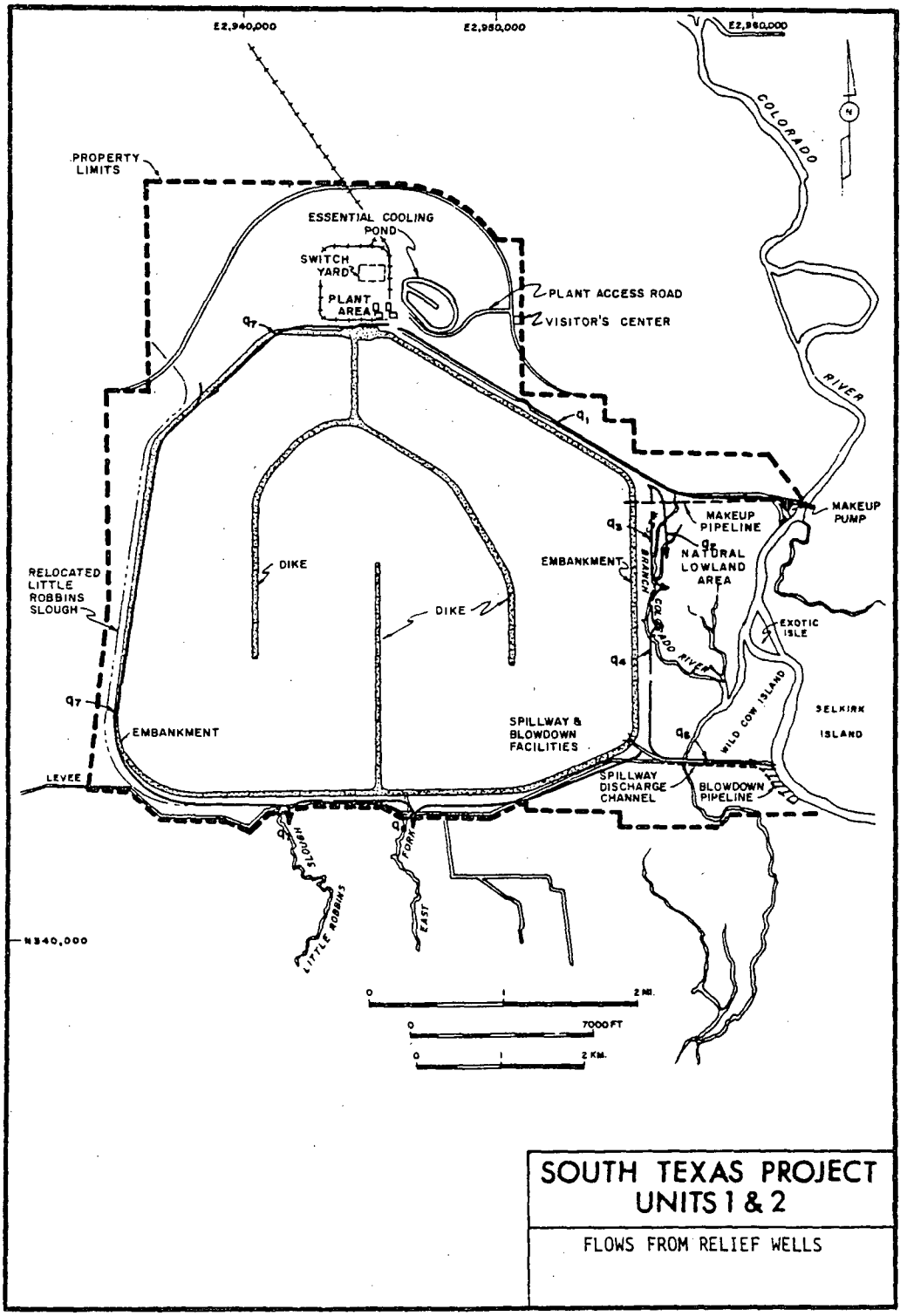

FIGURE 6.2.2-1. STP Plant Area (Source: Houston Power and Light 1978)

In a severe nuclear accident, radionuclides of various half-lives, initial quantities, toxicities, and ground-water transport parameters would be released. It is not necessary to determine the ultimate position of all classes of radionuclides. This study focuses on radionuclides that would be released into the ground-water system (as opposed to those that would constitute an atmospheric release). The radionuclides having long half-lives are of concern because they would not decay to low levels very soon after an accident. Radionuclides in large quantities that are not strongly sorbed are also of concern because they have the potential to migrate away from the site more quickly and in high concentrations.

The experience gained in the generic characterization of all nuclear power sites is used to select radionuclides that can serve as indicators of contamination. In unconsolidated silicates (i.e., sand, silt and clay), the radionuclides which best characterize contamination are strontium-90 and cesium-137.

There are several accident scenarios that could result in a nuclear power plant core melt. This study has conservatively assumed that the accident sequence that would release the largest portion of the nuclear inventory has occurred at this site. The amount of radionuclides contained in the core is based on the thermal output of the STP in relation to a theoretical reference reactor described by USNRC (1975). The thermal output and a partial core inventory of the two reactors are listed in Table 6.2.3-1.

TABLE 6.2.3-1. Initial Amounts of Indicator Radionuclides

Radionuclide	Half-Life (days)	Reference Reactor pCi (USNRC 1975)	South Texas Plant pCi (Single Unit)
Strontium-90	10519	3.71×10^{18}	4.53×10^{18}
Cesium-137	11042	4.67×10^{18}	5.70×10^{18}

The radionuclides contained in the core would be partitioned into the core debris, the sump water and the containment atmosphere. The accident sequence preceeding the core melt determines the percentage of the initial inventory that would reside in each of the above partitions under the assumption of the most likely accident sequence. The radionuclide partitioning for this study assumes that the most severe accident sequence has occurred. The resultant initial amounts of key radionuclides available for release are listed in Table 6.2.3-2. A more complete description of the core melt source term is given in Section 2.2.

6.2.3.2 Release of Radionuclides Into the Ground-Water System

The penetration of the core melt into the earth below the containment structure is a function of the accident sequence, size of the reactor, and the chemical composition of the geologic materials. Clay and sand at the STP would primarily be chemically composed of silicic minerals. The shape of core melt penetration into a silicate material has been calculated by Niemczyk et al.

TABLE 6.2.3-2. Release Fractions for the Indicator Radionuclides (Source: Niemczyk et al. 1981)

Radionuclide	Sump Water Release, %	Core Melt Debris Leach Release, %
Strontium-90	11	89
Cesium-137	100	0

(1981). The geometric configuration of the core debris would be approximately cylindrical with a radius of roughly 9 m (29 ft) and a depth of approximately 11 m (35 ft) below the basemat or about 25 m (80 ft below MSL). At this depth, the core debris would reside in the lower unit of the shallow-zone aquifer (see Section 6.3.2 for a detailed characterization of the STP site hydrogeology). The deep aquifer, which is used as a source of fresh water, would be isolated from the core melt by over 45 m (150 ft) of clay. The shallow aquifer sands are therefore the hydrostratigraphic unit that would transport the majority of radionuclides away from the site.

The heat contained in the core debris would temporarily vaporize the ground water adjacent to the melt and prevent transport under saturated conditions. It is estimated the top of the core melt in contact with sump water would cool below the boiling point of water in about six months. Similarly, the central portion of the core melt would cool in approximately one year (Niemczyk et al. 1981). The resaturation of the desiccation-alteration zone around the core debris would also delay the transport of contaminant. This study accounts for the temperature of the debris preventing saturation and conservatively does not consider the additional time required for resaturation.

The leach release of silicic materials occurs over a long period of time. Indeed, glass is often used as an isolation medium for radioactive wastes because of its isolation properties and low rate of decomposition. The dominant mechanism for the removal of radionuclides from core debris is matrix corrosion. The silicic leach processes are described more fully in Section 2.4.2. The majority of the radioactivity undergoes decay while still contained in the melt debris and does not enter the ground-water system. However, the leach release does continue for millennia at an exponentially decreasing rate. The leach rate is determined under the same assumptions as used in the generic examination of silicic core melts. The absolute rate is appropriately scaled to represent the thermal size of a single reactor at the STP. Figure 6.2.3-1 presents the release flux of strontium-90 from the core melt debris over time. Because almost 90% of the total strontium-90 present is contained in the core melt debris, sumpwater release, for simplicity, is not considered in this study.

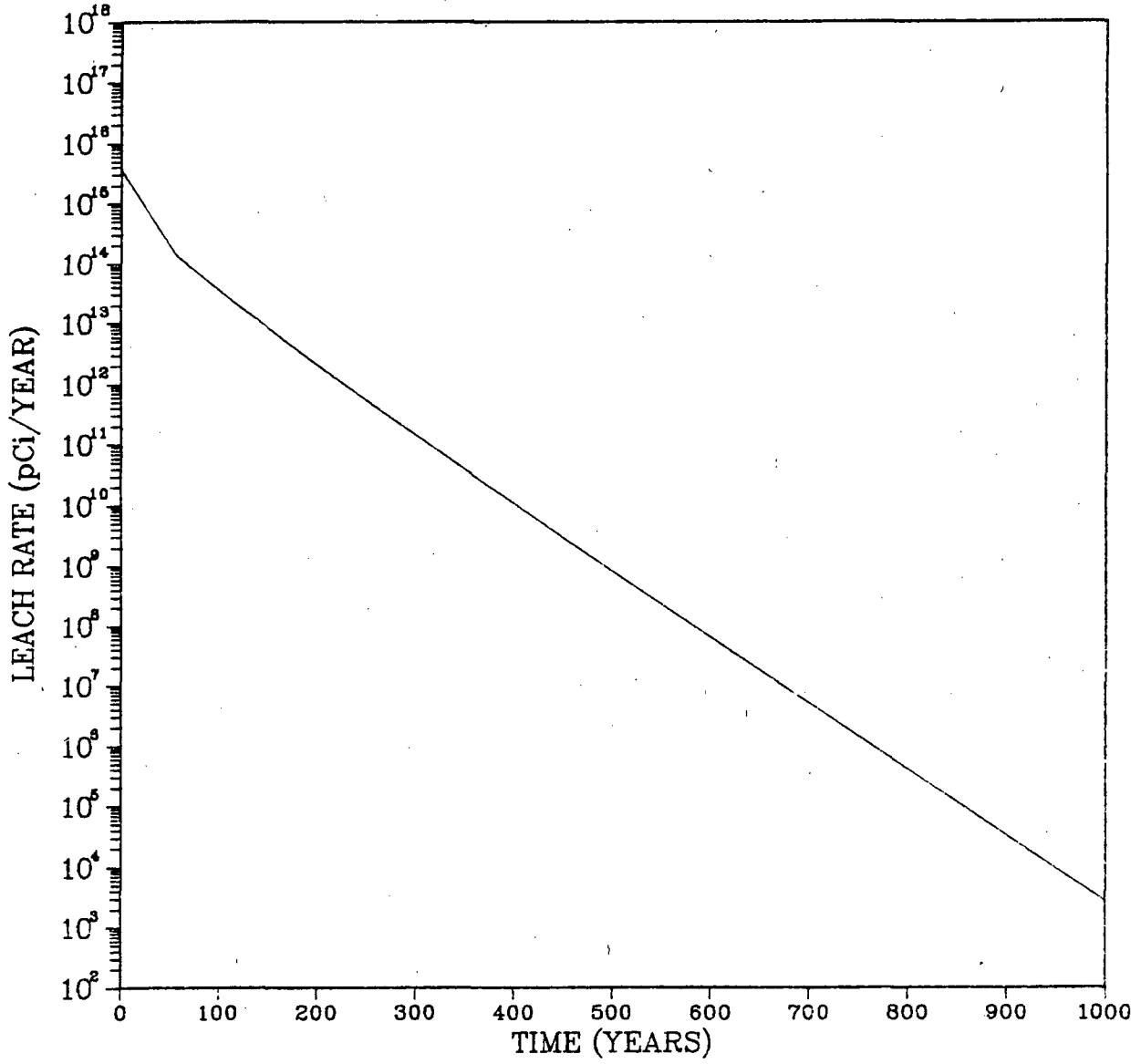

FIGURE 6.2.3-1. Hypothesized STP Leach Release of Strontium-90

6.3 REGIONAL ANALYSIS

6.3.1 Approach[a]

The regional hydrologic system is important in analyzing the hydrology and contaminant transport of more localized systems. This importance has been demonstrated in a ground-water modeling study of remedial action effectiveness

(a) English units of measure are used throughout the analysis because published data pertaining to the hydrogeologic properties of sites in the U.S. are typically in English units.

for the La Bounty Landfill in Charles City, Iowa presented by Cole et al. (1983). Their study also shows that boundary conditions for the local system must be determined from the regional system for pre-mitigative and post-mitigative flow conditions if reasonable estimates of travel times and ground-water flow rates are to be obtained. On this basis, a two stage modeling approach is developed for the STP site. The first stage consists of development of a coarse grid regional ground-water flow model, while the second stage involves development of ground-water flow and contaminant transport model for the immediate vicinity of the STP site.

The application of models to investigate ground-water flow and transport involves several areas of effort: data collection, data preparation for the model, history matching and predictive simulation (Mercer and Faust 1980). The interrelationships of these tasks is illustrated in Figure 6.3.1-1. The first phase of a ground-water model study consists of gathering the available geologic and hydrologic data on the ground-water system of interest. Typically this would include information on: surface and subsurface geology, precipitation, evapotranspiration, pumping, surface streamflows, soils, vegetation, irrigation, hydraulic potential, aquifer properties and boundary conditions. If available data are not adequate, a field data collection program may be required. All of the data are then used to develop a conceptual model of the basin.

As discussed by Boonstra and de Ridder (1981) a conceptual model is constructed based on preliminary assumptions regarding study area size, boundary conditions, number of geologic layers, ground-water flow direction, recharge and discharge locations, etc. The first step in developing the conceptual model is to identify the extent and nature of the ground-water system (e.g., does the system consist of a single aquifer or combination of multiple aquifers). Using the preliminary conceptual model, an appropriate computer code can be selected and development of the numerical model can begin. The model is first used to synthesize the various data and then to test the validity of the conceptual model. From this stage, refinement of the conceptual model and calibration of the numerical model involve an iterative process that continues until the two are consistent with each other and the numerical model adequately reproduces observed data. When this is accomplished, the numerical model is ready for predictive simulations.

The implementation of this process to the development of the STP regional model is described below.

6.3.2 Data Compilation and Conceptual Model Development

Numerical model development and calibration require a variety of quantitative hydrogeologic data that can be classified into two groups (Boonstra and de Ridder 1981):

1. data that define the physical framework of the ground-water system, and
2. data that describe the system inflow and outflow.

Specific data types within each group are listed in Table 6.3.2-1.

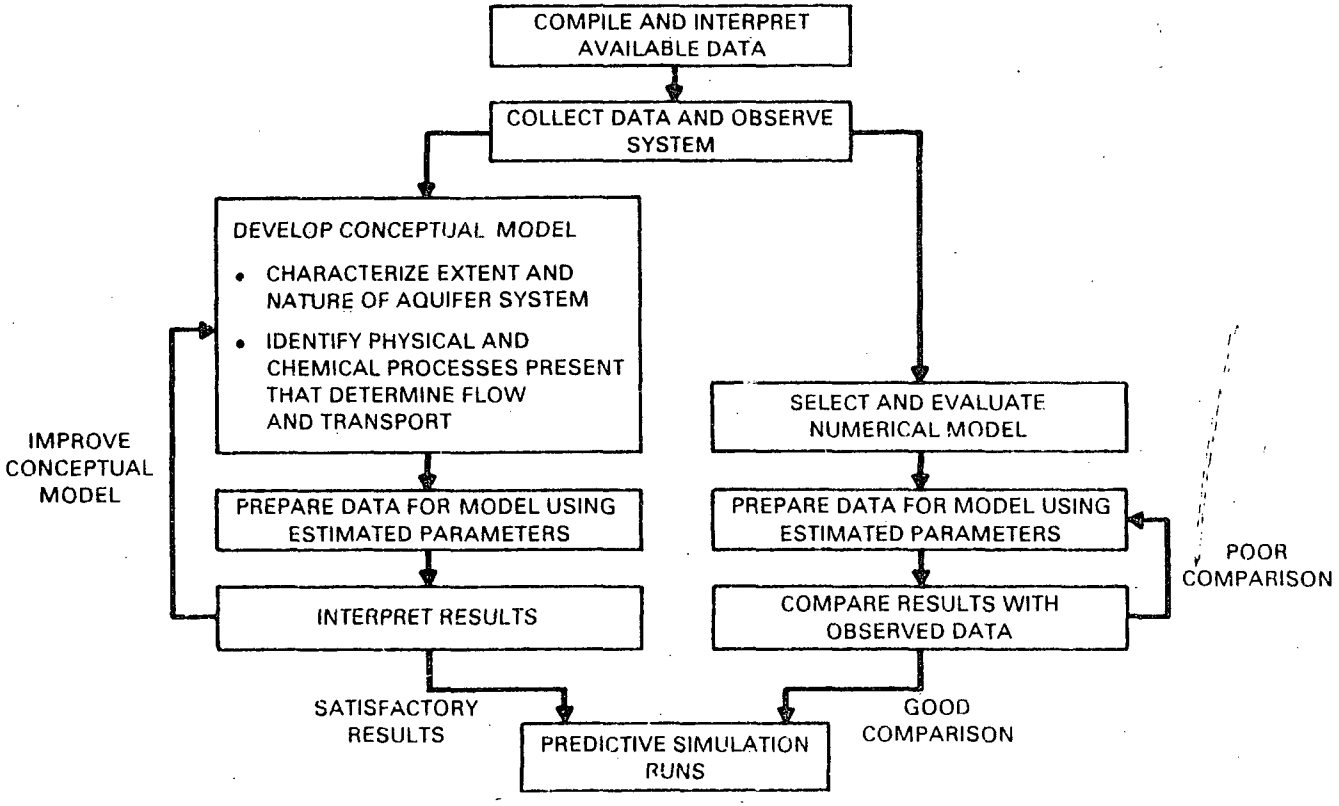

FIGURE 6.3.1-1. Major Steps in Ground-Water Model Applications (Source: Mercer and Faust 1980)

For a particular site there are many sources for the different types of data listed in Table 6.3.2-1. These sources include:

- Preliminary Safety Analysis Reports, Final Safety Analysis Reports, Environmental Reports, etc.
- Local water supply districts, well drillers, engineering consulting firms and other firms which deal with water problems.
- Local and regional Soil Conservation Service offices.
- State and county offices of natural resources, environment, health, or ecology.
- Local, state, regional and national offices of the U.S. Geological Survey (USGS), the U.S. Corps of Engineers, the U.S. Bureau of Reclamation, and the U.S. Environmental Protection Agency.
- Universities and colleges with programs in geology and hydrology.
- Local libraries.

In compiling data for the STP case study, readily accessible sources were used. Selected sections of the STP Final Safety Analysis Report (Houston Power and Light 1978) were relied upon as one of the principal data sources. Other key sources included the USGS and the Texas State Department of Water Resources. The remainder of this section presents the results of the STP hydrogeologic characterization. For each data type listed in Table 6.3.2-1, details of the data sources, analysis and interpretation are provided.

TABLE 6.3.2-1. Data Required for Ground-Water Modeling (Source: Boonstra and de Ridder 1981)

Physical Framework	Hydrologic Stress
1. Topography	1. Watertable elevation
2. Geology	2. Rate and extent of recharge areas
3. Types of aquifers	3. Rate and extent of point and and areal discharge
4. Aquifer boundaries	
5. Aquifer thickness and lateral extent	
6. Porous media material properties	

6.3.2.1 Topography

A basic requirement for conducting a ground-water study is a topographic map delineating surface water bodies, streams, man-made water courses and land surface elevation contours. Maps for the STP site were obtained from the USGS Map Distribution Center in Denver, Colorado. Figure 6.3.2-1 is a reduction of the topographic maps for the vicinity of the STP site. Features identified on

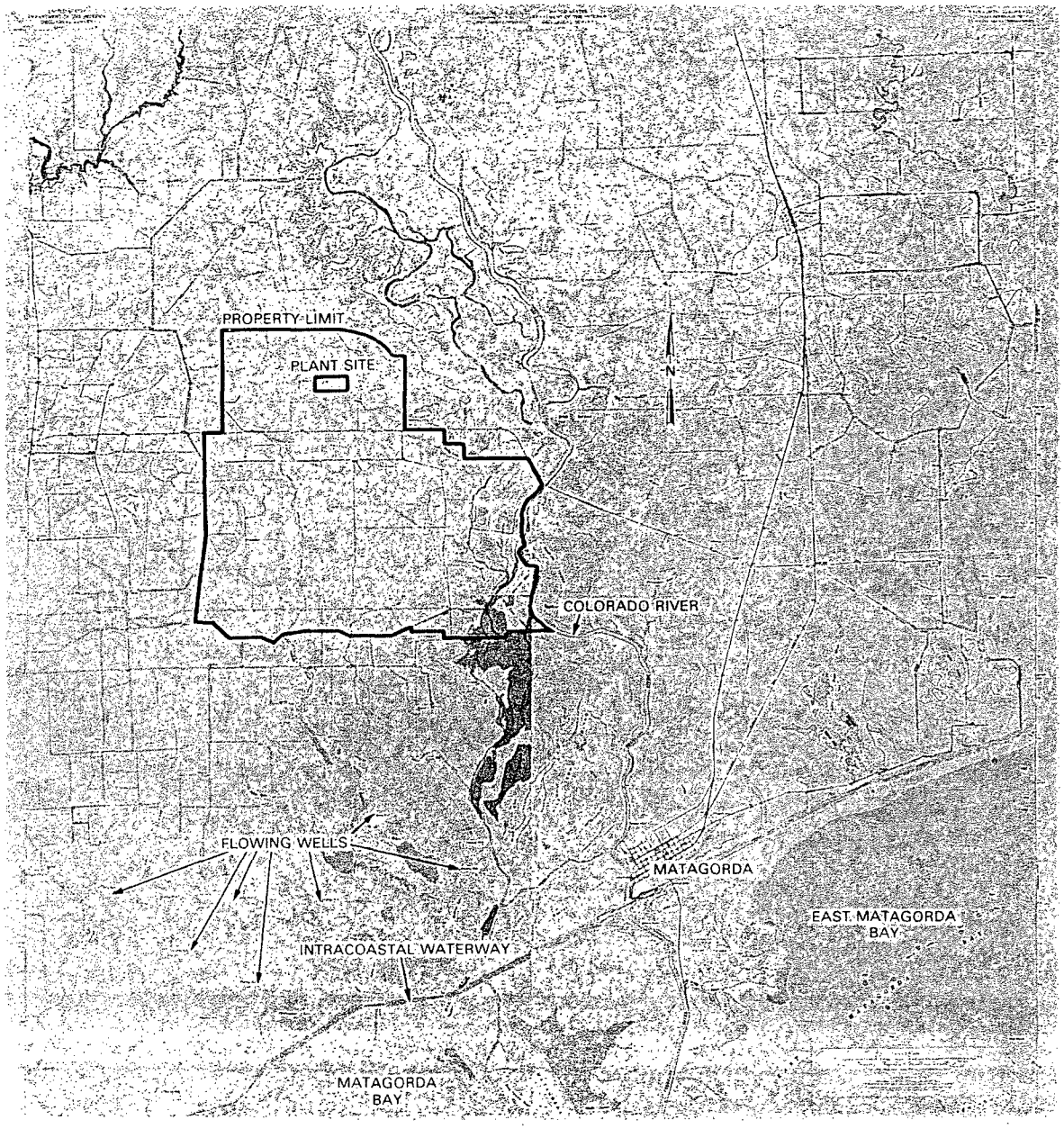

FIGURE 6.3.2-1. USGS Topographic Map for the Vicinity of the STP Site

the map include the approximate STP property limits and site location, Colorado River, Intracoastal Waterway and the Gulf of Mexico. In general, the topography is characterized by gently sloping terrain to the north of the site and flat swampy areas to the south. There are no structural geologic features discernable at the STP site. Local land-forms are subdued due to the gentle slope of the underlying geologic units, weathering and stream erosion.

6.3.2.2 Geology

The structural history the of Texas Gulf Coastal Plain on which the STP is located began in the late Jurassic Period. At this time, roughly 145 million years ago, the crust of the earth began to downwarp as a large regional feature known as the Gulf Geosyncline (Stokes 1966). Sediments eroded from the continental land mass to the north were transported by rivers and deposited in the geosyncline. These processes have accumulated over 50,000 feet of sedimentary material in the central depression of the geosyncline ranging in age from the Cretaceous Period to the present. The regular transportation of sediments in this region has resulted in the formation of the thick sedimentary units forming the Coastal Plain. There are two characteristic features of these geologic units: 1) the sediments are graded, that is, they become finer material (i.e., sand to clay) toward the center of the geosyncline; and 2) the layers of sediments become thicker toward the center of the geosyncline. This depositional formation has created extensive units known as sedimentary wedges that thicken and dip seaward. The southward dip of the older environment is greater than the more recent units because of the continued continental uplift inland and continued downwarp of the Gulf Geosyncline.

Deposition of the more coarse sediments occurred by alluvial processes along rivers and streams. As the rivers altered their channels and deposited additional material, the lateral accretion deposits (i.e., channel lag deposits, channel bar deposits, and point bar deposits) became vertically superimposed. The rivers continually migrated back and forth across the broad low relief depositional plain and created a series of coalescing alluvial and deltaic plains (Houston Power and Light 1978). This process formed geologic units of discontinuous interfingering beds which grade laterally over very short distances from clay to silt to sand to gravel (Hammond 1969). Taken in its entirety, the sediments are referred to as the Gulf Coast Aquifer (Baker and Wall 1976).

The near surface geologic units found in Matagorda County and their hydrologic significance are listed in Table 6.3.2-2. The STP is situated on the Pleistocene Beaumont Formation which extends at least 700 feet below the site. The base of the Beaumont Formation dips to the south at 10 to 20 feet/mile (Houston Power and Light 1978). The upper surface of the Beaumont Formation constitutes the present land surface. The formation is characterized as layers of clay, sandy clay, and thick sand units. The layers of sand are up to 100 feet thick and produce significant amounts of water for irrigation and mining (Hammond 1969). Clay layers of up to 150 feet thick hydraulically isolate the various sand layers.

TABLE 6.3.2-2. Geologic Description and Water-Bearing Properties of Stratigraphic Units Forming the Gulf Coast Aquifer (Source: Hammond 1969)

System	Series	Stratigraphic Unit	Estimated Thickness (ft)	Composition	Water-Bearing Properties and Distribution of Supply
Quaternary	Recent	Alluvium	0-200?	Silt, clay, fine to coarse sand and gravel with wooden debris and logs. Chiefly in eastern portions of Matagorda County.	Capable of yielding large amounts of fresh water. Highly permeable. All irrigation wells in extreme eastern Matagorda County and western Brazoria County are completed in this unit. Fresh water is underlain by saline water in coastal areas.
		Coastal Deposits	0-50?	Beach and dune sand and coastal marsh deposits.	Not capable of yeilding fresh water. Water present is highly mineralized.
		Beaumont Formation	250-900?	Sandy clay, clayey sand, calcareous, fine to medium sand often occurring in thick lenses, some shell beds and calcareous nodules.	Capable of yielding moderate to large amounts of fresh water. Fresh water is overlain and underlain by saline water in coastal areas.
		Montgomery Formation	40-80?	Medium to fine sand, silt and clay. Generally finer grained than underlying Bentley Formation.	Capable of yielding moderate to large amounts of fresh water. Fresh water is overlain and underlain by saline water in coastal areas.
	Pleistocene	Bentley Formation	400-1000?	Thickly bedded, fine to coarse sand and gravel interbedded with clay. Lense-like sand structure.	Capable of yielding large amounts of fresh water in most of the county with the exception of the coastal areas where formation contains highly mineralized water. Supplies water to irrigation wells in the north-central and northwestern portions of the county.
		Willis Formation	80-85?	Very fine to coarse sand and gravel, ferruginous, interbedded with clays.	Not capable of yielding fresh water. Water is highly mineralized except in extreme northwestern portion of the county.

The Beaumont Formation has been characterized in detail at the site of the South Texas Plant by drilling, bore hole logging and reflection geophysical profiling between bores. A hydrologic evaluation combining the geological evidence and piezometric data identified three major sand layers that are capable of transmitting large volumes of water. These sand layers are separated into two hydrostratigraphic units; a deep aquifer at depths greater than 300 feet, and a shallow aquifer consisting of an upper and lower unit ranging between 90 and 150 feet below land surface. A hydrostratigraphic unit is defined as a body of rock or series of formations with considerable lateral extent that compose a reasonably distinct hydrologic system. The distinction of the upper and lower units in the shallow aquifer is based on the presence of a 20 feet thick clay layer that locally separates the units and produces slightly different potentiometric levels. South of the site boundary this clay layer pinches out and the shallow aquifer becomes a single unit.

6.3.2.3 Types of Aquifers

An aquifer is defined as a geologic formation or group of formations that contain sufficient saturated permeable material to yield significant quantities of water (Boonstra and de Ridder 1981). Thus, determination of aquifer type(s) is accomplished by translating the known geologic and hydrologic information into terms of high yield waterbearing formations (aquifers), confining layers (very low permeability) or semi-confining layers (low permeability). Consecutive formations having similar water transmitting properties should be classified as a single aquifer system. For example, consecutive strata of clay, silty clay, sand clay, etc., though different in age and depositional conditions, represent a single layer having similar ground-water hydraulic properties. The three basic types of porous media aquifers; unconfined (watertable), confined (artesian) and semi-confined (leaky) are shown in Figure 6.3.2-2.

The primary sources of information for identifying the aquifer types in the vicinity of the STP site were the STP FSAR (Houston Power and Light 1978) and the Texas Water Development Board Report 91 by Hammond (1969). The aquifers in the site vicinity are found in the lower Gulf Coastal Plain, described as a thick composite of deltaic sediments extending locally to depths of as much as 2000 ft. These sediments are discontinuous, interfingering beds of clay, silt, sand and gravel seldom traceable over very appreciable distances. The different stratigraphic units in the Gulf Coastal Plain are described in Table 6.3.2-1. In Matagorda County, the Beaumont Formation supplies most of the usable ground water and extends from the ground surface to depths of about 700 feet in the area of the STP. Ground water in the Beaumont Formation is confined by an overlying zone of predominantly clay materials up to 150 feet thick. The main producing aquifer zone, designated as the deep aquifer zone, lies below depths of 200 to 300 feet in the site area.

Within the Beaumont Formation there is a shallow aquifer zone that occurs above depths ranging from 90 feet to 150 feet in the vicinity of the site. Based on geophysical and hydraulic tests as discussed in the STP FSAR (Houston Power and Light 1978), the upper zone is segmented into lower and upper confined units. Each unit is characterized by a different piezometric surface.

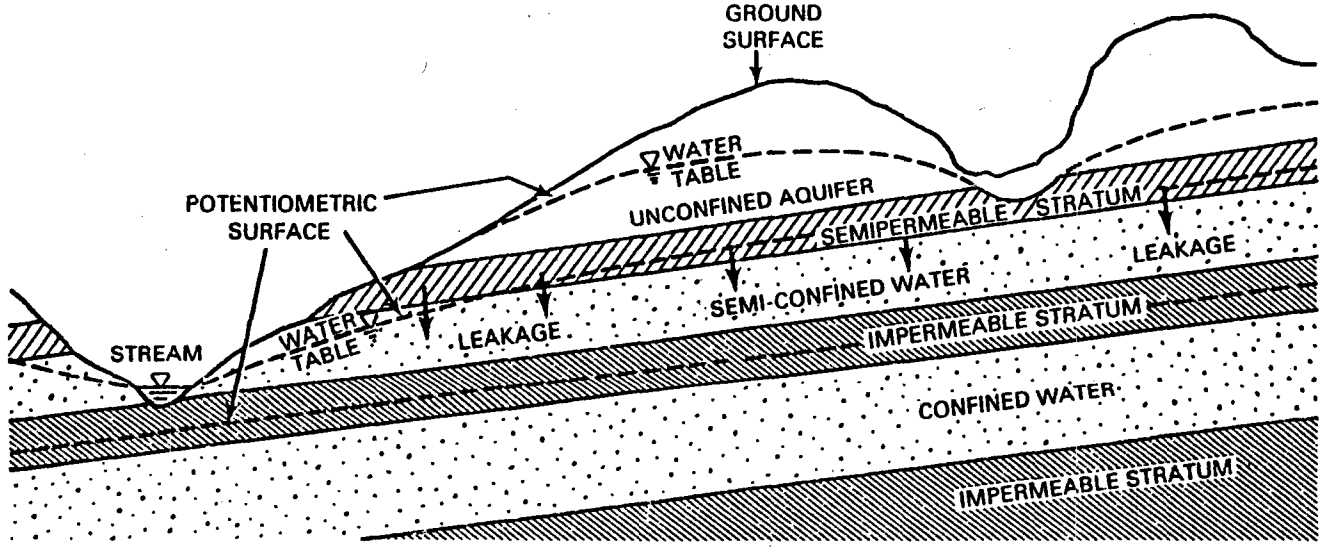

FIGURE 6.3.2-2. Illustration of the Three Basic Porous Media Aquifer Types

The regional geologic configuration in the vicinity of the site is illustrated by the geohydrologic-cross section shown in Figure 6.3.2-3. The cross-section clearly shows the deep aquifer zone overlain by the deep confining zone which ranges in thickness from over 150 feet to almost 250 feet. The shallow aquifer zone is located between the surface confining zone and the deep confining zone. The upper and lower units of the shallow aquifer zone are easily distinguishable, separated by a layer of predominantly impermeable material 25 feet to 50 feet in thickness. The piezometric levels shown on Figure 6.3.2-3 indicate both the shallow and deep aquifer zones are artesian units.

On the basis of the stratigraphy and relative locations of the aquifer units and the discussion of the postulated effects of a severe accident at the STP in Section 6.2.3.2, it is apparent that the molten core mass would penetrate to a depth corresponding to the lower unit of the shallow aquifer zone. Thus, flow and transport would occur under artesian conditions and, in the absence of significant inner-unit transfers, analysis can be limited to the lower unit of the shallow aquifer. This assumption precludes the need to perform detailed study of both the upper and lower units of the upper aquifer. Subsequent data analysis is conducted under this assumption. In an actual assessment of potential accident effects outside the context of a case study, this assumption would be subjected to extensive evaluation before proceeding.

6.3.2.4 Aquifer Boundaries

In addition to describing the thickness and lateral extent of the aquifer in question, the aquifer boundaries must also be properly defined. The different types of boundaries identified by Boonstra and de Ridder (1981) include:

- zero-flow boundaries.
- head-controlled boundaries.
- flow-controlled boundaries.
- free surface boundaries.

Since the free surface boundary is to be determined by the numerical model it will not be discussed here. These types of boundaries are illustrated in Figure 6.3.2-4 and briefly discussed below.

Zero-Flow Boundary

Conceptually, a zero-flow boundary is one across which flows are insignificant relative to flows in the main aquifer. Zero-flow boundaries can occur as either internal or external boundaries. For example, a massive unfractured crystalline formation along the outer edge of an aquifer or a ground-water divide would produce an external zero-flow boundary. A local outcrop of massive rock and an impermeable aquifer bottom would be representative of internal zero-flow boundaries. In developing a ground-water model of a basin, it is necessary to delineate the zero-flow boundaries on a map. Zero-flow is

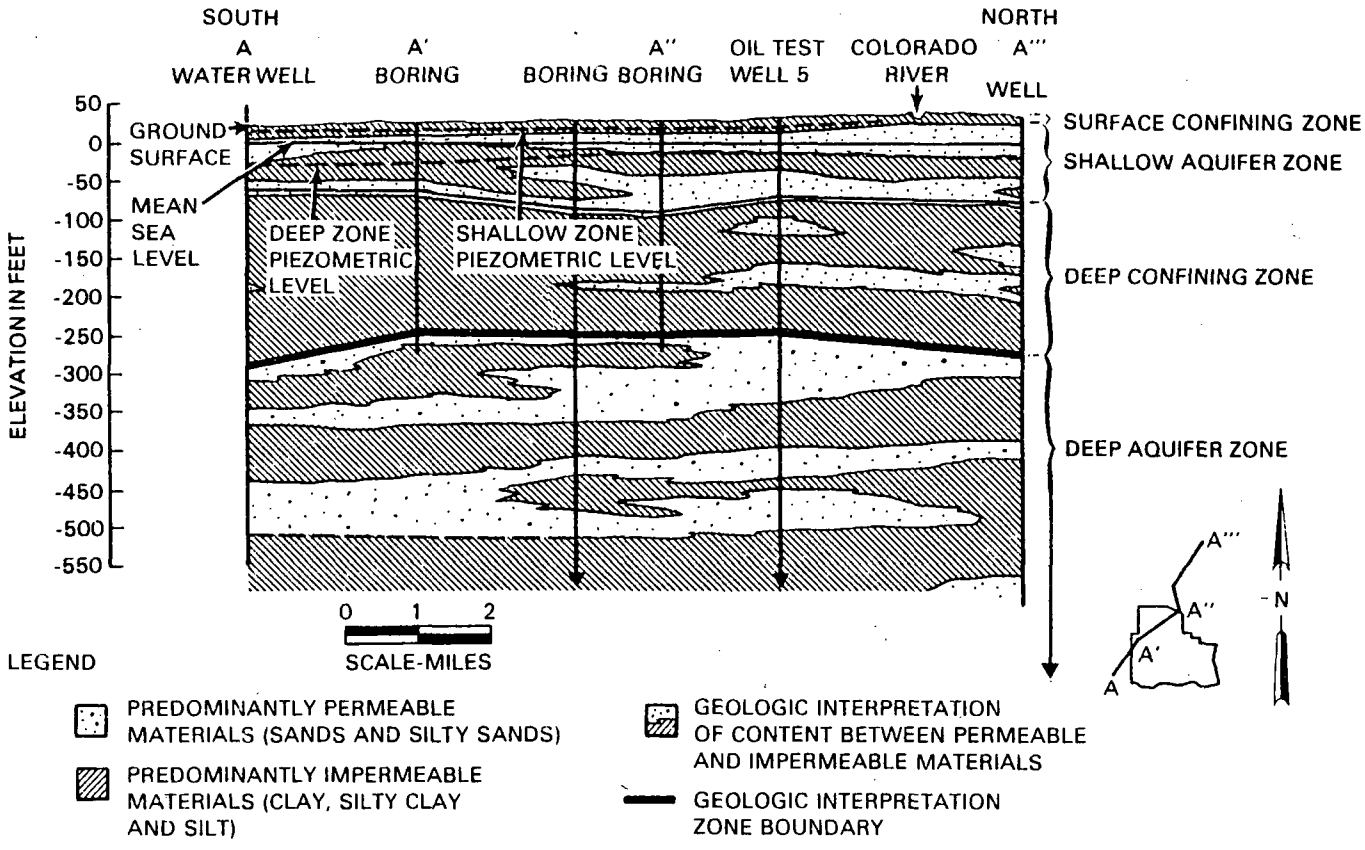

FIGURE 6.3.2-3. Geohydrologic Cross-Section A-A"' for the STP Site (From: Houston Power and Light 1978)

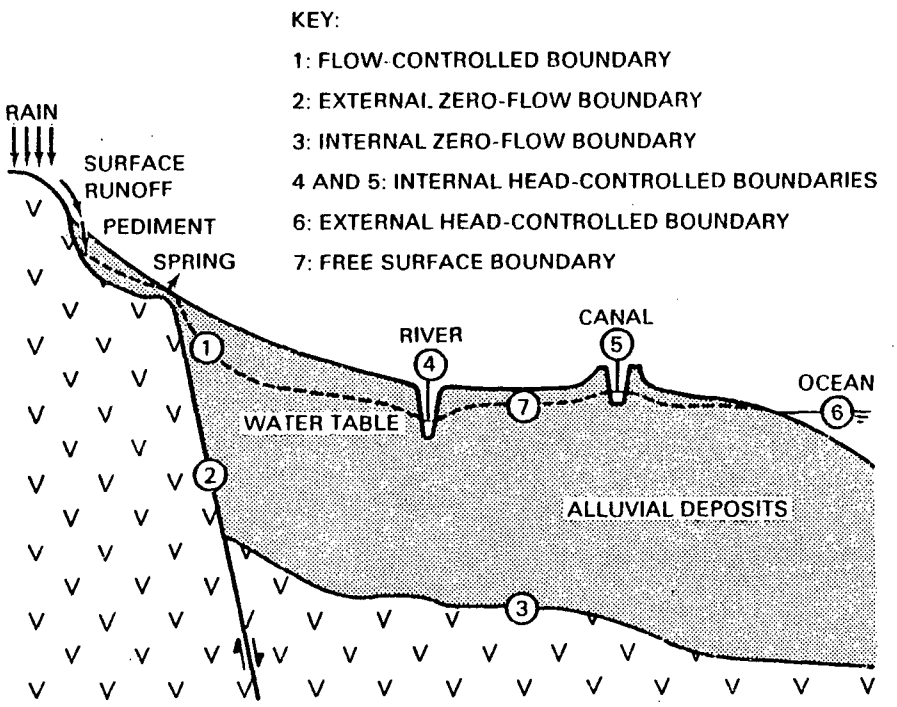

FIGURE 6.3.2-4. Illustration of Different Aquifer Boundary Types (Source: Boonstra and de Ridder 1981)

then achieved in the model by setting the hydraulic conductivity at the boundary equal to zero (Boonstra and de Ridder 1981).

Head-Controlled Boundary

A head-controlled boundary has a known hydraulic head which is either constant or varies with time and is not affected by potentiometric or permeability changes within the ground-water basin. Examples include large water bodies such as oceans and lakes or water courses with fixed water levels like irrigation canals. Similar to zero-flow boundaries, head-controlled boundaries can occur both internal and external to the aquifer. A stream in hydraulic contact with an aquifer inside its boundaries is an internal head controlled boundary while the ocean in direct contact with an aquifer is an external head-controlled boundary (Boonstra and de Ridder 1981).

Flow-Controlled Boundary

A flow-controlled boundary is a boundary through which ground water enters the aquifer at a certain rate from adjacent strata whose hydraulic head is not known. The volume of water transferred in this way is normally estimated by recharge based on rainfall and runoff data. The aquifer boundary may be a

zero-flow boundary but a portion of the incident precipitation may percolate into the colluvium and enter the aquifer at the boundary as ground-water flow (Boonstra and de Ridder 1981).

Selection of STP Boundary Conditions

During development of a ground-water model, it is advantageous in defining boundary conditions to select the external boundaries of the model so they coincide with head-controlled and/or zero-flow boundaries. If the model is being developed for only a portion of the basin, however, it might be necessary to arbitrarily choose a boundary where ground water flows into or out of the basin. In this case, the flow rate must be computed based on the boundary heads and hydraulic conductivity.

Selection of boundaries for the lower unit of the shallow aquifer in the STP site vicinity was based upon Hammond's (1969) general description of ground-water movement in Matagorda County and analysis of the observed hydraulic potentials in the vicinity of the site presented in the STP FSAR (Houston Power and Light 1978). As described by Hammond (1969), the ground water underlying Matagorda County moves continually from the principal areas of recharge, to the north in Wharton County, to the southeast toward the Gulf of Mexico where the primary discharge occurs. Hammond (1969) also points out that at times, though the Colorado River is completely dammed at a point below Bay City, its flow is partially resumed by ground-water seepage. Further, the STP FSAR (Houston Power and Light 1978) states: "shallow-zone discharge is into Matagorda Bay and the Colorado River estuary at least 5 miles to the southeast of the power station area." Thus, it was initially thought that the shallow aquifer discharges into Matagorda Bay except possibly where it is intercepted by the Colorado River. The pre-construction piezometric levels observed on March 14, 1974 for the upper unit of the shallow aquifer suggest this is occurring. The contours, presented in Figure 6.3.2-5, show a definite steepening in gradient as they approach the Colorado River, indicating the upper unit is hydraulically connected to the river. The contours for the lower unit, presented in Figure 6.3.2-6, show a tendency to align themselves with the river. However, the piezometric levels do not converge to the apparent water level of the river. This circumstance indicates that the lower unit only discharges a portion of its flow to the Colorado River as upward seepage through its confining layer.

On the basis of these observations, a regional study area was designed with the x-direction roughly parallel to the observed lower unit contours of equal hydraulic head. The rectangular area, partially outlined in Figure 6.3.2-7, superimposed on the site topography maps extends to the south into Matagorda Bay and East Matagorda Bay and to the north beyond the STP property limits. The exact regional boundaries were chosen arbitrarily at a distance far enough away from the STP site so that assigned boundary conditions would not greatly influence the local hydraulic conditions in the immediate vicinity of the STP. The complete grid, approximately 11.4 mi. by 13.3 mi. (2000 ft by 2000 ft grid elements) is shown in Figure 6.3.2-8.

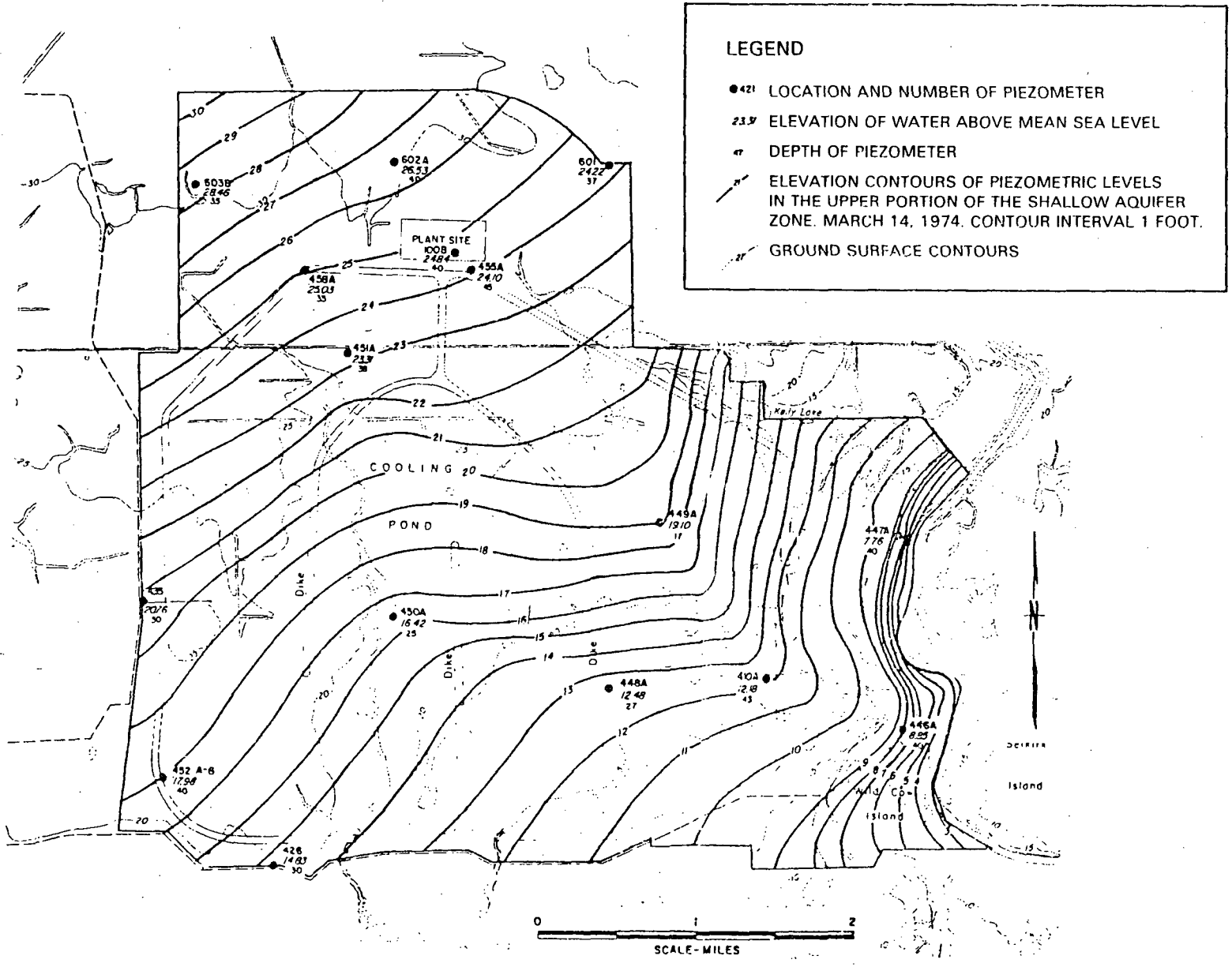

FIGURE 6.3.2-5. Observed Potential Contours for the Upper Unit of the Shallow Aquifer Zone (Source: Houston Power and Light 1978)

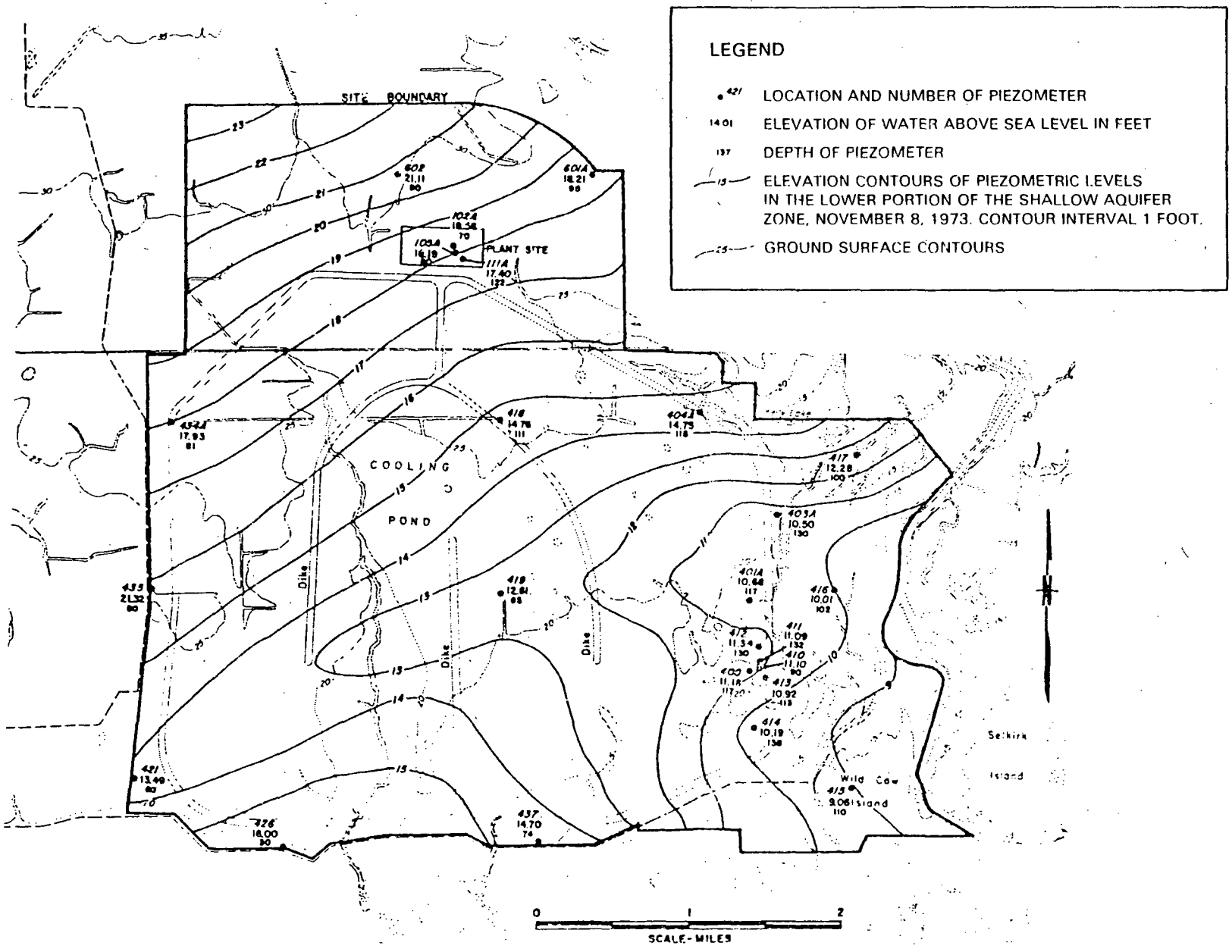

FIGURE 6.3.2-6. Observed Potential Contours for the Lower Unit of the Shallow Aquifer Zone (Source: Houston Power and Light 1978)

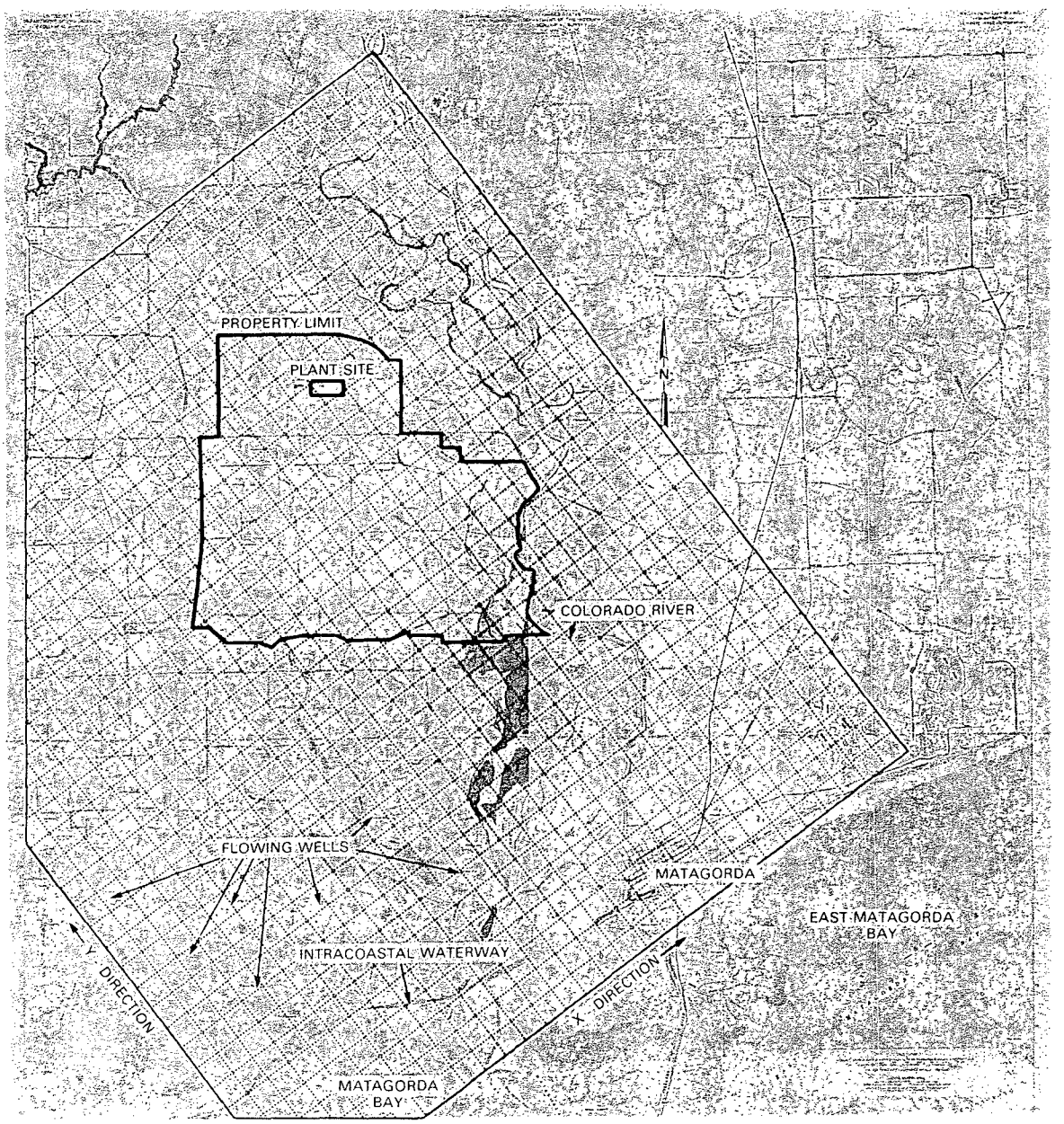

FIGURE 6.2.3-7. Partial Outline of Regional Study Area Superimposed on the STP Topographic Map

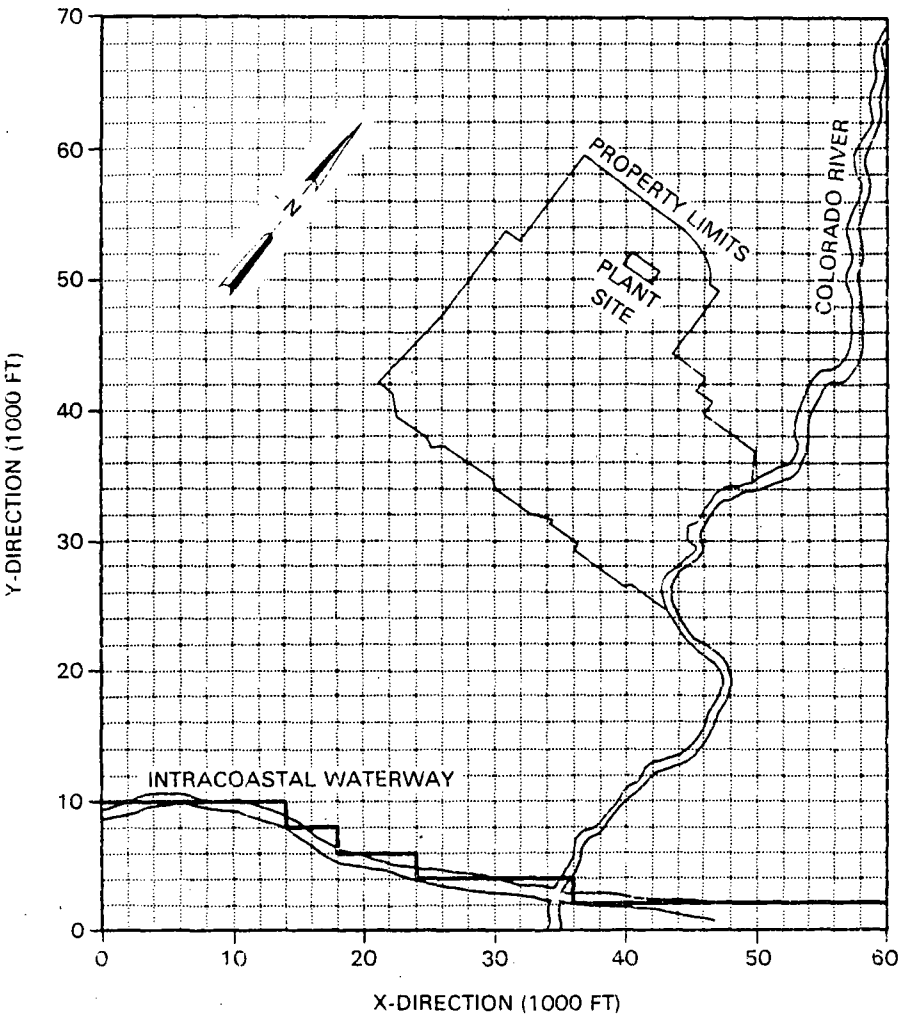

FIGURE 6.3.2-8. Complete Grid for the STP Regional Study Area

For the purposes of constructing the STP conceptual and numerical models it was necessary to determine the type and location of the aquifer boundaries for all four sides of the regional grid. The southern most boundary was assumed to be a head-controlled boundary coinciding with the Intracoastal Waterway. Tide gage records for the Waterway obtained from the USGS[a] indicate the mean tide level in the vicinity of Matagorda, Texas is approximately 1 foot MSL. The actual location of the 1 ft MSL constant head boundary is designated in Figure 6.3.2-8 by the heavy grid lines running along the Intracoastal Waterway.

Several of the observed contours of equal hydraulic head were extended the breadth of the regional grid. The contour extensions were based primarily on

(a) Letter from Robert K. Gabrysch, Chief, Houston Subdistrict, U.S. Geological Survey to Richard Skaggs, PNL.

the shape of the observed contours and additional facts such as the existence of a line of flowing wells at an approximate surface elevation of 6 ft MSL and an apparent ground-water mound in the center of the grid. Using the observed and estimated contours shown in Figure 6.3.2-9, hydraulic heads were estimated for each node in the regional grid using a 16-direction, steepest gradient, liner interpolation procedure. The results of the interpolation are presented in Figure 6.3.2-10, and designated as the "observed potential contours" for the STP regional area. Inspection of the interpolated contours shows an almost

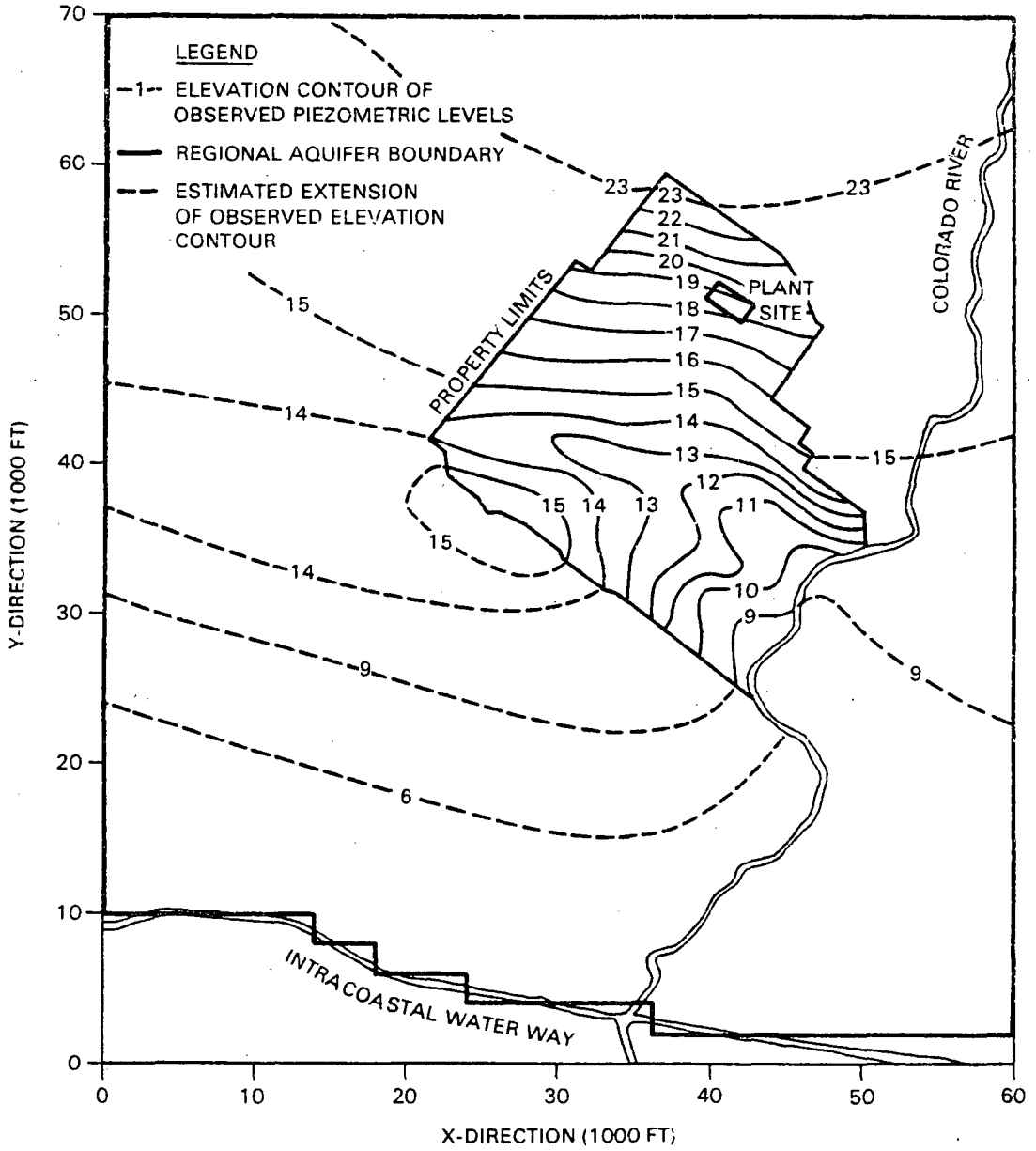

FIGURE 6.3.2-9. Observed and Estimated Potential Contours for STP Regional Study Area

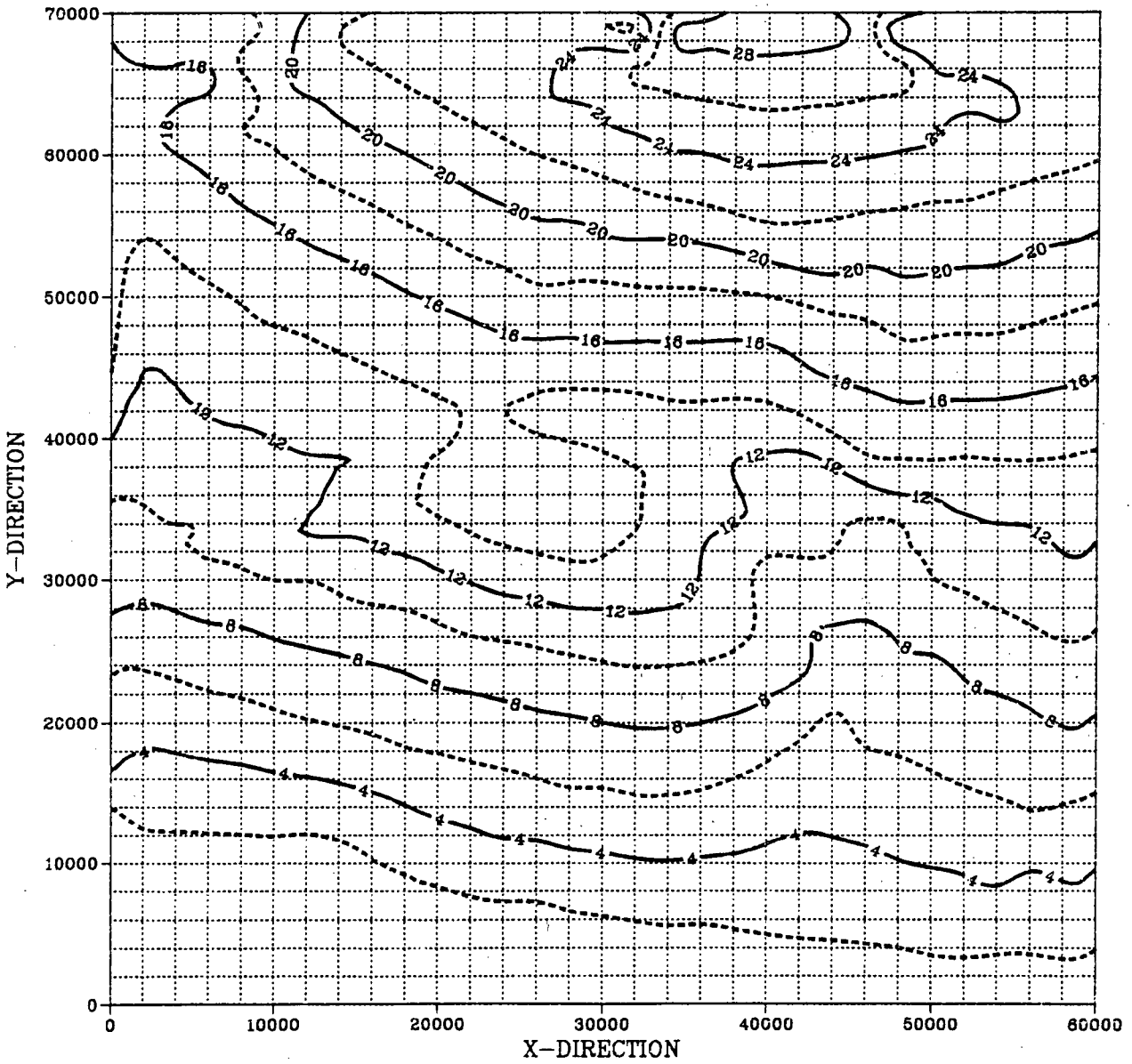

FIGURE 6.3.2-10. Observed Potential Contours for the STP Regional Area

exact match with the observed and estimated contours. However, due to the interpolation scheme used and the relatively large area over which the interpolation was made, minor peculiarities were produced. The 24, 26 and 28 foot contours appear to be closed indicating a ground-water mound that most likely does not exist. Also, the 12, 14, and 16 foot contours near the western edge of the area incorrectly bend upward. In both instances the net effect on the overall flow field, particularly in the vicinity of the STP site, is insignificant.

Inspection of the observed potentials shows that near the east and west grid boundaries the contours are approximately perpendicular to the y-direction. In the model, these boundaries are assumed to be head-controlled boundaries having constant head values equivalent to those shown in Figure 6.3.2-10.

The northern-most boundary is assumed to be a flow-controlled boundary where the head and flow at the boundary will be determined by the model.

6.3.2.5 Aquifer Thickness and Lateral Extent

Typically, the lateral extent and thickness of an aquifer vary considerably from one place to another. Fluvial basin aquifers commonly thin toward the rim of the basin while some basins show structural deformation due to downwarping and faulting. The primary sources of data for delineation of aquifer lateral extent are generally well and bore logs, and existing geologic maps. From these data, the aquifer top and bottom elevations are determined and the aquifer thickness calculated as the difference between the two.

The primary sources of information for the STP site were well and bore logging data presented in the STP FSAR (Houston Power and Light 1978). Useful information was also obtained from Hammond (1969). Over 100 oil or gas well electric logs, water well drilling logs, and soil borings were identified in the STP FSAR (Houston Power and Light 1978). Though the actual data from the logs and boring were not available for this study, three geohydrologic cross-sections interpreting the data were presented in the STP FSAR (Houston Power and Light 1978). Two cross-sections are shown in Figure 6.3.2-11 while the third is presented in Figure 6.3.2-3 above. The approximate locations of the three cross-sections relative to the STP site are indicated in Figure 6.3.2-12. It is clear from the figure that only a limited portion of the cross-sections extend outside the STP property limits. Therefore, for modeling purposes, it was necessary to infer from the cross-sections the top and bottom elevations of the lower unit for the study area.

The basic approach to accomplishing this is to compute values for the aquifer top and bottom at the node points of the regional grid using a fifth-degree polynomial interpolating function developed by International Mathematical and Statistical Libraries, Inc. (IMSL), (1980). Contour and surface maps showing the interpolated results for the top and bottom elevations are presented in Figures 6.3.2-13 and 6.3.2-14, respectively. The (0,0) coordinate for both figures corresponds to the lower left hand corner of the study grid.

To summarize data presented thus far, the conceptual model for the STP case study consists of the lower unit of the shallow zone aquifer. The lower unit is a confined or semi-confined aquifer that extends continuously over the study area. The aquifer interfaces at its bottom with the very low permeability deep confining zone and at its top with a zero or low permeability layer segregating the lower unit from the upper unit of the shallow aquifer.

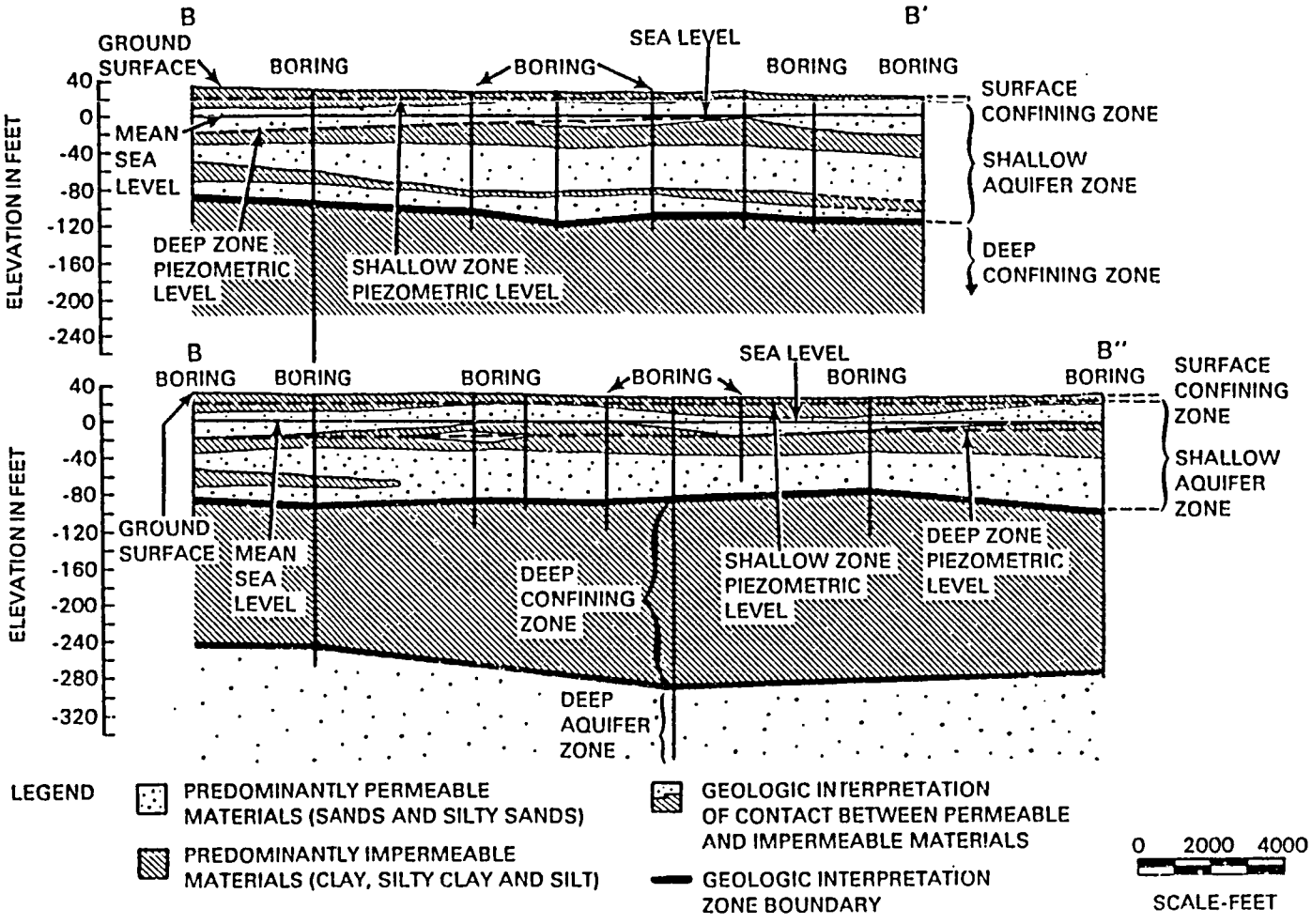

FIGURE 6.3.2-11. Geohydrologic Cross-Sections B-B' and B-B" for the STP Site (Source: Houston Power and Light 1978)

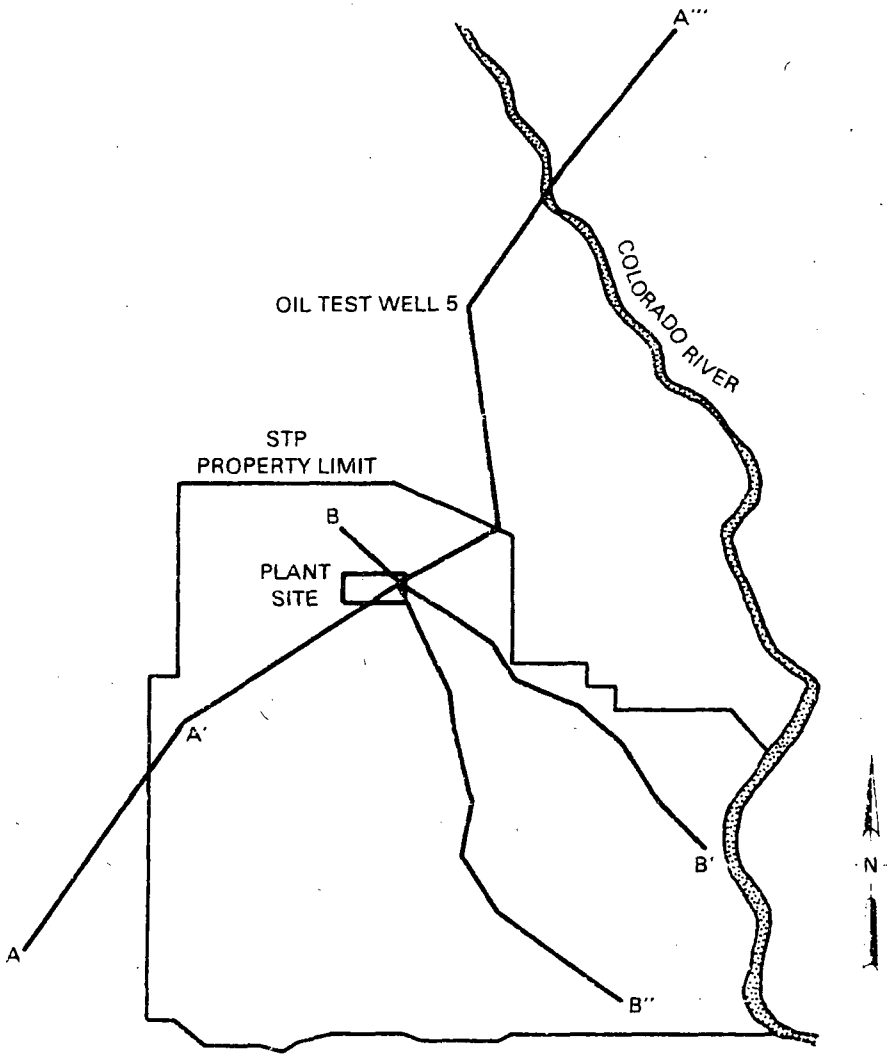

FIGURE 6.3.2-12. Locations of the Geohydrologic Cross-Section A-A''', B-B' and B-B'' (Source: Houston Power and Light 1978)

The bottom of the aquifer varies from approximately -60 feet mean sea level (MSL) to -120 feet MSL. Similarly, the top varies from about -30 feet MSL to -60 feet. Both the aquifer top and bottom dip from the northwest to the southeast which is consistent with the slope of the underlying Beaumont Formation as described by Hammond (1969). The thickness of the lower unit varies from about 28 feet to 62 feet. An overlay of the lower unit aquifer top and bottom illustrating the spatial distribution of the thickness is presented in Figure 6.3.2-15.

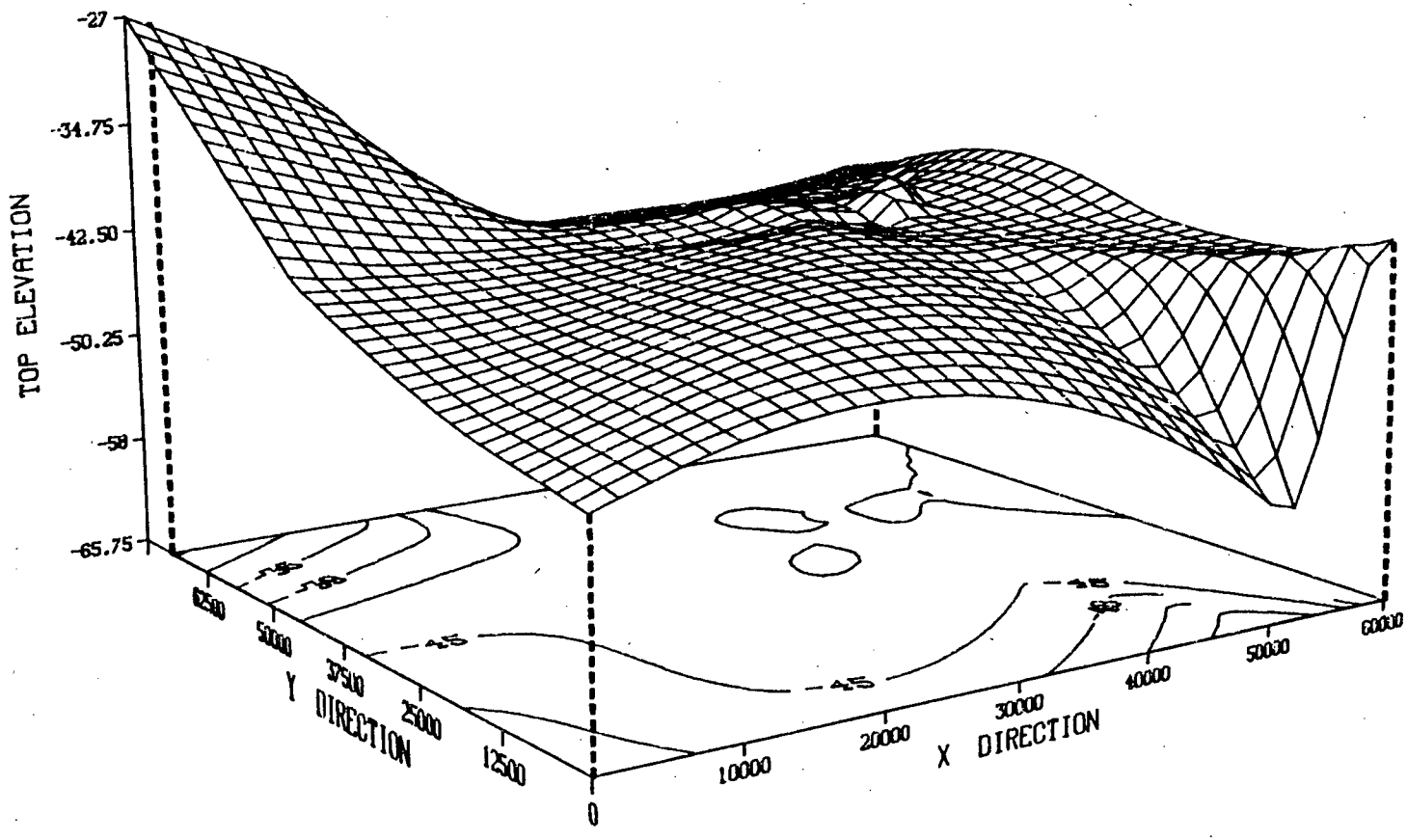

FIGURE 6.3.2-13. Top Elevation Contour and Surface Maps for the Lower Unit of the Shallow Aquifer Within the STP Regional Study Area

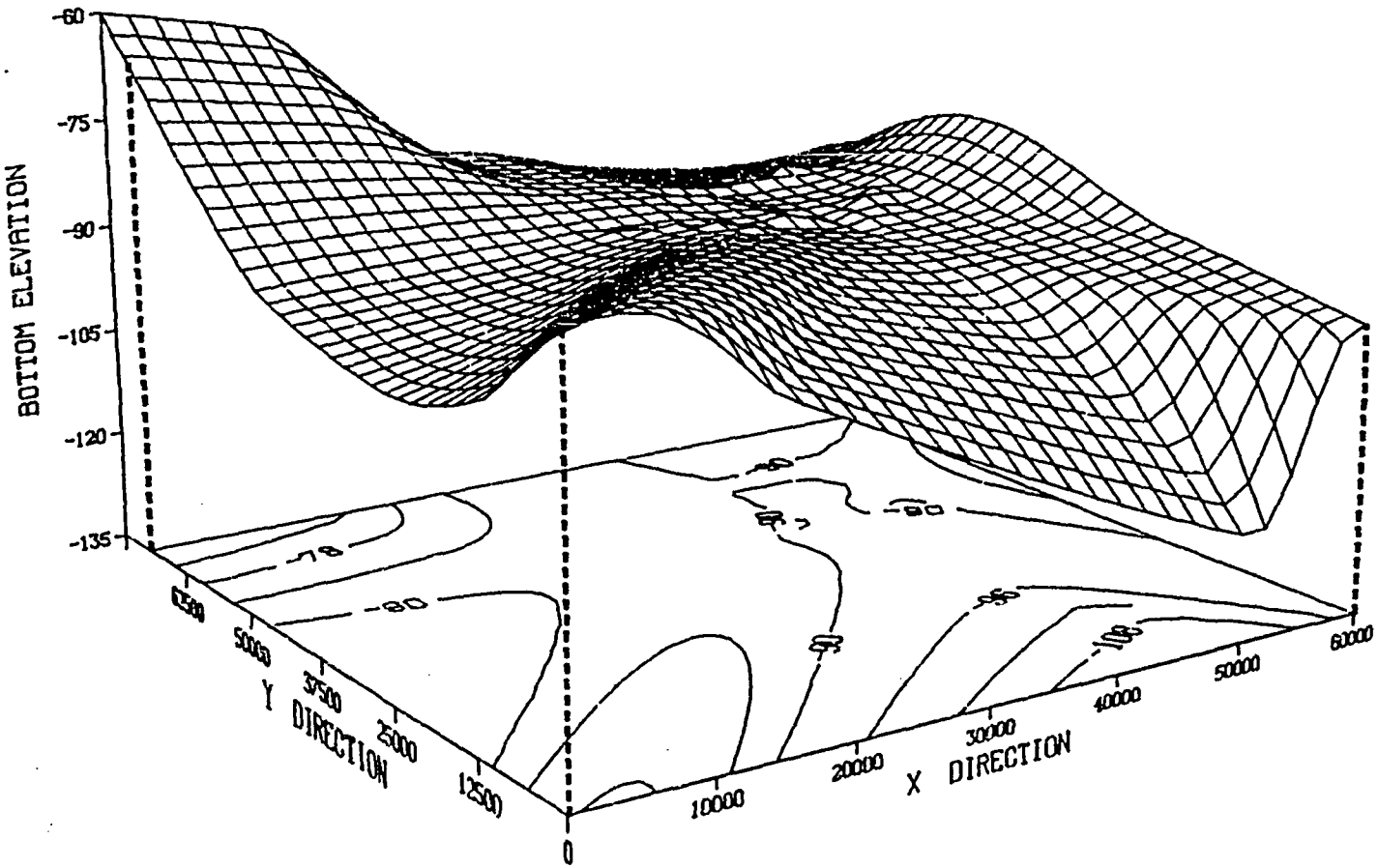

FIGURE 6.3.2-14. Bottom Elevation Contour and Surface Maps for the Upper Unit of the Shallow Aquifer Within the STP Regional Study Area

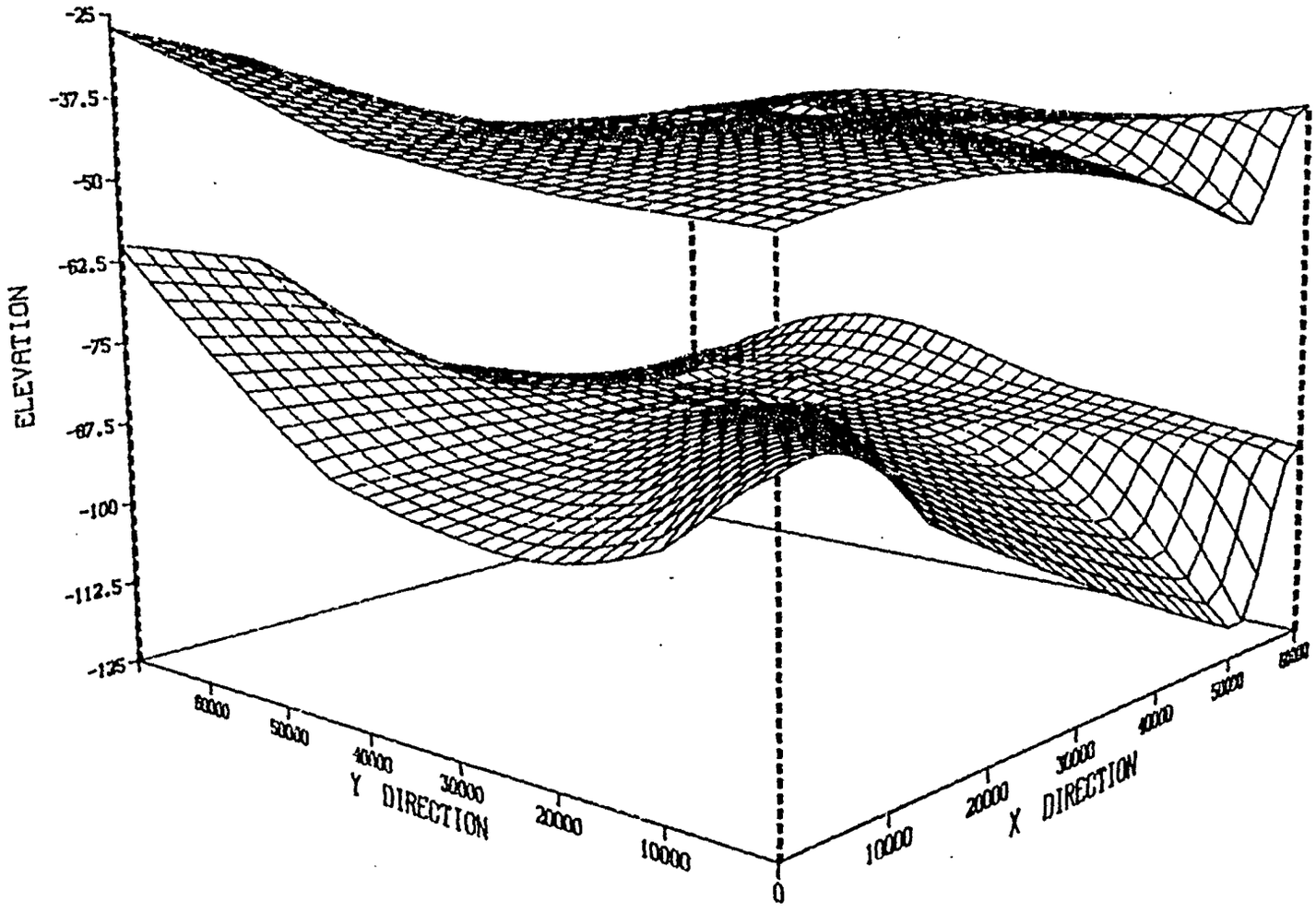

FIGURE 6.3.2-15. Overlay of the Top and Bottom Elevations for the Lower Unit of the Shallow Aquifer Within the STP Regional Study Area

6.3.2.6 Porous Media Hydraulic Properties

The magnitude and spatial distribution of a number of material properties must be specified for the aquifer under study. Table 6.3.2-3 presents some of the required properties for each of the aquifer types (Boonstra and de Ridder 1981). A variety of field, laboratory and numerical methods have been developed to determine the different hydraulic properties. For discussions of the various methods, the reader is referred to Bentall (1963), Krusemand and de Ridder (1970), Office of Water Data Coordination (1977) and Boonstra and de Ridder (1981).

The data and information concerning the hydraulic properties for the lower unit of the shallow aquifer zone were compiled primarily from the results of four pumping tests conducted in the shallow zone within the STP property limits (Houston Power and Light 1978). The depths of the tests and the test results are summarized in Table 6.3.2-4.

Based on the test depths, pump test 3 most likely measures the conditions in the upper unit while the remaining test depths coincide with the lower unit. Therefore, hydraulic conductivities in the lower unit are in the range of 400 to 600 gpd/ft^2 while storage coefficients vary from 0.00045 to 0.0007.

TABLE 6.3.2-3. Required Porous Media Hydraulic Properties

Property	Aquifer Type		
	Confined	Unconfined	Semi-Confined
Hydraulic Conductivity, K	X	X	X
Hydraulic Conductivity for Overlying Confining Layer, K'			X
Storage Coefficient, (for transient simulation only), S	X		X
Specific Yield, μ		X	
Porosity, n	X	X	X
Effective Porosity, n_e	X	X	X

X designates required property.

TABLE 6.3.2-4. Aquifer Test Summary (Source: Houston Power and Light 1978)

Pump Test Number	Test Depth (ft)	Transmissivity (gpd/ft)	Hydraulic Conductivity (gpd/ft^2)	Storage Coefficient
1	60-140	33,000	410	0.00071
2	59-83	13,000	600	0.00045
3	20-43	1,100	65	0.0017
4	30-45	10,500	420	0.0007

Additional information regarding hydraulic properties related to analyses of accidental radionuclide releases in the lower aquifer unit is presented in the STP FSAR (Houston Power and Light 1978). For the analysis discussed, the following properties were assumed:

- hydraulic conductivity 635 gpd/ft^2
- porosity: 37%.

Complementing the information obtained from the STP FSAR, Hammond (1969) describes the hydraulic characteristic of the Gulf Coast aquifer. Though Hammond's discussion emphasizes the heavily pumped deep aquifer zone, the information provides a framework for evaluating the FSAR pumping tests data. Pumping tests in Matagorda County and surrounding areas provide values of hydraulic conductivity for the sands of the Gulf Coast aquifer ranging from 103 to 3,950 gpd/ft^2 and averaging about 570 gpd/ft^2. Generally, the deeper sands, because of increased compaction and cementation, have lower hydraulic conductivities. Table 6.3.2-5 presents the results of the pump tests for the two wells in Matagorda County that are partially screened in the lower unit aquifer. The transmissivities for both wells are relatively high compared to 70,000 gpd/ft average value for the deeper wells.

The hydraulic conductivity value in Table 6.3.2-5 is also much higher than the pump test results presented in the FSAR (Table 6.3.2-4). This is explained in part by Hammond's observation that lower permeabilities are generally found near the coast due to finer grain size sediments. The sands away from the coast are part of the Colorado River alluvial deposits and tend to have coarser size distributions.

The storage coefficients of the STP pump tests 1, 2, and 3 were in the neighborhood of 5×10^{-4} to 7×10^{-4} (Houston Power and Light 1978). The single value for storage coefficient shown in Table 6.3.2-5 is similar in magnitude, having a value of 1.1×10^{-3}. These values are typical for a confined aquifer and confirm the conceptual model based on bore logs.

The values for porosity provided by Hammond (1969) are representative ranges for sedimentary material. These are presented below in Table 6.3.2-6. On the basis of the values shown, the value for porosity of 37% assumed in the

TABLE 6.3.2-5. Pump Test Results for Wells in Matagorda County (Source: Hammond 1969)

Well Number	Date	Screened Internal (ft MSL)	Hydraulic Conductivity (gpd/ft^2)	Transmissivity (gpd/ft)	Storage Coefficient
TA-65-58-107	10-04-66	75-202	---	176,000	1.1×10^{-3}
TA-65-58-803	05-01-66	91-215	3,950	399,000	---

TABLE 6.3.2-6. Representative Porosities for Sedimentary Material (Source: Hammond 1969)

Material	Porosity, %
Soils	50-60
Clay	45-55
Silt	40-50
Medium to coarse mixed sand	35-40
Uniform sand	30-40
Fine to medium mixed sand	30-35
Gravel	30-40
Gravel and sand	20-35
Sandstone	10-20
Shale	1-10

FSAR (Houston Power and Light 1978) is within the range for medium to coarse mixed sand (35-40%) and uniform sand (30-40%). The assumed value is slightly outside the 30% to 35% range for the fine to medium mixed sand.

6.3.2.7 Hydraulic Head (Ground-Water Potential)

Generally, a ground-water basin experience a number simultaneously occurring of hydrologic stresses (Boonstra and de Ridder 1981). These stresses include: infiltration of rainfall and/or irrigation water, streambed percolation, evapotranspiration, ground-water discharge by streams or springs and well pumpage. At any given time, the combined effects of the stresses are reflected in the configuration and fluctuation of the basin hydraulic heads. Consequently, the collection and evaluation of watertable data are important parts of ground-water model development (i.e., calibration by history matching). Simulated hydraulic heads are compared with measured values to ensure the ground-water model is representing the various stresses that are being exerted on the basin. The data requirements for quantifying the hydrologic stress and the results obtained for the STP site are discussed below.

The magnitude and distribution of the hydraulic head within a basin and at the boundaries are determined by observation wells and/or piezometers. For confined and unconfined aquifers, only observation wells screened in the aquifer of study are required. In a semi-confined aquifer, however, hydraulic head measurements are required in the study aquifer as well as in the aquifer overlying the permeable confining layer. Though not used directly, the heads for the overlying aquifer are required to compute recharge/discharge through the confining layer. Under normal conditions, the observation wells should be measured periodically (dependent on local conditions) for one to two years to establish temporal hydraulic head level fluctuation trends.

The results of the water level measurements are best presented in the form of maps of equal contours of hydraulic hgeads, hydrographs, and, if applicable, head-difference maps. The necessary map(s) must be generated for the beginning of the study period to establish the initial conditions for the basin. If sufficient change in the head contours occurs within the basin over time due to recharge, discharge, pumping, etc., then maps are also needed for each successive time period chosen for modeling. If steady-state conditions are assumed for the basin, the model is calibrated only for the specified initial conditions. For a semi-confined aquifer, two hydraulic head contour maps must be drawn; one for the study aquifer and one for the aquifer above the confining layer.

At the STP site, hydraulic head data are limited to those available in the STP FSAR (Houston Power and Light 1978). Contours of the observed data for the lower and upper units of the shallow aquifer zone are presented in Figures 6.3.2-5 and 6.3.2-6. As discussed in Section 6.3.2.4, the contours were extrapolated over the study region based upon the available information. The results of this process for the lower unit are presented in Figure 6.3.2-10. The same procedure is followed to extrapolate data for the upper unit. Since the available data are limited to measurements taken on a single day (i.e., May 14, 1974 from the upper unit and November 8, 1973 for the lower unit) the following assumptions are made:

1. post-construction potential levels rebounded to those measured,
2. steady-state conditions prevail in the upper and lower unit aquifers, and
3. the measured data are representative of steady-state conditions.

The primary reason for making these assumptions is that the data required to characterize dynamic conditions within the basin and the efforts of construction were unavailable.

The main source of temporal change within the basin is the Colorado River which under normal conditions can experience stage changes of up to 10 feet within a given year. Figure 6.3.2-16 shows the response of the Colorado River to typical rainfall period in 1973 and the associated response of the lower and upper units of the shallow aquifer zone. It can be seen that the response of the lower unit is attenuated significantly compared to that of the upper unit. With regard to the first assumption, the single greatest potential effect is due to construction of the Cooling Reservoir (see Figure 6.2.2-1).

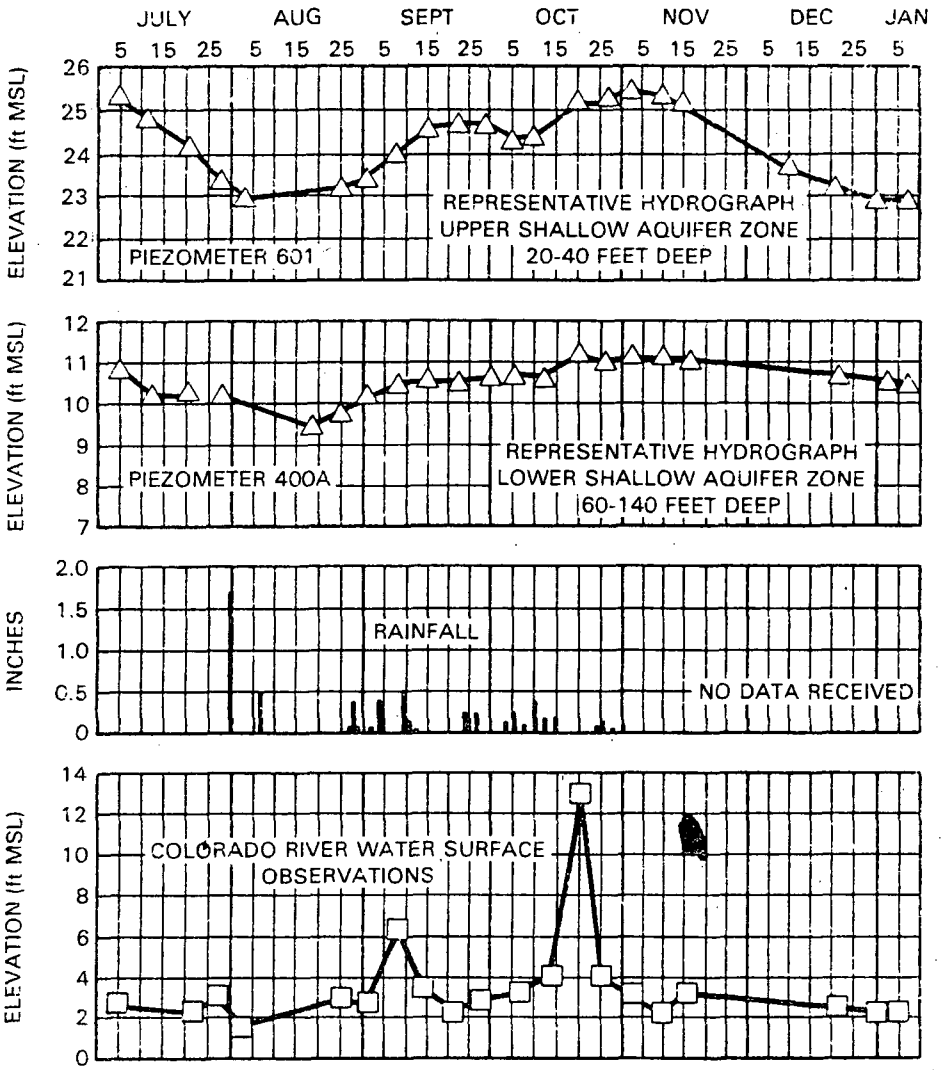

NOTES:

1. RIVER LEVEL MEASUREMENTS MADE AT FM ROAD 521 BRIDGE APPROXIMATELY TWO MILES EAST OF SITE.
2. RAINFALL MEASUREMENTS FROM SOUTH TEXAS PROJECT METEOROLOGICAL TOWER.

FIGURE 6.3.2-16. 1973 Water Level Observations in the Vicinity of the STP Site (Source: Houston Power and Light 1978)

As stated in the STP FSAR (Houston Power and Light 1978), the normal maximum operating level for the Cooling Reservoir is 49 feet MSL which is over 20 feet above the surrounding ground surface. Thus, seepage from the Cooling Reservoir will tend to raise local ground-water potentials. However, the reservoir embankment is designed to use compacted fill, to insure that the piezometric levels of the soil in the plant area remain below the ground surface. Since pre-construction levels in the upper aquifer were 2 to 3 feet below the ground surface, this would indicate the ground-water mounding will be less than 2 to

3 feet. Further, since the seepage from the Cooling Reservoir will discharge directly into the upper unit, the effect in the lower unit will be limited to the increased leakage that will occur due to the higher hydraulic head.

From the above discussion, it is apparent that changes in hydrologic stresses with time and changes due to the STP construction will modify the potentials measured for the upper and lower units of the shallow aquifer. However, based on the evidence presented it appears that the effects of these changes are not severe in the lower unit. Therefore, in light of the stated objectives of the case study, the limitations associated with making the stated assumptions regarding the use of available hydraulic head data are considered acceptable by the authors.

6.3.2.8 Aquifer Recharge/Discharge

A key element of any ground-water study is the estimation of the type and magnitude of aquifer recharge/discharge. For the case of unconfined aquifers Freeze and Cherry (1979) define ground-water recharge as the entry of water into the saturated zone at the water table surface accompanied by flow away from the watertable within the saturated zone. Unconfined aquifers having a deep watertable can be recharged by rainfall percolation, streambed percolation and percolation of irrigation water. In confined aquifers, recharge in the strict sence occurs along the rim of the basin where the aquifer intersects the land surface. In a manner similar to that for unconfined aquifers, the sources of recharge at the confined aquifer outcrop are rainfall percolation, streambed percolation and surface runoff from adjacent areas. Another important source of recharge for semi-confined aquifers may be water flow through over- or under-lying confining layers.

Freeze and Cherry (1979) similarly define discharge as the removal of water from the saturated zone across the watertable surface accompanied by flow within the aquifer toward the watertable surface. In both confined and unconfined aquifers, discharge can occur as spring flow, seepage into streams, evapotranspiration and through underlying or overlying confining layers.

The delineation of recharge and discharge areas may require information on topography, surface and subsurface geology, and climate. If the aquifer is semi-confined and exchange of water between aquifers occurs, data on hydraulic potential surfaces is necessary. Several methods can be used to estimate aquifer recharge and discharge. Examples include computations using Darcy's equation or analysis of measured stream flow hydrographs. These and others are described by Boonstra and de Ridder (1981).

According to the STP FSAR (Houston Power and Light 1978), recharge of the shallow-zone aquifer probably occurs within a few miles north of the site. The available data indicate that the upper confining layer prevents any appreciable recharge within or to the south of the site. Consequently, analysis of recharge for the lower unit of the shallow aquifer is limited to seepage from the upper unit. Discharge from the lower unit, as discussed previously regarding boundary conditions, is assumed to occur at the Intracoastal Waterway and

by vertical seepage, particularly at the Colorado River. The recharge and discharge of the lower unit were calculated by applying a form of Darcy's equation (Freeze and Cherry 1979):

$$Q = -K' \frac{(h - h')}{m'} \Delta x \, \Delta y$$

where

Q = recharge/discharge rate (gpd)
K' = vertical hydraulic conductivity in confining bed (gpd/ft)
h = hydraulic head in aquifer (ft MSL)
h' = hydraulic head in covering layer (ft MSL)
m' = thickness of confining bed (ft)
Δx = x-dimension of regional grid elements (ft)
Δy = y-dimension of regional grid elements (ft).

A negative value for (h - h') indicates flow of water into the lower unit. Conversely, a positive value signifies water is being discharged by the lower unit as vertical upward seepage.

The initial evaluations of recharge and discharge were computed at each node of the regional grid based upon an assumed uniform vertical hydraulic conductivity, the previously determined potentials for the upper and lower units of the shallow aquifer, values of the confining layer thickness interpolated from the available geohydrologic cross-sections, and the values of Δx and Δy determined directly from the regional study grid. The vertical hydraulic conductivity was initially set at 0.005 gpd/ft^2 based on the range of 0.01 gpd/ft^2 to 0.00001 gpd/ft^2 provided by Freeze and Cherry (1979) for unconsolidated, unweathered marine clay. The result of the initial evaluation was a net recharge to the aquifer of 1.6×10^6 gpd or 3.7×10^{-4} gpd/ft^2 of aquifer.

According to Hammond (1969), in some parts of Matagorda County, available data indicate that sands in the deep zone aquifer are replenished by water from overlying shallower sands through the bore holes of idle water wells. Obviously, this is not directly accounted for in the recharge/discharge analyses. If this represents a significant form of water loss which has affected observed potentials, it will ultimately be reflected in the model through the calibration procedure by reducing the recharge from the overlying unit to achieve the necessary water balance. Another possibility not accounted for is downward vertical seepage from the lower unit shallow aquifer to the deep zone aquifer. Though there is significant head differential between the two aquifers, as much as 30 feet, it is believed that the 100 to 200 foot thick deep confining zone would limit the seepage to insignificant levels.

Hammond (1969) reports that most of the irrigation, public supply and industrial wells in Matagorda County produce water from the 200 to 700 foot depth interval. Due to the high salinity of the shallow zone aquifer, only minor pumpage for some domestic and livestock wells produce from shallower depths. A summary of estimated 1973 ground-water usage within a 10-mile radius of the STP site is shown in Table 6.3.2.7 (Houston Power and Light 1978). The total 130 acre-ft/yr withdrawal from the shallow-zone aquifer, equivalent to

TABLE 6.3.2.7. Summary of Estimated 1973 Ground-Water Use in the Vicinity of the STP (Source: Houston Power and Light 1978)

Ground-Water Use	Total Wells in Operation		Estimated Pumpage (acre-ft/yr)	
	Shallow Aquifer Zone	Deep Aquifer Zone	Shallow Aquifer Zone	Deep Aquifer Zone
Irrigation	-	17	-	1,750
Industrial	-	1	-	160
Public and Municipal	-	7	-	100
Stock and Domestic	49	69	100	140
Drilling Supply	1	1	30	30
TOTAL	50	95	130	2,180

1.2×10^5 gal/day, is less than 7% of the computed net recharge rate. The pumpage was not directly accounted for in developing the ground-water model of the lower unit of the shallow aquifers.

6.3.2.9 Conceptual Model

The preceding sections describe a majority of the data obtained and analyzed for the STP case study. In the sections following, the numerical model development, calibration and simulations are presented. The bridge linking the two efforts is the conceptual model of the ground-water flow system that determines transport of radionuclide releases due to a postulated severe accident at the STP site.

A conceptual model, defined by Simmons and Cole (1985) is the modeler's perception of the physical behavior of a ground-water system. Conceptual model development is simply the process by which a preliminary description and understanding of a ground-water system is obtained based on available data, experience and fundamental hydrologic principles. The conceptual model thus becomes, a simplified composite picture of what is known about the study area, hydrogeologic boundaries and boundary conditions, geologic and stratigraphic layers, ground-water flow directions and quantities, flow barriers, recharge/discharge areas, time dependencies of the flow system, etc.

A general rule suggested by Simmons and Cole (1985) for developing a conceptual model is: "a model should be made as simple as possible and only the detail necessary to explain the available data and observed phenomena relevant to the study objectives should be included." Further, as depicted in Figure 6.3.1-1, development of the conceptual model is a continuing process that

occurs parallel to the numerical model development. As new data and new understanding about the system are gained, the conceptual model is updated as required throughout the study.

The objective of the STP case study requires the development a ground-water model to simulate the transport of radionuclides released by a severe accident. Given the postulated accident scenario, it is assumed the molten reactor core mass would ultimately rest approximately 35 ft below the STP containment building basemat within the lower unit of the shallow-zone aquifer. On the basis of this assumption, development of the conceptual model focused on the lower unit. The key features of the conceptual model are listed below and illustrated in Figure 6.3.2-17:

- The lower unit of the shallow-zone aquifer is a semi-confined aquifer situated between the deep confining zone and a semi-permeable confining layer that divides the shallow aquifer.

- The general flow direction within the lower unit of the shallow aquifer is the southwest toward Matagorda Bay, its primary discharge point.

- From available lower unit aquifer tests the average hydraulic conductivity is assumed to be 600 gpd/ft^2. The vertical hydraulic conductivity through the upper confining layer is assumed to be 0.005 gpd/ft^2.

- The lower unit aquifer top ranges in elevation from approximately -30 ft MSL to -60 ft MSL, the bottom varies from -60 ft MSL to -120 feet MSL, and its from 30 to 60 ft thick.

- Over most of the study region, the lower unit aquifer receives recharge as vertical seepage from the upper unit aquifer. The exception to this, where discharge occurs, is just west of the river all the way to the east study boundary. Within the study region, the net recharge to the lower unit is estimated to be 1.6 x 10^6 gpd.

6.4 REGIONAL MODEL DEVELOPMENT

A two-stage modeling approach is used to characterize the ground-water system at the STP site. The first stage consists of developing a coarse grid regional hydrologic flow model, whereas the second stage involves developing flow and contaminant transport models for the immediate vicinity of the STP site.

The purpose of the regional model is to establish boundary conditions for the local model. The local model then simulates the ground-water system in the immediate area of the plant in greater detail. The usual procedure for determining boundary conditions is to extend the regional model from the area of interest to where the conditions are known (i.e., constant head along a river, no flow along a ground-water divide, etc.). The problem, however, is that if one goes too far from the area of interest, the resolution around the area of

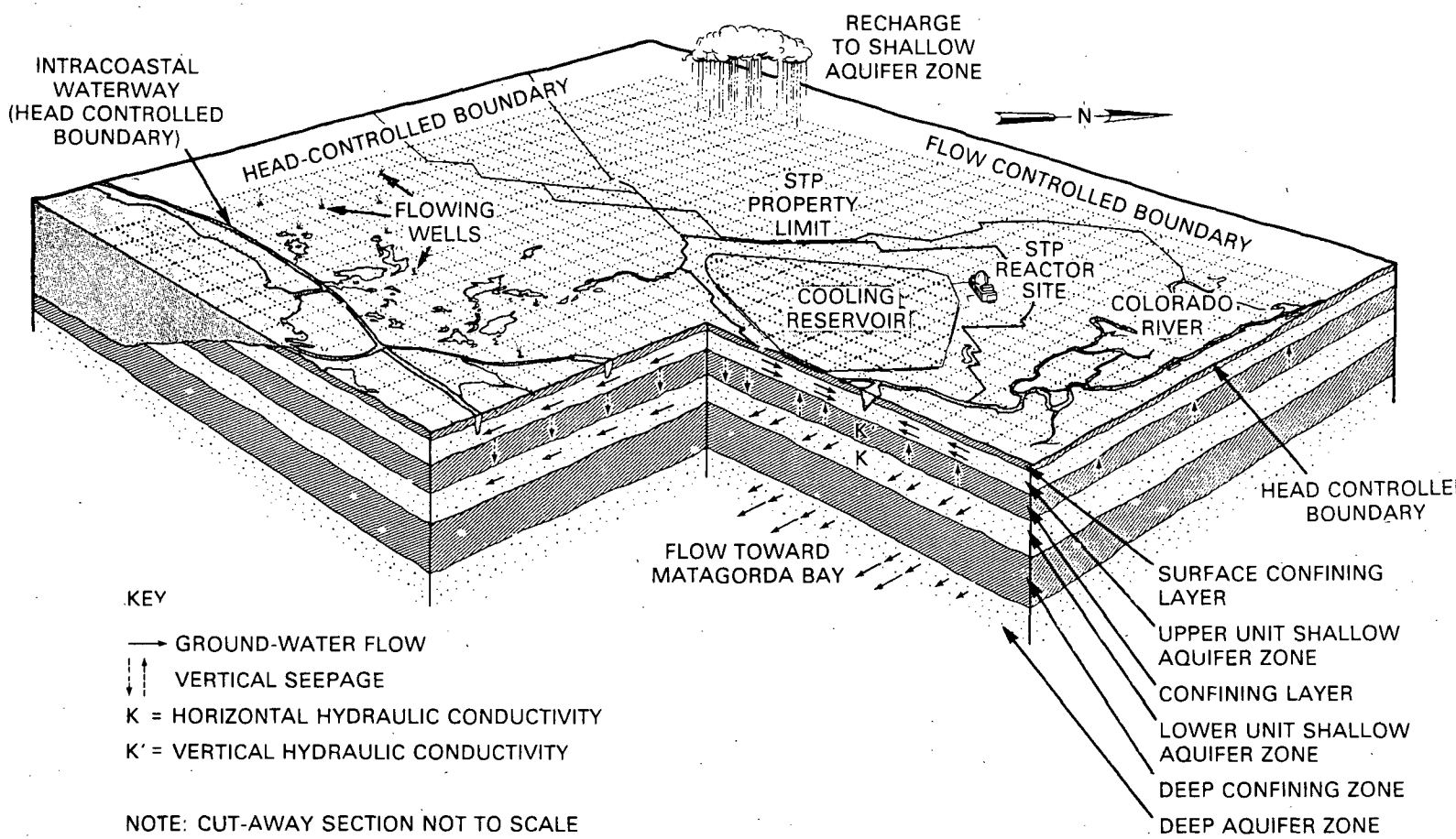

FIGURE 6.3.2-17. Illustration of the Conceptual Model for the STP Site

interest is reduced because of numerical model size restrictions (i.e., the number of nodes). This problem can be alleviated by using a two-stage modeling approach. The regional model should be coarse enough to enable its boundaries extend out to either where the hydrologic conditions were "known", and/or to where the boundary is far enough away that it would have little influence on the area of immediate interest (i.e., local model area).

Again, referring to Figure 6.3.1-1, and subsequent to data collection and initial conceptual model development, construction of a ground-water model involves three additional steps:

1. selection of an appropriate computer code,

2. preparation of data for model using determined parameters (Initial Model Development), and

3. compare results with observed data (Model Calibration).

6.4.1 Code Selection

A computer code is the numerical implementation of a set of equations that describe, in simplified form, the important physical processes acting within a ground-water system (Simmons and Cole 1985). Quite often and incorrectly, the computer code is said to be the model and model development is thought to be merely the selection of an appropriate code. However, the two processes are quite distinct. There are a number of different codes that may solve the same equations; but selecting an appropriate code for the analysis of a site specific ground-water flow and transport problem requires analyses of several factors. It is unlikely that there is a "best" code for all study purposes and objectives. For example, a code that is appropriate for flow in a porous medium may be totally inappropriate for similar analyses in a fractured environment. Codes should be selected on the basis of demonstrated numerical accuracy and faithful description of the dominant physical processes. Further, the selected code should have the necessary regional simulation capabilities (e.g., representation of spatial variations in hydraulic conductivity).

Preliminary code selection for the STP case study is based on a study of available ground-water flow and transport code capability summaries (Kincaid et al. 1983). The specific criteria used in the final code selection include:

Is the theoretical basis of the code technically sound, is it well documented, and has it been previously implemented and verified?

Does the code simulate the dominant hydrologic and transport processes identified in the preliminary STP conceptual model?

Does the code provide for varying structure of the hydrologic flow and transport system?

Will the code accept spatially varying parameters (e.g., hydraulic conductivity, transmissivity, etc.)?

- Can the code accept the appropriate boundary conditions (head-controlled and flow-controlled), interior impermeable boundaries, recharge, and withdrawal/injection?

From the results of the review, the TRANS code was selected for use in the STP case study local and regional modeling. TRANS is an extensively documented, generalized computer code which simulates the effects of convection, dispersion and to a limited extent, chemical reaction. Ground-water flow is computed using a variable grid, finite difference formulation. Solutions are included for nonsteady/steady flow problems in heterogeneous aquifers under confined, unconfined or leaky aquifer conditions. The code also accounts for time-varying withdrawal and injection, ground-water recharge and evapotranspiration. The solute transport portion of the code is based on a Lagrangian particle technique for the convective mechanisms and a random-walk technique for the dispersion. With its many features, TRANS provides the means to evaluate the performance of both active and passive interdiction methods that may be implementable at the STP with reasonable accuracy and efficiency. For a detailed description of the code formulations, the reader is referred to Prickett and Lonnquist (1971), and Prickett, Naymik and Lonnquist (1982). The basic equations for flow and transport in the TRANS code are described in Appendix C.

6.4.2 Initial Regional Model Development

Development of the initial ground-water model is essentially the process of translating the conceptual model into a discretized form consistent with the input format of the selected code. This process can be streamlined considerably if in the data collection and analysis stage of the study, the need for discretization is anticipated. If so, the data analysis can be done node by node and the results converted directly into the appropriate code format. Such was the case in constructing the conceptual model for the lower unit of the shallow zone aquifer at the STP site. All aquifer system parameters that required spatial discretization were discretized using the previously selected regional grid (Figure 6.3.2-8). The primary TRANS input data requirements and the source of the initial data values used are summarized in Table 6.4.2-1.

The results of the initial model steady-state simulation are presented in Figure 6.4.2-1 which shows the simulated potential contours. Comparison of the simulated potentials to the observed potentials, general slopes are similar and they match at the boundaries, (Figure 6.3.2-10), reveals quite a difference, even though general slopes are similar and they match at the boundaries. The observed ground-water mound just to the left of the grid center is missing in the simulated results. The observed low potential extending from the lower right corner of the grid toward the mound is also not simulated. In general, the simulated potentials on the left half of the grid are too high.

6.4.3 Regional Model Calibration

Before the initial model of the study area can be used to predict hydraulic potentials or contaminant concentrations resulting from implementation of various mitigative action alternatives, it must be calibrated.

TABLE 6.4.2-1. TRANS Input Requirements and Source of Data for Initial Regional Model

Parameter (Required for Each Node)	Source
Aquifer top and bottom elevations	Interpolated from available geohydrologic cross-sections
Hydraulic Conductivity, (K)	Uniform value (600 gpd/ft^2) selected from well test results
Storage Coefficient, (S)	Uniform value (0.00045) selected from well test results
Effective Porosity, (n_e)	Uniform value (0.37) from the STP FSAR
Actual Porosity, (n)	Uniform value (0.37); assumed n_e equals n for sandy aquifers
Vertical Hydraulic Conductivity for Confining Layer, (K')	Uniform value (0.005 gpd/ft^2) from Freeze and Cherry (1979)
Recharge/Discharge Rate	Computed directly from K' and aquifer thickness (top elevation minus bottom elevation)
Initial Hydraulic Heads	Observed potential contours

Calibration means that a check is made to determine how well the model can correctly generate the past behavior of hydraulic potentials (hydrologic flow model) and/or contaminant movement (contaminant transport model) as they are established from historical records. Adjustments are then made in model parameters until an acceptable re-creation of historical patterns is achieved.

The calibration procedure begins by selecting a period of time for which historical records are available. The required modeling information is then input to the model (as discussed in the previous section on initial model development) and an initial potentiometeric surface is calculated. The predicted values are then compared with values observed (measured) in the field for the period of historical record. Typically, there is a discrepancy between the simulated and the observed.

Because geologic and hydrologic information can be interpreted in a number of different ways, and because of inherent measurement errors which are incorporated in historical records or incompleteness in historical records, the input parameters must be adjusted to a certain extent. A re-evaluation of the hydrogeologic information and/or the historical records is required to formulate a new input data set for the model. The historical period is then

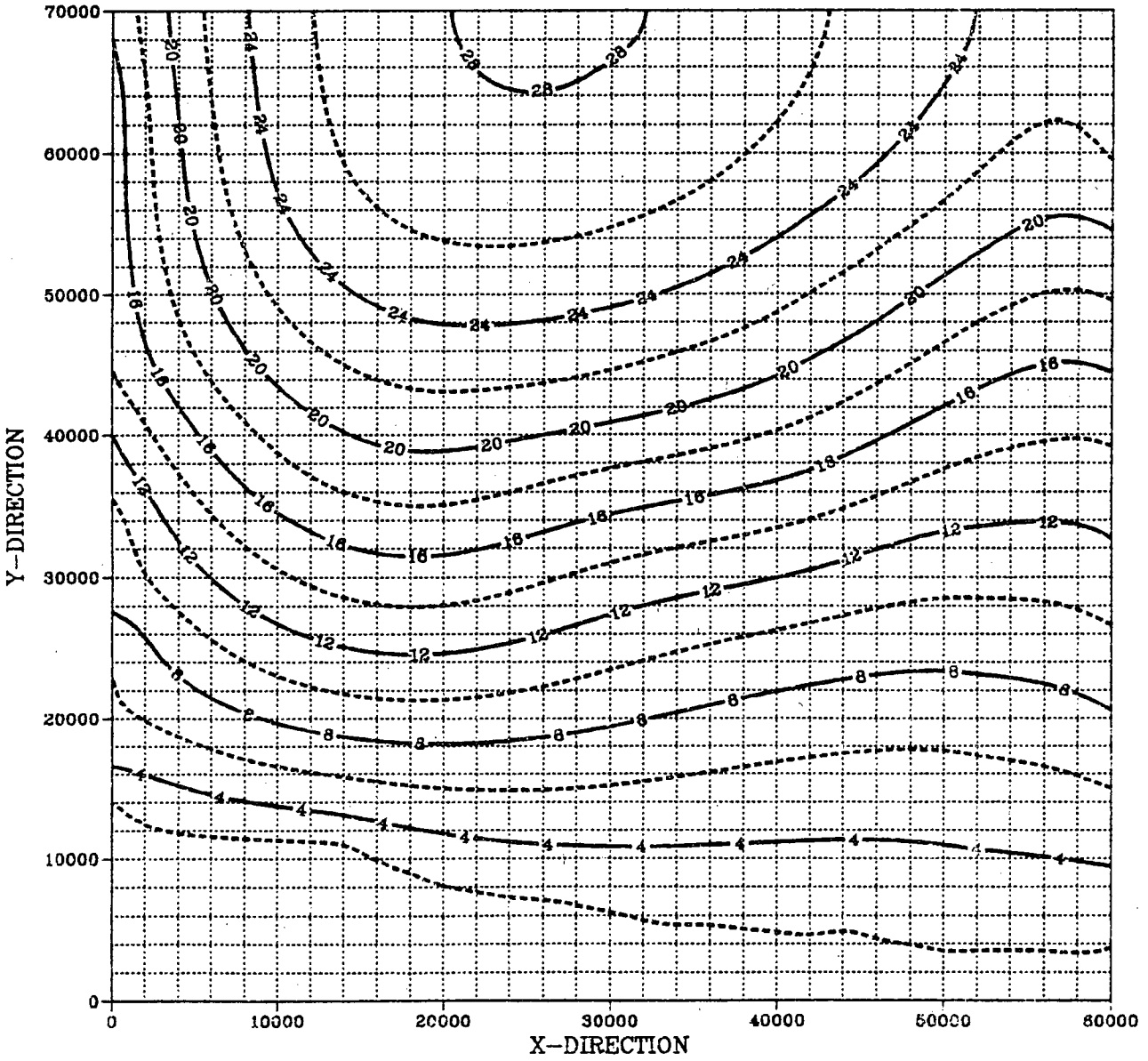

FIGURE 6.4.2-1. Potential Contours Simulated by the Initial STP Region Model

simulated with the new data set and the results compared to observed potentials. The process is repeated until an adequate fit of simulated results to observed behavior is reached.

At the STP site little data were available from available literature regarding the hydraulic potentials or the hydraulic properties of the lower unit of the shallow-zone aquifer. Because of the lack of data and associated

uncertainties adjustments must be made in the input data set in order to adequately calibrate the model. Because of these uncertainties the model is helpful in understanding the ground-water flow system. Many changes in parameter values can be made relatively quickly and inexpensively in the model. This facilitates comparison of model response to changes in parameter values and appreciation of model sensitivity to these changes. The adjustments made in the calibration process are based on refinements/improvements in the data set and in the understanding of the ground-water flow system. The model only indicates that changes are needed. It does not describe the changes. Arbitrary changes not supported by data or bound by understanding should be avoided.

It is often difficult to define a satisfactory match. Obviously, the longer the historical record of hydrologic measurements/observations used for calibration, the better the results will be. Since long-term hydrologic records are seldom available, models are usually calibrated with data covering only a relatively short time period. For example, at the STP site, because of data limitations it was necessary to calibrate the model to a single set of hydraulic potential measurements covering a limited portion of the study region.

Calibration is often the most difficult and one of the most time consuming aspects of ground-water modeling. However, calibration is of utmost importance. Depending on the desired accuracy and the difficulties experienced with scarcity of data, tens of runs can be required to obtain a satisfactory match. However, a model becomes a reliable prediction tool on which to base decisions once it is properly calibrated (Boonstra and de Ridder 1981).

The procedure used to calibrate the STP regional flow model was to run the initial model, compare observed with model-predicted results, make the appropriate changes in the initial data set and rerun the model. This process continued for a number of runs until an acceptable match between simulated hydraulic potentials and observed potentials was achieved. Because the available hydraulic potential data are limited, the focus in the calibration had to be duplication of the hydraulic head within the STP property limits.

The parameters adjusted in the regional model calibration process (i.e., those parameters to which were most sensitive) were the hydraulic conductivity, (K), and the recharge/discharge rates. After several iterations, an acceptable match was achieved between observed and model predicted potentials. The original hydraulic conductivities (i.e., uniformly 600 gpd/ft^2) were adjusted as shown in the three-dimensional plot presented in Figure 6.4.3-1. The relative adjustments made were guided by the differences in the observed potential contours and those simulated by the initial model. For example, simulation of the observed ground-water mound left (or west) of the study area center required relatively low hydraulic conductivities within and down-gradient of the mound (540 gpd/ft^2) and a high hydraulic conductivity immediately up-gradient of the mound (4200 gpd/ft^2). Similarly, the trough (i.e., low potential levels) in the lower right corner (or southeast) of the study area was simulated by increasing hydraulic conductivities to 2340 gpd/ft^2.

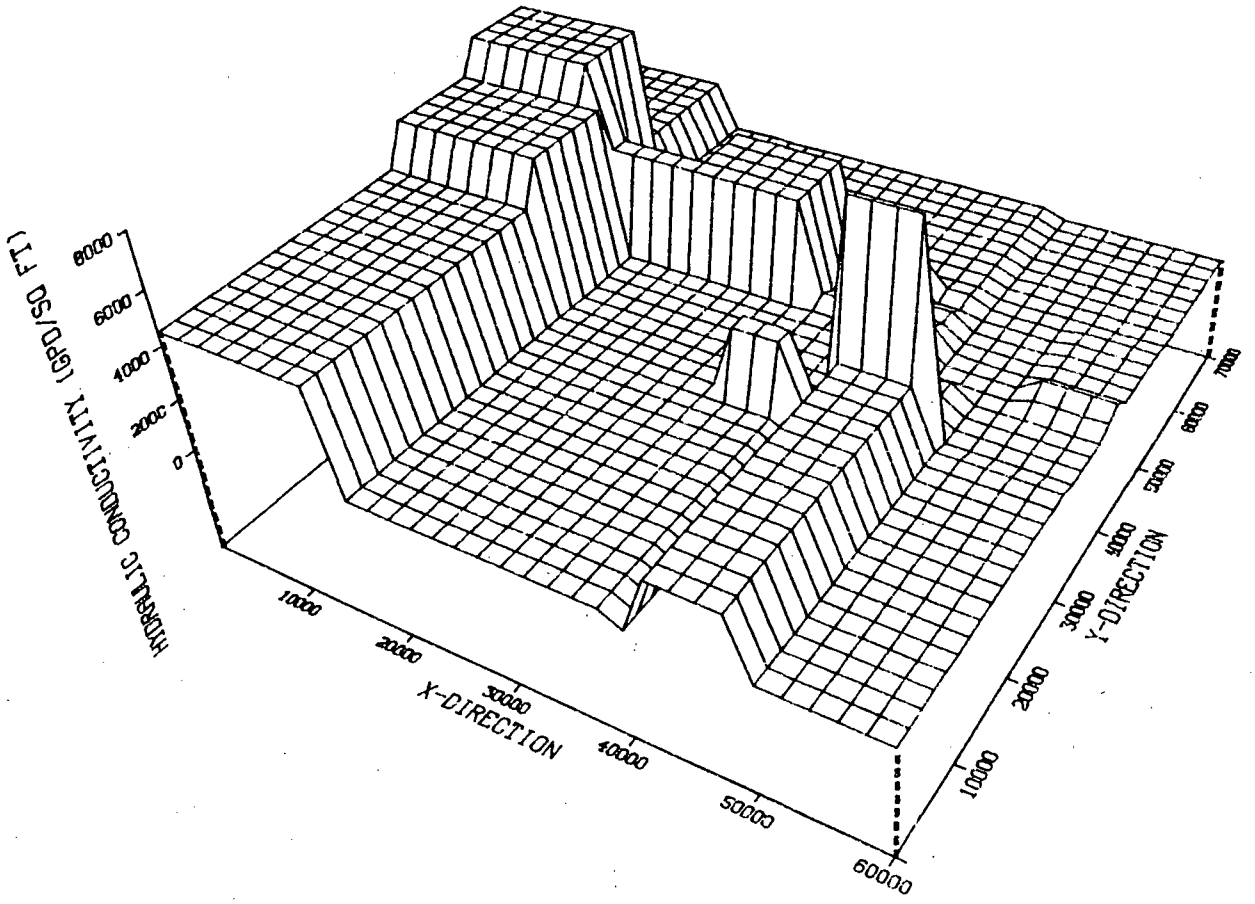

FIGURE 6.4.3-1. Calibrated Hydraulic Conductivities for the STP Final Regional Model

The recharge/discharge rate adjustments were accomplished by adjusting the vertical hydraulic conductivity (K'). Adjustments were made primarily to simulate the water mound to the left of the grid center which is characteristic of increased recharge, and the trough which is characteristic of decreased recharge. The final recharge/discharge distribution is shown in Figure 6.4.3-2. Overall, the recharge to the study region was increased above initial estimates by about 70% to 2.8×10^7 gpd.

Potential contours from the final STP model simulation are presented in Figure 6.4.3-3. Though the match is not exact, the key features which would most effect flow paths and velocities (i.e., general trends in the potential gradient, the ground-water mound and trough) are acceptably reproduced. To further verify the reasonableness of the final model results, Figure 6.4.3-4 shows streamlines beginning at the approximate location of the STP (coordinate 42000 ft, 51000 ft) based on the observed and the simulated potentials. The streamlines, which closely approximate the contaminant trajectory, are approximately the same.

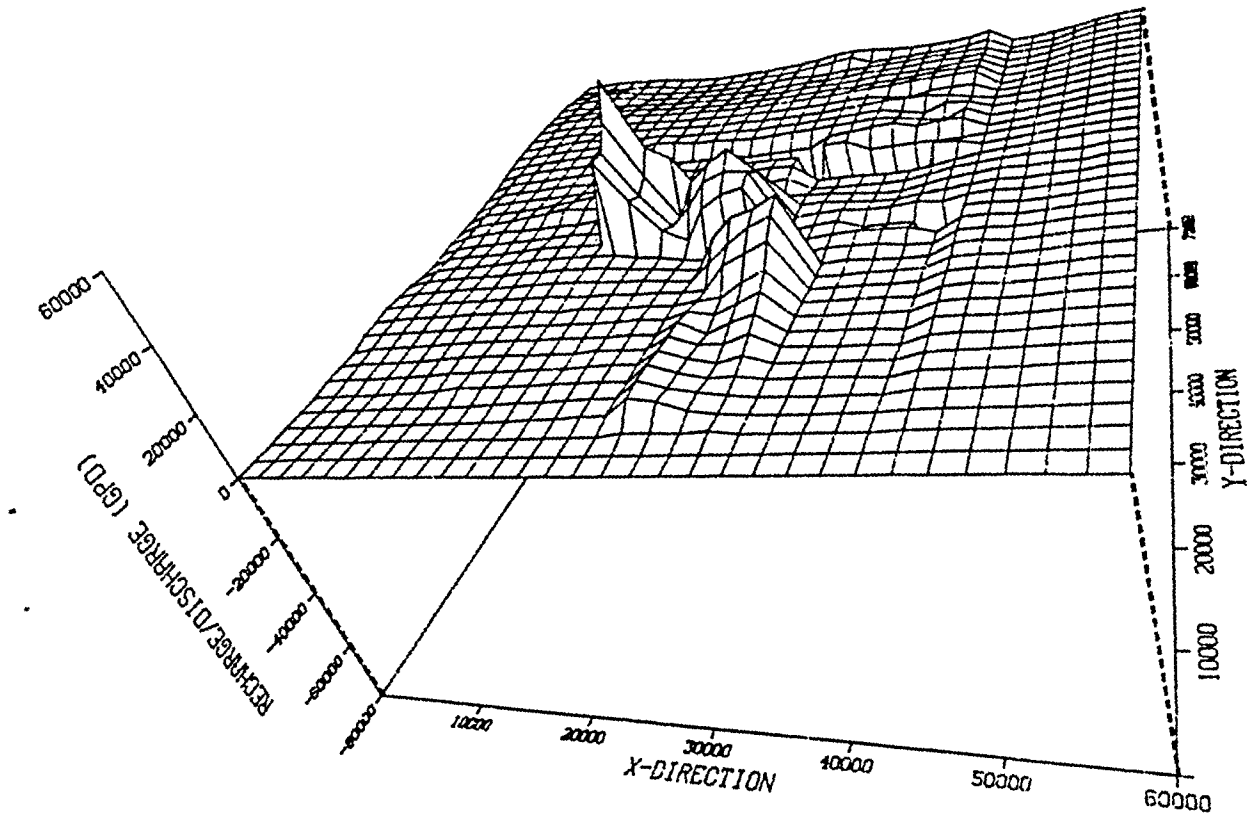

FIGURE 6.4.3-2. Calibrated Recharge/Discharge for the STP Final Regional Model

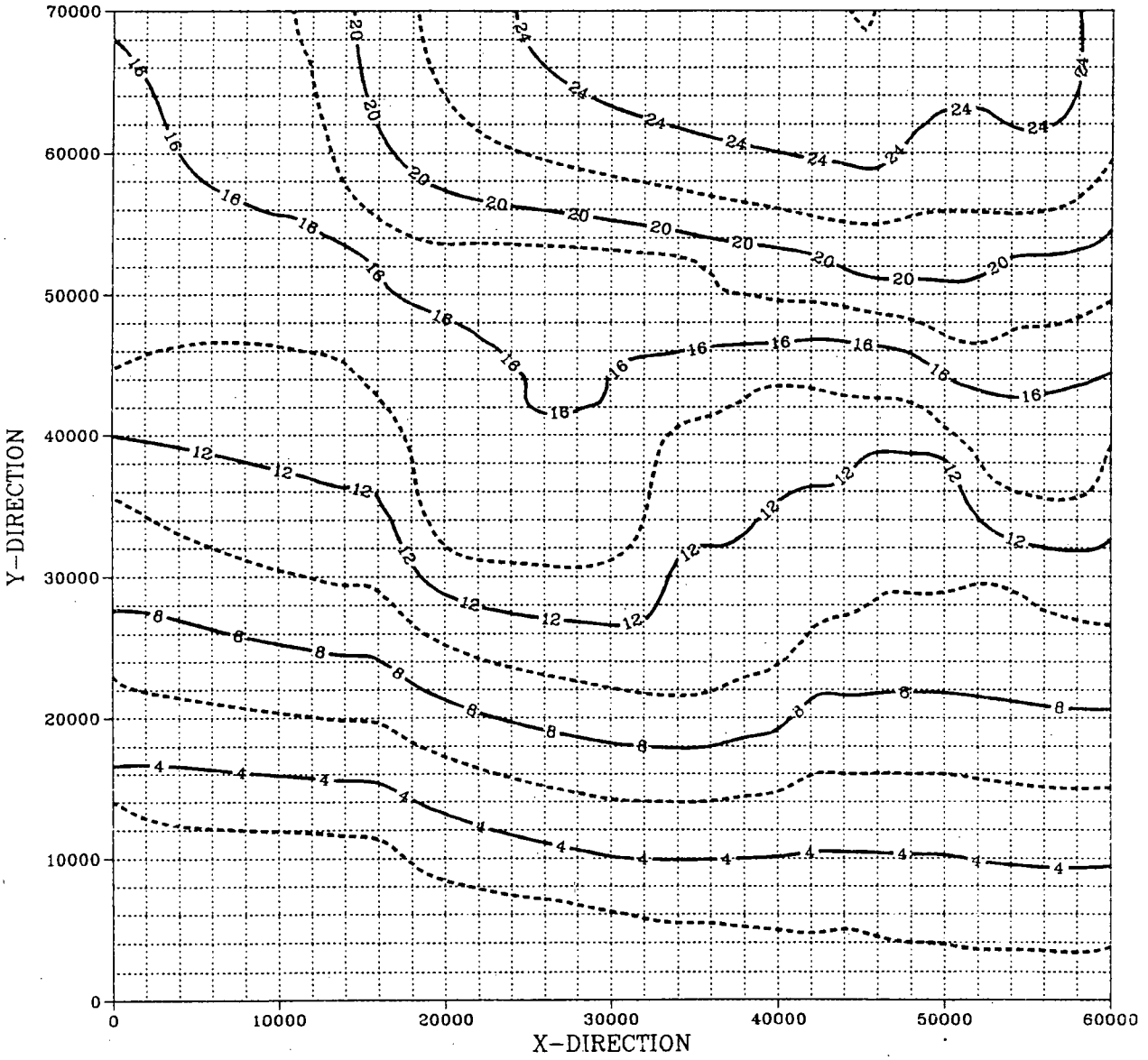

FIGURE 6.4.3-3. Potential Contours Simulated by the Final STP Regional Model

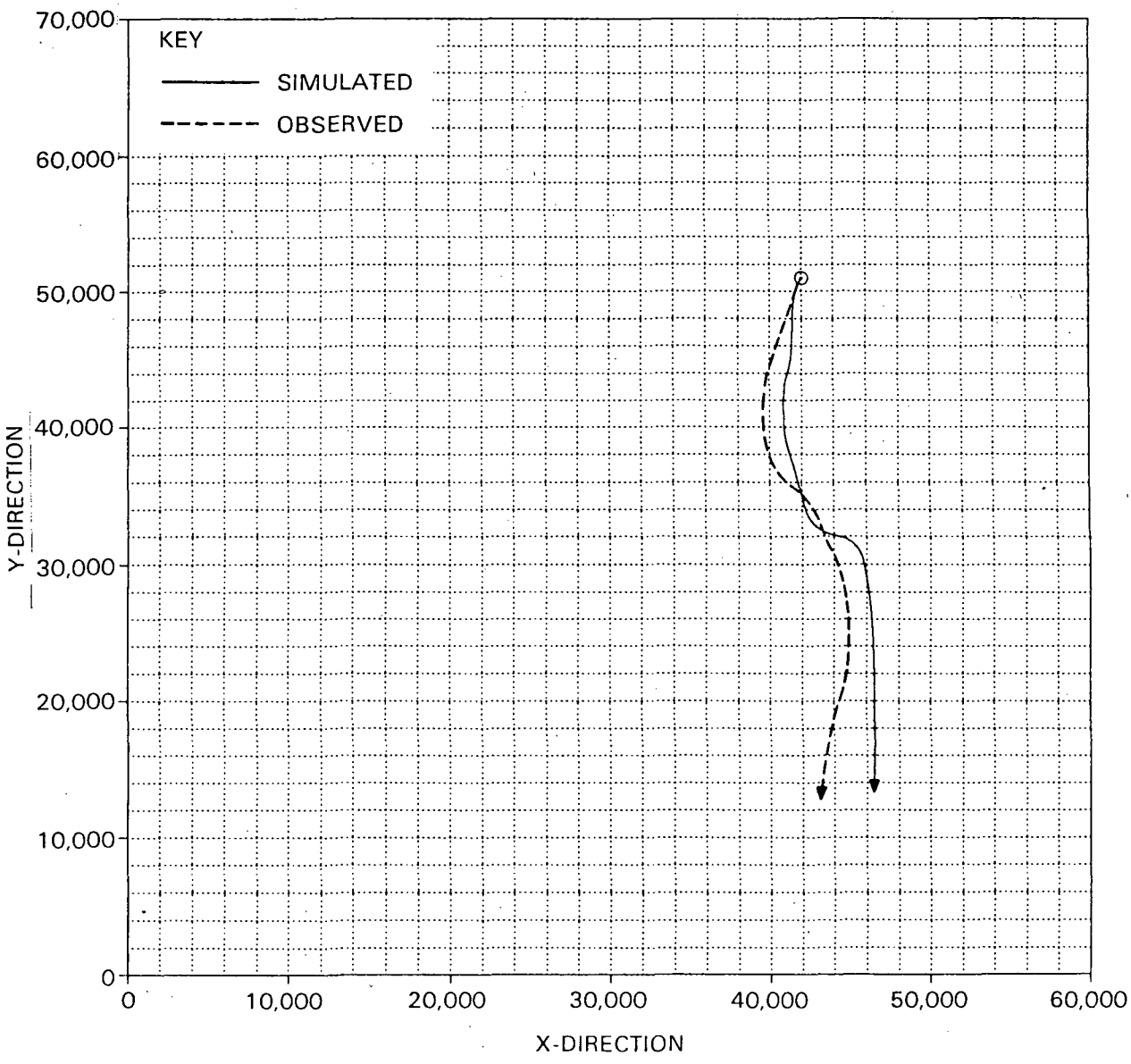

FIGURE 6.4.3-4. Estimated Streamlines From the STP Site Based on Observed and Simulated Potentials

6.5 LOCAL MODEL DEVELOPMENT

6.5.1 Local Area Size and Boundary Conditions

The local model covers an area of 11.2 square miles within the regional study area as shown in Figure 6.5.1-1. The model boundaries were chosen to encompass the STP site and the area down-gradient to the Colorado River.

The boundaries of the local model are located far enough away from the plant site such that implementation of the various mitigative strategies in the vicinity of the plant would not greatly affect the flow field at the boundaries. At the same time the local study area was made small enough to allow a detailed look at flow and transport from the plant (i.e., use a fine mesh) without using an excessive number of nodes. The irregular local model grid, was designed to minimize grid cell size around the STP (coordinate 42000 ft, 51000 ft) and have increasing cell size away from the plant. This was done to allow flexibility in locating and sizing barriers and injection/withdrawal wells for the evaluation of the performance of various mitigative strategies.

As previously discussed, the boundary conditions for the local model are determined directly from the regional model. The procedure for implementing the two models (i.e., regional and local) for pre-mitigative and post-mitigative analyses is to first run the regional model, set the local boundary conditions from the regional results, then run the local model. The boundary conditions in the local model are head-controlled for all boundaries.

The structural top and bottom of the lower shallow-zone aquifer were defined the same as in the regional model as were also the hydraulic conductivities and the recharge/discharge rates. The transfer of these properties from the regional model grid to the irregular local grid was accomplished using an IMSL interpolation routine (IMSL 1980).

The observed and simulated potential contours for the local area are presented in Figures 6.5.1-2 and 6.5.1-3, respectively. It can be seen that the observed trends in the gradient and contour shapes are basically reproduced by the local model. This is particularly true immediately down-gradient of the approximate plant location (i.e., coordinate 42000 ft, 51000 ft), indicating an acceptable model calibration.

6.6 PRE-MITIGATIVE LOCAL FLOW AND TRANSPORT MODELING

Ideally, development of a transport model parallels that for the flow model. Beginning with the final local flow model, initial values of the transport parameters are estimated from available data and subsequently calibrated to obtain a reasonable match between field-measured and model-predicted contaminant concentrations. However, when developing a model to evaluate mitigative techniques for the control of radionuclide contaminants due to severe nuclear power plant accidents, radionuclide contaminant field data are not likely to exist. Consequently, one must rely on initial estimates of the transport parameters (e.g., primarily the effective porosity, retardation

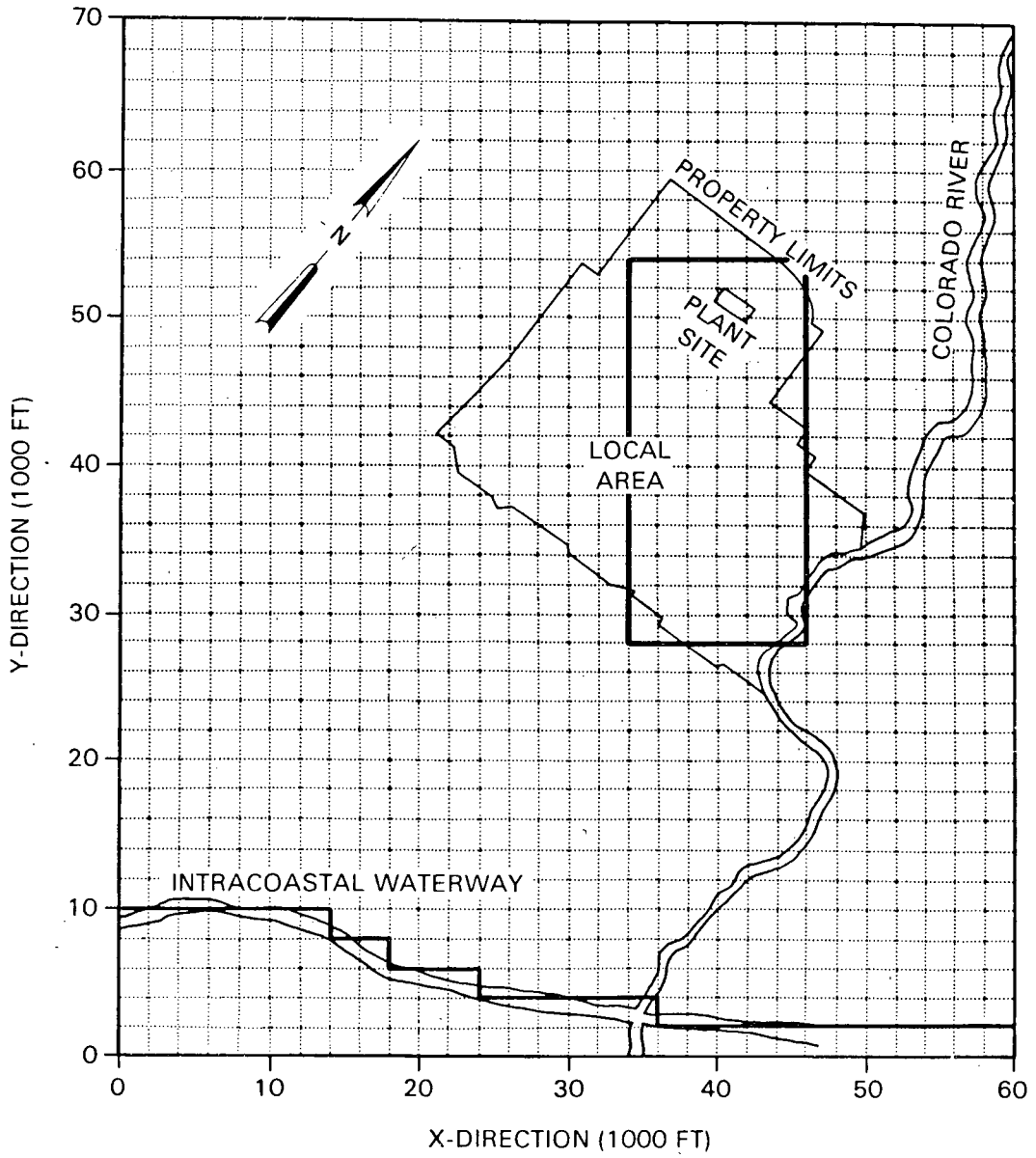

FIGURE 6.5.1-1. STP Local Model Study Area

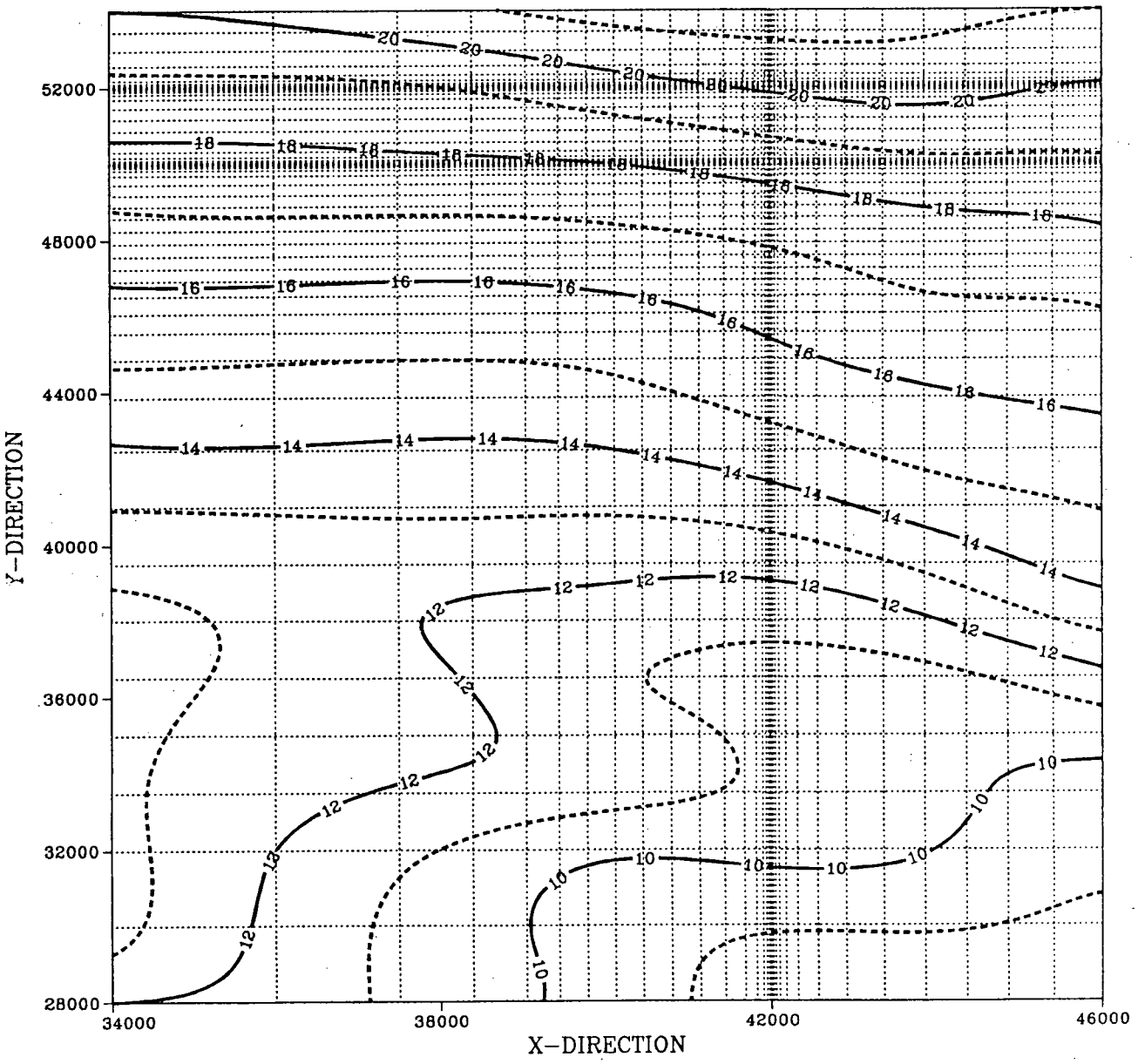

FIGURE 6.5.1-2. STP Local Area Observed Potential Contours

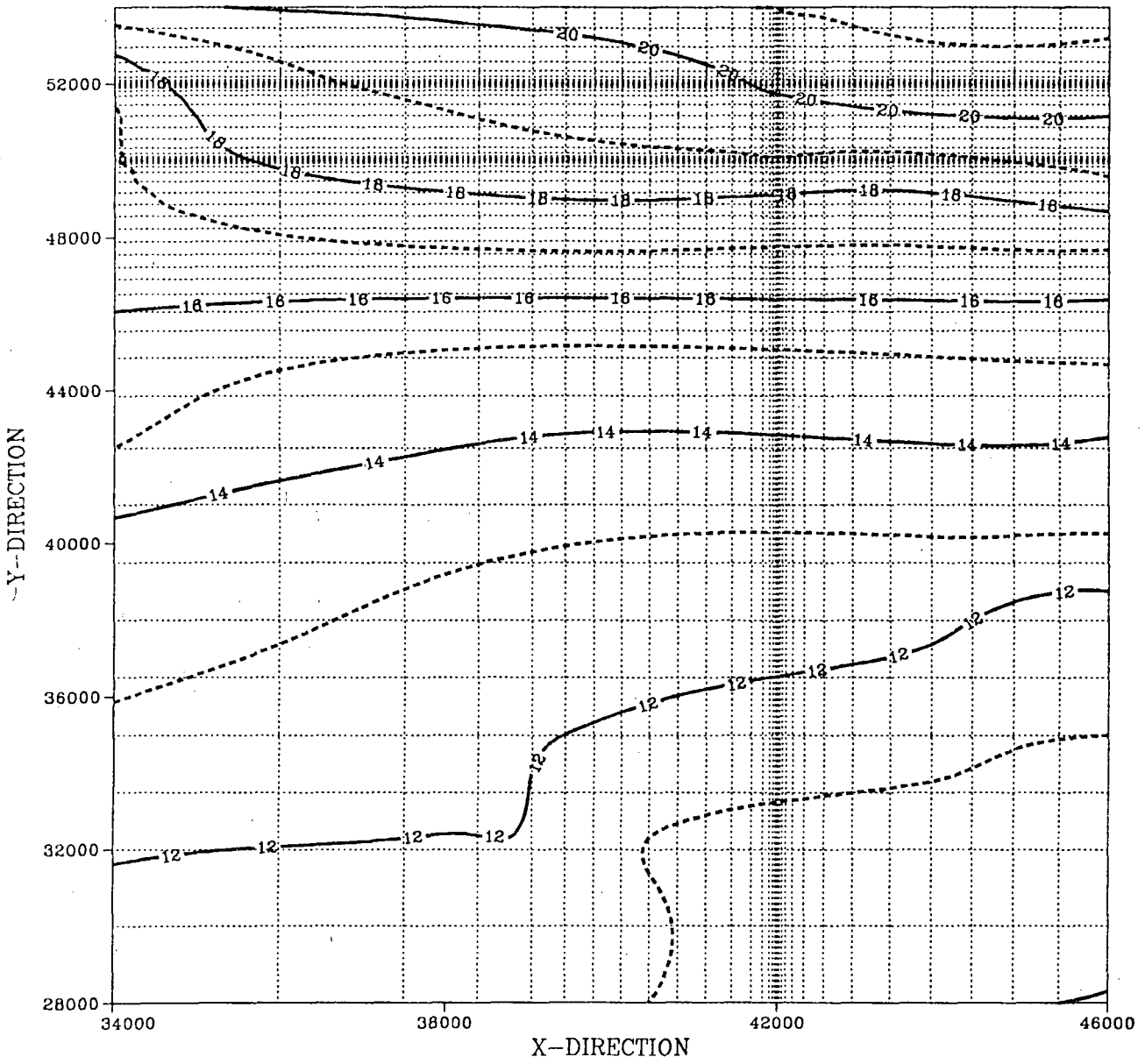

FIGURE 6.5.1-3. STP Local Model Simulated Potential Contours

factor and dispersivity coefficients), based on available information. Generally, once satisfactory estimates are obtained, these same values are used for the baseline pre-mitigative simulations as well as the post-mitigative performance comparisons.

6.6.1 Transport Parameter Estimations

The data and parameters required to simulate transport are:

1. longitudinal and transverse dispersivity coefficients,
2. contaminant source characteristics including leach rate and contaminant decay constant,
3. adsorption data such as distribution coefficient, bulk density and effective porosity.

The determination of the required parameters and data for the pre- and post-mitigative transport analysis is discussed below.

6.6.1.1 Dispersivity Coefficients

Simmons and Cole (1985) describe dispersion in a ground-water system as a combination of molecular diffusion, which occurs even under conditions of no flow, and hydrodynamic dispersion. Hydrodynamic dispersion results from variation in the local water velocity within the medium with respect to its average value as described by convection. This variation in velocity exists at any scale, from microscopic (in the pores) to macroscopic (due to uncharacterized heterogeneity of the medium) and even megascopic (due to large scale variations in medium properties like fractures). Dispersion is important because it produces mixing and spreading both longitudinally and transversely with respect to the flow direction of the trahsported contaminants. Estimation and measurement of hydrodynamic dispersion for field conditions is presently a topic of intensive research (Molz et al. 1983; Wang and Anderson 1982; Simmons 1982). The problems in dealing with spatial variability of hydrologic properties and field-scale dispersion processes have resulted in questions about the adequacy of the classical convective-dispersive approach with its inherent assumptions regarding dispersion. However, as long as the appropriate effective dispersion coefficients can be defined the convective-dispersion approach is considered applicable.

In TRANS contaminant transport is computed on the basis that the distribution of contaminant concentrations in the ground water can be represented by a finite number of discrete particles. Each particle represents a fraction of the total mass of contaminant involved and is assumed to move with the ground-water flow. The technique, designated by Prickett, Naymick and Lonnquist (1981) as the "random-walk" method, is founded on the concept that dispersion in porous media is a random process such that particles move through an aquifer with two types of motion. One motion is that of the mean flow along computed streamlines. The other type is random motion governed by scaled probabilities related to flow length and the longitudinal and transverse dispersion coefficients. The "random-walk" concept is illustrated in Figure 6.6.1-1.

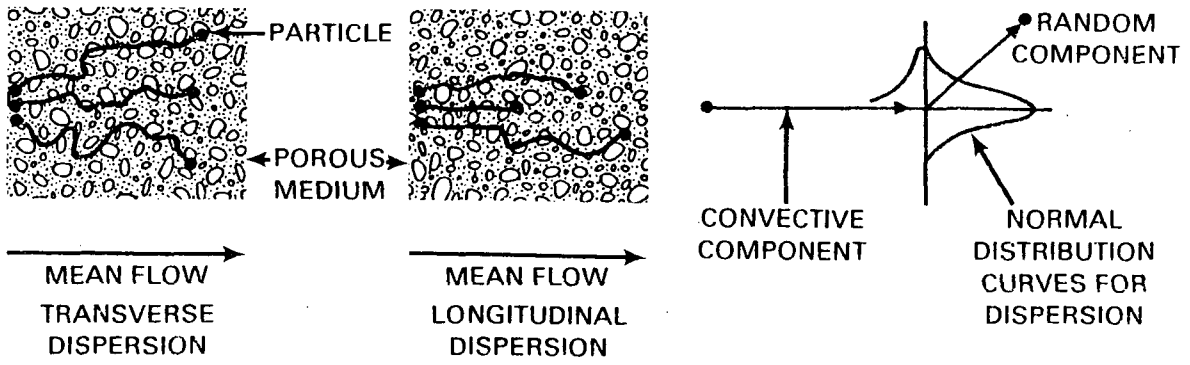

FIGURE 6.6.1-1. Illustration of "Random-Walk" Concept Employed by TRANS (Source: Prickett, Naymik and Lonnquist 1981)

Because of a total lack of data related to dispersivity in the study aquifer, initial estimates of longitudinal (D_L) and transverse (D_T) dispersivity coefficients were made based on information in the literature. One source (Yeh 1981) provided estimates of D_L for various materials which are presented in Table 6.6.1-1.

The geologic material in the study aquifer most likely fits in the sandy silt to sand range resulting in a valve equal to 25 m to 50 m or approximately 80 ft. to 165 ft. According to Fried and Combarnous (1971) based on laboratory studies D_T is equal to about 1/20 D_L. Therefore, the equivalent range for D_T is 4 ft. to 8 ft. Data presented by Gelhar and Axness (1981), shown in Figure 6.6.1-2, demonstrate that the value of D_L is a function of scale.

TABLE 6.6.1-1. Estimated Longitudinal Dispersivity (D_L) for Various Geologic Materials (Source: Yeh 1981)

Geologic Material	Estimated Longitudinal Dispersivity (D_L), m
Clay-Silt	1
Silty Clay	5
Silty Marl	10
Sandy Silt	25
Sand	50

Though there is considerable scatter in the data it shows a distinct increase in D_L with travel distance. For reference, the line for D_L equal to one-tenth the travel distance is shown. The estimated down-gradient travel distance from the STP to the Colorado River is about 5 miles (8000 m). For distances of this magnitude measured dispersivities shown in Figure 6.6.1-2 range from about 5 m to 500 m. The values suggested by Yeh (1981) falls well within this range and would be at about the midpoint on the log-log plot. Consequently, the value for sand (50 m) is used for the initial transport analysis.

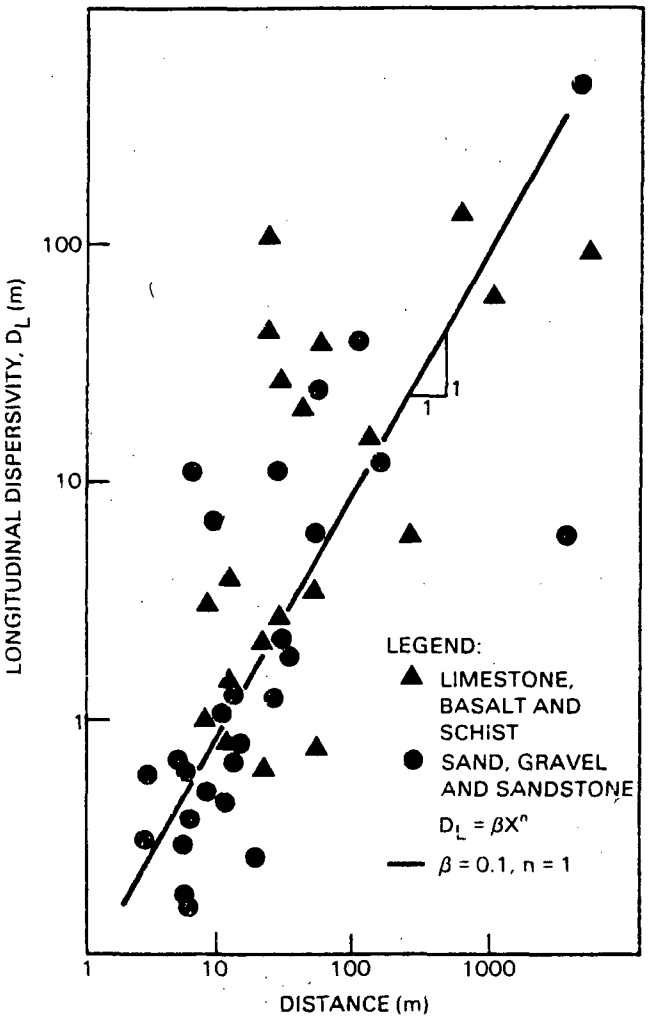

FIGURE 6.6.1-2. Field Observations of Longitudinal Dispersivity (After: Gelhar and Axnes 1981)

6.6.1.2 Source Characteristics

Data requirements for characterization of a radionuclide contaminant source are the source leach rate and decay constants for the radionuclides present. As noted in Section 6.2.3 this case study and methodology demonstration will address the leaching of radionuclides from the core melt debris following a postulated severe reactor accident at the STP. Further, strontium-90 will be used as the indicator radionuclide for the pre-mitigative transport modeling.

The hypothesized leach release of strontium-90, shown in Figure 6.2.3-1, decreases exponentially from approximately 4×10^{15} pCi/year at the time leaching begins to 2×10^{3} pCi/year after 1000 years. With TRANS, the source must be input as a sequence of slug releases, each occurring over a specified time period (i.e., the time step used for the transient transport simulation). Given the strontium-90 half-life of 10,519 days and the large amounts of radionuclide hypothesized to be released, simulation times of several hundred years are anticipated. Therefore, the release rate curve was integrated in 100-year intervals to obtain an equivalent curve consisting of a series of constant release rates. The resulting stepped curve (Figure 6.6.1-2) decreases from about 4×10^{14} pCi/year for the first 100 years to 1×10^{4} pCi/year at the end of 1000 years.

6.6.1.3 Adsorption Related Parameters

Distribution Coefficient

In TRANS, reversible equilibrium controlled adsorption is described in terms of a retardation coefficient. In turn, the retardation coefficient is related to the distribution coefficient, K_d, of the concentration isotherm for a particular chemical species and the bulk density and effective porosity of the aquifer medium. In effect the retardation coefficient represents the reduction in solute travel velocity relative to the ground-water flow velocity such that an adsorbed contaminant moves more slowly, but without being permanently affixed to the medium (Simmons and Cole 1985).

Simmons and Cole (1985) state that the estimation and use of distribution coefficients is currently at issue within the technical community. Measurements of K_d under static laboratory conditions may not be comparable to those obtained from a dynamic field experiment. This brings into question transferability of laboratory measurements to field conditions. Usually discrepancies can be explained in terms of violation of chemical equilibrium assumptions. However, retardation coefficients may have phenomenological meaning when estimated inversely to match a field-scale tracer test, even though values may not conform to laboratory conditions. In this light, an estimate of K_d for strontium-90 which was obtained from the representative K_d's is presented in Table 3.3.2-2. Values in the table are 10 ml/g for porous silicate and 50 ml/g for porous silicate containing clay and silt. Conservatively, a value of 10 ml/g is selected for the analysis.

Effective Porosity

The available information regarding effective porosity for the study area was limited to an assumed value of 37% obtained from the STP FSAR (Houston Power and Light 1978) and the representative porosity values for various sedimentary material shown in Table 6.3.2-6 (Hammond 1969). The ranges given are 30% to 40% for uniform sand and 30% to 35% for fine to medium mixed sand. The 37% value assumed in the STP FSAR (Houston Power and Light 1978) falls within or near these ranges and thus appears to be reasonable.

Bulk Density

In addition to effective porosity, determination of the retardation factor requires a known bulk mass density which can be determined from the relationship (Freeze and Cherry 1979):

$$n_e = 1 - \frac{\rho_b}{\rho_m}$$

where

n_e = effective porosity
ρ_m = particle mass density (2.65 g/cm^3 for most mineral soils), and
ρ_b = bulk mass density.

From this relationship, assuming an effective porosity of 37%, the bulk mass density for the lower unit is 1.7 g/cm^3 or 104 lb/ft^3.

6.6.1.4 Additional TRANS Parameters

As previously discussed, the total mass of contaminant is represented in TRANS by a discrete number of particles, with the idea that as the number of particles approaches the molecular level the exact solution to the convective-diffusion equation would be obtained. Prickett et al. (1981) suggest that relatively few particles (less than 5000) are needed to obtain an acceptable solution for most engineering applications. Measured contaminant data necessary to test their assertion were not available. However, in initial model tests several transport runs were made with different numbers of particles. The results indicated that simulation results did not change appreciably due to increasing the number of particles from 5000 to 7000, though computer simulation time increased significantly. Consequently, the number of particles was set equal to 5000 for all simulations in this case study.

The final parameter values determined for the pre-mitigative transport simulations and their sources are summarized in Table 6.6.1-1.

6.6.2 Pre-Mitigative Local Transport Results

There are two primary objectives in performing a pre-mitigative transport analysis:

1. quantitatively assess the need for mitigation following a severe accident release of radionuclides to the ground-water system, and

2. when mitigation is found to be necessary, provide a baseline for evaluating the effectiveness of selected mitigation techniques.

To meet these objectives for the case study, TRANS was used to simulate radionuclide transport from the STP for a 1000-yr period from the time leach releases begin. The transient simulation was made using 100 year time steps and the discretized leach rate curve shown in Figure 6.6.1-3. The radionuclide

TABLE 6.6.2-1. Summary of TRANS Transport Parameter Values for STP Transport Simulations

Parameter	Value	Source
Longitudinal Dispersivity (D_L)	50 m (164 ft)	Gelhar and Axness (1981)
Transverse Dispersivity (D_T)	2.5 m (8 ft)	Computed; $D_L/20$
Distribution Coefficient (K_d)	10 ml/g	Table 3.3.2-2
Effective Porosity (n_e)	37%	STP FSAR (Houston Power and Light 1978)
Bulk Density (ρ_b)	104 lb/ft^3	Computed
Retardation Factor (R_d)	46	Computed
Number of Particles (NP)[a]	5000	Prickett et al. (1981)

(a) TRANS specific parameter

release is assumed to be a point source at spatial coordinates 42,000 ft in the x-direction and 51,000 ft in the y-direction. The basis for assessing the need for mitigation is the potential for significant release of radionuclides to the Colorado River.

The results of the pre-mitigative transport simulation indicate that the strontium-90 plume, because of the high retardation, would migrate less than 2400 ft from the STP in 1000 years. Three-dimensional plots of the distribution of strontium-90 concentrations at 100 years and 1000 years are shown in Figures 6.6.2-1 and 6.6.2-2. At 100 years the maximum concentration is approximately 1×10^{5} pCi/ml while at 1000 years the maximum has decreased to 2.5×10^{-5} pCi/ml, well below the maximum permissible concentration of strontium-90 of 0.3 pCi/ml according to 10 CFR/Part 20 (USNRC 1978).

With regard to the first objective of the pre-mitigative transport analysis, based on the simulations using strontium-90 as an index radionuclide, significant contamination of the Colorado River would not occur. Consequently, mitigation of radionuclide movement in ground water following a severe accident at the STP would not be necessary.

Though mitigation would not actually be required at the STP, the ground-water model for the site still provides an excellent vehicle for demonstrating site specific evaluation of mitigative techniques. To this end, the following sections describe a detailed analysis of feasible mitigative techniques. The analysis is based upon the STP local and regional models and a hypothetical contaminant that is assumed to move only advectively with the ground water (i.e., the distribution coefficient and dispersivities are equal to zero). In Figure 6.6.2-3, the pathline for ground-water flow from the STP to the Colorado

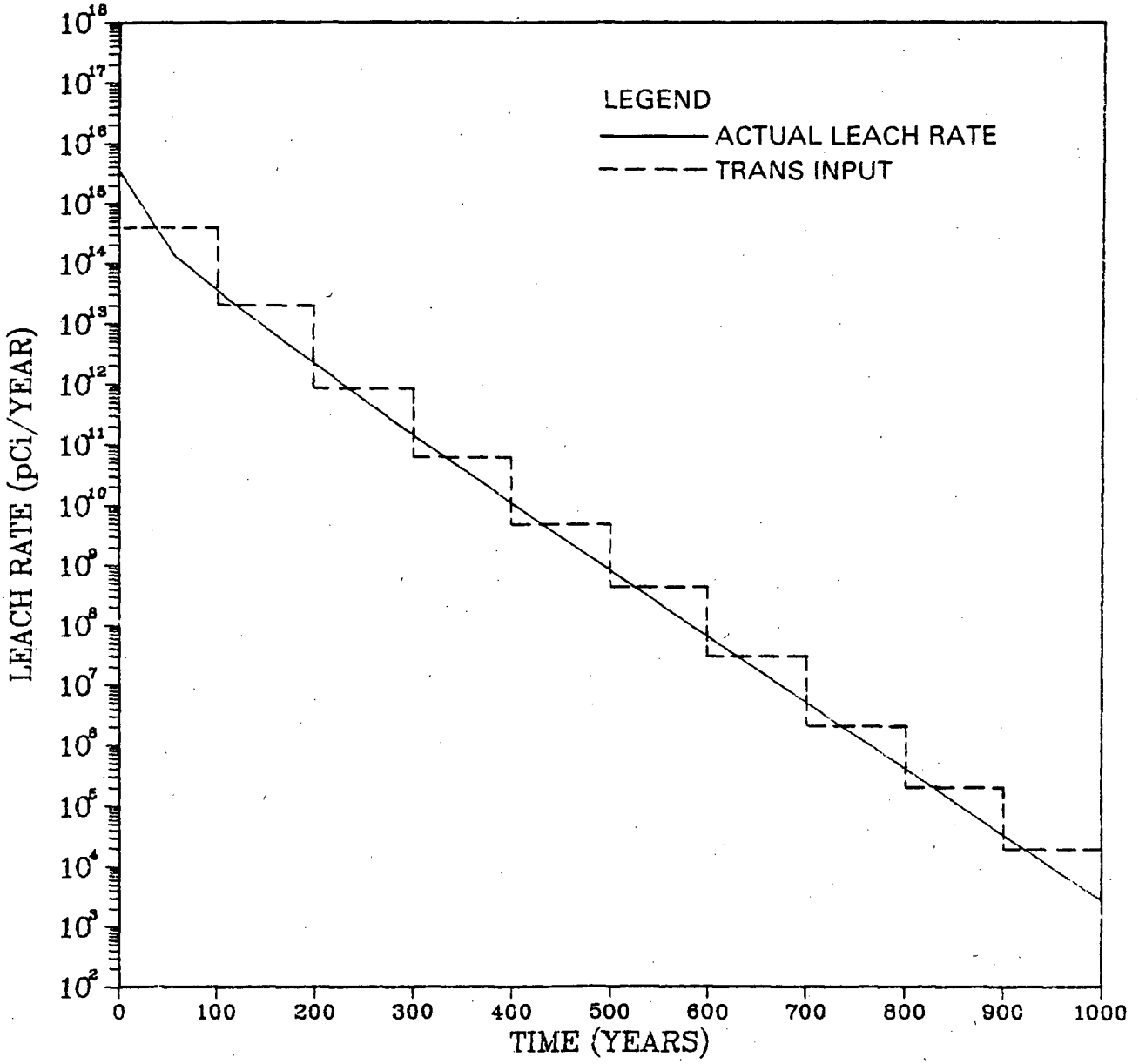

FIGURE 6.6.1-3. Stepped Source Leach Rate Curve for Strontium-90

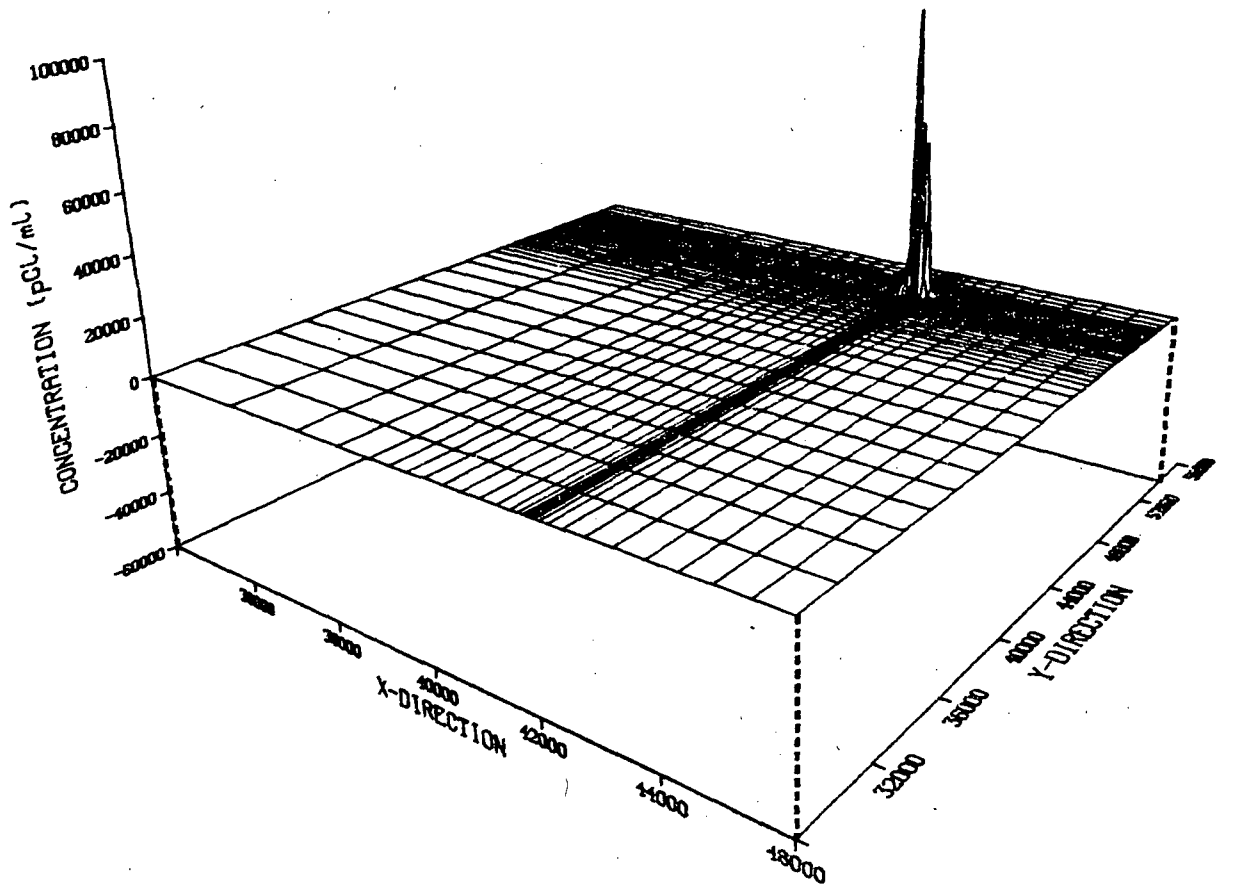

FIGURE 6.6.2-1. Simulated Pre-Mitigation Strontium-90 Concentrations at 100 Years

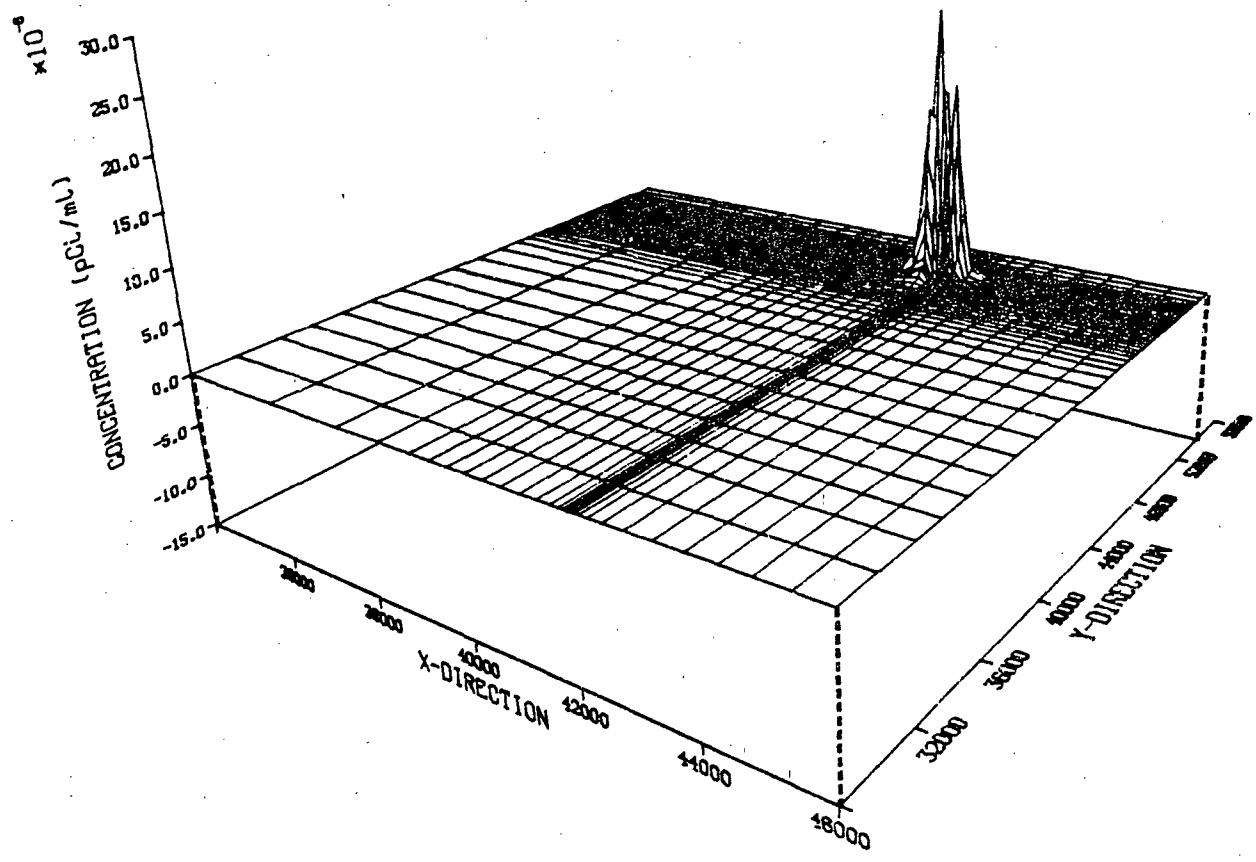

FIGURE 6.6.2-2. Simulated Pre-Mitigation Strontium-90 Concentrations at 1000 Years (Note Vertical Scale Exaggeration as Compared to Figure 6.6.2-1)

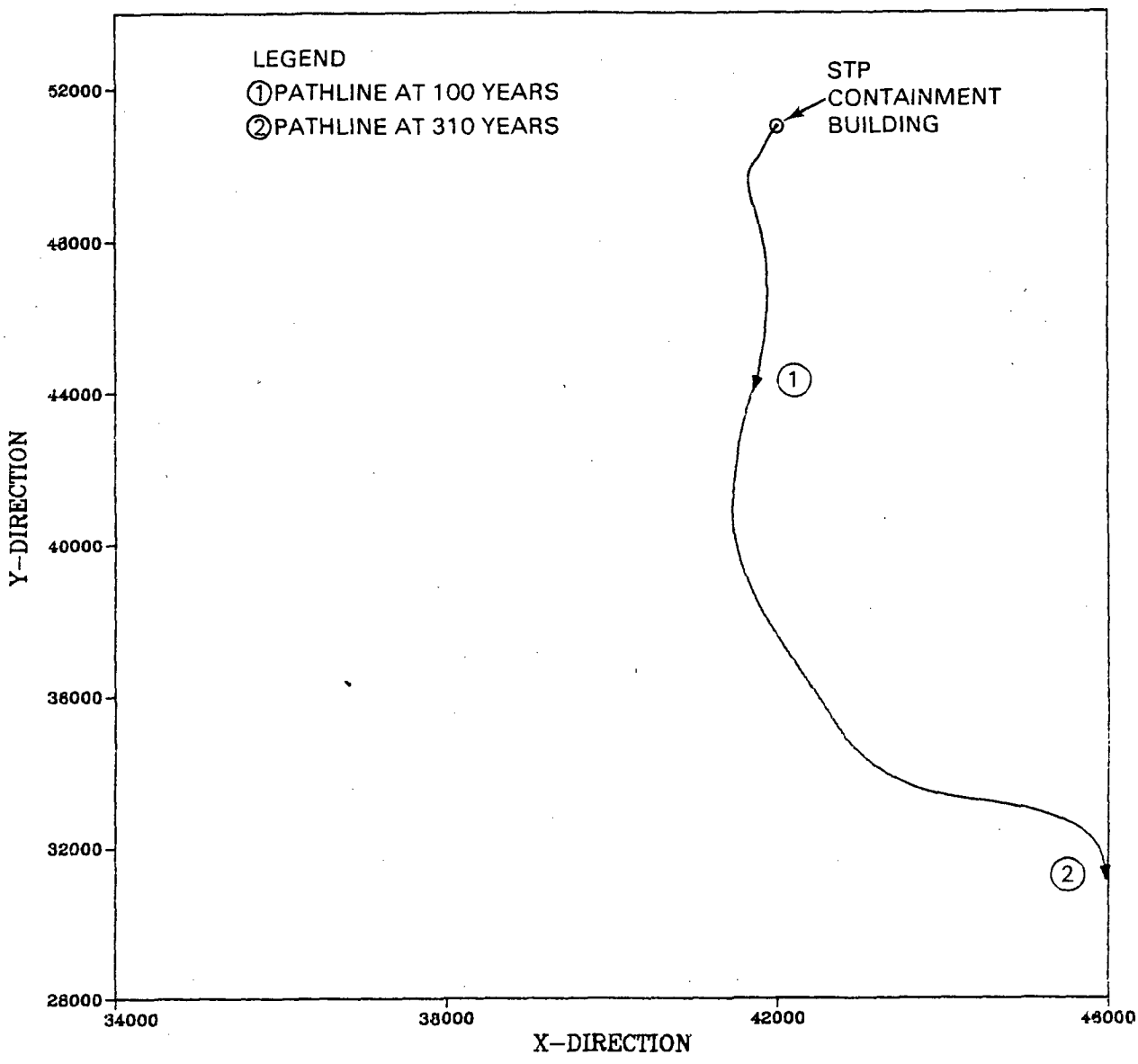

FIGURE 6.6.2-3. Pre-Mitigation Pathline From the STP

River is shown. The estimated time of arrival is 310 years. This value will serve as the baseline for evaluating the effectiveness of the mitigation techniques to be considered.

6.7 EVALUATION OF MITIGATIVE TECHNIQUES

The previous sections of this chapter discuss the procedures for developing a mathematical model for analysis of flow and contaminant transport at porous media nuclear power plant sites and then demonstrates the procedures by applying them to the STP. This pattern is continued in this section wherein the emphasis is in demonstrating the general approach to evaluate mitigative techniques while giving only limited attention to the specific characteristics and configuration of the STP.

6.7.1 Approach

The first step in the evaluation of mitigative techniques involves preliminary screening of those methods that clearly are not feasible given site-specific hydrogeologic conditions. Engineering judgment and an understanding of the design, construction and performance considerations of the different techniques are usually sufficient to determine those methods most likely to be applicable. The review of mitigation techniques presented in Chapter 4.0 provides information necessary for this screening phase.

Following the initial screening, the remaining mitigative techniques are subjected to a detailed assessment in terms of their effectiveness in achieving the desired level of mitigation and in formulating a their preliminary design. Recent studies by Silka and Mercer (1982); and Cole et al. (1983) demonstrate the usefulness of computer modeling in the feasibility study process. While it may be straightforward to determine that grouts are applicable to a relatively porous hydrogeologic unit, mathematical models are required to assess the performance of a grout cutoff as a function of location (i.e., up-gradient or down-gradient) and orientation and dimension. The trade-offs in performance lead one to conceptual design specifications for a technique. Once a model is developed for a site, any number of alternatives can be evaluated with minimal additional effort. Further, predictions of contaminant concentrations can be obtained for any location of interest such as site boundaries, surface water discharge points, or drinking water wells (Boutwell et al. 1984).

6.7.2 Screening of Mitigative Techniques

Within the generic site classification scheme discussed in Chapter 3.0, the STP site is categorized as porous unconsolidated silicate. As such, a wide range of mitigative techniques or strategies are potentially feasible (see Table 5.6.2-1). However, due to site specific data obtained from the hydrogeologic characterization and assessment performed on the STP the range of feasible strategies can be narrowed.

Both particulate (i.e., cement-based) and more probably non-particulate (i.e., chemical) grouts may be feasible for construction of ground-water cutoffs to the migration of radionuclides from the STP. The general material properties of the shallow zone aquifer indicate that both the upper and lower shallow zone aquifers could be successfully grouted with the intervening clay layer acting as a key-in and a natural ground-water flow barrier. The average permeability of the host material at the STP is approximately 85 ft/day (0.03 cm/sec) which falls in the middle of the "easy" to grout range of permeabilities listed in Table 5.6.2-1. The relatively high permeability coupled with the low average ground-water velocity (i.e., roughly 0.3 ft/day) facilitates successful chemical grouting of ground-water cutoffs. According to data presented in Table 4.3.1-3 permeation grouting with sodium silicate, lignochrome gel, colloidal solutions, or prepolymer grouts would be recommended. In granular materials, such as those present at the STP, there may be a filtration of cement-based grouts, thus diminishing their suitability for development of a low permeability barrier. However, detailed laboratory analyses would be required to estimate the degree and overall effect of the filtration as a constraint on the feasibility of implementing cement-based grouts. The soil size limitations on grout permeation presented in Figure 4.3.1-1 suggest that silicate grouts may be most suitable for the STP. Silicate grouts may also be somewhat more resistant to the potential prolonged exposure to saltwater that may be possible at the STP depending on the eventual location of the cutoff. Finally, the normal range of pH (i.e., roughly 6 to 8) observed for the ground-water in vicinity of the STP (Hammond 1969) would not prohibit the use of a silicate grout.

Because of the depth to which a constructed barrier would have to be placed to be effective in mitigating the consequences of contamination of the lower shallow zone aquifer, the use of steel sheet piling is infeasible and the construction of slurry trench cutoff walls would be impractical. A realistic value for the depth of cutoff, including key-in to the underlying confining bed, that would be required for the STP is roughly 100 ft below MSL. This depth coupled with a surface elevation of 25 ft would require excavation of over 125 ft of material. The depth of excavation could be reduced by locating the slurry trench in an area where the bottom of lower shallow zone aquifer is closer to the ground surface. However, this approach may result in a grossly non-optimal placement of the cutoff. The alternate-slot method would be recommended for construction of a slurry trench cutoff at depths approaching 125 ft. Because of structural integrity, the depth of the wall and the relatively high permeability of the site lean-concrete would most likely be preferred for the construction of the cutoff. Also, because of the depth and looseness of the host material, trench cave-in may prohibit the construction of a slurry trench cutoff.

Creation of a hydraulic barrier to the specific path or trajectory of the contaminant plume resulting from a possible severe accident at the STP would also be a feasible mitigative strategy for the STP site. Due to the conceptual nature of these dynamic strategies, their feasibility, which is directly related to performance, must be addressed via some form of model evaluation of the effects of varying withdrawal and/or injection rates at various locations on ground-water flow and contaminant transport. Since the aquifer for which

potential surface modification would be sought is deep (125 ft) and confined, deep wells would most likely be installed that have high pumping capacities. The wells would only be screened in the lower shallow-zone aquifer in order to prevent avoidable contamination of the upper shallow zone aquifer. Strategies that involve injection would be preferable to a significant amount of withdrawal because of the potential for contamination of the surface environment. Readily available sources of injection water could be obtained from the Colorado River although filtration would be required for efficient injection. An alternative to filtering Colorado River water would possibly be to locate a high volume discharge well a suitable distance away so that drawdown did not appreciably undermine the creation of a hydraulic barrier. The well discharge would then be used as injection water. Such a scheme would require development of an overland pipeline and small retention storage. The STP cooling reservoir could also be useful as both a source of injection water and/or a storage basin for water withdrawn from the aquifer, depending upon the degree to which it would be contaminated by atmospheric releases of radionuclides. According to Davis and DeWiest (1966) water yields of between 200 and 300 gpm are normally associated with coastal plain aquifers. Therefore, ground-water withdrawal rates should not exceed this limit by any appreciable amount. Acceptable injection rates should be achievable because of the relatively high porosity (i.e., 0.37) and high permeability in the vicinity of the STP.

Interceptor trenches and permeable treatment beds would not be practically feasible at the STP site for two specific reasons. First, the depth limitations on excavation for development of slurry trenches also apply to development of interceptor trenches. Second, the characteristics of ground-water flow and contaminant transport in the shallow zone aquifer prohibit implementation of collection systems. Because of the very flat hydraulic gradient associated with the lower shallow zone aquifer and the relatively high effective porosity ground-water velocities are very low. Consequently, dispersive behavior may contribute to the spread of a contaminant plume much more so than advective transport of radionuclides. Therefore, to be efficient any collection system (i.e., interceptor trenches or permeable treatment beds) would require artificial inducement (possibly through withdrawal and injection) to counter the effect of dispersion in intercepting the contaminant. Because of the depth and confined nature of the lower shallow zone aquifer and the dispersive influence of the hydraulic properties of the aquifer, collection systems would be impractical.

Ground-water freezing would also be impractical for construction of a barrier to ground-water flow because of the obvious limitations of cost and climate. Thermal erosion due to the warm climate and frequent precipitation could continually prohibit closure of a frozen cutoff. Air injection would not be recommended due to the lack of experience in designing and implementing air injection systems as barriers to ground-water flow.

In summary, the ground-water contaminant mitigative techniques that appear most suitable for implementation at the STP based on the reconnaissance level hydrogeologic characterization and the pre-mitigative ground-water flow and contaminant transport analysis are:

1. a fully penetrating and properly keyed grouted cutoff, and
2. a hydraulic barrier to ground-water flow and transport created by injection and/or withdrawal.

6.7.3 Assessment of Feasible Alternatives

The two basic mitigation techniques identified in the screening phase as most feasible for the STP site are a grouted cutoff wall and the development of a hydraulic barrier by ground-water injection and withdrawal. In reality there are any number of implementable conceptual designs for each of these techniques, either individually or in combination. It is not the purpose of this case study to attempt to evaluate all of these possibilities or even to identify the "best" or most effective design. The intent here is to provide information regarding the use of quantitative methods to make such an evaluation and to demonstrate their use for selected alternatives.

The approach used to assess the above alternatives involves quantifying their effectiveness in increasing ground-water travel time from the STP to the Colorado River and, hence, enhancing natural decay of radionuclides. Selected model parameters and inputs for the local transport model were adjusted to simulate the impact each alternative would have on ground-water flow. Steady-state simulations of ground-water flow were then made and the results were compared with the pre-mitigated results to obtain a measure of effectiveness.

6.7.3.1 Cutoff Walls

Cutoff walls are vertical barriers emplaced to either prevent contaminated ground water from migrating away from the site, or to divert incoming ground water away from the contaminant source. There are several alternative cut-off design configurations including (Boutwell et al. 1984):

1. an up-gradient cutoff extending to an impermeable layer,
2. a down-gradient cutoff extending to an impermeable layer,
3. both up-gradient and down-gradient cutoffs, and
4. a cutoff that extends completely around the site.

For this case study, up-gradient and down-gradient cutoffs having lengths of 2000 ft, 3000 ft and 4000 ft are considered. The effectiveness of each cutoff is simulated by introducing a line of nodes having zero permeability 1000 ft up-gradient or down-gradient, from the STP. The 2000 ft cutoffs are centered relative to the plant as illustrated in Figure 6.7.3-1 and Figure 6.7.3-2. The 3000 ft and 4000 ft cutoffs are simply increased in length by adding to the west. The results of the simulations show that ground-water travel times are increased from 310 years for the pre-mitigative case to 540 years, 530 years and 525 years for the 2000 ft, 3000 ft, and 4000 ft cutoffs, respectively. Figure 6.7.3-3 compares the pathline produced by the 2000 ft cutoff with that for the pre-mitigated case. It can be seen that there is very little difference in the two paths, but due to the lowering of the gradient below the plant, the cutoff reduces the distance traveled in the first 100 years substantially. The pathlines for the longer cutoff designs, not shown, are practically identical to that for the 2000 ft cutoff. From these

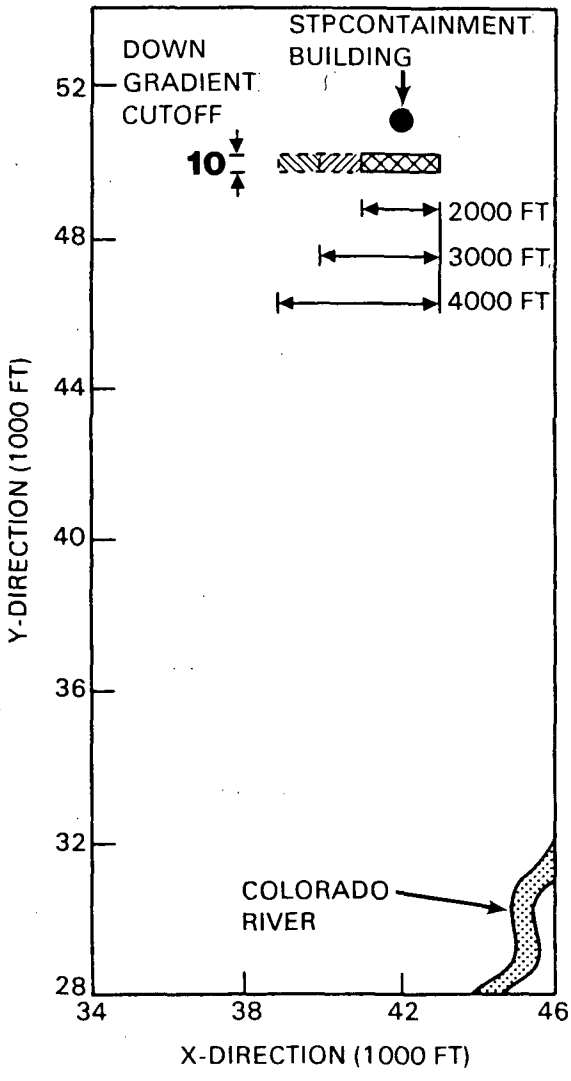

FIGURE 6.7.3-1. Location of Down-Gradient Cutoff Wall

results, it is apparent that for the flow field at the STP, once the up-gradient cutoff is sufficiently long to divert up-gradient flows and flatten the gradient at the site, there is no advantage to increasing the cutoff length to the west.

The ground-water mounding effects produced by the 2000 ft cutoff are illustrated by the potential surface in Figure 6.7.3-4. The maximum hydraulic head increase behind the cutoff, relative to the pre-mitigated condition, is about 1 ft. Thus no significant "bathtub effect" would be evidenced in the confined lower shallow zone aquifer.

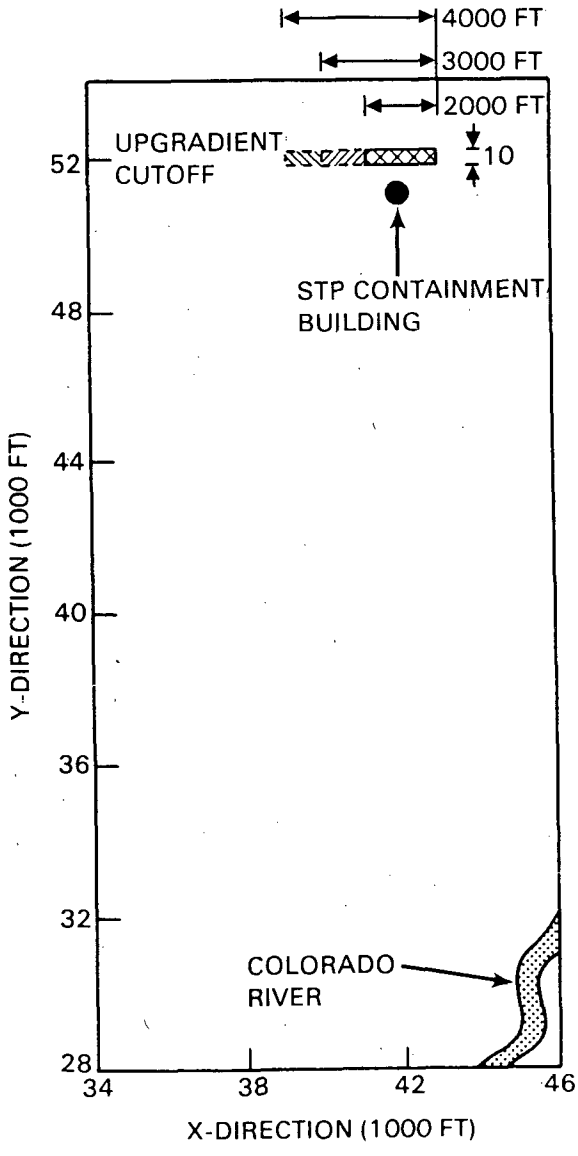

FIGURE 6.7.3-2. Location of Up-Gradient Cutoff Wall

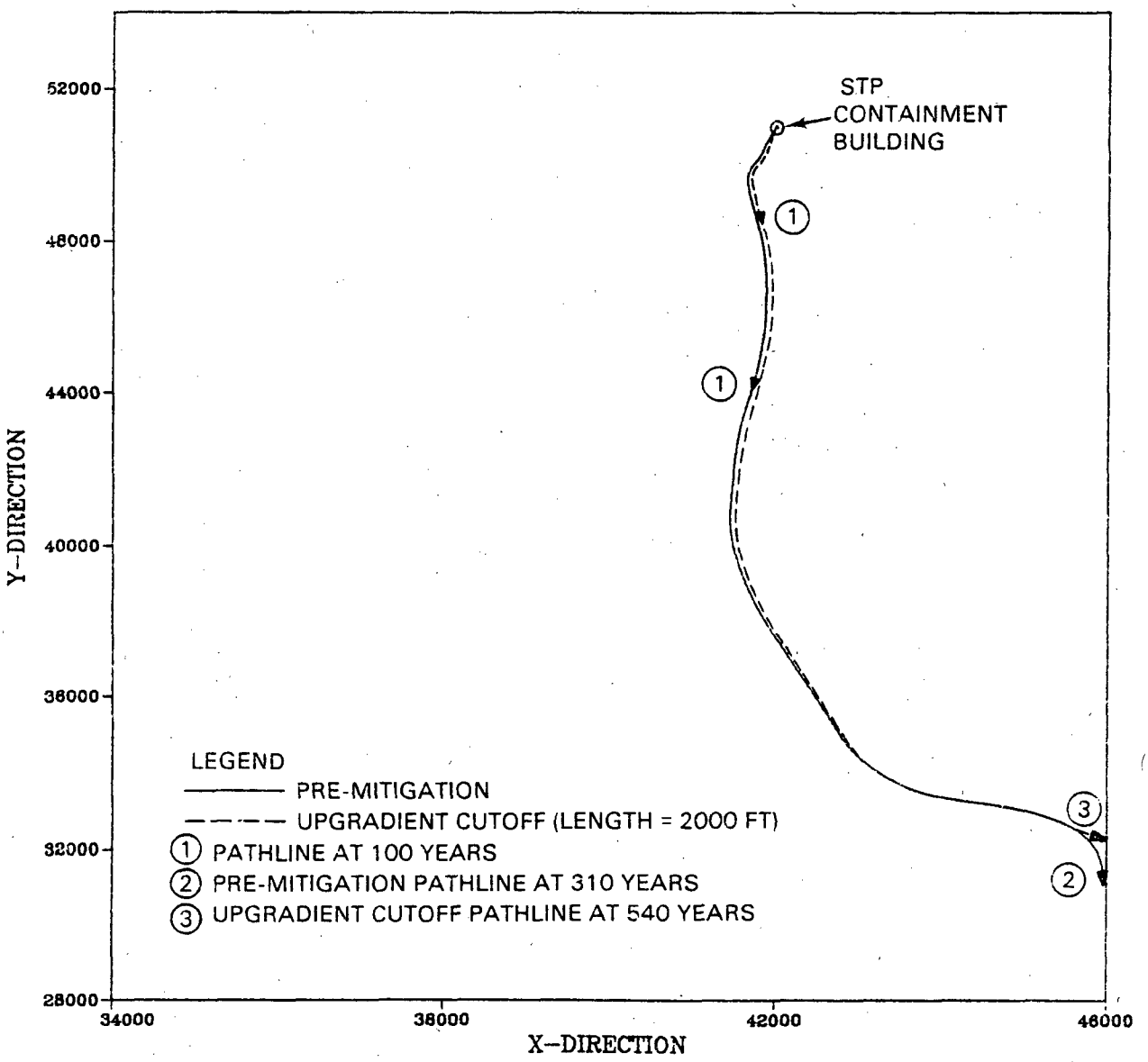

FIGURE 6.7.3-3. Pathline from the STP With 2000 ft Up-gradient Cutoff

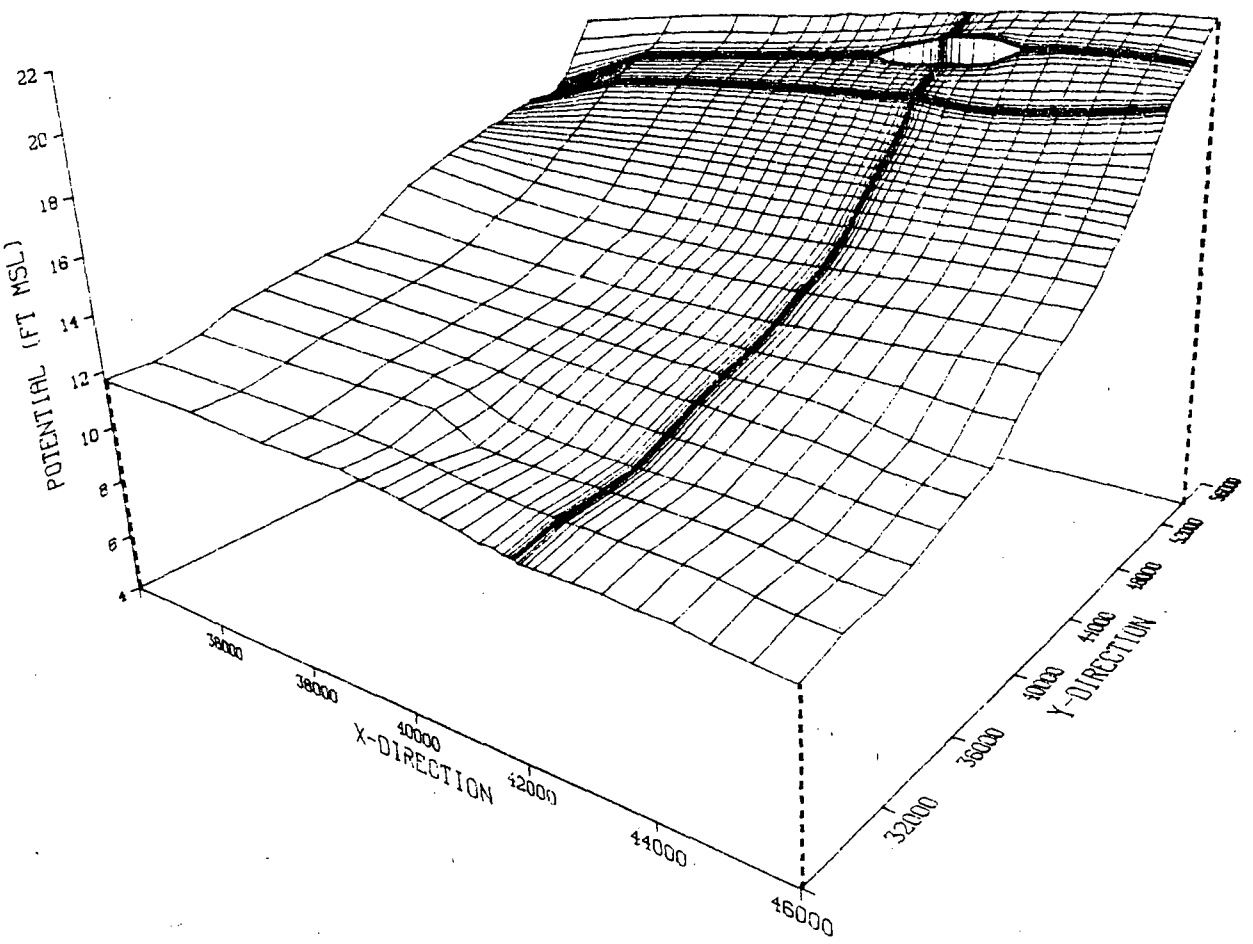

FIGURE 6.7.3-4. Simulated Potential Surface: With a 2000 ft Up-gradient Cutoff

The simulated travel time results for the down-gradient cutoffs, with increasing length, are 450 years, 475 years, and 565 years, respectively. The pathlines for the three cases shown in Figure 6.7.3-5, clearly demonstrate the circuitous routes produced by directly obstructing the pre-mitigative ground-water flow. In contrast to the up-gradient cutoffs, increasing the down-gradient cutoff length directly increases the path length and, therefore, increases the travel time.

Ground-water mounding effects produced by the 4000 ft down-gradient cutoff wall are illustrated by the potential surface presented in Figure 6.7.3-6. The maximum hydraulic head increase behind the cutoff is about 2 ft.

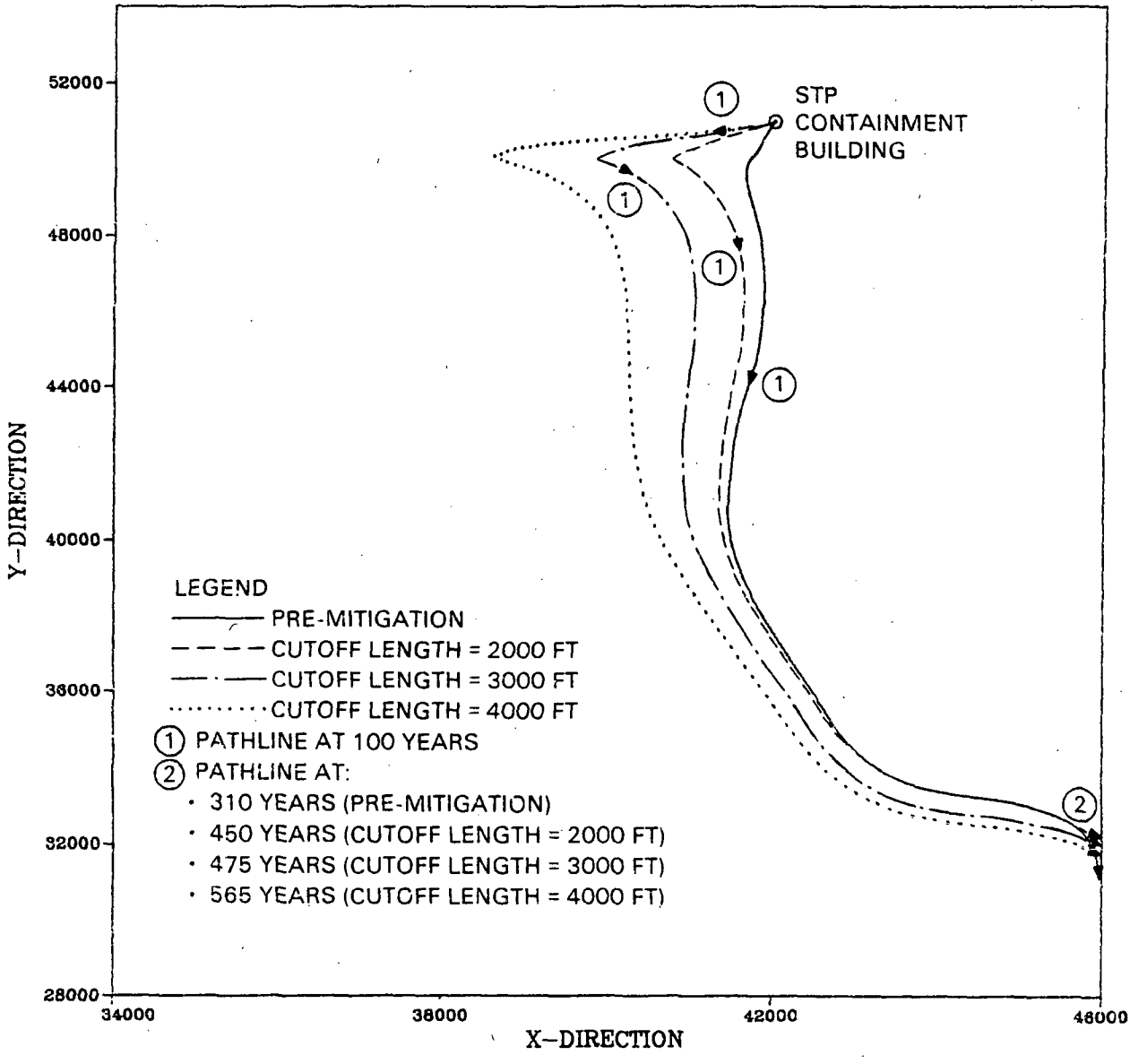

FIGURE 6.7.3-5. Simulated Pathlines from the STP: With Down-gradient Cutoffs

A summary of results for the six cutoff design evaluations is presented in Table 6.7.3-1. The table contains the design length, travel time and percentage increase in travel time for each cutoff design. In addition, to provide some perspective on how these designs would effect transport of radionuclides, an estimate is made of the radioactivity remaining in the ground water at the time of arrival at the Colorado River assuming an initial release at time zero of 1×10^{16} pCi of a hypothetical radionuclide having a 10,000 day half-life. In all cases, the increased travel times produced by the cutoffs results in a 2 to 3 orders of magnitude reduction in pCi remaining at the time of arrival.

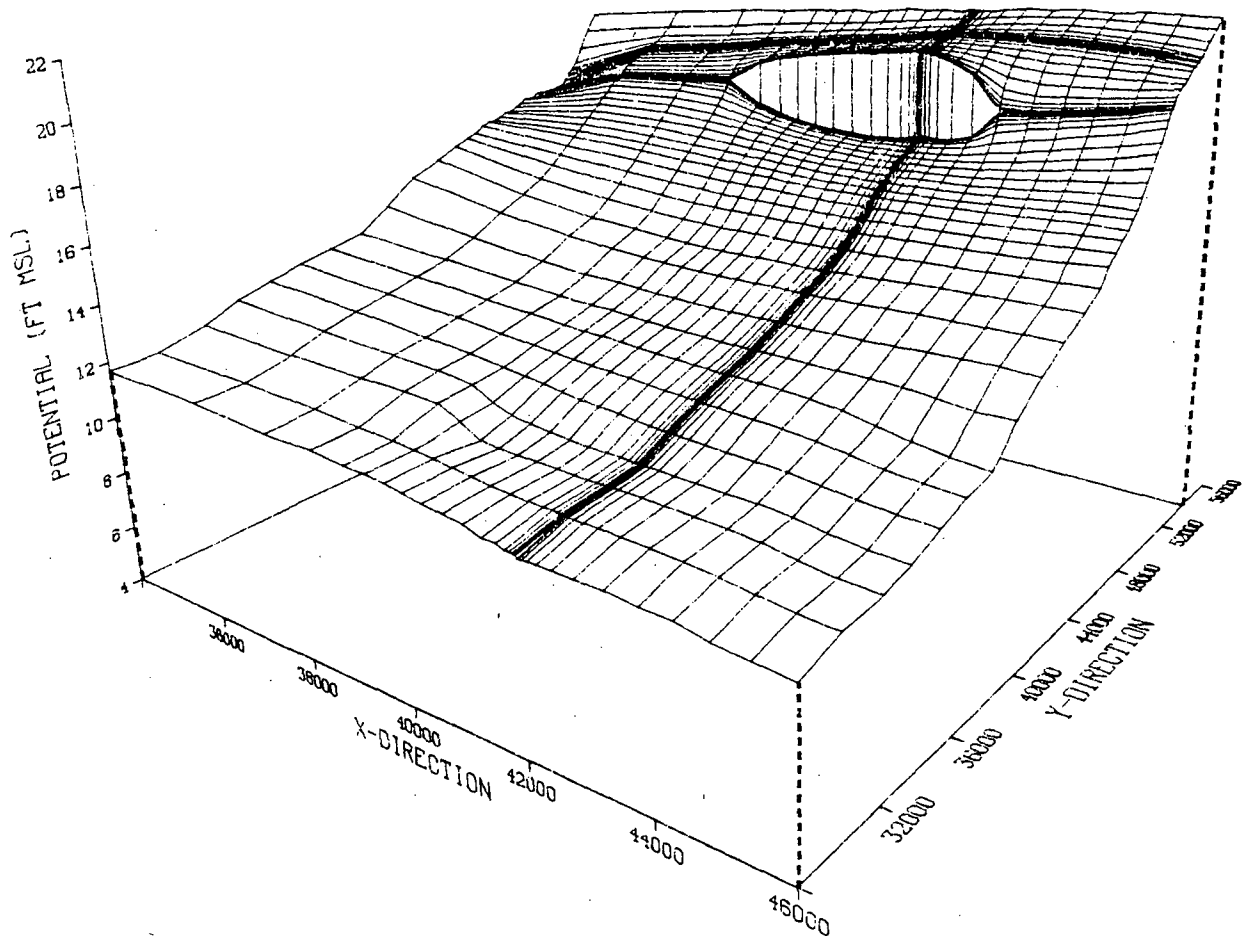

FIGURE 6.7.3-6. Simulated Potential Surface: With a 4000 ft Down-gradient Cutoff

6.7.3.2 Hydraulic Barriers

Hydraulic barriers to ground-water contaminant transport can often be created by ground-water withdrawal and injection which changes the potental surface in some advantageous way. The strategy selected for the STP was development of a hydraulic barrier to divert ground-water flow toward a less potentially hazardous route, that is a longer travel distance (thus greater decay) to the Colorado River. One of the main objectives is to divert the flow without withdrawing contaminated ground water and consequently creating a treatment or disposal problem.

In complicated ground-water flow regimes, where multiple wells may be installed to implement a hydraulic barrier, it can be very difficult to determine pumping rates that achieve the required level of mitigation through control of the trajectory of the contaminant plume. The method used to determine optimum steady-state pumping rates necessary to achieve a specific contaminant

TABLE 6.7.3-1. Summary of Cutoff Design Evaluations

Design	Cutoff Length, ft	Travel Time to Colorado River, yr	Increase Relative to Pre-mitigated Case	Radioactivity[(a)] Remaining, pCi
Pre-mitigation	--	310	--	3.9×10^{12}
Up-gradient Cutoff	2000	540	74%	1.2×10^{10}
	3000	530	71%	1.5×10^{10}
	4000	525	69%	1.7×10^{10}
Down-gradient Cutoff	2000	450	45%	1.1×10^{11}
	3000	475	53%	6.1×10^{10}
	4000	565	82%	6.2×10^{9}

(a) Assuming an arbitrary half-life of 10,000 days and a release of 1×10^{16} pCi at time zero.

control objective once the number and location of the wells have been established is as follows. A nonlinear optimization procedure is coupled with a two-dimensional, steady-state ground-water flow model (similar to TRANS) and a transient, advective contaminant transport model. The optimization algorithm drives the flow modeling component which in turn provides the hydraulic gradient information for the transport analysis. The whole process iterates on pumping rates until the rates that cause the contaminant trajectory and/or travel time to best meet a desired trajectory and/or travel time are determined.

The objective used in the above approach can be any sort of mathematical statement that describes the desired or mitigated contaminant transport. The objective can be in terms of the arrival location of the contaminant travel path and/or the arrival time of a contaminant trajectory, as long as the locations and times can be stated mathematically. This approach can be used to determine the pumping rates necessary to influence the potential surface (which controls contaminant transport) in a manner that will cause the contaminant to be diverted from the unmitigated (and potentially hazardous) travel path into a different and less hazardous trajectory.

Two general injection/withdrawal schemes for hydraulic barrier development at the STP are evaluated:

1. Near-field injection/withdrawal, and
2. Far-field injection/withdrawal.

The results of the evaluations are discussed below.

Near-field Injection/Withdrawal

Initially, a near-field scheme consisting of 10 wells, located as shown in Figure 6.7.3-7, was input to the optimization procedure. The objective stipulated for the optimization in simple terms was that the flow from the STP be directed away from the Colorado River while minimizing the injection rate. The result of the optimization indicated that only two of the ten injection wells are necessary to satisfactorily divert the contaminant trajectory. The specified injection rates were 34 gpm and 2 gpm, respectively. Considering the average yields for irrigation wells in Matagorda County of 1,955 gpm, and the high aquifer transmissivities and porosities, this appears to be an easily achievable injection rate. Further, 34 gpm could easily be withdrawn from the Colorado River and filtered. In this regard the cooling reservoir could also be used as a settling and/or storage basin.

The pathline for ground-water flow from the STP produced by the near-field scheme is shown in Figure 6.7.3-8. It can be seen that the travel time to the Colorado River is over 1300 years. The potential surface resulting from implementation of the near-field scheme is shown in Figure 6.7.3-9. The spike produced by the scheme represents a maximum increase in potential relative to the pre-mitigated case of approximately 2 ft.

Far-field Injection/Withdrawal

The initial scheme for the far-field case included three wells at the locations shown in Figure 6.7.3-10. Again the target was to divert ground-water flow away from the Colorado River with a minimum combined injection rate. In this case the optimization procedure results stipulated that Well No. 1 pump with a steady-state injection rate of 31 gpm. The simulation results show that the travel time to the model boundary is also about 1300 years, a factor of three times the pre-mitigated travel time to the Colorado River. Figure 6.7.3-11 shows the travel path with this scheme which exits the model region along the X-axis. The modified of the potential surface, as illustrated in Figure 6.7.3-12, though more pronounced than that for the other schemes, represents only a 4 ft increase in head relative to the premitigated case.

A summary of results for the injection scheme evaluations is presented in Table 6.7.3-2. The table contains the total injection rate, travel time to the Colorado River and percentage increase in travel time relative to the pre-mitigated case. Similar to what was presented for the cutoff designs, an estimate is made of the radioactivity remaining in the ground water at the time of arrival at the Colorado River assuming a hypothetical release of 1×10^{16}pCi of a radionuclide having a 10,000 day half-live. Both schemes produced a greater than three-fold increase in the travel time, reducing the remaining radioactivity by 10 orders of magnitude.

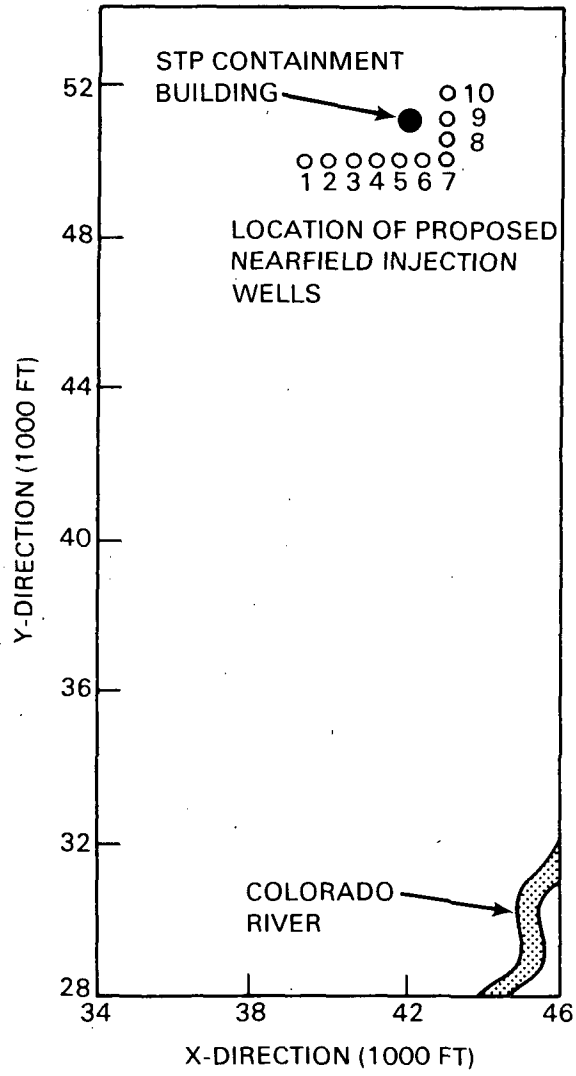

FIGURE 6.7.3-7. Proposed Near-Field Injection Scheme

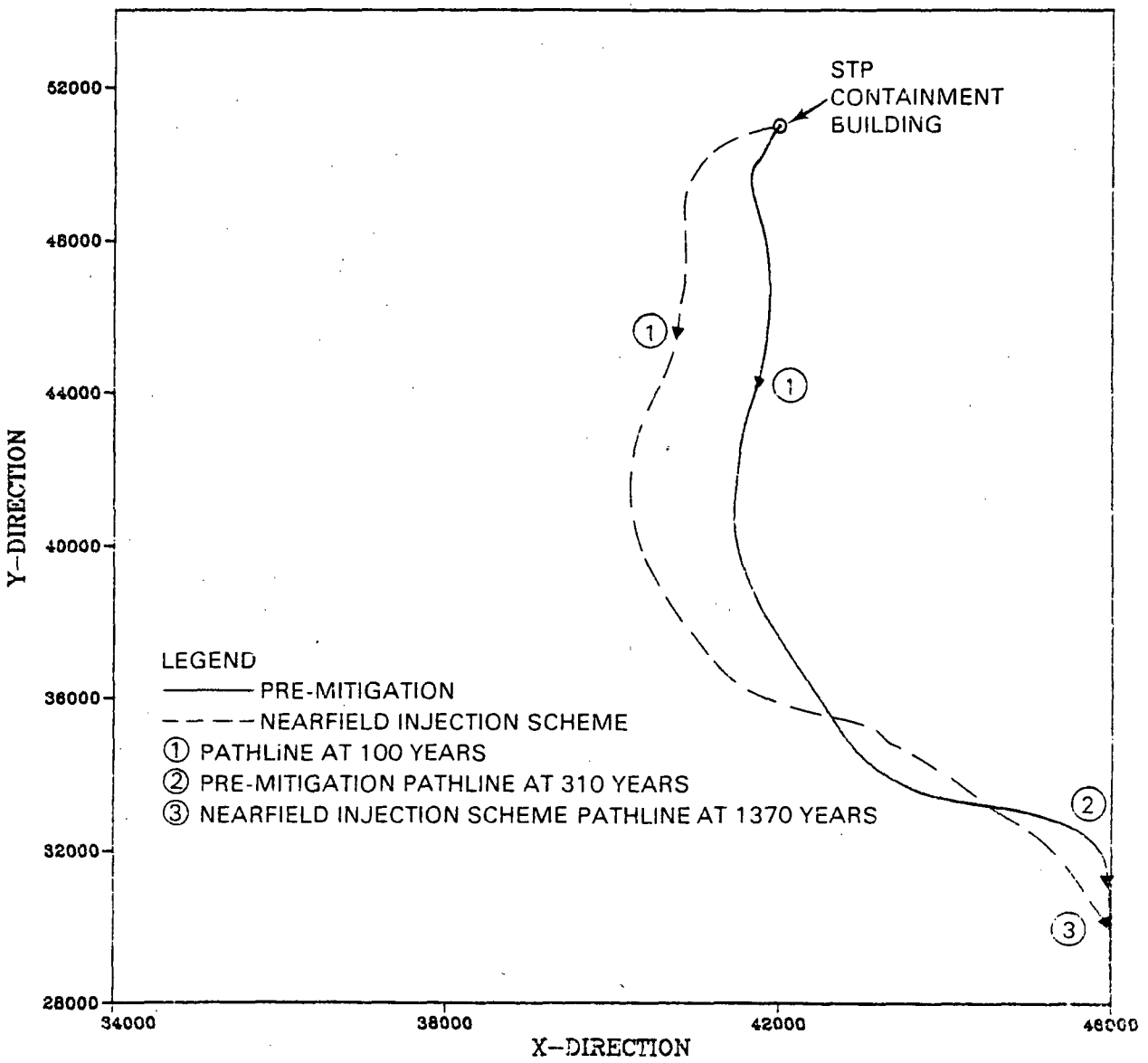

FIGURE 6.7.3-8. Simulated Pathline from the STP: With the Near-Field Injection Scheme

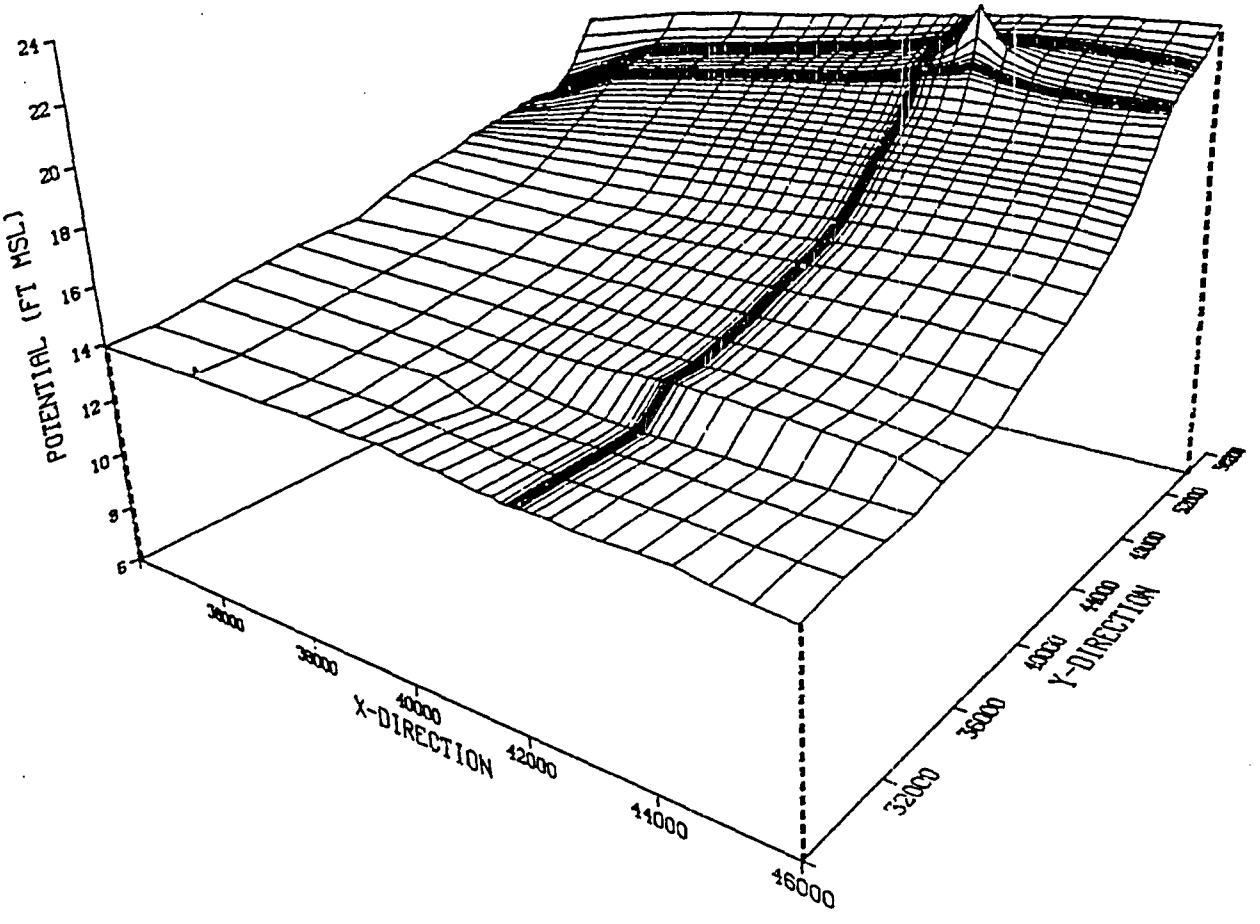

FIGURE 6.7.3-9. Simulated Potential Surface: With the Near-Field Injection Scheme

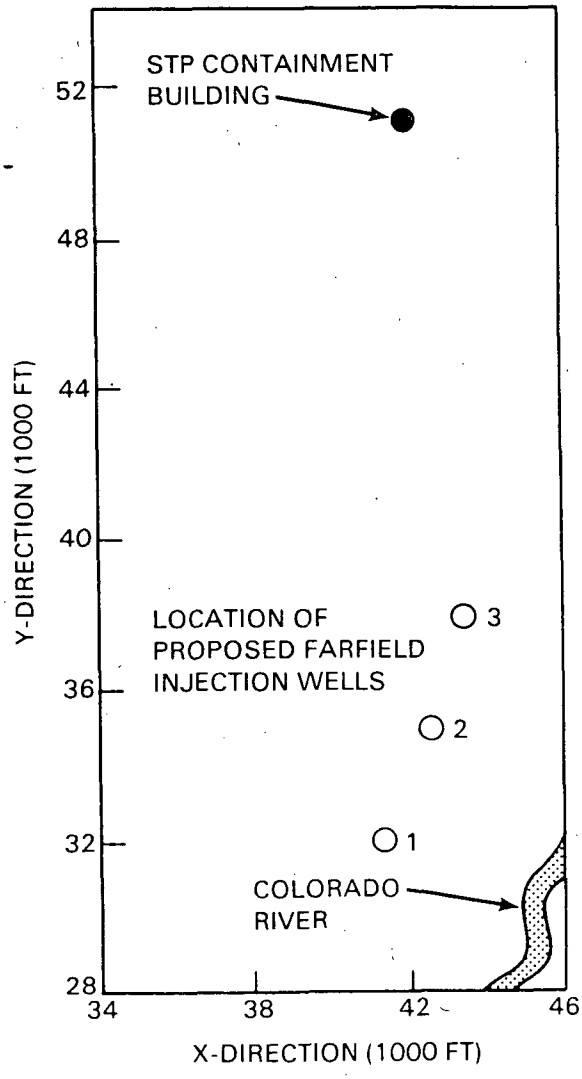

FIGURE 6.7.3-10. Proposed Far-Field Injection Scheme

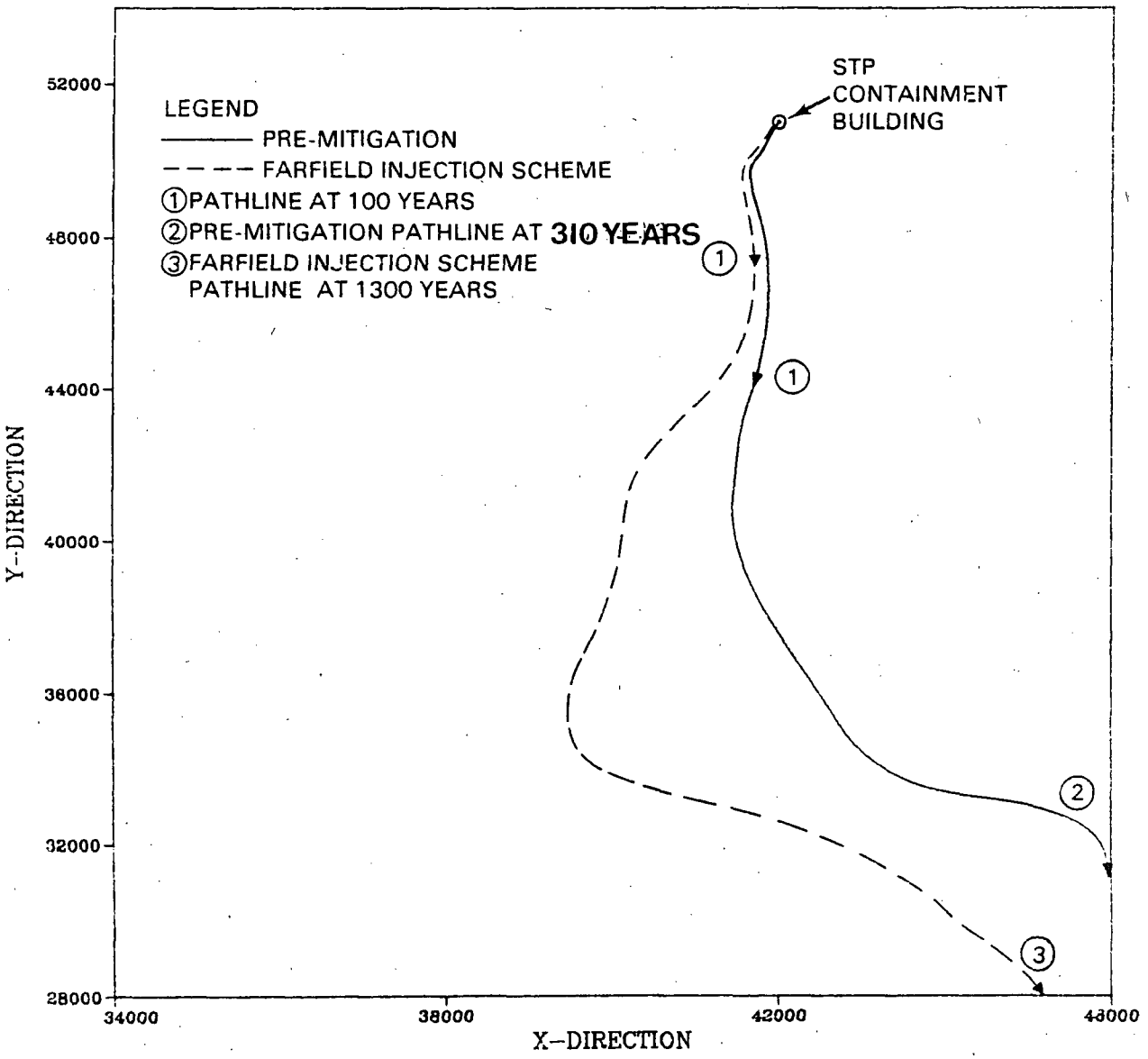

FIGURE 6.7.3-11. Simulated Pathline from the STP: With the Far-Field Injection Scheme

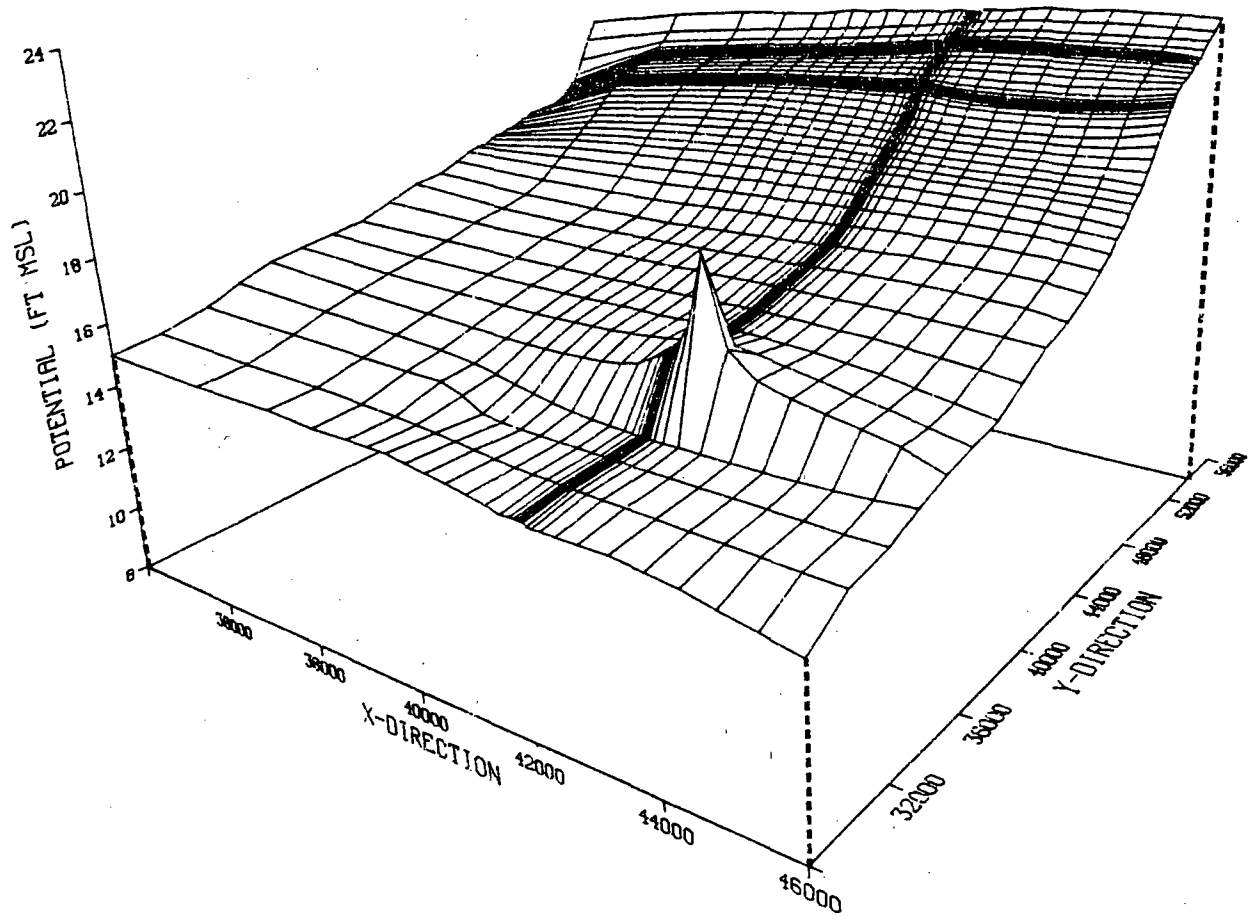

FIGURE 6.7.3-12. Simulated Potential Surface: With the Far-Field Injection Scheme

TABLE 6.7.3-2. Summary of Injection Scheme Evaluations

Scheme	Total Injection Rate, gpm	Travel Time to Colorado River, yr	Increase Relative to Pre-Mitigative Case	Radioactivity Remaining, pCi[(a)]
Pre-Mitigative	--	310	--	3.9×10^{12}
Near-field	36 gpm	1370	342%	8.9×10^{0}
Far-field	31 gpm	1300	320%	5.2×10^{1}

(a) Assuming an arbitrary half-life of 10,000 days and a release of 1×10^{16} pCi at time zero.

6.7.4 Conclusions

The primary objective of the STP case study is to develop and demonstrate general methodology for evaluating the desirability and feasibility of implementing ground-water contaminant mitigation strategies following a severe nuclear power plant accident. The study was conducted with readily available data sources including the STP Final Safety Analysis Report, regional hydrology reports, and the open literature. The level of technical detail attained in the case study results is commensurate with a reconnaissance or better level of analysis. The STP case study results include:

1. a detailed hydrogeologic characterization of a Texas Gulf Coastal Plain aquifer,

2. a complete discussion of data requirements, sources and procedures for the hydrogeologic characterization,

3. a two-dimensional ground-water flow and contaminant transport numerical model development based on the hydrogeologic characterization,

4. a baseline pre-mitigative analysis of radionuclide transport, and

5. a limited evaluation of the effect of selected engineered barriers and hydraulic barriers on radionuclide transport.

Major conclusions from the study results are the following:

1. flow and transport model simulation results show that following a severe accident at the STP ground-water radionuclide concentrations would be well below maximum permissible concentrations, therefore, mitigative action would not be necessary,

2. for the STP, all mitigation techniques evaluated significantly increased ground-water and contaminant travel times, and

3. model evaluations indicate that hydraulic and constructed barriers could prove to be effective in mitigating radionuclide discharges at the STP.

6.8 REFERENCES

Baker, E. T., Jr., and J. R. Wall. 1976. "Summary Appraisals of the Nations Ground-Water Resources - Texas Gulf Region," U.S. Geological Survey Professional Paper 813-F. U.S. Government Printing Office, Washington, D.C.

Bentall, R. 1963. "Methods of Determining Permeability, Transmissivity and Drawdown," Geological Survey Water-Supply Paper 1536-I. U.S. Department of the Interior, U.S. Geological Survey, Arlington, Virginia.

Boonstra, J., and N. A. de Ridder. 1981. Numerical Modeling of Groundwater Basins, International Institute for Land Reclamation and Improvement, Wageningen, The Netherlands.

Boutwell, S. H., S. M. Brown and B. R. Roberts. 1984. Selection of Models for Remedial Action Assessment, Anderson-Nichols and Co., Inc., Palo Alto, California.

Cole, C. R., F. W. Bond, S. M. Brown and G. W. Dawson. 1983. Demonstration/ Application of Ground-Water Modeling Technology for Evaluation of Remedial Action Alternatives, prepared by Pacific Northwest Laboratory, Richland, Washington, for the Municipal Environmental Research Laboratory, Environmental Protection Agency, Cincinati, Ohio.

Espenshade, E. B., Jr., ed. 1970. Goodes World Atlas, Rand McNally and Company, Chicago, Illinois.

Fried, J. J. and M. A. Combarnous. 1971. "Dispersion in Porous Media," in Advances in Hydroscience, Academic Press, New York, pp. 169-282.

Freeze, R. A., and J. A. Cherry. 1979. Groundwater, Prentice-Hall, Inc., Englewood Cliffs, New Jersey.

Gelhar, L. W. and C. J. Axness. 1981. Stochastic Analysis of Macrodispersion in Three-Dimensionally Heterogeneos Aquifers, Report No. H-8, Hydrologic Research Program, New Mexico Institute of Mining and Technology, Socorro, New Mexico.

Hammond, W. W., Jr. 1969. Ground-Water Resources of Matagorda County, Texas, Report 91, prepared by the Texas Water Development Board in cooperation with the Lower Colorado River Authority and Matagorda County Commissioners Court, Austin, Texas.

Houston Power and Light. 1978. Final Safety Analysis Report, South Texas Project Units 1 and 2, Houston, Texas.

Hunt, C. B. 1967. Physiography of the United States, W. H. Freeman and Company, San Francisco, California.

International Mathematical and Statistical Libraries, Inc. 1980. The IMSL Library Reference Manual. Edition 8. Houston, Texas.

Kincaid, C. T., J. R. Morrey and J. E. Rogers. 1983. Geohydrochemical Models for Solute Migration, Volume I, The Selection of Computer Codes and Description of Solute Migration Processes, prepared by Battelle, Pacific Northwest Laboratories, Richland, Washington, for the Electric Power Research Institute, Palo Alto, California.

Kruseman, G. P. and N. A. de Ridder. 1979. "Analysis and Evaluation of Pumping Tests Data," Bulletin 11, ILRI, Wageningen, The Netherlands.

Mercer, J. W., S. D. Thomas and B. Ross. 1982. Parameters and Variables Appearing in Repository Siting Models, prepared by Geotrans, Inc. under contract to Teknekron Research, Inc. for the U.S. Nuclear Regulatory Commission, NUREG/CR-3066.

Mercer, J. W. and C. R. Faust. 1980. "Ground-Water Modeling: An Overview," Ground Water, 15(2) pp. 108-115.

Molz, F. J., O. Guven and J. G. Melville. 1983. "An Examination of Scale Dependent Dispersion Coefficents," Ground Water, 21(6), pp. 715-725.

National Oceanic and Atmospheric Administration. 1980. Local Climatological Data-Annual Summaries for 1980, National Climatic Center, Asheville, North Carolina.

Niemczyk, S. J., et al. 1981. The Consequences from Liquid Pathways After a Reactor Meltdown Accident. U.S. Nuclear Regulatory Commission, NUREG/CR-1596.

Office of Water Data Coordination. 1977. National Handbook of Recommended Methods for Water-Data Acquisition, U.S. Geological Survey, Reston, Virginia.

Prickett, T. A., T. G. Naymik and C. G. Lonnquist. 1981. "A Random-Walk Solute Transport Model for Selected Groundwater Quality Evaluations," Bulletin 65, Illinois State Water Survey Division, Champaign, Illinois.

Prickett, T. A., and C. G. Lonnquist. 1971. Selected Digital Computer Techniques for Groundwater Resource Evaluation, Illinois State Water Survey Division, Urbana, Illinois.

Simmons, C. S. 1982. "A Stochastic-Convective Transport Representation of Dispersion in One-Dimensional Porous Media Systems," Water Resource Res., 18(4) pp. 1193-1214.

Simmons, C. S. and C. R. Cole. 1985. Guidelines for Selecting Codes for Groundwater Transport Modeling of Low-Level Waste Burial Sites. PNL-4980, Pacific Northwest Laboratory, Richland, Washington.

Stokes, W. L. 1966. Essentials of Earth History, Prentice-Hall, Inc., 2nd Ed., Englewood Cliffs, New Jersey.

U.S. Nuclear Regulatory Commission. 1978. Liquid Pathways Generic Study, NUREG-0440.

U.S. Nuclear Regulatory Commission. 1975. Reactor Safety Study: An Assessment of Accident Risks in U.S. Commercial Nuclear Power Plants, NUREG-15/014 USNRC, U.S. Government Printing Office, Washington, D.C.

Wang, H. S. and M. P. Anderson. 1982. Introduction to Groundwater Modeling-Finite Difference and Finite Element Methods, W. H. Freeman and Co., San Francisco.

Yeh, G. T. 1981. AT123D: Analytical Trans One-, Two-, and Three-Dimensional Simulation of Wast Transport in the Aquifer System, ORNL-5602, Oak Ridge National Laboratory, Oak Ridge, Tennessee.

7.0 SOUTH TEXAS PLANT - CASE STUDY NO. 2

7.1 INTRODUCTION

The South Texas Plant (STP) case study presented in this chapter is a continuation of analyses and results of Case Study No. 1 discussed in Chapter 6.0. The first case study focused on the hydrogeologic characterization and ground-water flow analysis for the STP. The study served to demonstrate the methods, procedures, and analyses necessary to evaluate, based on available information, the impact of mitigation on the ground-water flow regime of a specific site. Building on these results, Case Study No. 2 illustrates a more comprehensive (though not exhaustive) performance evaluation and trade-off analysis of mitigative strategy conceptual designs. Also provided is a discussion of the STP site configuration and the accompanying constraints the layout of plant facilities could have on the design, construction and implementation of mitigative measures. Referring to Figure 1.5-2, the STP case studies in composite are an illustrative example of a site-specific, reconnaissance level analysis and evaluation of strategies to mitigate the migration of radionuclides in a porous, unconsolidated geologic formation following a severe nuclear accident. It should be noted by the reader that much of the background information concerning the STP site characterization, data sources, etc., included in Chapter 6.0 are only summarized here. When appropriate, the reader is referred to specific sections in Chapter 6.0 if more detail is desired.

7.1.1 Case Study Objectives

The objectives of STP Case Study No. 2 are to utilize the conceptual and numerical models developed for STP Case Study No. 1 to accomplish the following:

- evaluate performance of an extensive array of mitigation alternatives including upgradient and downgradient engineered barriers (linear, L-shaped and U-shaped) and hydraulic barriers,
- assess the sensitivity of mitigation measure performance to design characteristics such as length, distance from the source, and effective barrier permeability,
- investigate the effects of hydrogeologic characteristics (e.g., hydraulic conductivity, retardation, dispersivity, etc.) on mitigation,
- consider the importance of the STP facilities' spatial configuration on mitigation measure design, and
- discuss cost as a factor in the evaluation and selection of mitigative strategies.

7.1.2 Case Study No. 2 Approach and Limitations

The two STP case studies were conducted based on the general methodology outlined in Section 6.1.3. Briefly, this methodology consists of four main steps:

Step 1. Survey of regional ground-water hydrogeologic characteristics and regional flow analysis to determine local boundary conditions.

Step 2. Pre-mitigative local ground-water flow and transport analysis.

Step 3. Performance evaluation of feasible mitigative techniques based on ground-water and contaminant transport simulation.

Step 4. Sensitivity analyses of contaminant transport to hydrogeologic parameters.

Part of the focus of Case Study No. 1 was to accomplish Step 1 above for the STP site. The available hydrogeologic data were reviewed and analyzed leading to the development of conceptual and numerical models for the STP site regional ground-water flow system (described in Sections 6.2, 6.3, and 6.4). Also within the first case study, a pre-mitigative local transport analysis and limited evaluations of selected mitigative techniques were conducted.

Taking advantage of the site characterization conducted for the first case study, Case Study No. 2 begins with a pre-mitigative flow and transport analysis and continues with a comprehensive performance evaluation of numerous mitigation alternatives and the sensitivity of their performance to specific hydrogeologic parameters. The TRANS two-dimensional ground-water flow and transport code (Prickett et al. 1981) was used throughout the two studies. A brief description of the capabilities and the main governing of the TRANS code are provided in Appendix C. As discussed in Section 6.1.4, only previously published data are used. Required data that are unavailable are estimated based on the best information available and/or engineering judgment. Other limitations to the analysis discussed in Section 6.1.4 apply equally to Case Study No. 2.

7.2 DEFINITION OF CASE STUDY NO. 2

As noted above, the reader is referred to Chapter 6 for a detailed description of the STP site location, reactor design and underlying ground-water system. In this chapter it is sufficient to present a brief summary of this information.

7.2.1 Physical Setting and Site Description

The STP is located in south-central Matagorda County, Texas adjacent to the Colorado River approximately 10.6 mi inland from Matagorda Bay, which opens into the Gulf of Mexico. The surrounding area consists of low relief, abandoned river valleys and marshes, and it is within the humid subtropical region of Texas. The plant is situated on the Pleistocene Beaumont Formation

which extends at least 700 ft below the site. The formation consists of clay, sandy clay, and thick sand units. Available data indicate there are two hydrostratigraphic units underlying the site: a deep aquifer at depths greater than 300 ft, and a shallow aquifer consisting of upper and lower units ranging between 90 ft and 150 ft below the land surface. The two units of the shallow aquifer are separated locally by a 20-ft thick clay layer that pinches out south of site (Houston Power and Light 1978). For the convenience of the reader Figure 6.3.2-17, an illustration of the conceptual model for the STP site, is included here as Figure 7.2.1-1. The figure depicts the underlying geologic units and the general directions of ground-water flow in the vicinity of the plant.

7.2.2 STP Facilities Description and Configuration

For several reasons, the general configuration of the STP facilities would be an important factor in the design and implementation of possible mitigative actions subsequent to a severe accident. The power station is composed of two identical pressurized water reactors (PWR). Several of the plant structures important to safe operation and shutdown of the plant (located in Figure 7.2.2-2) are shared by both units including the cooling reservoir, makeup pumping station, spillway and blowdown facilities, essential cooling pond, emergency transformer and switchyard (Houston Power and Light 1978). If continued operation of one unit is important, a key element of any mitigation design would be maintenance of essential functions such as reactor cooling and power transmission. For example, engineered barriers would have to be located outside the cooling reservoir and essential cooling pond to maintain their integrity as reliable sources of cooling water.

Plant structures also serve as physical obstacles that would influence location of engineered barriers (e.g., it might be difficult to construct a grout curtain or slurry wall within the switchyard). Another consideration would be the likelihood that water impounded by the cooling reservoir and essential cooling pond will be contaminated by atmospheric fallout. To prevent release of contaminated, reservoir water, it would be necessary to avoid damaging the impoundment embankments during mitigation construction.

Each of the principal site structures and their functions are discussed below. The influence each of these structures would have on design of specific mitigation measures is discussed in Section 7.5.

The STP site occupies approximately 12,220 acres with principal structures placed as shown in Figure 7.2.2-1. Each of the two units has a reactor core-rated thermal power of 3,800 MWt and net electrical power output of 1,250 MWe. The two units, located on a detailed plan view of the plant area in Figure 7.2.2-2, are approximately 600 ft apart. The reactor containment structures for both units are post-tensioned concrete cylinders with steel liner plates, hemispherical tops and flat bottoms. The cylinders have inside diameters of 150 ft, are 166 ft 3 in. high and 4-ft thick walls. The basemat is 18 ft thick. The containments are designed to withstand the internal pressure and temperature associated with the mass and energy release of a loss of coolant accident (Houston Power and Light 1978).

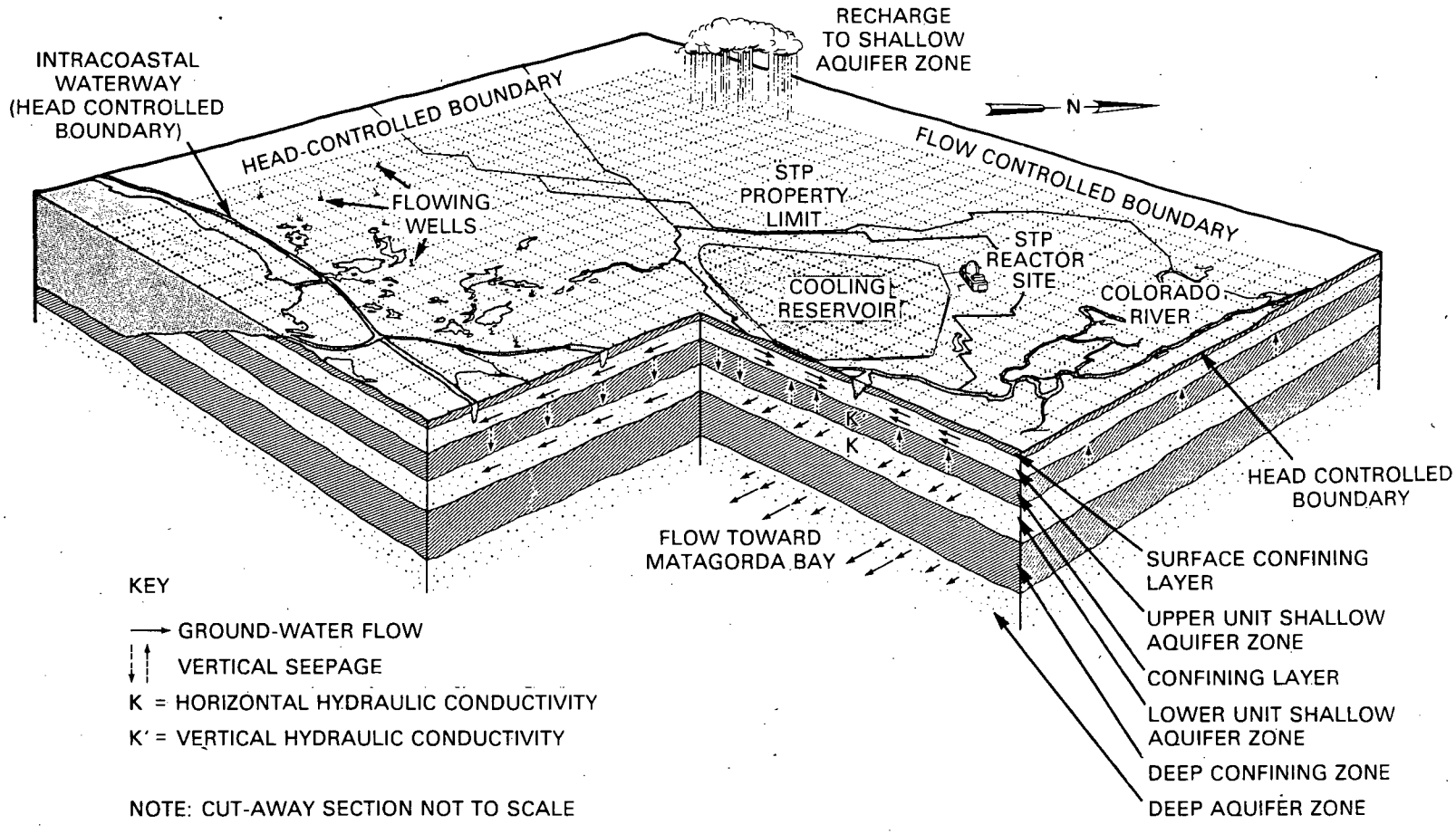

FIGURE 7.2.1-1. Illustration of the Conceptual Model for the STP Site.

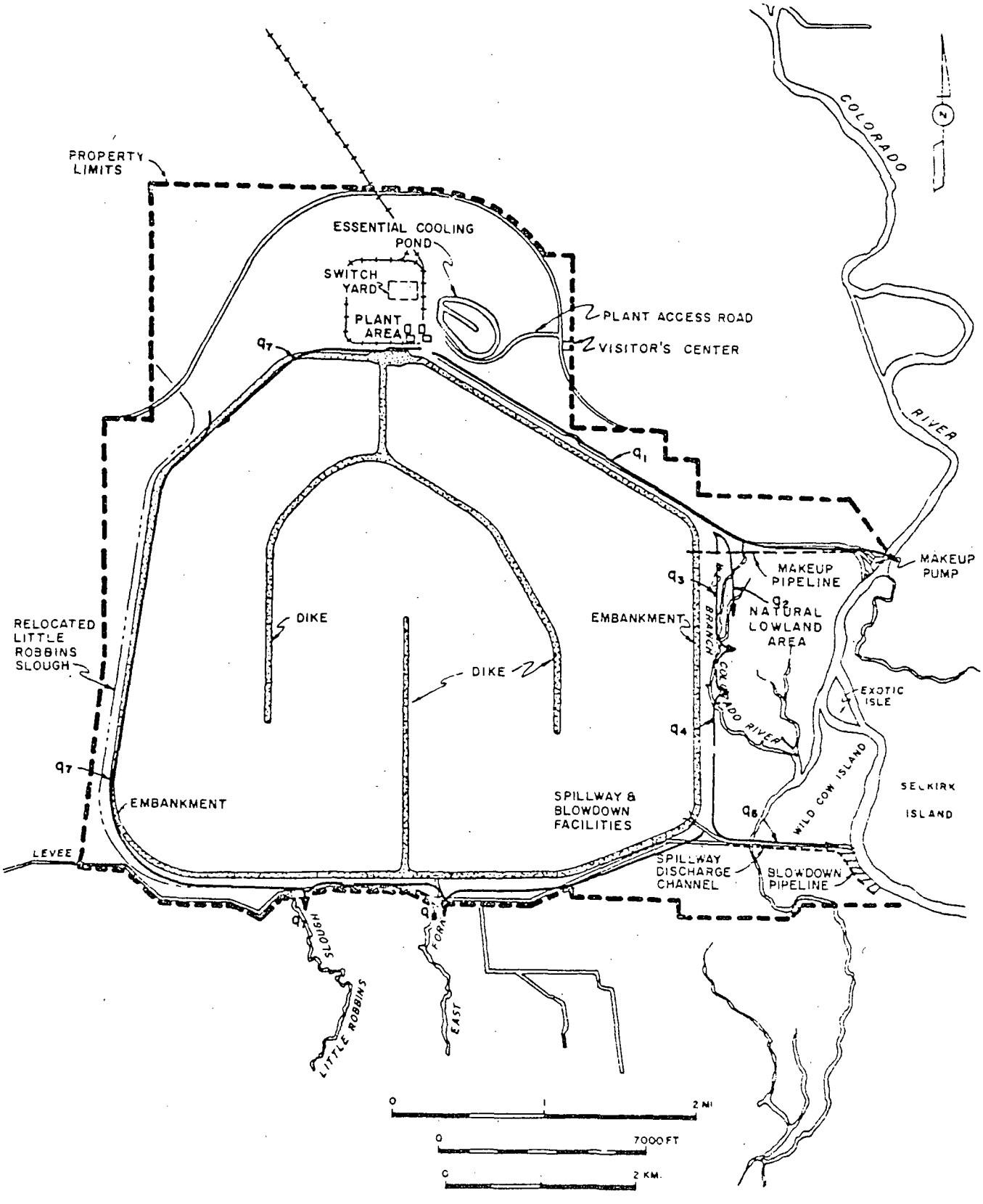

FIGURE 7.2.2-1. STP Plant Area (Source: Houston Power and Light 1978).

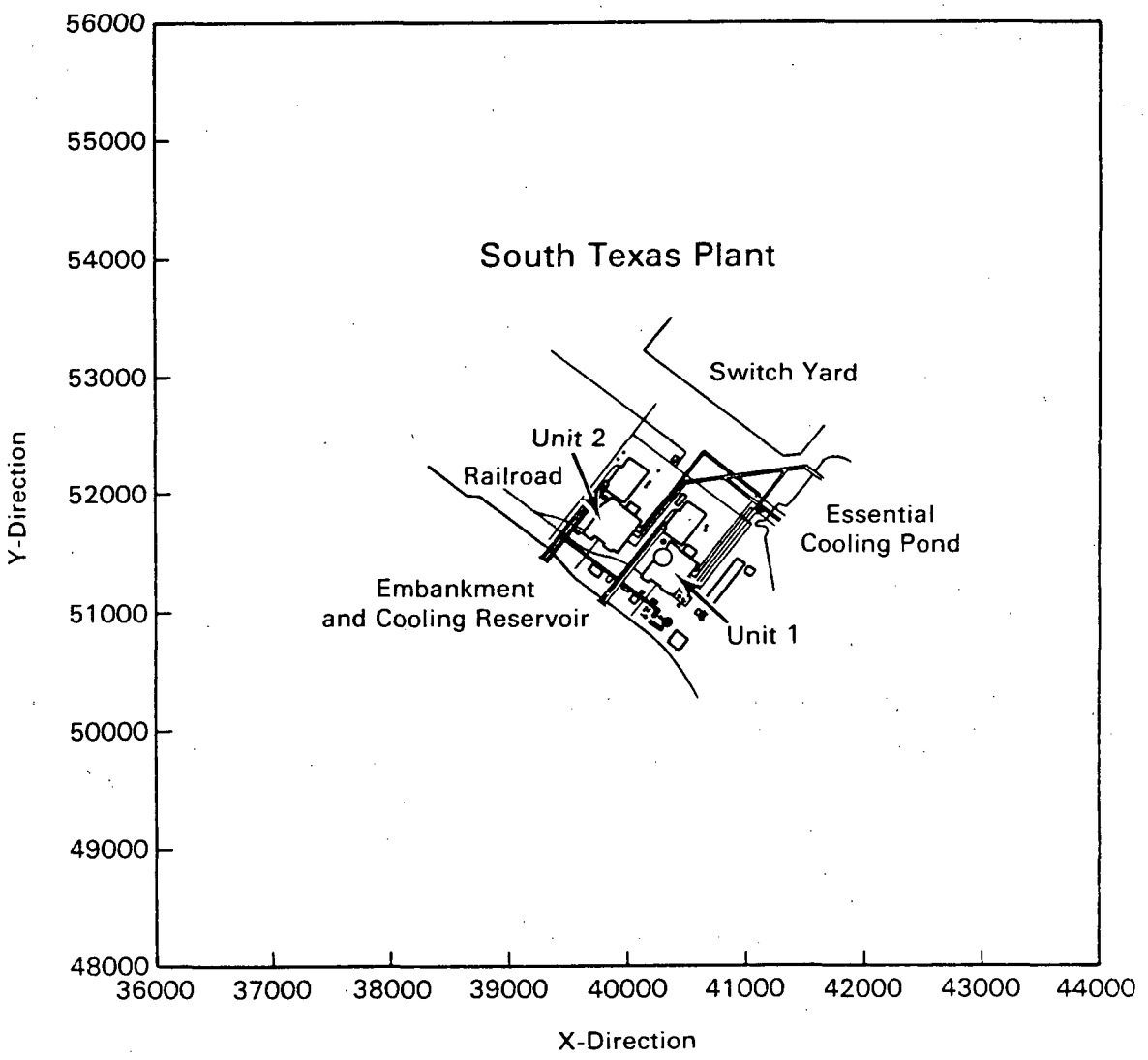

FIGURE 7.2.2-2. Detailed Plan View of STP Configuration.

The STP cooling reservoir covers an area of 7,000 acres and is contained within an 65,500-ft embankment having a crest elevation of 66.25 ft MSL (plant grade elevation is 28 ft MSL). The reservoir is over 3 mi long extending from its north embankment about 550 ft south of the reactor containment buildings to the south end of the STP property limit. The purpose of the reservoir is to dissipate the excess heat from the circulating cooling water. Condenser cooling water is discharged into the western half of the reservoir and directed along a circuitous path by a baffle system to the power plant intakes located in the eastern half of the reservoir. Water for the reservoir is supplied from the Colorado River. Blowdown to control reservoir water quality is discharged into the Colorado River near the southeast corner of the reservoir. The essential cooling pond is a 48-acre offstream impoundment located east of the plant area that derives water from the cooling reservoir and has a 530-gpm

backup well. The pond supplies cooling water for safe shutdown of the plant during normal operations and serves as the ultimate heat sink under postulated accident conditions. The STP's transmission system facilities, located north of the plant area, include a 345-kV switchyard and a 138-kV emergency transformer. The switchyard covers a rectangular area of about 12 acres. When power is unavailable from the main generator, the system provides reliable power for simultaneous normal shutdown of both units or concurrent shutdown of one unit and a design basis accident in the other (Houston Power and Light 1978).

7.2.3 Definition of Accident Scenario

The STP is a PWR incorporating a double loop for removal of heat from the reactor core. As discussed in Section 6.2.3, the postulated severe accident for the STP occurs when insufficient heat is removed from the reactor and the core materials overheat to the melting point. The hot core materials could then melt through the concrete basemat of the reactor containment building, allowing radioactive debris to enter geologic materials below the plant (USNRC 1975). The debris containing nuclear fuel, steel and liquefied geomaterials would begin cooling and solidifying once it entered the substratum. A period of approximately one year would be required for sufficient cooling of the debris to occur to allow ground water to flow through and around the melt mass and begin transporting contaminant away from the site (Niemczyk et al. 1981).

In addition to core debris, another possible source of contamination following a severe accident at the STP is the cooling water and water used in emergency spray systems. This water (referred to as sump water) could collect in the containment building sump, become contaminated in the accident process, and be released to the stratum beneath the plant.

The depth of penetration of the core melt into the earth below the containment basemat is a function of the accident sequence, size of the reactor and the chemical composition of the geologic materials. The clay and sand units underlying the STP are composed primarily of silicic minerals. The shape of the core melt penetration into silicate material has been calculated by Niemczyk et al. (1981): the core debris would be approximately cylindrical with a radius of roughly 29 ft at a depth of 35 ft below the basemat. At the STP site, this depth would coincide with an elevation of about 80 ft below MSL. Thus, the core debris would reside in the lower unit of the shallow-zone aquifer (see Section 6.3.2 for a detailed characterization of the STP site hydrogeology). The deep aquifer, which is the source of fresh water in the region, would be isolated from the core melt by a 150-ft-thick clay confining layer. Thus, it is assumed that the lower unit of the shallow aquifer would transport the majority of the radionuclides away from the site. Figure 7.2.3-1 is a schematic showing the final configuration of the core melt debris relative to the reactor basemat and the underlying units.

For the purposes of pre- and post-mitigation contaminant transport analysis following a severe accident at the STP, the focus is on radionuclides that: 1) have long half-lives and would not decay to low levels very soon after an accident, or 2) are in large quantities that are not strongly sorbed and

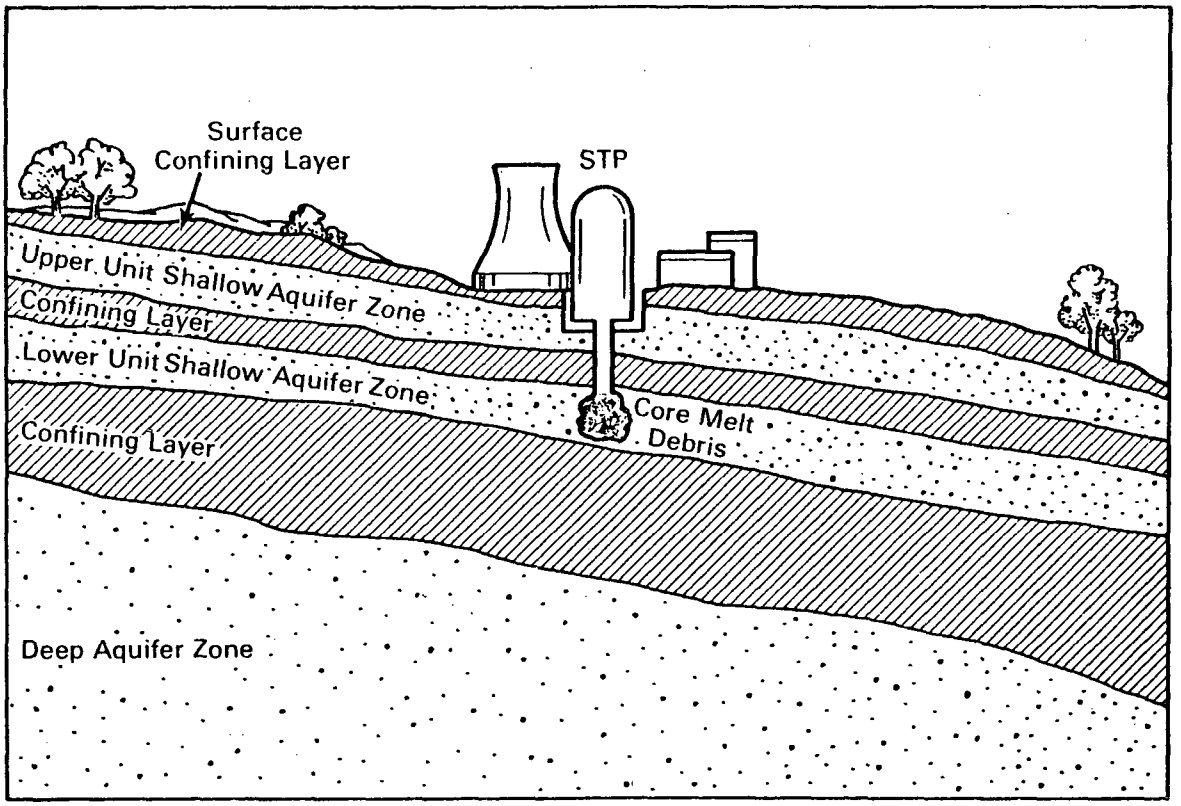

FIGURE 7.2.3-1. Assumed Location of the Core Melt Debris Subsequent to a Severe Reactor Accident at the STP.

thus could potentially migrate away from the site in high concentrations. As discussed in Section 6.2.3, strontium-90 was selected as the most appropriate indicator radionuclide on which to base pre- and post-mitigation transport analyses at the STP. The hypothesized leach release rate of strontium-90 into the shallow aquifer as a function of time following the initiation of leaching (approximately one year after the accident) is plotted in Figure 7.2.3-2. This curve includes only the core melt debris leach release and was determined assuming 4.53×10^{18} pCi of strontium-90 are initially present following a severe accident for a single unit of the STP and that 89% of the strontium-90 is contained in the core melt debris leach release and the remaining 11% in the sump water release.

7.3 MODEL DEVELOPMENT

The ground-water flow and transport analyses for the STP site are accomplished using a two-stage modeling approach. The first stage utilizes a course grid regional hydrologic flow model. The purpose of the regional model is to establish boundary conditions for the local model under both pre- and post-mitigation conditions. The local model is then used to simulate the ground-water system in the immediate area of the plant in greater detail.

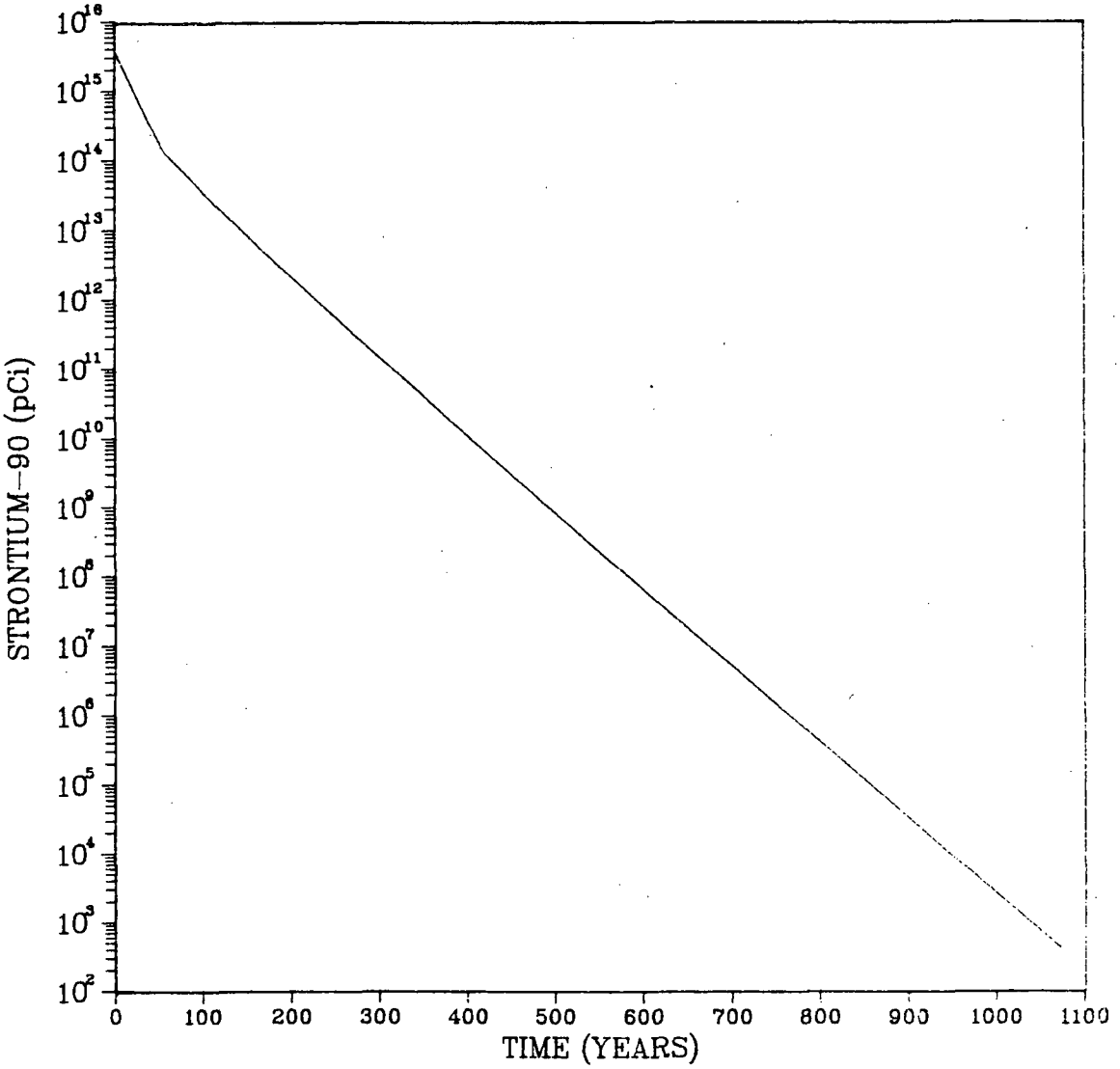

FIGURE 7.2.3-2. Hypothesized STP Leach Release of Strontium-90.

While the regional model used in this case study is the same as that developed for STP Case Study No. 1 without modification, a modified, higher resolution local model is employed.

Development of the regional model is discussed in Section 6.4, including: use of available data, model parameter values selected, and model calibration results. The new local model allows consideration of the STP plant facilities configuration and provides greater flexibility in siting mitigation measures (i.e., engineered and hydraulic barriers) within the model grid. This is accomplished by reducing the areal extent of the local model from 11.2 square miles (12,000 ft x 26,000 ft) to 2.3 square miles (8,000 ft x 8,000 ft) and by increasing the number of grid nodes from 33 x 58 to 55 x 63. The location and extent of the new local study area relative to the regional model grid and

original local study area is delineated in Figure 7.3-1. Figure 7.3-2 shows the STP facilities superimposed on the new local grid. The reader is reminded that the model grids are oriented such that the general ground-water flow direction is approximately parallel to the y-direction.

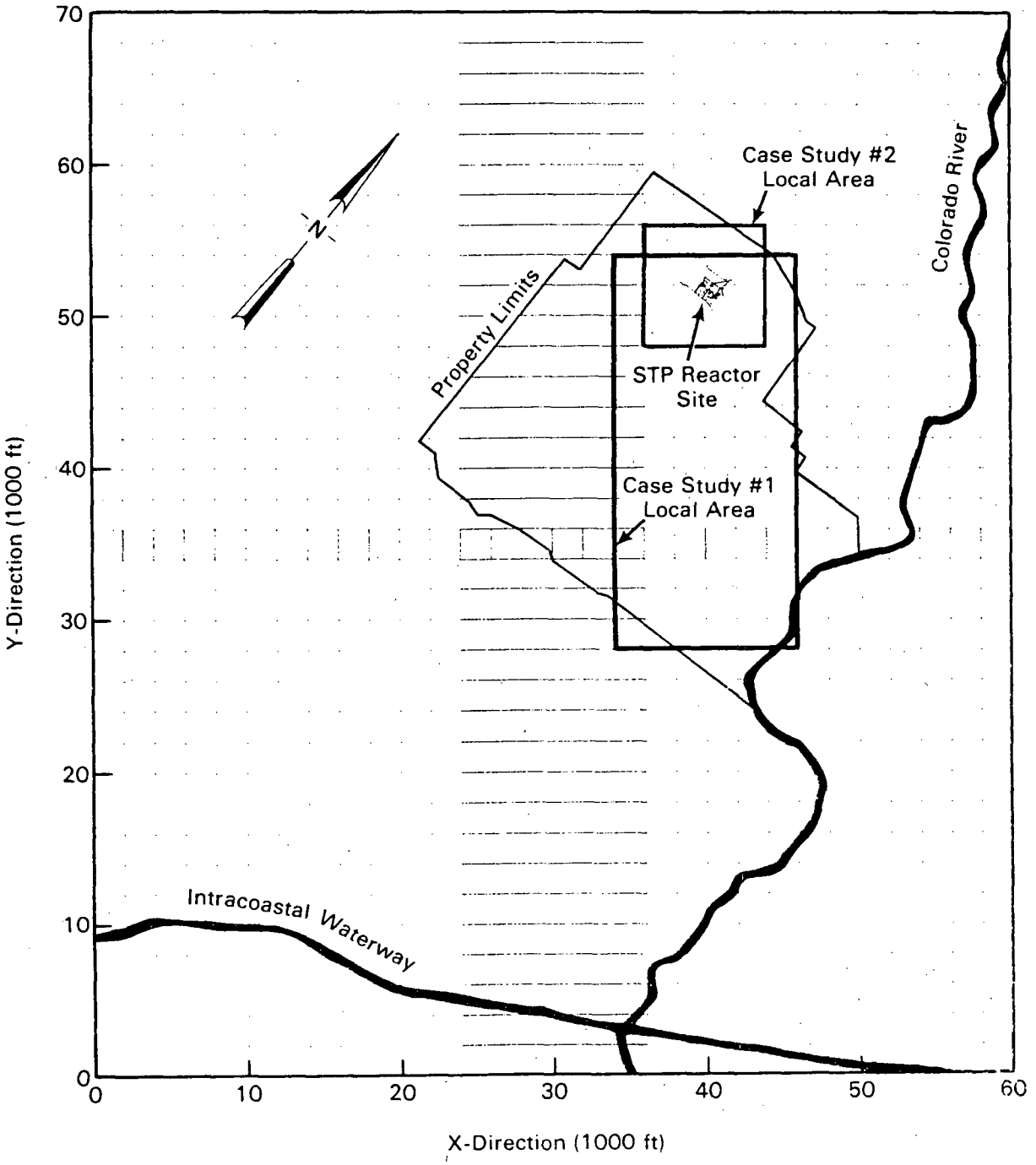

FIGURE 7.3-1. STP Case Study No. 2 Local Study Area.

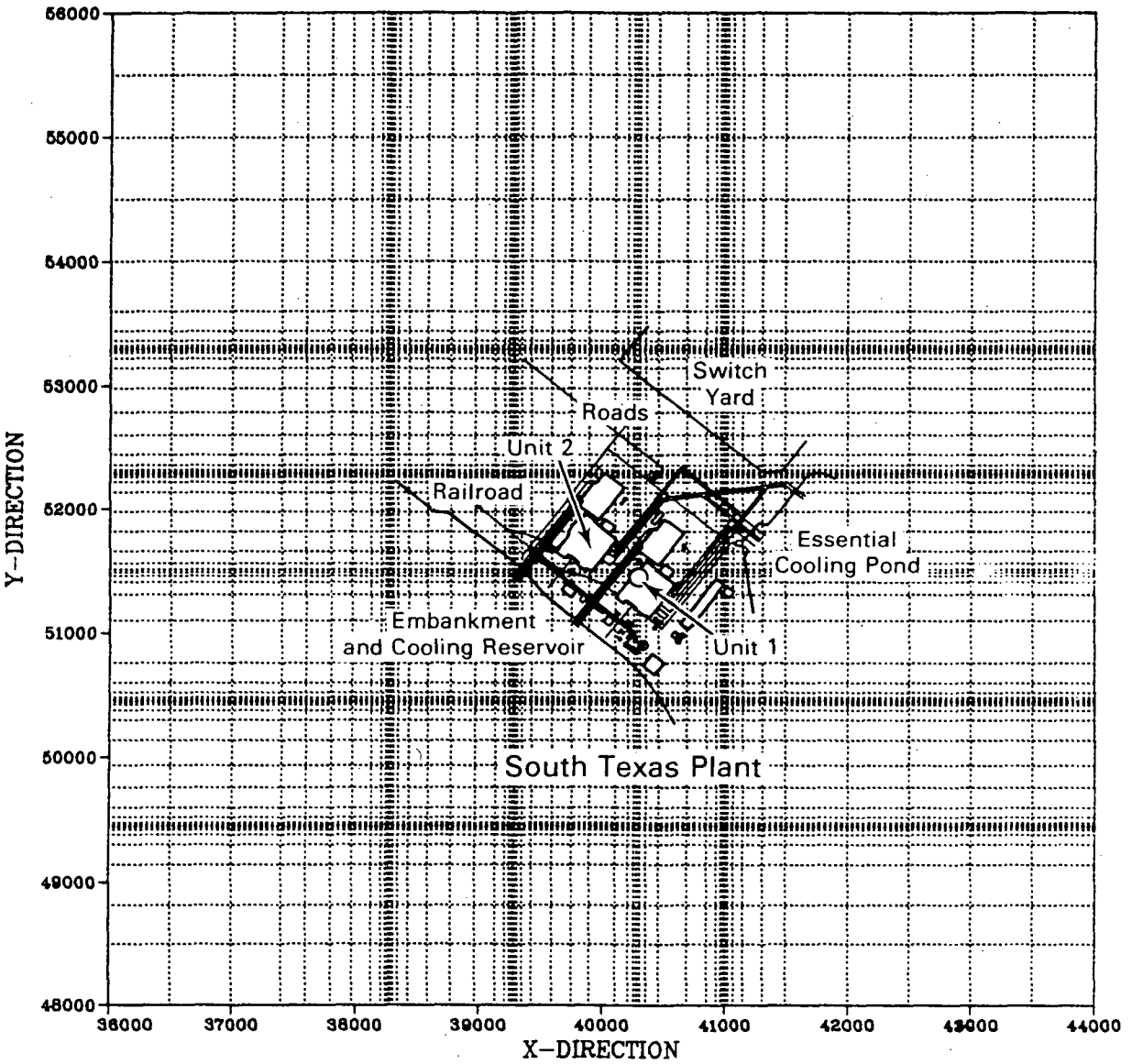

FIGURE 7.3-2. STP Case Study No. 2 Local Model Grid.

The boundary and initial conditions for the new local model are determined directly from the regional model. The procedure followed is to first run the regional model and then determine the potentials for the local model boundary from the regional model simulation results. Other local model parameters were also interpolated directly from the regional model including the lower shallow-zone aquifer top and bottom, hydraulic conductivities and the recharge/discharge rates from/to the upper shallow-zone aquifer. Potential contours for the local study area (plotted in Figure 7.3-3) vary somewhat uniformly from about 22 ft MSL at the upper boundary to 17 ft MSL at the lower boundary, producing a relatively flat average gradient of about 0.0006 ft/ft. The spatial distribution of hydraulic conductivities is illustrated by the

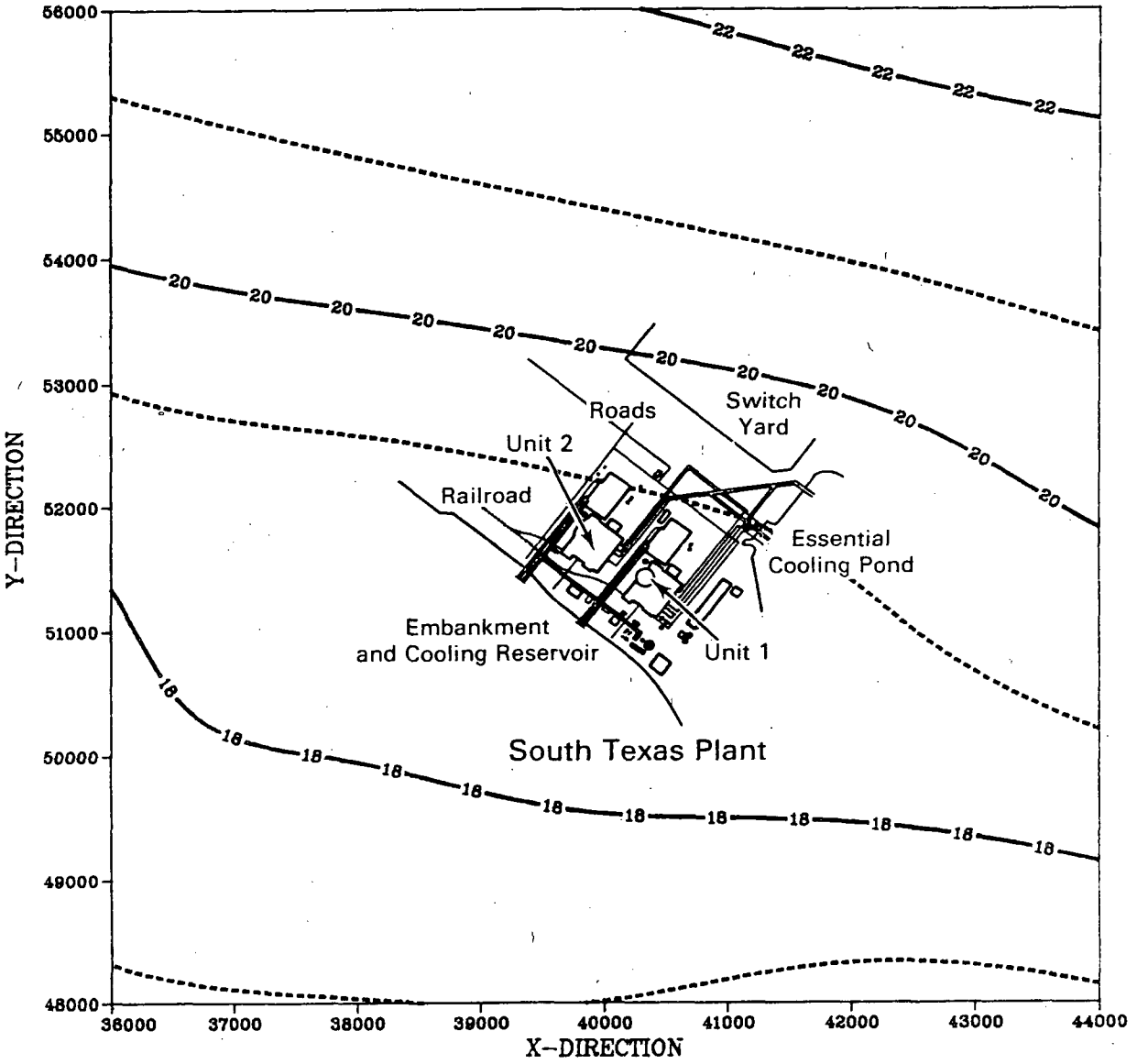

FIGURE 7.3-3. Observed Potential Contours For the Local Study Area.

three-dimensional surface plot presented in Figure 7.3-4. In contrast to the regional model distribution in Figure 6.4.3-1 which show distinct discontinuities (as determined through calibration), the surface for the local hydraulic conductivities includes the minor smoothing effects due to the transfer to the local model by interpolation. The variation in conductivities in the local area is characterized by a region of high values of about 1,500 gpd/sq ft in the center of the local area extending to the west boundary. Values are lower over the rest of the area, generally ranging from about 200 to 500 gpd/sq ft. In the immediate vicinity of the plant (noted in Figure 7.3-4) the conductivity is high and decreases in the down-gradient direction. Vertical ground-water movement within the local area is from the upper zone of the shallow aquifer

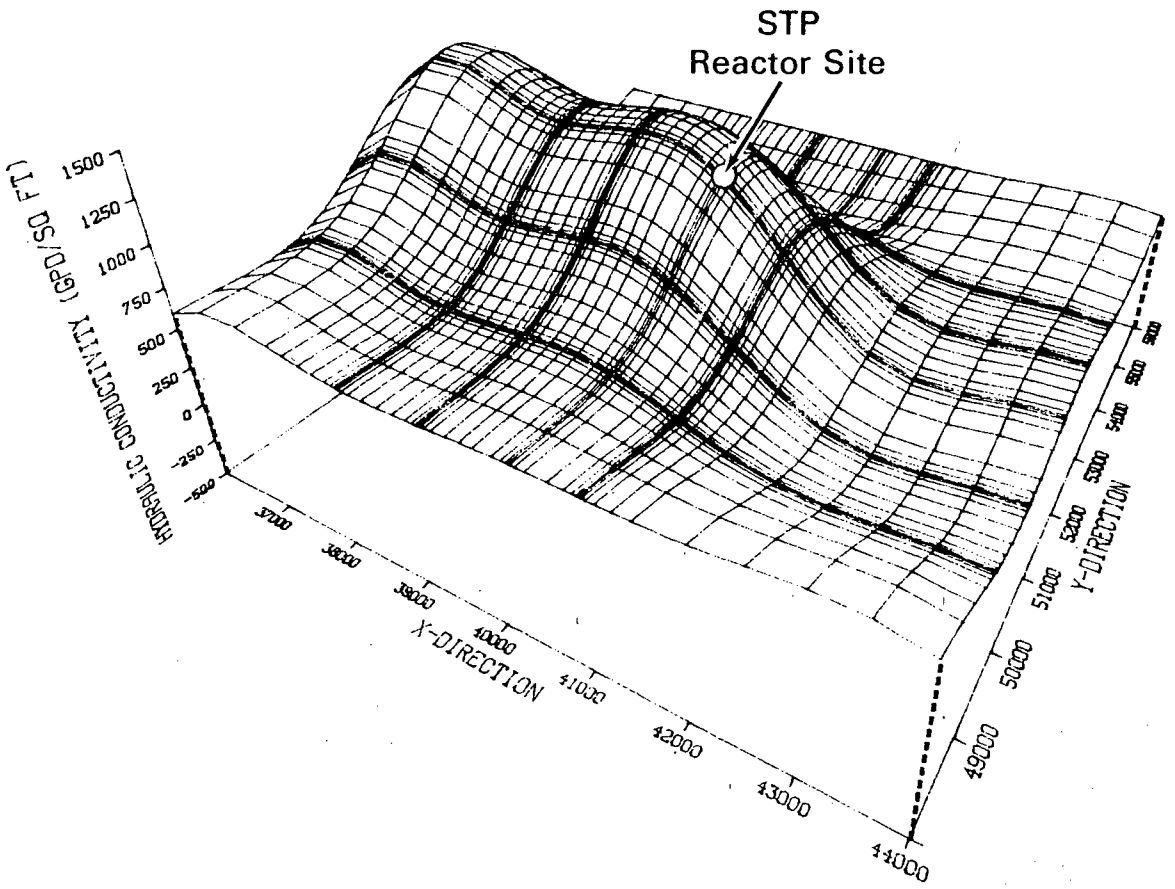

FIGURE 7.3-4. Hydraulic Conductivities for the STP Local Model.

into the lower zone (i..e., recharge to the study aquifer) and is spatially fairly uniform. The estimated average recharge rate over the local area, based on calibration of the regional model (see Section 6.4.3) is approximately 0.0005 gpd/sq ft or about 0.3 in/year.

As a check on the interpolation process used in transferring parameters and aquifer properties from the regional model to the local model, the potential contours were simulated by the local model and compared to the observed values. The simulated potentials are plotted in Figure 7.3-5. The greatest difference between the two sets of contours occurs in the center of the model area where the simulated results are about 0.5 ft lower than the observed. Overall the simulated and observed values compare favorably, providing a psuedo-verification that the local model adequately represents the ground-water flow system and can be useful in evaluating pre- and post-mitigation analyses.

Because of the total lack of observed radionuclide transport data at the STP site, estimates of transport modeling parameters (i.e., soil bulk density, effective porosity, retardation factor, and dispersivity coefficients) are

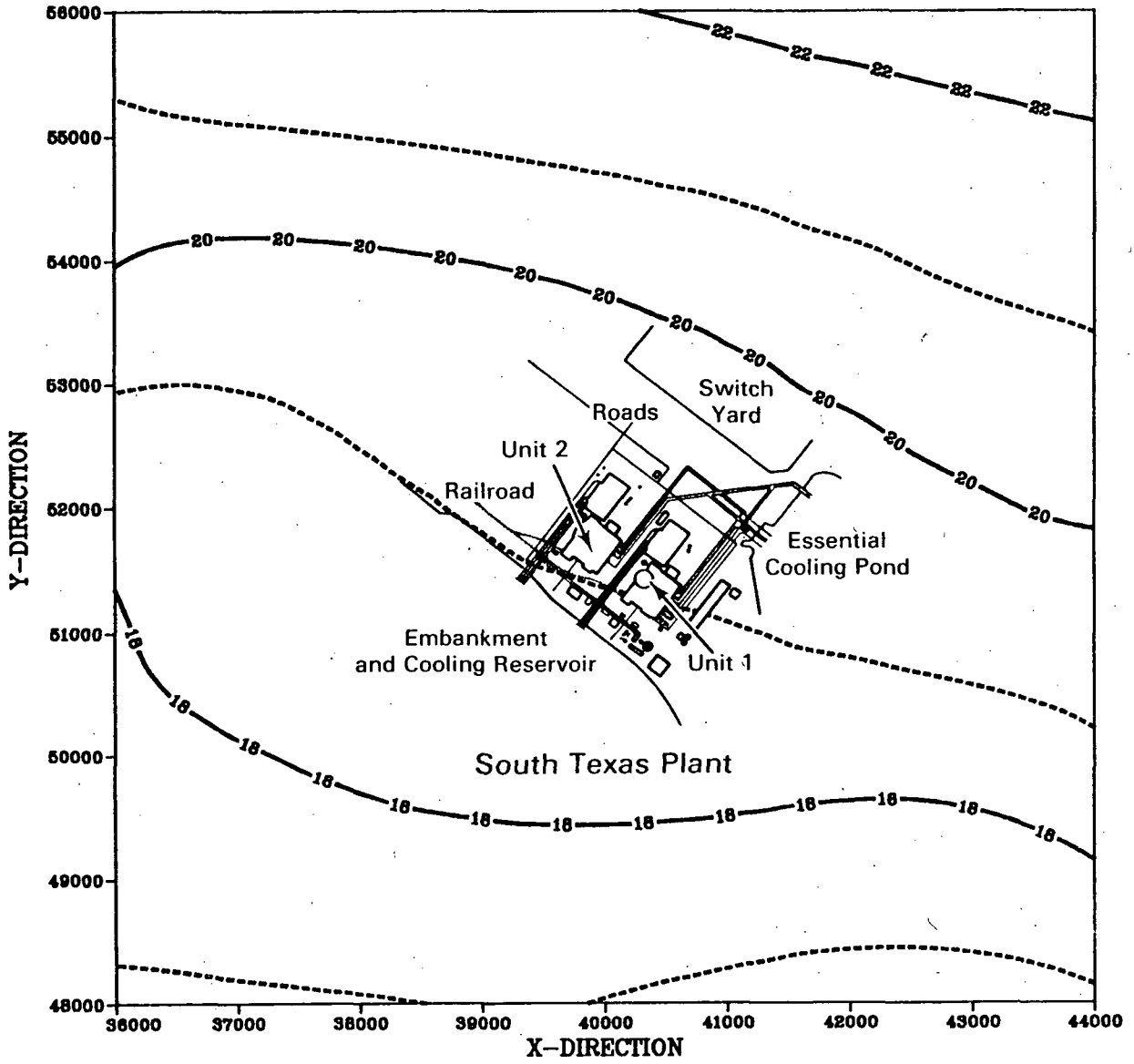

FIGURE 7.3-5. Simulated Potential Contours for the Local Study Area.

based entirely on previously published information. The values used for the local model utilized in Case Study No. 2 are the same as those used in the first case study with one exception. The values used and the information source for each are discussed in Section 6.6.1 and listed in Table 7.3-1. The only change to this list is the increase of the number of particles (NP) from 5,000 to 10,000; therefore, individual particles represent half as much contaminant, providing greater resolution for analyzing the transport simulation results. A sensitivity analysis of these parameters and their effect on mitigation performance is presented in Section 7.5.

TABLE 7.3-1. Summary of TRANS Transport Parameters for STP Case Study No. 2 Transport Simulations

Parameter	Value	Source
Longitudinal Dispersivity (D_L)	164 ft	Gelhar and Axness (1981)
Transverse Dispersivity (D_T)	8 ft	Computed; DL/20
Distribution Coefficient (K_d)	10 ml/g	Table 3.3.2-2
Effective Porosity (η_e)	37%	STP FSAR [Houston Power and Light (1978)]
Bulk Density (ρ_b)	10^4 lb/ft^3	Computed
Retardation Factor (R_d)	46	Computed
Number of Particles (Np)	10,000	Prickett et al. (1981)

7.4 PRE-MITIGATIVE LOCAL TRANSPORT RESULTS

The purpose of the a severe accident pre-mitigative transport analysis is twofold:

1. quantitatively assess the need for mitigation, and

2. when mitigation is found to be necessary, provide a baseline for evaluating relative mitigation performance.

On the basis of Case Study No. 1 results it was determined that after 1000 years subsequent to the assumed severe accident, transport of significant quantities of radionuclides was limited to a distance of approximately 2400 ft. The results also indicate that by 1000 years dilution and natural decay would reduce the maximum concentration within the contaminant plume to about 20×10^{-4} pCi/ml, a level well below the maximum permissible concentration of 0.3 pCi/ml set for strontium-90 by 10 CFR Part 20 (USNRC 1978).

However, as previously noted, the STP still provides a vehicle far analyzing mitigation performance. Conclusions regarding the need for mitigation in Case Study No. 1 were based on the prevention of significant radionuclide releases to the Colorado River. The new local model, which encompasses a smaller area with greater spatial resolution, facilitates incorporation of an alternative objective for possible mitigation measures, (i.e., containment of radionuclide contamination within, or close to the immediate plant area). Such would be the case if it were determined that the ultimate course of action in response to a severe accident was site restoration (i.e., removal and safe storage of contaminated material). It would then be desirable to minimize, through mitigation, the quantity of geologic material contaminated by migrating radionuclides. In light of this possibility, the pre-mitigation radionuclide transport for the STP was reanalyzed using the new local model to determine the extent of the unmitigated contaminant migration

with time and to provide the basis for evaluating the relative benefits (i.e., reduction in contaminant flux) derived from selected mitigation measure designs. The approach used to assess the pre-mitigated condition at the STP was to simulate the steady-state flow condition and the transient leach release and transport of the strontium-90.

The results of the pre-mitigation analysis are consistent with those of Case Study No. 1. Three-dimensional plots showing the simulated spatial distribution of strontium-90 concentration at 100 years and 1000 years following the accident are presented in Figures 7.4-1 and 7.4-2, respectively. Similar to the results obtained from the Case Study No. 1 local model, these plots illustrate significant reduction in concentrations with time due to dilution and natural decay. In addition, both models indicate that the combination of fairly flat potential gradient in the study aquifer and the sorption of strontium-90 limit the extent of migration to approximately 2000 ft downgradient of the reactor site.

In analyzing the pre-mitigation simulation results as the baseline for evaluation of mitigation alternatives, the objective of the mitigation is very important. As discussed above, the assumed purpose of the mitigation measures in Case Study No. 2 is to limit the areal extent of radionuclide migration to allow future contaminant removal and site restoration at minimal risk to the environment and minimal cost. Figures 7.4-1 and 7.4-2 illustrate qualitatively the concentration levels and lateral extent of the pre-mitigative radionuclide movement at their respective times. These plots do not provide for quantitative comparison between pre-mitigative and post-mitigation results. Therefore, the approach used to assess mitigation performance is to determine the resulting contaminant flux as a function of time at a common downgradient location. The section 800 ft downgradient from the reactor site was selected as the location for the flux determinations for all cases, and is referred to as the "breakthrough section." This section is sufficiently distant from the site while being upstream of the downgradient mitigation measures to be evaluated. The effectiveness of a given mitigation measure in reducing contaminant flux serves as an index to its performance in contamination containment. For example, Figure 7.4-3 shows superimposed on the source release curve, the pre-mitigated flux (pCi/yr) of strontium-90 at the breakthrough section. The travel time for strontium-90 to the breakthrough is greater than 200 years. The maximum flux rate is about 6.2 x 10 9 pCi/yr and decays to less than 3 x 10 5 pCi/yr by the year 1000. The main implication from the pre-mitigated results is that on the order of 200 years are available for implementation of mitigation. Also, if site restoration were desirable prior to that time the contamination would be limited to a distance of less than 500 ft from the plant.

Implementation of mitigation measures to reduce the flux rate at the breakthrough section, in effect, also meets the proposed mitigation objective of decreasing downgradient migration. Furthermore, impeding movement of the radionuclides serves as an in situ treatment process by allowing more time for natural decay to occur close to the source. The significance of decay in analyzing radionuclide transport is illustrated by the two curves in Figure 7.4-4. The lower curve, pre-mitigated flux 800 ft downgradient of the source, is the same as shown in Figure 7.4-3. The upper curve is the flux that

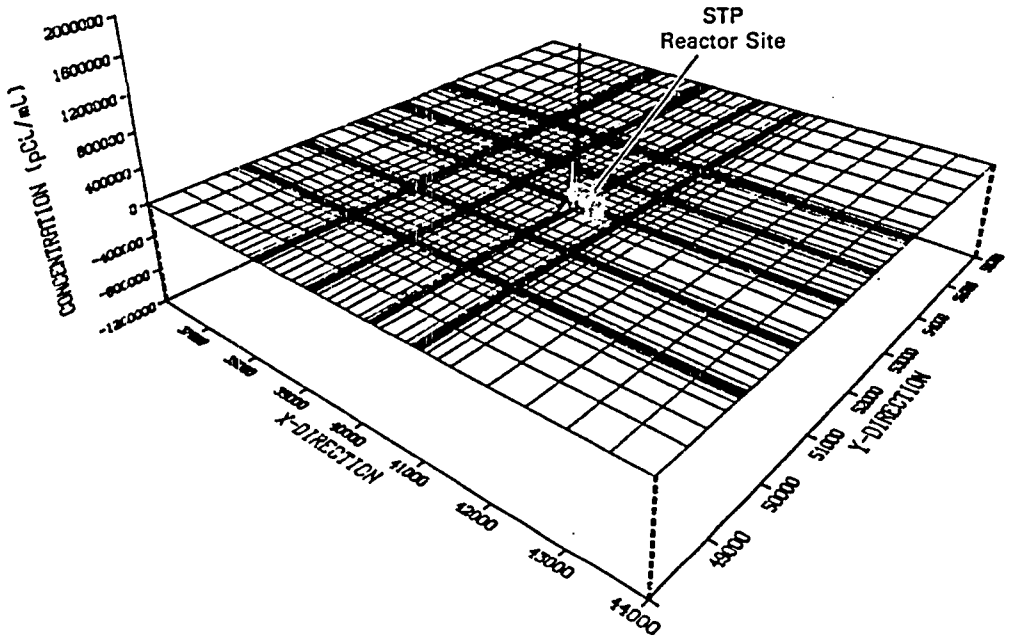

FIGURE 7.4-1. Simulated Pre-Mitigation Strontium-90 Concentrations at 100 Years.

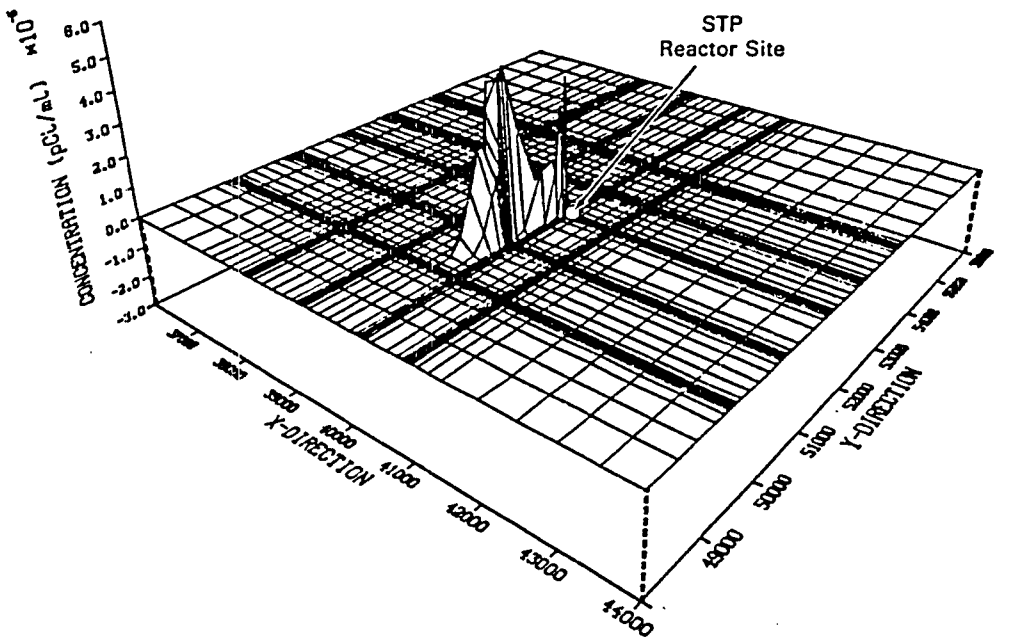

FIGURE 7.4-2. Simulated Pre-Mitigation Strontium-90 Concentrations at 1000 Years.

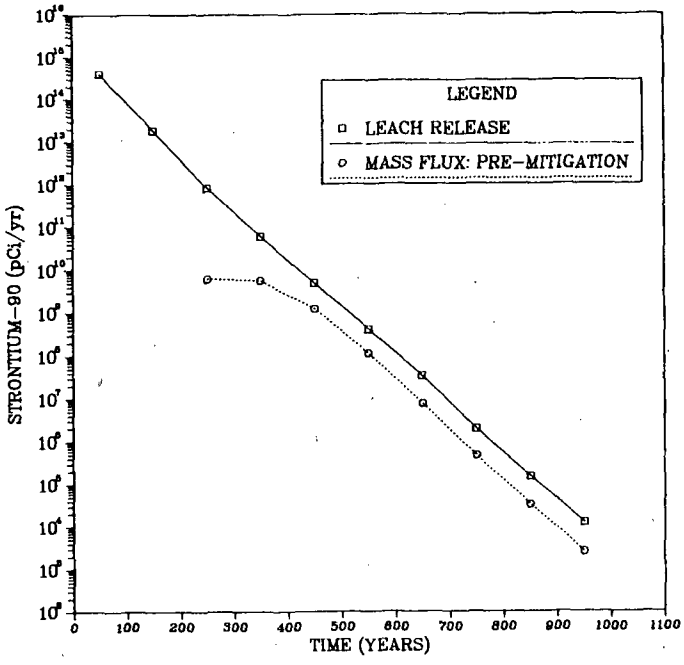

FIGURE 7.4-3. Pre-Mitigation Strontium-90 Flux Rate with Time 800 ft Down-Gradient of STP Reactor Site.

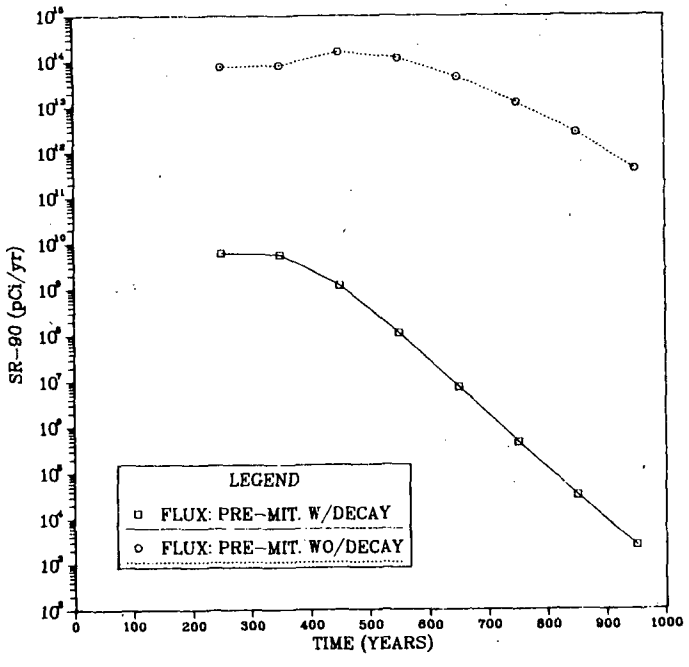

FIGURE 7.4-4. Comparison of Pre-Mitigation Strontium-90 Flux Rate With and Without Natural Decay.

would occur assuming the same release curve, flow velocities, retardation, etc., but without including natural decay with time. The non-decaying curve shows the first arrival of the plume, the passing of the peak and the effects of the continually decreasing source release rate. The curve with decay on the other hand, is much lower, produces maximum values early and continually decreases at a rate slightly greater than the release curve. Clearly the beneficial effects of natural decay point to an overall mitigation strategy that takes advantage of decay by delaying transport of radionuclides away from the source, limiting the areal extent of contamination and reducing the flux levels from the site.

7.5 EVALUATION OF MITIGATIVE TECHNIQUES

The first step in evaluation of mitigative techniques involves preliminary screening of those methods that clearly are not feasible given site-specific hydrogeologic conditions. A broad spectrum of measures may be considered for a particular site including grout cutoffs, slurry cutoffs, hydraulic barriers or interceptor trenches and treatment beds. The applicability of each of these approaches to the STP site is discussed in Section 6.7.2. To summarize, the ground-water contaminant mitigative techniques that appear most suitable for implementation at the STP, based on the reconnaissance level hydrogeologic characterization and pre-mitigative ground-water flow and transport analysis in Chapter 6.0, are:

1. a fully penetrating and properly keyed grouted cutoff, and

2. a hydraulic barrier to ground-water flow and transport created by injection.

The general material properties of the shallow zone aquifer indicate that the upper- and lower-zone aquifers could be successfully grouted with the intervening clay layer acting as a key-in and a natural ground-water flow barrier. A schematic illustrating an in-place grout cutoff such as might be used at the STP is presented in Figure 7.5-1. The average permeability of the host material at the site is 85 ft/day which falls in the middle of the "easy" to grout range of permeabilites listed in Table 5.6.2-1. Combined with the low average ground-water velocity (less than 0.1 ft/day), the relatively high permeability facilitates successful chemical grouting of ground-water cutoffs. The soil size limitations on grout permeation presented in Figure 4.3.1-1 indicate that silicate grouts may be most suitable for the STP site.

Acceptable injection rates should be achievable at the STP due to the relatively high porosity (0.37) and high permeability. Because the lower unit of the shallow aquifer is relatively deep (125 ft) and confined, deep wells with high capacities would most likely be installed. The wells would be screened only in the lower shallow aquifer zone to prevent contamination of the upper unit. The Colorado River serves as a readily available source of injection water. Other alternatives include location of a high volume

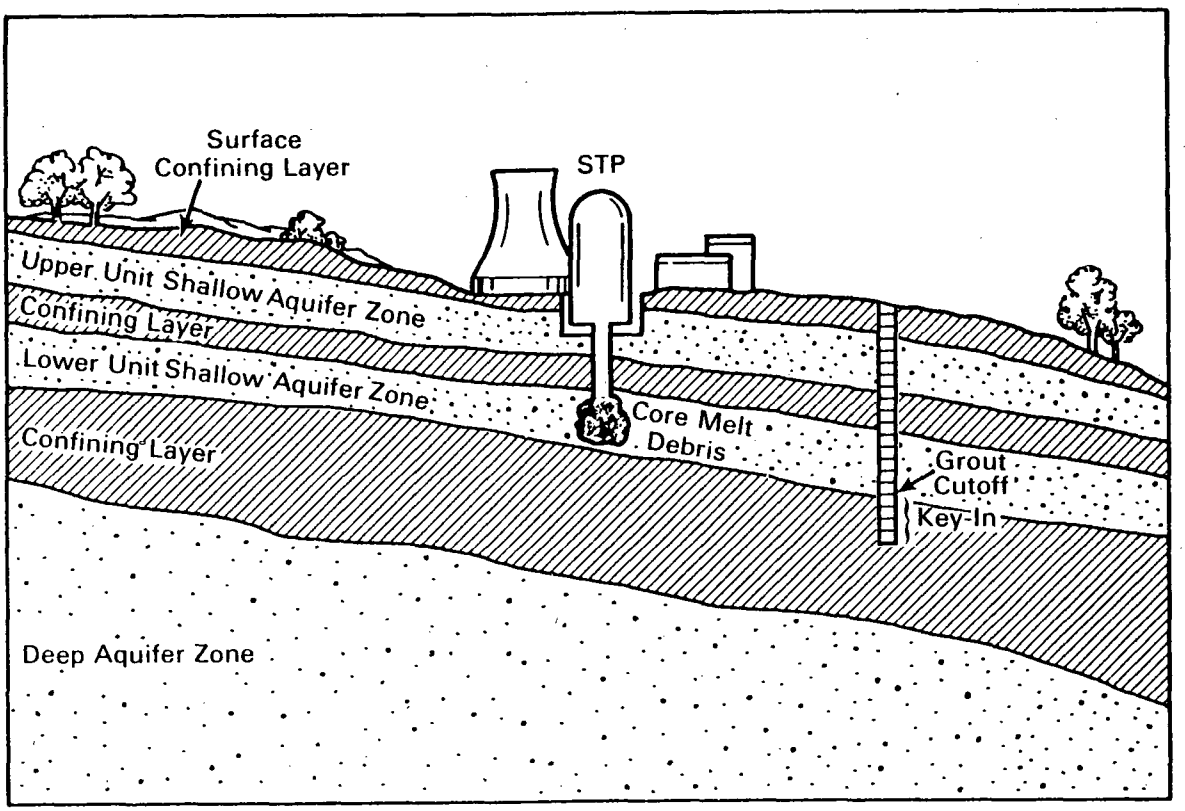

FIGURE 7.5-1. Schematic of Typical Grout Curtain Placement for the STP.

discharge well a suitable distance away from the STP or use the STP cooling reservoir as both a source of injection water and storage basin, depending on the level to which it would be contaminated by atmospheric releases of radionuclides. Injection strategies would be preferable to withdrawal because of the need for disposal of contaminated water discharged by withdrawal schemes.

While grout cutoffs and hydraulic barriers are identified as the most feasible techniques for the STP, there are an unlimited number of alternative designs utilizing these techniques individually or in combination. It's beyond the scope of this effort to determine a "best" design alternative. However, 28 different designs are considered in this case study including upgradient and downgradient cutoffs, one combination design and a limited number of downgradient hydraulic barriers. Keeping the mitigation objective in mind (i.e, minimizing contaminant migration from the site vicinity) the purposes of the evaluations presented are to:

1. evaluate the general effectiveness of selected mitigation alternatives in limiting contaminant migration from the immediate reactor site,

2. investigate the relative importance of specific design parameters including barrier length, distance from the site, orientation to the

site (i.e., centered or offset), shape (linear, L-shaped, U-shaped), permeability of grout cutoffs and upstream vs. downstream location, and

3. consider the sensitivity of mitigation performance to hydrogeologic and transport parameters such as hydraulic conductivity, dispersivity, and retardation factor.

The selection of conceptual designs to be considered, while somewhat arbitrary, was based on several factors. Because of the potential for high levels of surface and subsurface contamination in the immediate vicinity of the reactor due to atmospheric fallout, it was assumed that barriers would have to be placed approximately 1000 ft away from the reactor site. A sufficient number of alternatives were considered to provide insight into the performance characteristics of a wide range of design variations. Both downgradient and upgradient cutoffs were considered while only downgradient hydraulic barriers were assessed. Also, one combination design was included which utilizes both an upgradient and a downgradient barrier. Costs, while discussed in a later selection, played no role in the initial design selections.

The approach to analyzing the flow and transport for the mitigation conditions was to adjust the local flow model parameters (i.e., hydraulic conductivity) to simulate the impact each alternative would have on groundwater flow. The transport of strontium-90 was then simulated under these conditions.

The format for discussion of the mitigation conceptual designs and their performance is the following. First, each of the individual designs and their performance (i.e., reduction in contaminant flux) relative to the pre-mitigated case are discussed as part of a set. For example, one set of downgradient designs includes four separate grout cutoffs 1000 ft from the reactor site, with centered orientation, and having lengths of 500, 1000, 2000 and 3000 ft. Second, mitigation performance as a function of design parameters is considered wherein designs from more than one set are compared to one another. Finally, the results of the parameter sensitivity studies will be presented. Throughout the discussions, graphics are used liberally to present simulation results and to avoid overly repetitious descriptions of plume shapes, potential surfaces, etc.

7.5.1 Downgradient Mitigation Measures

Each of the downgradient designs and their performance relative to the pre-mitigated case are discussed in this section. Sketches are provided to illustrate the location, shape, and length of each design. Also, example three-dimensional plots of resultant potential surfaces and contamination distributions are provided. At the end of the section Table 7.5.1-1 is included which summarizes the alternatives evaluated, their general design parameters and their performance. Specifically, for each alternative the summary table lists the design shape, length, and permeability. The table also includes the average potential gradient created by the design, approximate contaminant travel time and peak and total contaminant flux at the breakthrough section.

7.5.1.1 Downgradient Plant Configuration Design Considerations Alt. #1, Alt. #2 and Alt. #3 (with Cooling Reservoir)

The primary plant feature in the downgradient direction from the plant which might effect design and placement of mitigation measures is the cooling reservoir. As discussed in Section 7.2.2, there may be certain circumstances wherein, following a severe accident, the cooling capacity for the second unit would have to be maintained. Or, if the reservoir water is heavily contaminated by atmospheric fallout, for a period of time following a severe accident it might not be feasible to drain it. If either of these possibilities were the case, construction of a grout curtain in the shallow aquifer through and beneath the reservoir might be infeasible. Worker safety considerations might preclude drilling activities in and around contaminated reservoir water, and the presence of the reservoir water might make the drilling and injection operations associated with grout cutoff construction much more difficult.

In light of these concerns, the first set of design alternatives are conceptualized assuming grout cutoff construction beneath the cooling reservoir is precluded. Three designs are assessed: having lengths of 500, 1000, 2000 ft (designated as Alt. #1, Alt. #2, and Alt. #3, respectively) each offset to the east such that the west end of the cutoff terminates at the reservoir embankment. The cutoffs are simulated assuming they have zero permeability, penetrate to the confining layer beneath the shallow aquifer and are 10-ft wide. An illustration showing their approximate location relative to the STP is presented in Figure 7.5.1-1.

The relative effect the three cutoffs have on the local model potential surface is illustrated in Figures 7.5.1-2, 7.5.1-3, and 7.5.1-4. Each of the figures show the offset position of the cutoffs relative to the reactor site. The drop across the cutoffs range from 0.5 ft for the 500-ft cutoff to 1.75 ft for the 2000-ft cutoff. In general, the cutoffs produce a very flat gradient immediately upgradient and immediately downgradient of the cutoff center. At the cutoff edges, gradients steepen toward the cutoff centers. The flux rates produced by the cutoffs are compared to the pre-mitigated flux in Figure 7.5.1-5. For the pre-mitigated case flux begins at about year 250. Results for the mitigated cases show flux begins at about 150 years. In all three cases the flux rate is increased by the cutoffs; in fact, the increase is directly related to cutoff length. Over the 1000-year simulation period, the total pre-mitigated flux is increased from 1.3×10^{12} pCi to 3.5×10^{12}, 4.4×10^{12}, and 3.4×10^{12} pCi, respectively for the three cutoff designs. The cause for the negative impact of the cutoffs can be seen clearly in the potential surface plots. The reactor site is located almost directly upgradient of the west end of each of the cutoffs. Thus, as the contaminant plume approaches the vicinity of the cutoff it moves into an area of steep gradient and increased velocity. Consequently, the contaminant is transported rapidly toward and past the cutoff locations, producing markedly increased flux rates. The surface plot of strontium-90 concentrations for the 2000-ft cutoff at 1000 years (Figure 7.5.1-6) further illustrates the effect of the offset grout cutoffs. Compared to the pre-mitigated concentrations in Figure 7.4-2, the front of the main plume has advanced approximately 500 ft farther after the same period of time.

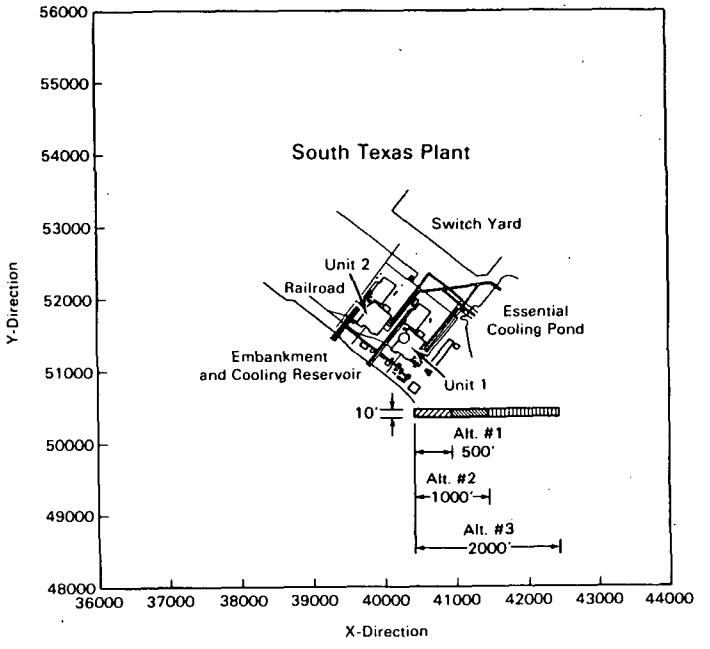

FIGURE 7.5.1-1. Location of Alt. #1 (L=500 ft), Alt. #2 (L=1000 ft) and Alt. #3 (L=2000 ft).

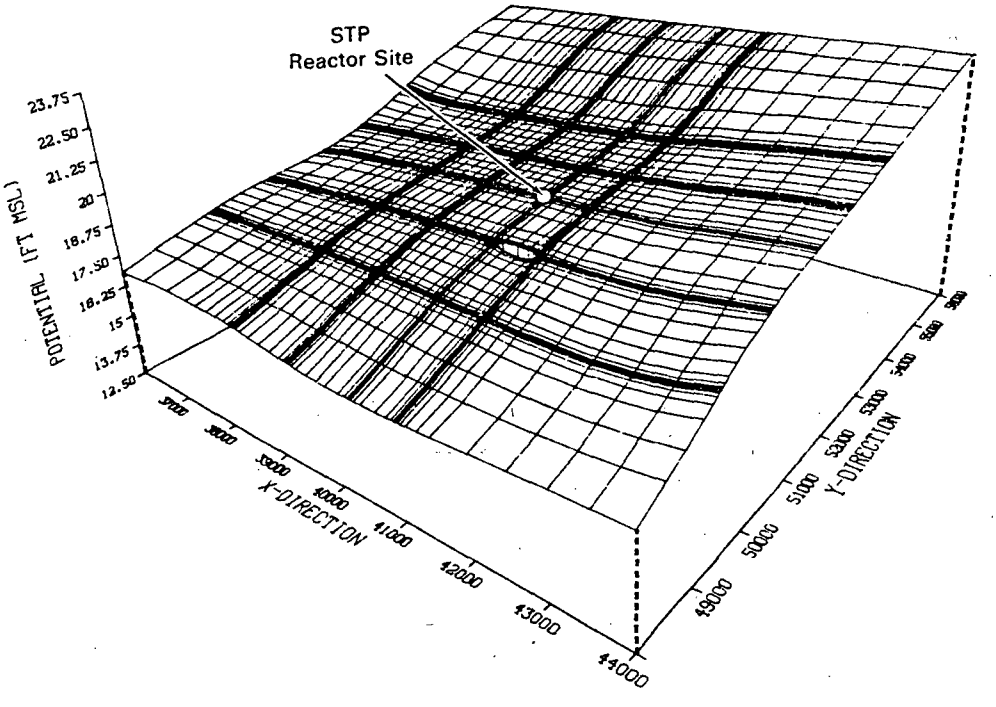

FIGURE 7.5.1-2. Simulated Potential Surface Alt. #1: 500-ft Cutoff, East of the Cooling Reservoir, 1000 ft Downgradient.

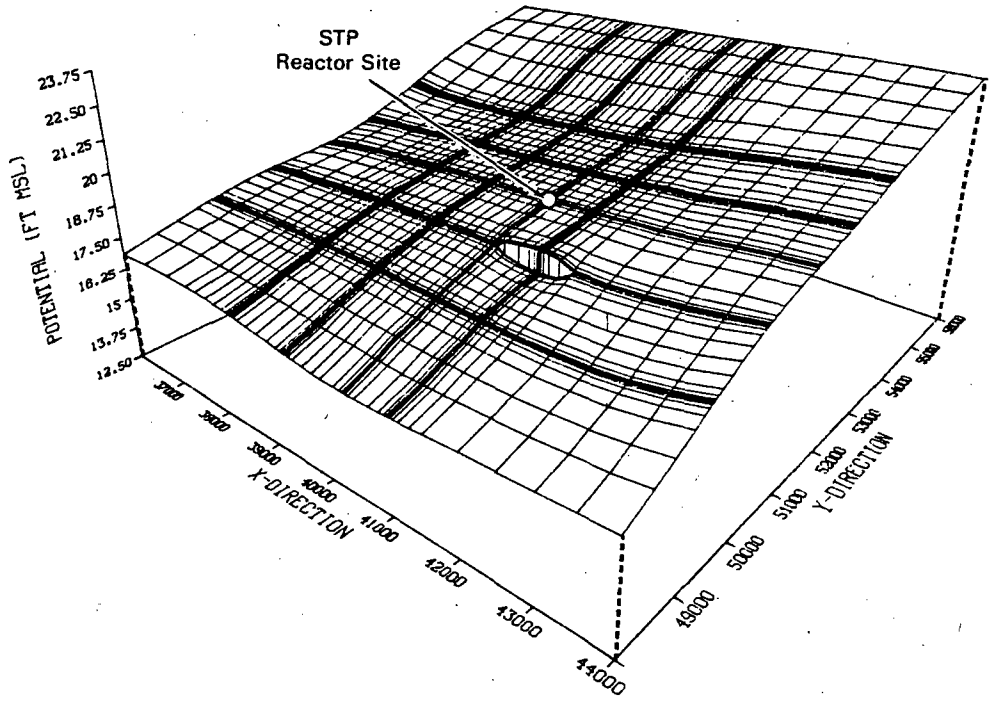

FIGURE 7.5.1-3. Simulated Potential Surface Alt. #2: 1000 ft Cutoff, East of the Cooling Reservoir, 1000 ft Downgradient.

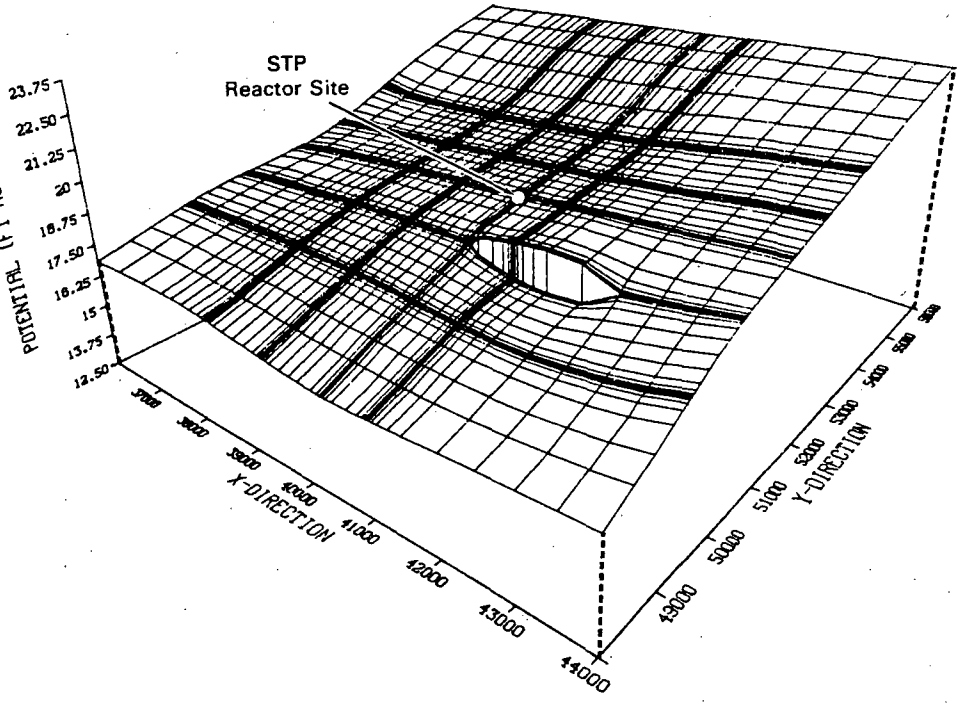

FIGURE 7.5.1-4. Simulated Potential Surface Alt. #3: 2000 ft Cutoff, East of the Cooling Reservoir, 1000 ft Downgradient.

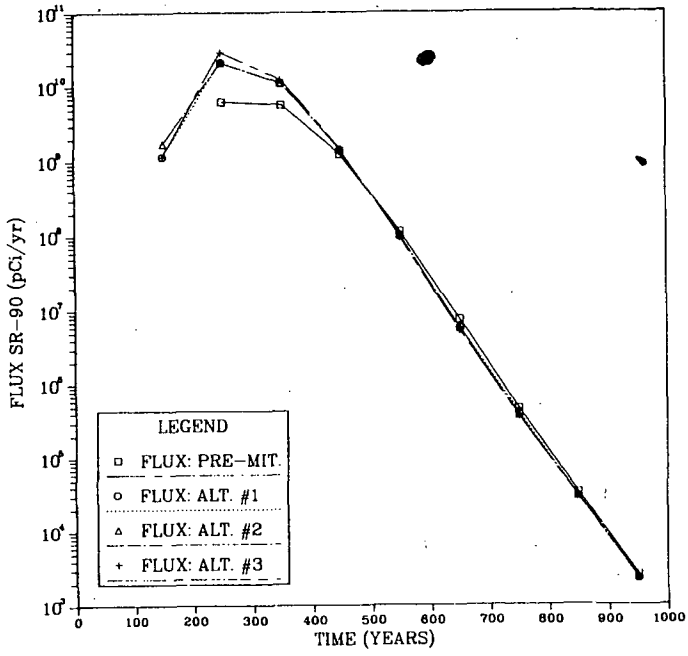

FIGURE 7.5.1-5. Simulated Flux Rates: Alt. #1 (L=500 ft), Alt. #2 (L=1000 ft), and Alt. #3 (L=2000 ft).

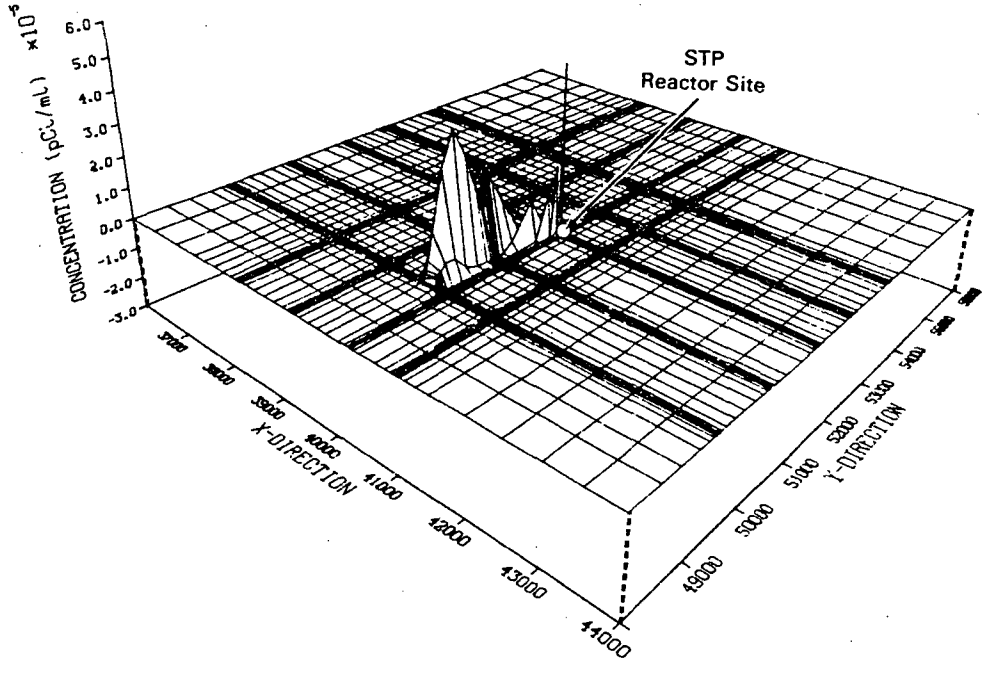

FIGURE 7.5.1-6. Simulated Strontium-90 Concentrations at 1000 years: Alt. #3 (L=2000 ft).

On the basis of these results, downgradient cutoffs, if constructed outside the cooling reservoir, provide no benefit and actually increase transport of radionuclides from the STP site. Therefore, if grout cutoffs are to be constructed in the downgradient direction it will be necessary to locate them with a more centered orientation relative to the reactor site. If mitigation were delayed sufficiently to allow the potentially contaminated water in the reservoir to be disposed of or to evaporate such that dangerously high surface contamination is removed, grout cutoffs could be effectively implemented downgradient of the reactor site. Assuming this to be the case, the remainder of the downgradient grout cutoffs evaluated are conceptualized without the constraint of remaining outside the reservoir area.

7.5.1.2 Additional Downgradient Grout Cutoff Design Evaluations Alt. #4, Alt. #5, Alt. #6, and Alt. #7 (without Cooling Reservoir)

The next set of alternatives considered consists of four linear cutoffs. These cutoffs are centered relative to the reactor site and located 1000 ft downgradient. As noted above, it was assumed that the closest possible location for cutoff construction following a severe accident was about 1000 ft from the reactor. This assumption is largely arbitrary; however, it was made recognizing that in reality a limit will exist. Contrary to the previous designs, this set is intended to maximize, per unit length of linear barrier, the impact on the transport of radionuclides from the reactor site. Therefore, they are located at the assumed minimum distance from and centered relative to the reactor. Four designs are evaluated at this location, including lengths of 500, 1000, 2000 and 3000 ft. The locations are shown in Figure 7.5.1-7. As examples, the resulting potential surfaces with the cutoffs in place are shown for the 500-ft and 3000-ft cutoffs in Figures 7.5.1-8 and 7.5.1-9. The 500-ft cutoff acts merely as a small obstruction to flow, again creating a drop of only 0.5 ft and only minor backwater effect. The 3000-ft barrier on the other hand produces a 2.1-ft drop and significant backwater effects, reducing the gradient at the site to 0.7×10^{-4} ft/ft.

The resultant flux with time for the cutoff designs are compared in Figure 7.5.1-10. The simulations show that the 500-ft design actually increases the flux rate with arrival of strontium-90 occurring at the breakthrough point after less than 200 years while the 1000-ft design only marginally reduces the flux rate. The results for the two longer cutoffs demonstrate that, for increasing lengths beyond 1000 ft, there is substantial increase in first arrival time. Consequently, because of natural decay, the flux rates are reduced. The total flux of strontium-90 for the 1000-year simulation period is reduced from 1.3×10^{12} pCi for the pre-mitigated case to 8.4×10^{11}, 1.7×10^{10}, and 1.2×10^{8} pCi for the 1000-, 2000- and 3000-ft designs, respectively. An example of the spatial distribution of strontium-90 concentration for the centered cutoff is presented in Figure 7.5.1-11. For this case, the 3000-ft design at 1000 years, the contaminant is totally contained behind the barrier and lateral spreading at the plume front is increased. Overall concentrations are approximately the same as in the pre-mitigated case.

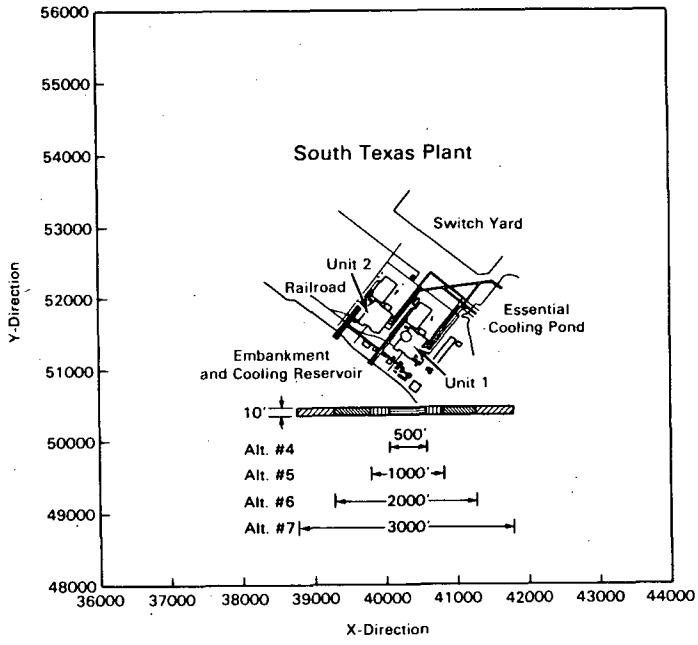

FIGURE 7.5.1-7. Location of Alt. #4 (L=500 ft), Alt. #5 (L=1000 ft), Alt. #6 (L=2000 ft), and Alt. #7 (L=3000 ft).

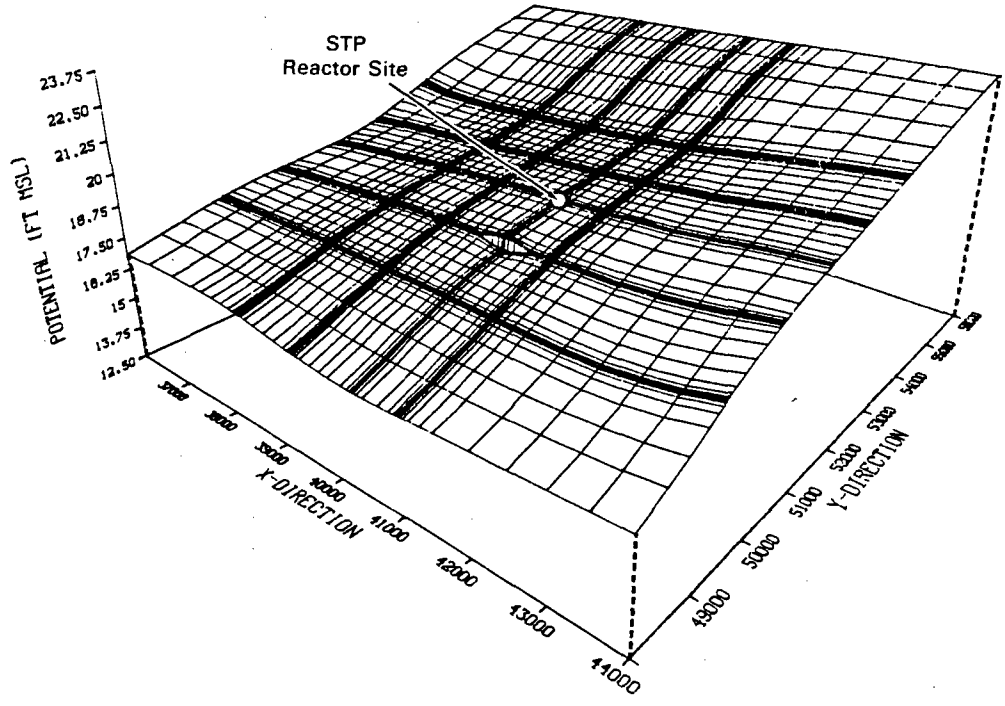

FIGURE 7.5.1-8. Simulated Potential Surface Alt. #4: 500-ft Cutoff, Centered, 1000 ft Downgradient.

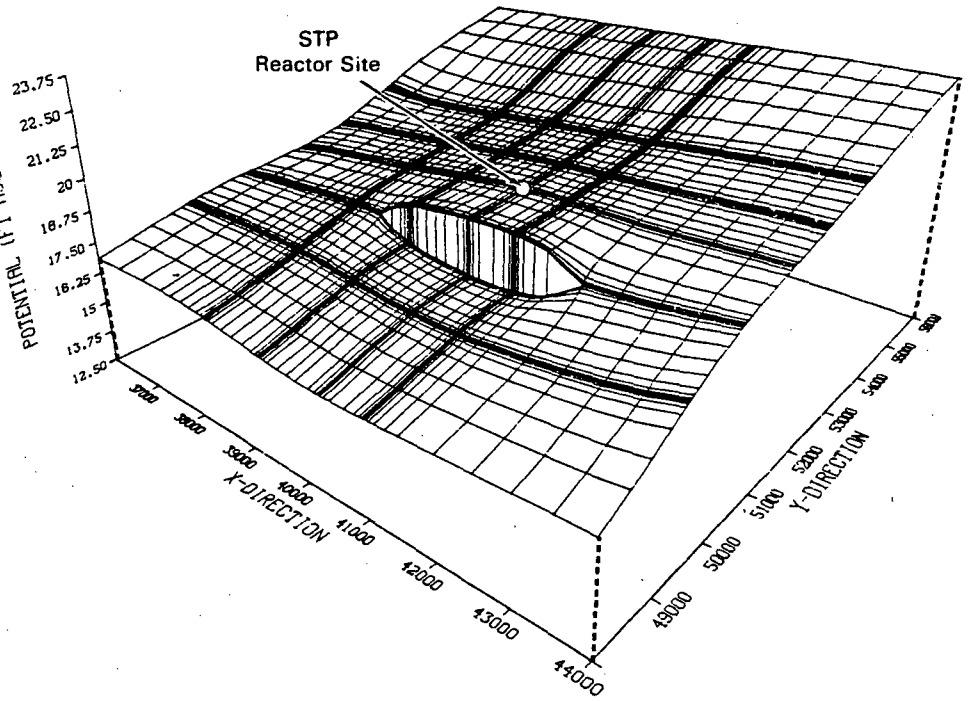

FIGURE 7.5.1-9. Simulated Potential Surface Alt. #7: 3000-ft cutoff, Centered, 1000 ft Downgradient.

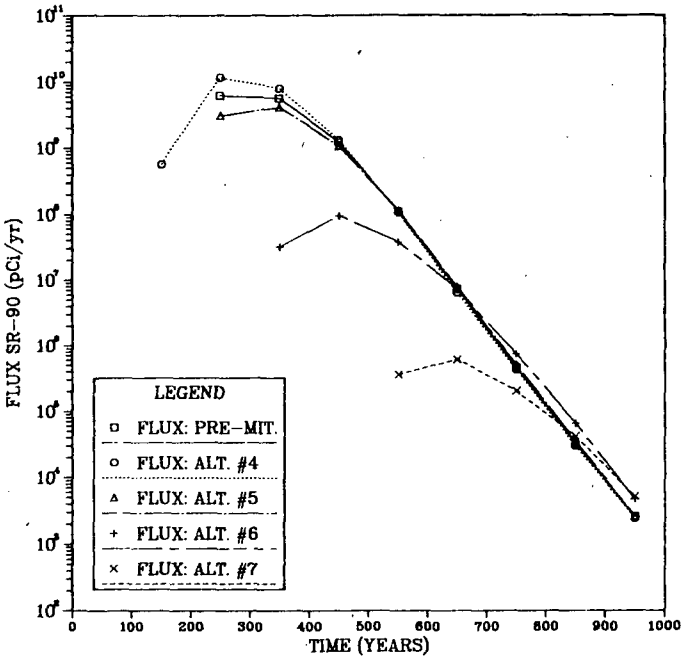

FIGURE 7.5.1-10. Simulated Flux Rates: Alt. #4 (L=500 ft), Alt. #5 (L=1000 ft), Alt. #6 (L=2000 ft), and Alt. #7 (L=3000 ft).

Alt. #8 and Alt. #9 (Offset)

To investigate the possible advantages and disadvantages of partially offsetting the cutoffs relative to the reactor location, Alt. #8 and Alt. #9 are 3000 ft in length and located 1000 ft downgradient. As can be seen in Figure 7.5.1-12, relative to the reactor site, the centers are offset 1000 ft to the east and west, respectively. The simulated potential surfaces for the designs are presented in Figures 7.5.1-13 and 7.5.1-14. It's noteworthy that the drop across Alt. #8 is greater due to the lower hydraulic conductivities in the eastern portion of the study area (see Figure 7.3-4). The maximum drop across Alt. #8 is 3.2 ft compared to 2.5 ft for Alt. #9. Though the higher drop results in greater backwater effect in the y-direction, it also produces an increased gradient in the x-direction from east to west. The effect of the lateral gradient can be seen by comparing the 1000-year concentration surface plots for the two designs in Figures 7.5.1-15 and 7.5.1-16. The lateral gradient produced by Alt. #8 allows the strontium-90 to escape around the western end of the cutoff and continue to move away from the site. Alt. #9, on the other hand, completely contains the plume. This difference is also evident in the simulated contaminant flux for the two designs plotted in Figure 7.5.1-17. In both cases the flux is significantly reduced relative to the pre-mitigated case; however, for the same length of cutoff, Alt. #9 exhibits much better performance. Total flux for Alt. #8 is 3.3×10^{10} pCi compared to 2.0×10^{10} pCi for Alt. #9.

Alt. #10 (2000 ft Downgradient)

Intuitively, the closer a barrier is placed to the contaminant source, the better its performance will be in terms of decreasing potential gradients and flow velocities and increasing travel distances. However, conditions could exist such that a barrier would have to be placed a greater distance away. To provide a measure of the impact increased distance would have on cutoff performance, Alt. #10 is evaluated, a 3000 ft long, centered cutoff located 2000 ft downgradient from the reactor (shown in Figure 7.5.1-18). The potential surface for Alt. #10 is shown in Figure 7.5.1-19. The drop across the cutoff is about 2.5 ft and the backwater effect extends a considerable distance upgradient. The contaminant plume after 1000 years, presented in Figure 7.5.1-20, is completely contained within 1000 ft downgradient of the reactor. The mitigated flux, compared to the pre-mitigated flux in Figure 7.5.1-21, is substantially reduced and the first arrival is delayed approximately 100 years. These results indicate that even at greater distances from the reactor successful mitigation can be achieved without dramatically increasing cutoff size.

Alt. #11, Alt. #12, and Alt. #13 (L- and U-Shaped)

These designs, two L-shaped cutoffs and a U-shaped cutoff, are evaluated to investigate possible advantages of modifying cutoff shape. All three designs have a total length of 3000 ft and are located 1000 ft downgradient of the reactor. The L-shaped cutoffs, illustrated in Figure 7.5.1-22, consist of a 2000-ft leg in the x-direction and a 1000-ft leg in the y-direction. The potential surfaces produced by the L-shaped cutoffs are plotted in

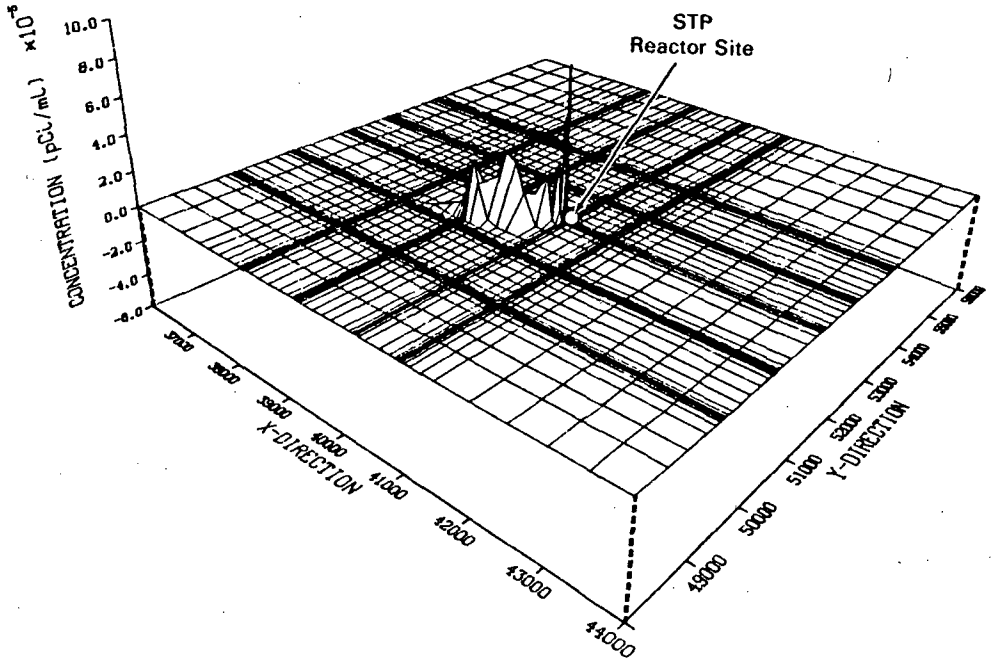

FIGURE 7.5.1-11. Simulated Strontium-90 Concentrations at 1000 years: Alt. #7 (L=3000 ft).

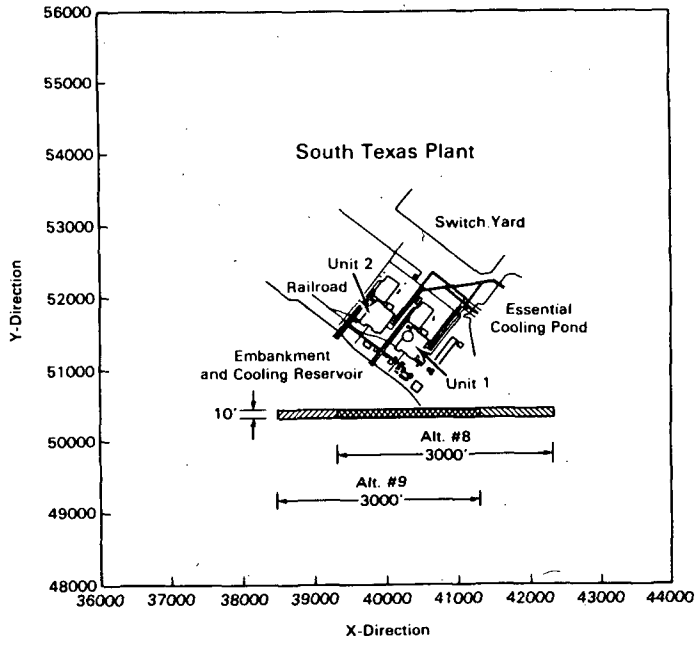

FIGURE 7.5.1-12. Location of Alt. #8 (L=3000 ft, Offset-East) and Alt. #9 (L=3000 ft, Offset-West).

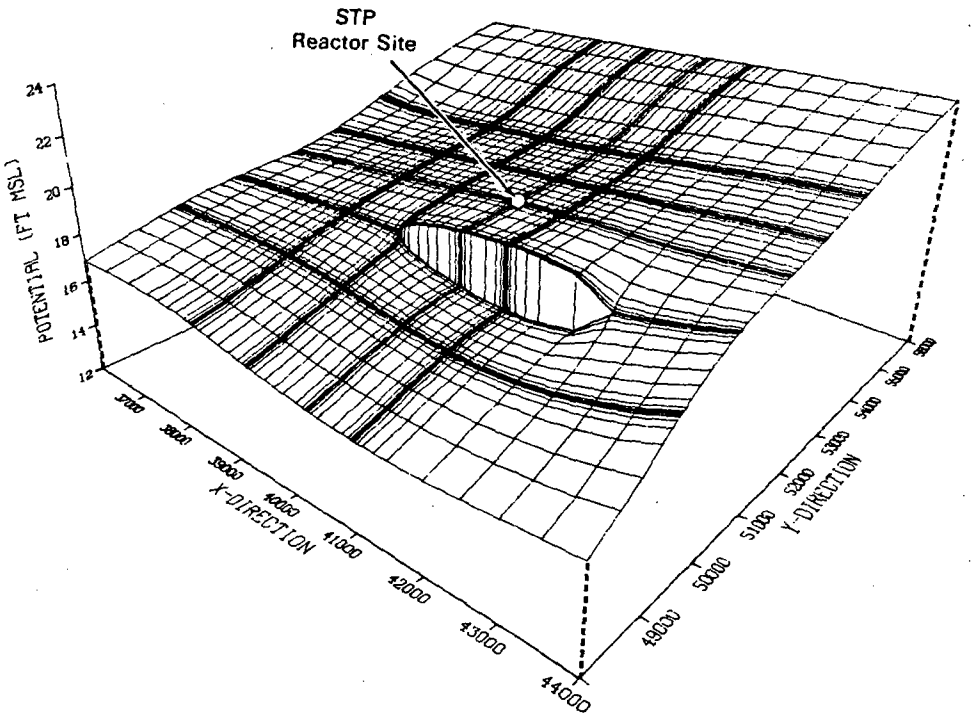

FIGURE 7.5.1-13. Simulated Potential Surface, Alt. #8: 3000 ft Cutoff, Offset-East, 1000 ft Downgradient.

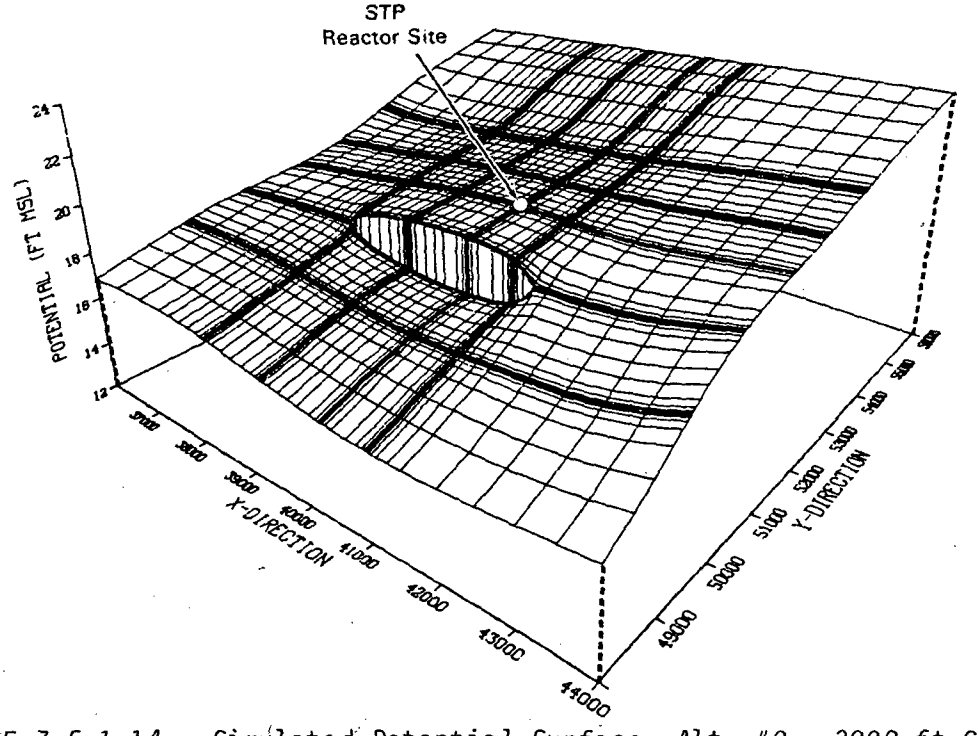

FIGURE 7.5.1-14. Simulated Potential Surface, Alt. #9: 3000 ft Cutoff, Offset-West, 1000 ft Downgradient.

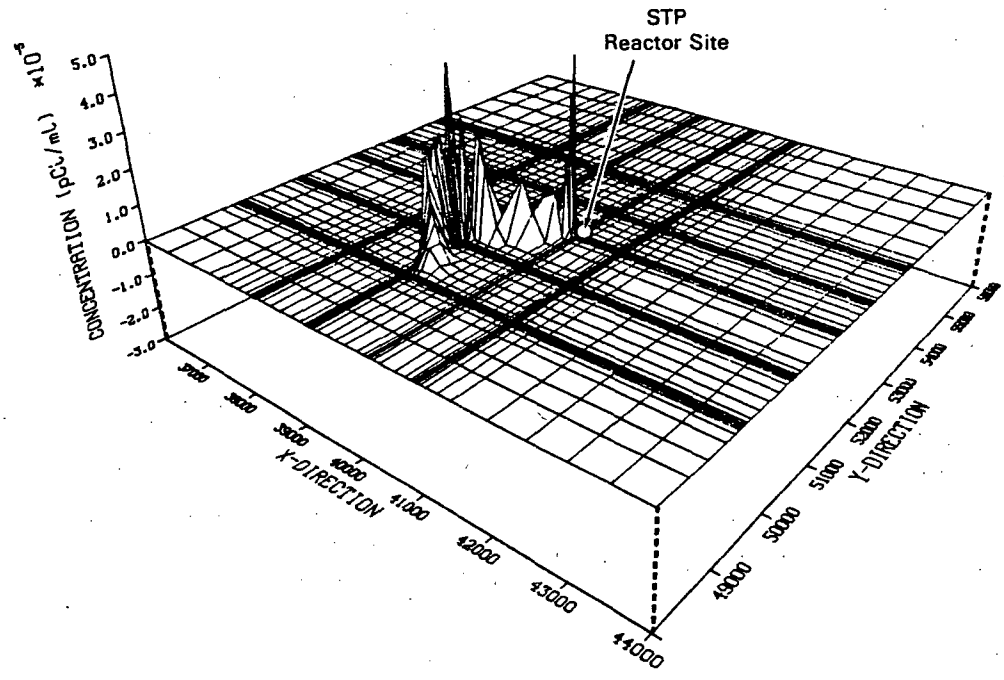

FIGURE 7.5.1-15. Simulated Strontium-90 Concentrations at 1000 Years: Alt. #8 (L=3000 ft, Offset-East).

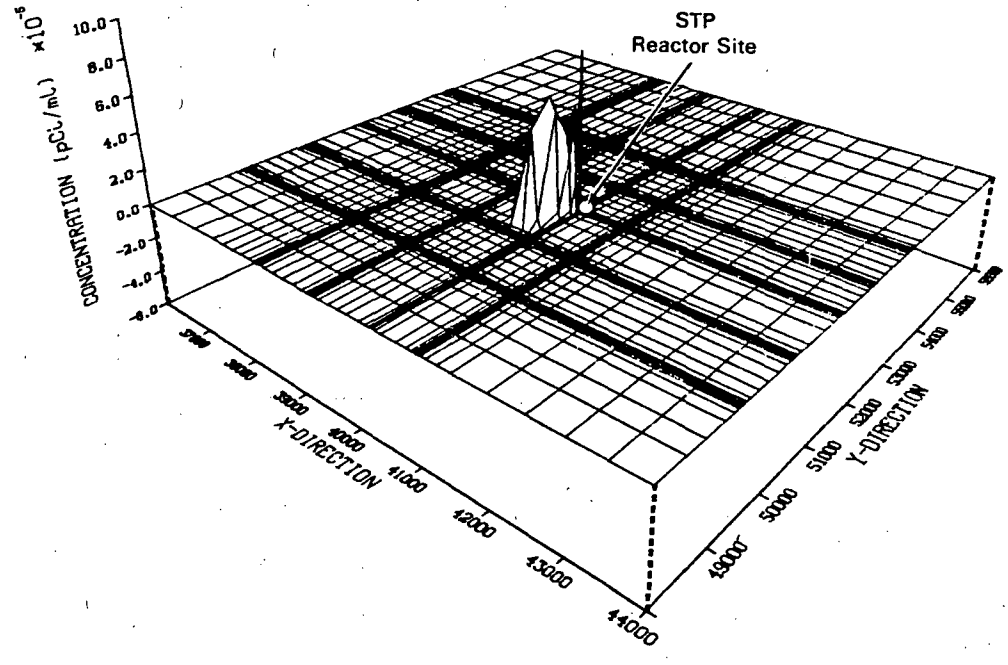

FIGURE 7.5.1-16. Simulated Strontium-90 Concentrations at 1000 Years: Alt. #9 (L=3000 ft, Offset-West).

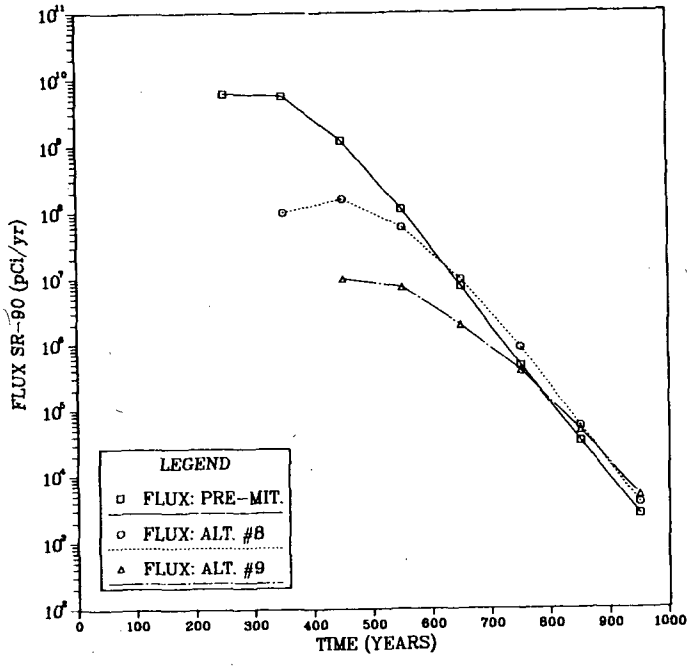

FIGURE 7.5.1-17. Simulated Flux Rates: Alt. #8 (L=3000 ft, Offset-East) and Alt. #9 (L=3000 ft, Offset-West).

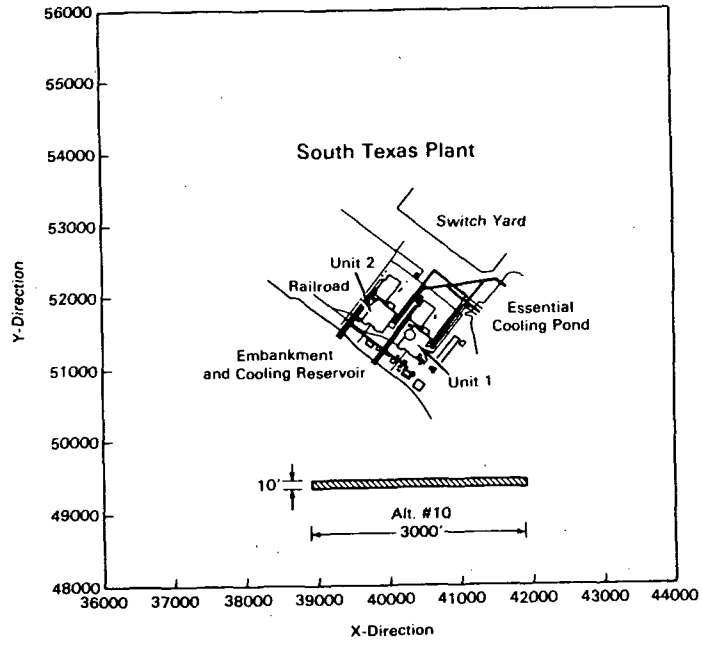

FIGURE 7.5.1-18. Location of Alt. #10 (L=3000 ft), 2000 ft Downgradient.

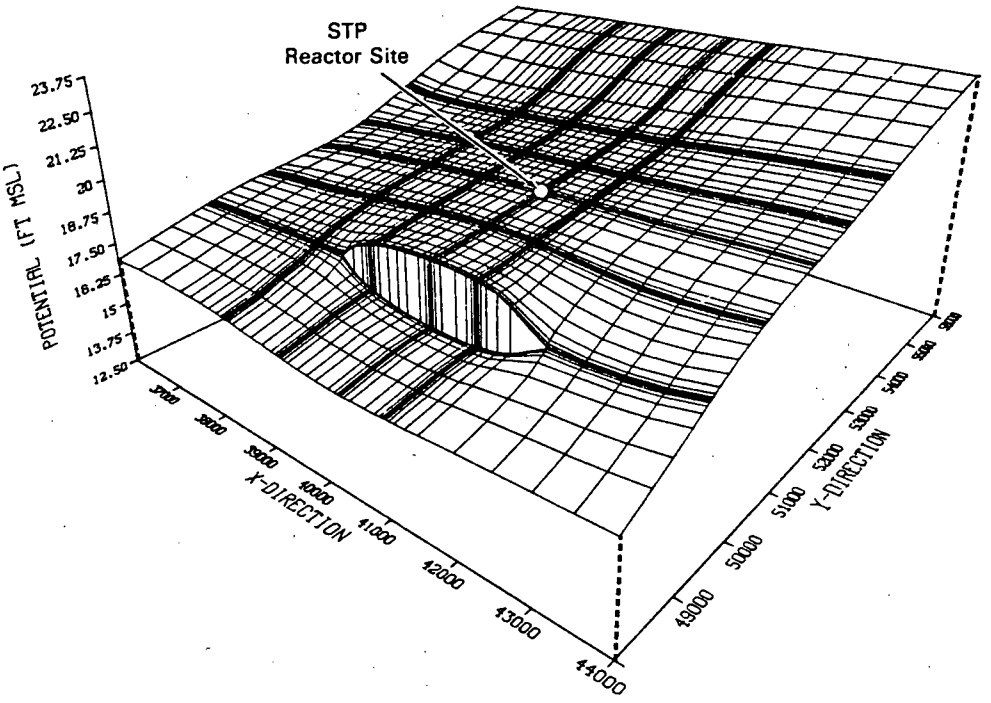

FIGURE 7.5.1-19. Simulated Potential Surface, Alt. #10 (L=3000 ft), 2000 ft Downgradient.

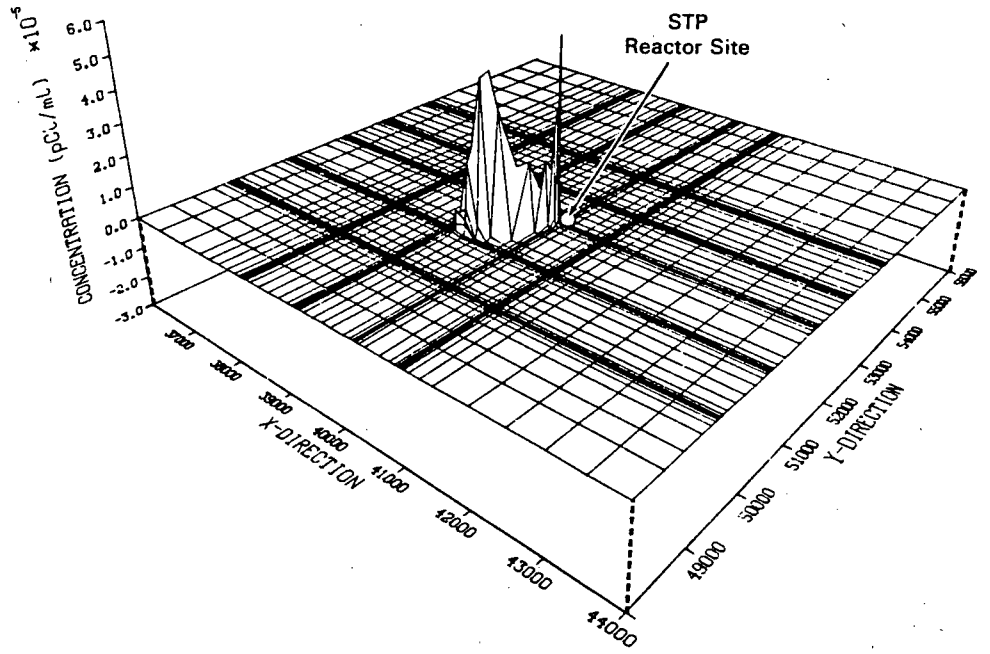

FIGURE 7.5.1-20. Simulated Strontium-90 Concentrations at 1000 years: Alt. #10 (L=3000 ft), 2000 ft Downgradient.

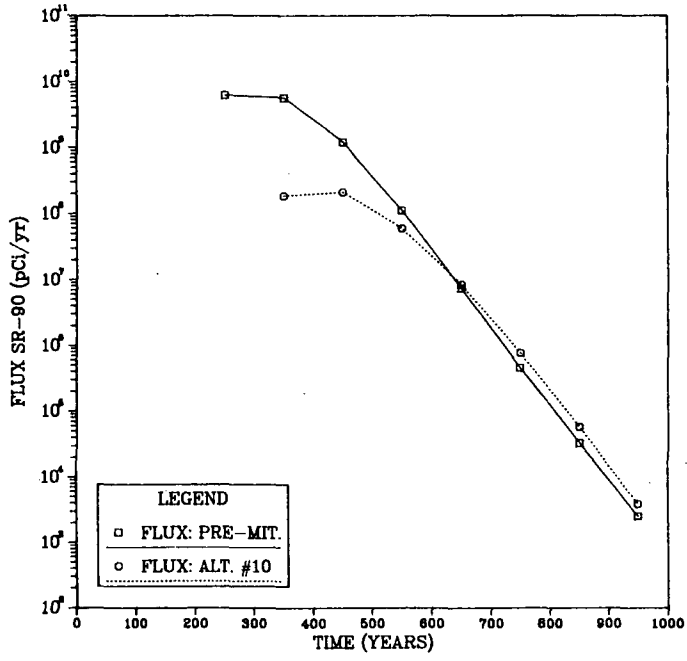

FIGURE 7.5.1-21. Simulated Flux Rates: Alt. #10 (L=300 ft), 2000 ft Downgradient.

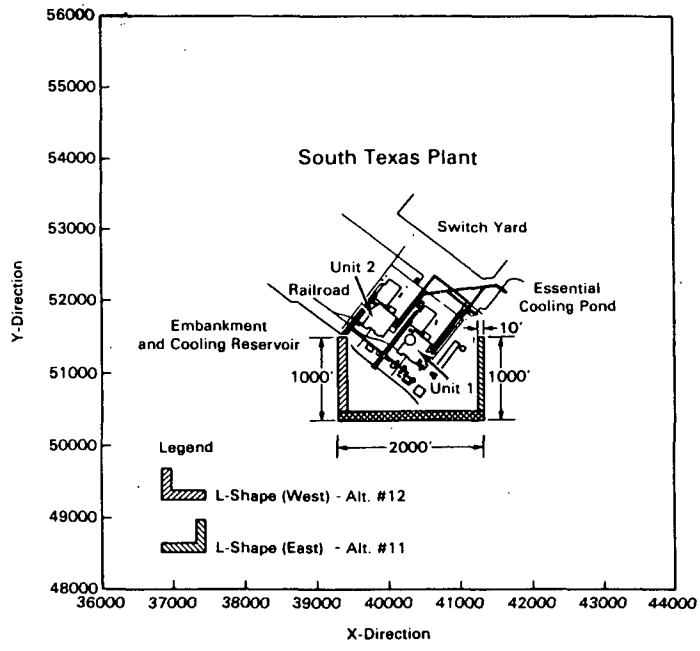

FIGURE 7.5.1-22. Location of Alt. #11 (L-Shaped-East) and Alt. #12 (L-Shaped-West).

Figures 7.5.1-23 and 7.5.1-24. The surface generated by Alt. #11 is very similar to that for Alt. #6, a 2000-ft linear cutoff, indicating the 1000-ft leg has little effect. Because of the low conductivities in the eastern portion of the study area, the lateral velocities are low and are not greatly affected by the cutoff leg. In contrast Alt. #12, with the leg added to the western end, produces observable drop and backwater in the x-direction which contributes to the reduction in potential gradient at the site. The gradient at the reactor created by Alt. #12 is 0.7×10^{-4} ft/ft compared to 1.4×10^{-4} ft/ft for Alt. #11. The difference in potentials produced by the two designs is clearly manifested in the resulting concentration distributions presented in Figures 7.5.1-25 and 7.5.1-26. The lateral velocities generated by Alt. #11 transport the strontium-90 laterally along the upstream face of the cutoff toward the west, allowing it to escape around the end. The 1000-ft leg on Alt. #12, on the other hand obstructs both lateral and longitudinal flow and transport, and effectively contains the contaminant plume near the reactor site.

The U-shaped design of Alt. #13, shown in Figure 7.5.1-27, utilizes the same length of cutoff as the L-shaped designs but consists of a centered 2000-ft section placed 1000-ft downgradient of the reactor, with 500-ft legs attached at each end. Similar to Alt. #12, the design significantly reduces the gradient at the reactor to 0.8×10^{-4} ft/ft and creates observable potential drop in the x-direction (see Figure 7.5.1-28). The resultant distribution of contaminant at 1000 years, shown in Figure 7.5.1-29, is totally contained upgradient of the cutoff. However, the lateral spreading is greater than that for Alt. #12. As indicated by Figure 7.5.1-30, all three designs reduce flux relative to the pre-mitigated case, but Alt. #12 and #13 are clearly better designs. In fact, the attachment of the cutoff leg to the western end as is done for both designs, almost completely eliminates flux from the reactor area within the 1000-year simulation period. The total flux for Alt. #12 and #13 are 6.3×10^{3} and 1.8×10^{4} pCi, respectively, eight orders of magnitude less than pre-mitigated flux. Because of their effectiveness in reducing gradients, the two designs delay the first arrival of contaminant at the breakthrough section until after 800 years. Several conclusions can be drawn from these results. First, the attachment of the leg in the area of low hydraulic conductivity (east) does not significantly increase performance. Installation of barriers to flow in both the x- and y-directions greatly enhances performance. The 500-ft leg (U-shape) on the western end performs nearly as well as the 1000-ft leg (L-shape), leading to the fact that if costs are important, a shorter leg for the L-shape design might provide adequate mitigation. Finally, a more general conclusion is that the spatial distribution of hydraulic conductivity plays an important role in the relative performance of specific designs and should be considered accordingly in the site characterization phase of the study.

Alt. #14, Alt. #15, and Alt. #16 (Injection Scheme)

The final set of downgradient designs evaluated are three injection schemes. The schemes consist simply of an injection well (or wells) located directly 1000-ft downgradient of the reactor site at the location shown in Figure 7.5.1-31. The total injection rates for the three schemes are 20, 30,

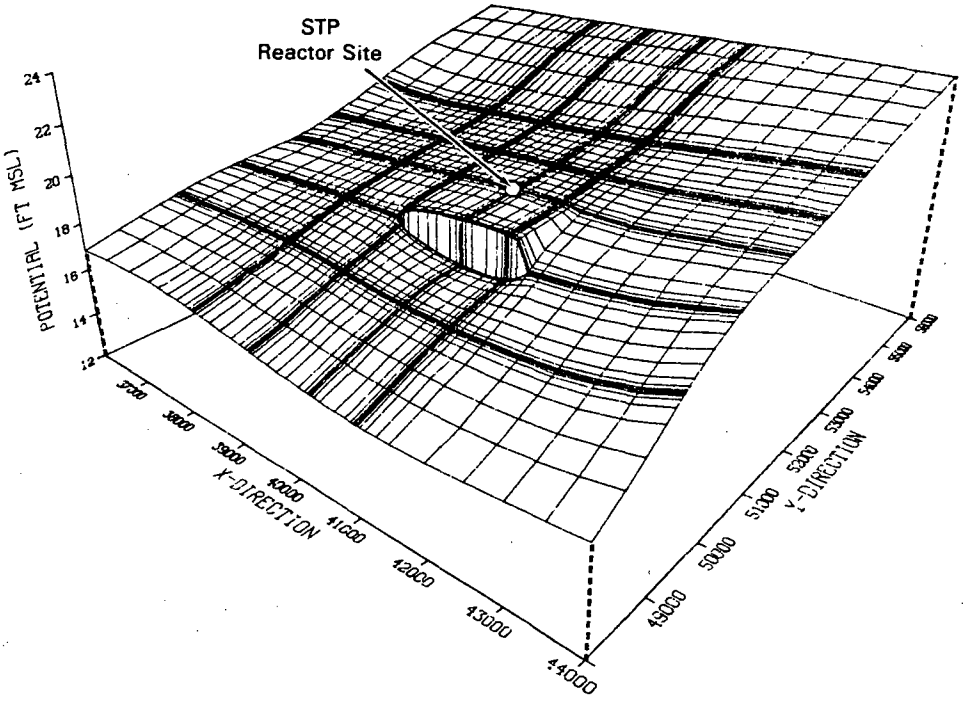

FIGURE 7.5.1-23. Simulated Potential Surface, Alt. #11 (L-Shaped-East).

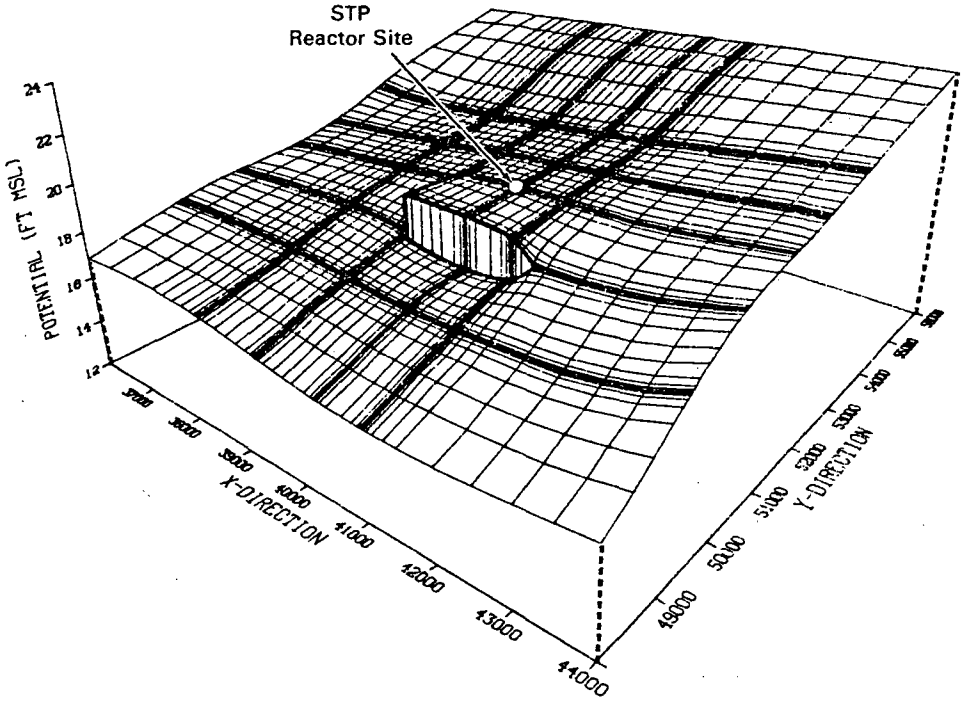

FIGURE 7.5.1-24. Simulated Potential Surface, Alt. #12 (L-Shaped-West).

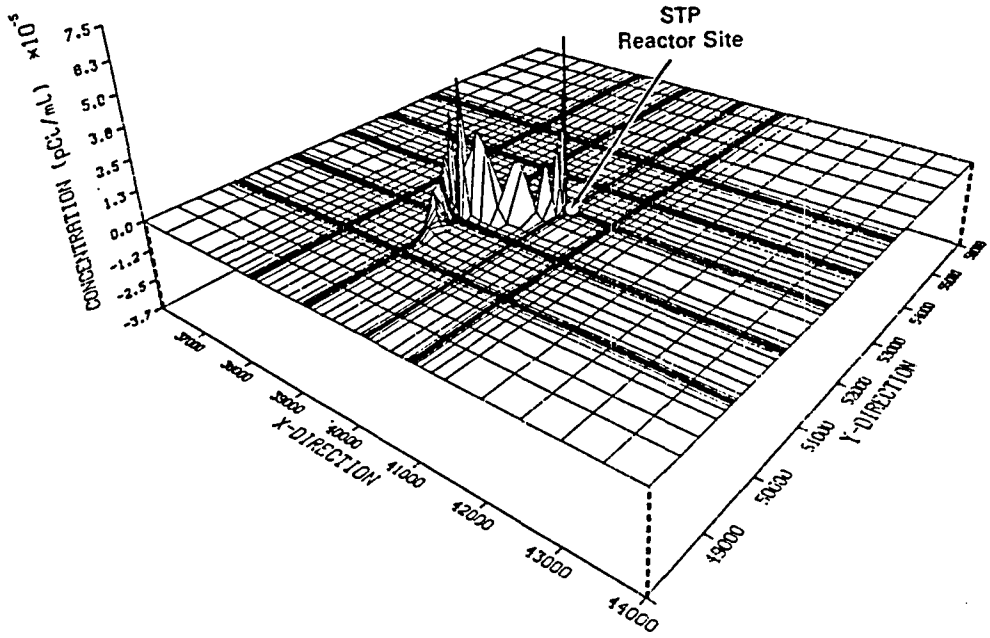

FIGURE 7.5.1-25. Simulated Strontium-90 Concentrations at 1000 years: Alt. #11 (L-Shaped-East).

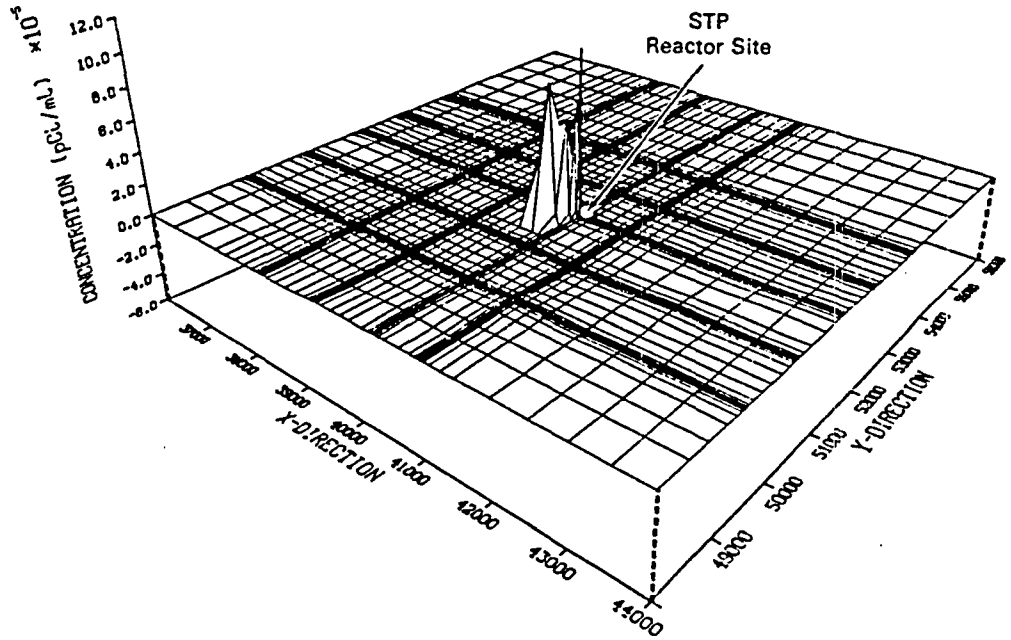

FIGURE 7.5.1-26. Simulated Strontium-90 Concentrations at 1000 years: Alt. #12 (L-Shaped-West).

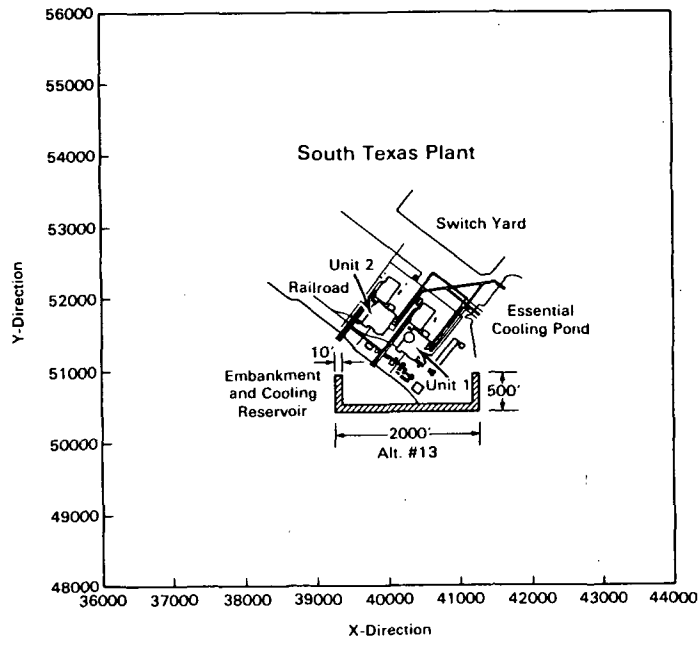

FIGURE 7.5.1-27. Location of Alt. #13 (U-Shaped).

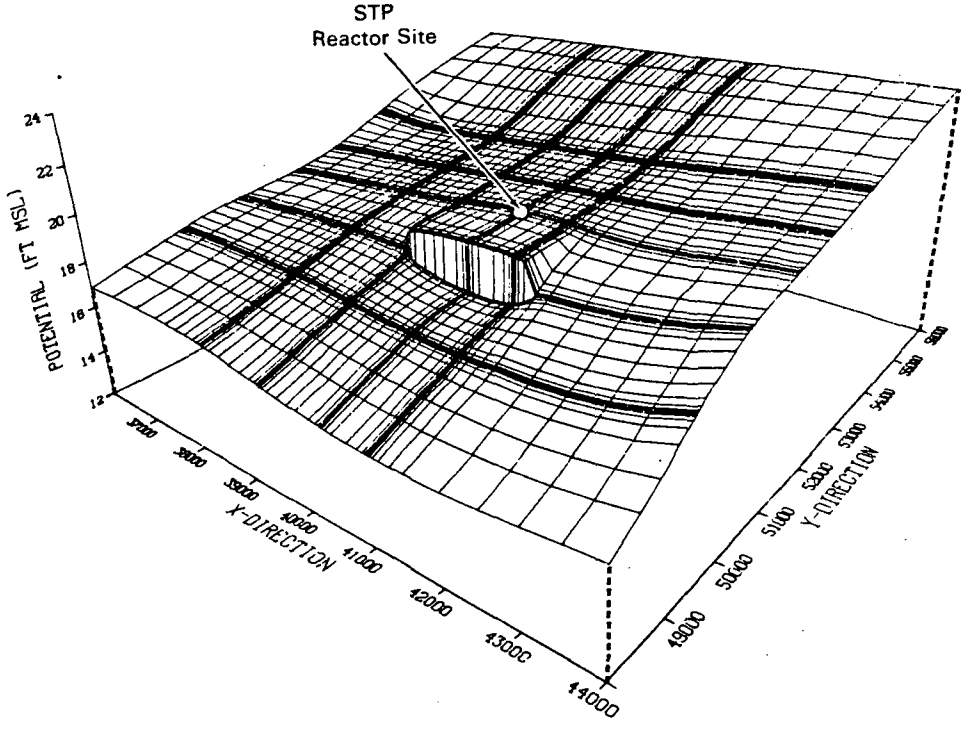

FIGURE 7.5.1-28. Simulated Potential Surface, Alt. #13 (U-Shaped).

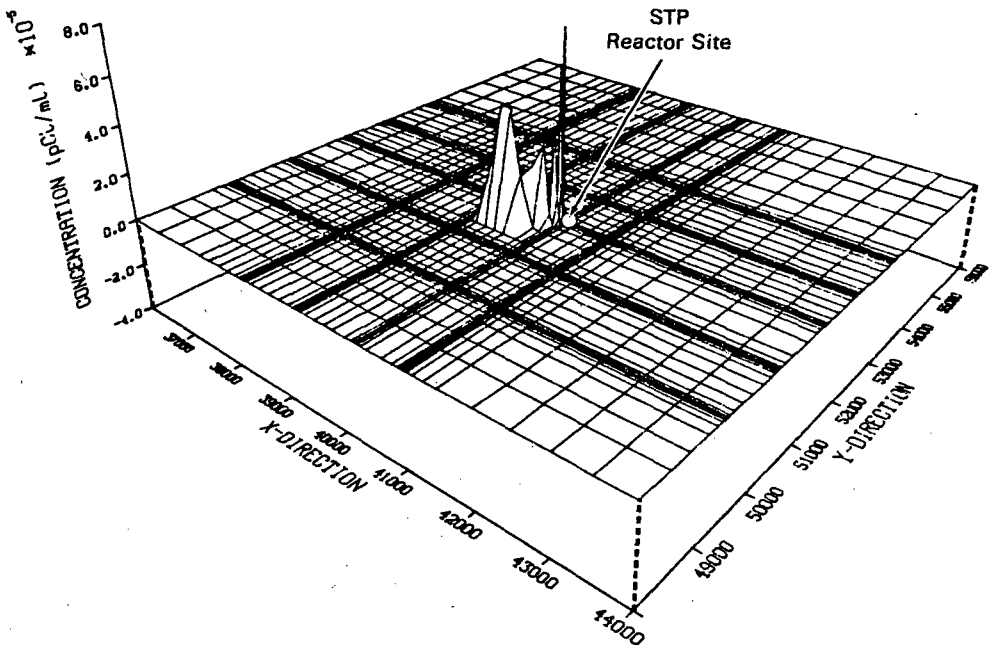

FIGURE 7.5.1-29. Simulated Strontium-90 Concentrations at 1000 years: Alt. #13 (U-Shaped).

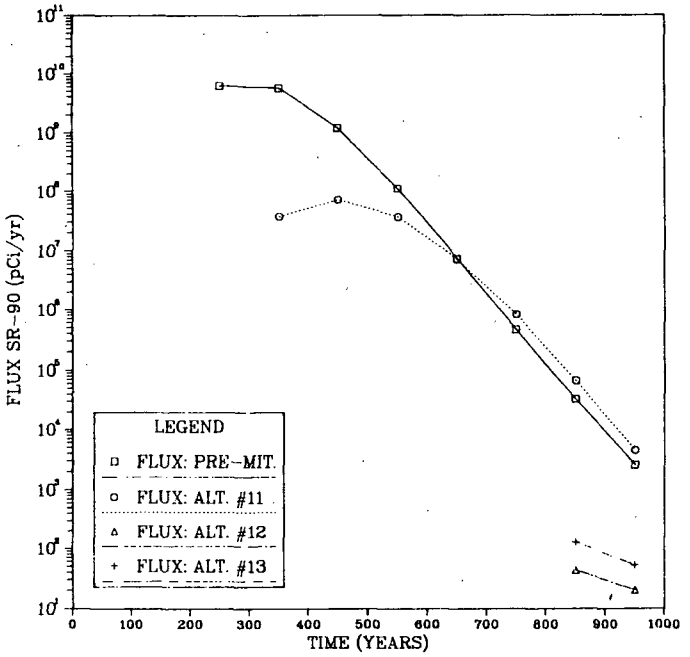

FIGURE 7.5.1-30. Simulated Flux Rates: Alt. #11 (L-Shaped-East), Alt. #12 (L-Shaped-West), and Alt. #13 (U-Shaped).

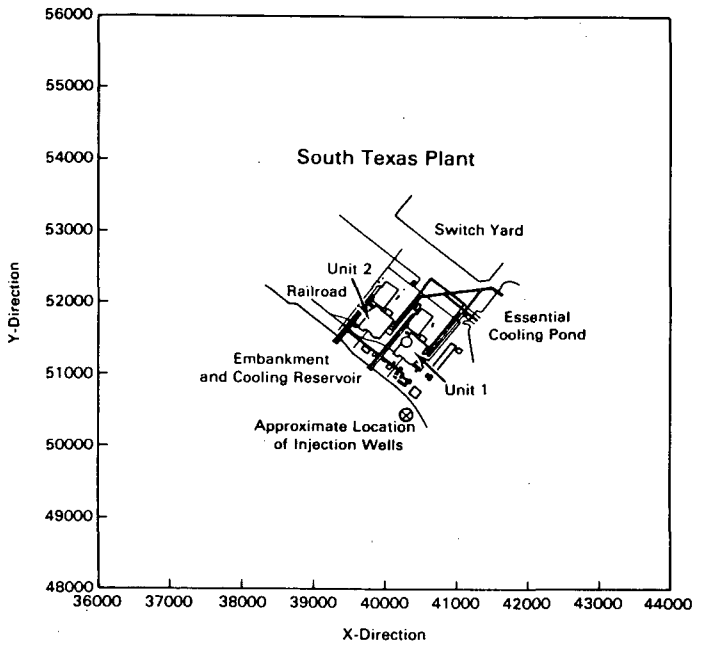

FIGURE 7.5.1-31. Location for Injections Wells: Alt. #14, Alt. #15, and Alt. #16.

and 40 gpm, respectively. The impact of injection on the potential field is creation of a mound which increases in magnitude and areal extent with increasing injection rate. This is illustrated by the potential surface plots for the 20-gpm and 40-gpm schemes in Figures 7.5.1-32 and 7.5.1-33. The mound for the 20-gpm injection scheme is barely discernible while that for the 40-gpm scheme is quite prominent. Similar to the cutoff designs, the preferred direction for contaminant movement is around the hydraulic barrier created by the injection, to the west. This can be most clearly seen in Figure 7.5.1-34, the strontium-90 distribution at 1000 years for the 20-gpm scheme. The majority of the plume is upgradient of the injection location; however, the leading edge is advanced a few hundred feet beyond that point. For the 40-gpm case, though some spreading has occurred, the majority of the plume is contained. The contaminant flux rates resulting from the injection schemes are compared to the pre-mitigated case in Figure 7.5.1-35. In general the curves are similar to those from the cutoff designs, having high initial values and then showing the effects of the decreasing source term and natural decay. The curves also show the increasing effectiveness in containing the strontium-90 with increasing injection rate. All three schemes reduce flux relative to pre-mitigation. Doubling the injection rate from 20- to 40-gpm delays the first arrival from about 350 years to about 450 years, decreases the maximum flux rates by over two orders of magnitude and reduces the total flux from 3.8×10^{10} pCi to 2.8×10^{8} pCi.

A summary of design characteristics and performance for the downgradient alternatives is provided in Table 7.5.1-1.

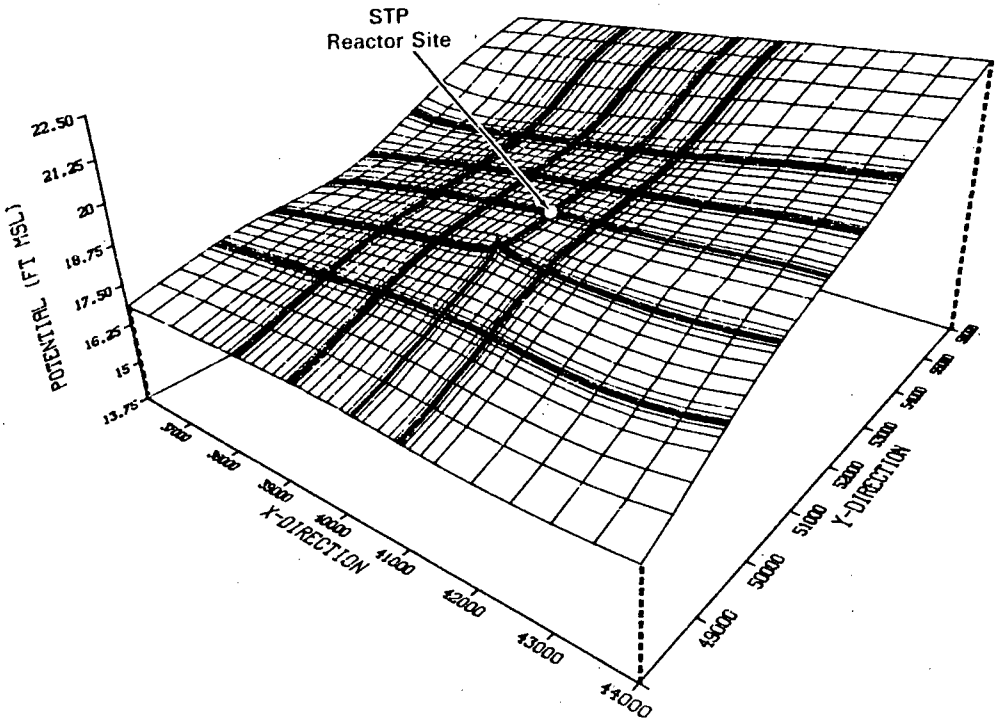

FIGURE 7.5.1-32. Simulated Potential Surface, Alt. #14 (20 gpm).

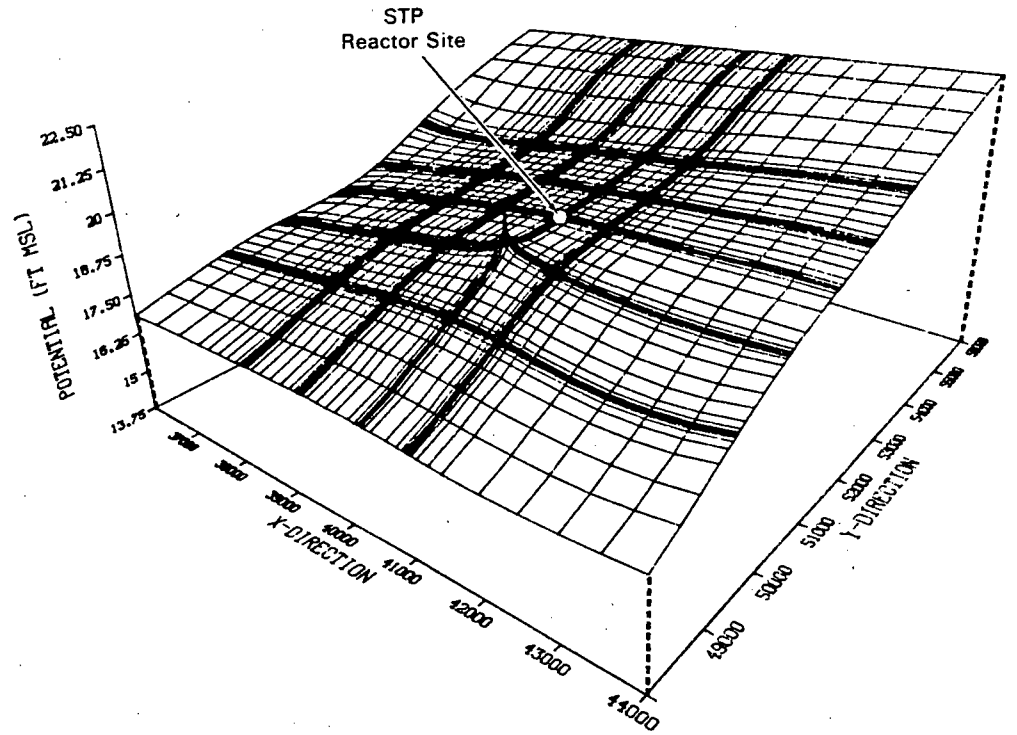

FIGURE 7.5.1-33. Simulated Potential Surface, Alt. #16 (40 gpm).

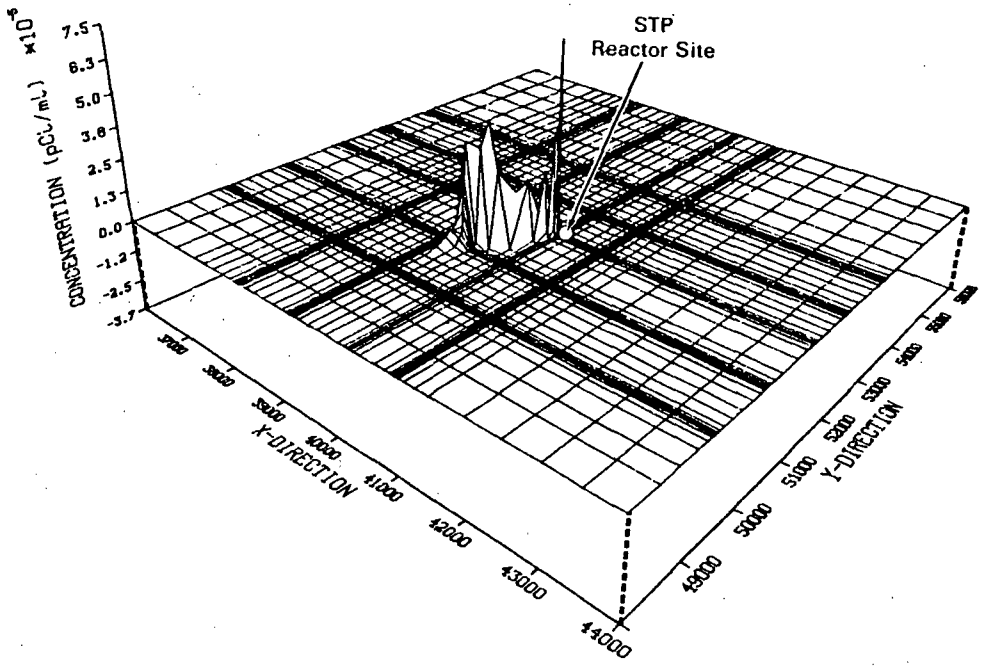

FIGURE 7.5.1-34. Simulated Strontium-90 Concentrations at 1000 years: Alt. #14 (20 gpm).

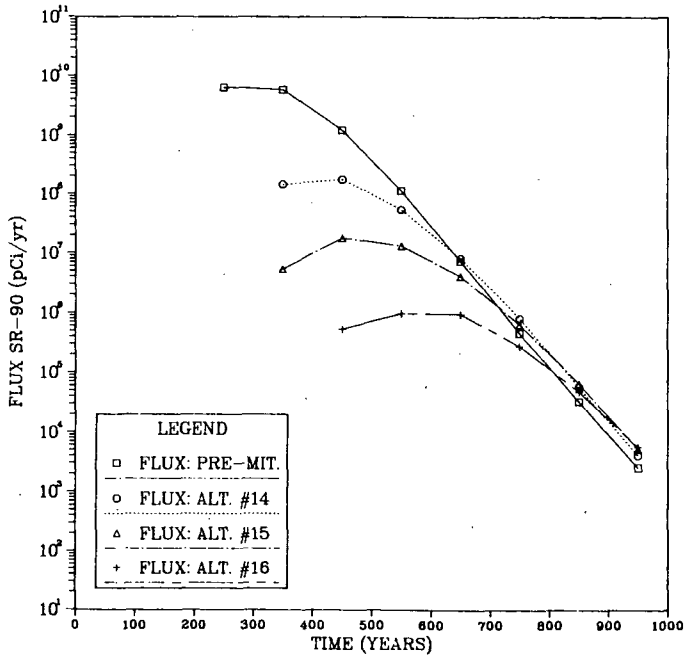

FIGURE 7.5.1-35. Simulated Flux Rates: Alt. #14 (20 gpm), Alt. #15 (30 gpm), and Alt. #16 (40 gpm).

TABLE 7.5.1-1. Summary: Downgradient Design Parameters and Performance

Alternative	Type/Shape	Distance from STP Reactor (ft)	Length (ft)	Cutoff Permeability (gpd/ft^2)	Maximum Heat Drop (ft)	Potential[a] Gradient at the STP Reactor (ft/ft)	Approximate Strontium-90[b] First Arrival Time (yr)	Maximum Flux Rate[b] of Strontium-90 (pCi/yr)	Total Flux[c] of Strontium-90 (pCi)
Pre-Mitigation	-	-	-	-	-	4.0×10^{-4}	250	6.2×10^{9}	1.3×10^{12}
#1	Cutoff/Linear (Offset)	1000	500	0.0	0.4	5.4×10^{-4}	150	2.0×10^{10}	3.5×10^{12}
#2	"	1000	1000	0.0	0.8	5.6×10^{-4}	150	2.0×10^{10}	4.4×10^{12}
#3	"	1000	2000	0.0	1.8	6.3×10^{-4}	150	2.9×10^{10}	3.4×10^{12}
#4	Cutoff/Linear (Centered)	1000	500	0.0	0.7	2.8×10^{-4}	150	1.2×10^{10}	2.2×10^{12}
#5	"	1000	1000	0.0	1.4	1.7×10^{-4}	250	4.1×10^{9}	8.4×10^{11}
#6	"	1000	2000	0.0	2.2	1.1×10^{-4}	350	9.5×10^{7}	1.7×10^{10}
#7	"	1000	3000	0.0	3.2	0.7×10^{-4}	550	6.1×10^{5}	1.2×10^{8}
#8	Cutoff/Linear (Offset-East)	1000	3000	0.0	3.2	0.8×10^{-4}	350	1.6×10^{8}	3.3×10^{10}
#9	Cutoff/Linear (Offset-West)	1000	3000	0.0	2.5	1.5×10^{-4}	450	1.0×10^{7}	2.0×10^{10}
#10	Cutoff/Linear (Centered)	2000	3000	0.0	2.5	1.3×10^{-4}	350	2.1×10^{8}	4.6×10^{10}
#11	Cutoff/L-East (Centered)	1000	3000	0.0	1.9	1.4×10^{-4}	350	7.1×10^{7}	1.5×10^{10}
#12	Cutoff/L-West (Centered)	"	3000	0.0	2.0	0.7×10^{-4}	850	4.3×10^{1}	6.3×10^{3}
#13	Cutoff/U-Shape (Centered)	"	2000	0.0	2.0	0.8×10^{-4}	850	1.3×10^{2}	1.8×10^{4}
#14	Injection (20 gpm)	1000	-	-	-	-	350	1.7×10^{8}	3.8×10^{10}
#15	Injection (30 gpm)	1000	-	-	-	-	350	1.8×10^{7}	4.1×10^{9}
#16	Injection (40 gpm)	1000	-	-	-	-	450	9.7×10^{5}	2.8×10^{8}

(a) Average potential gradient over the distance 1000 ft downgradient of the STP reactor site.
(b) At the breakthrough section 800 ft downgradient of the reactor site.
(c) During the 1000 year simulation period.

7.5.2 Upgradient Mitigation Measures

It is the intent of the above section on downgradient cutoff design evaluations to illustrate several of the many possible variations that could be employed in the design of contaminant mitigation measures. To avoid duplication, the focus of this section is to provide a basis for comparison of upgradient vs. downgradient cutoff design performance. Therefore, only a few examples are presented in detail. One in particular, is a combination design which utilizes concurrently an upgradient and a downgradient cutoff. Injection schemes are not included since they are not applicable as upgradient measures. While withdrawal schemes might be functional in this regard, they are not considered because of the potential danger of capturing and discharging contaminated water to the surface environment. In addition to those designs that are discussed, the characteristics and performance for a large number of additional upgradient designs are summarized for the interested reader in Table 7.5.2-1 at the end of this section.

7.5.2.1 Upgradient Plant Configuration Design Considerations

The upgradient plant features that may directly influence mitigation design at the STP, with the exception of the buildings in the immediate plant area, are the essential cooling pond and the switchyard. The concerns associated with the cooling reservoir are equally applicable to the pond (i.e., the water may become highly contaminated due to atmospheric deposition and/or it may be necessary to keep the pond functional in the near term following a severe accident). Similarly, the the operability of the switchyard facilities may be required under post-accident conditions or the facilities and their foundations may simply be obstacles to convenient or expedient cutoff construction. Therefore, because of these concerns, the primary location for upgradient cutoffs was selected just upgradient of the essential cooling pond (approximately 800 ft upgradient of the reactor), maintaining its integrity and minimizing interference with the switchyard. A secondary location approximately 1800 ft upgradient of the reactor was also evaluated. At these locations there are no constraints on cutoff placement, thus designs analogous to Alt. #1, #2, and #3 were not evaluated.

While downgradient cutoffs serve to increase the travel path length and reduce the potential gradient, upgradient cutoffs accomplish only the latter. However, they do offer an advantage in that because they are upgradient, the possible hazards associated with contaminated ground water are greatly reduced. For the same reason it might also be possible to initiate upgradient cutoff construction sooner than downgradient alternatives following an accident.

7.5.2.2 Upgradient Design Evaluations

Alt. #17, Alt. #18, Alt. #19, Alt. #20, and Alt. #21 (Centered)

This set of upgradient cutoffs, shown in Figure 7.5.2-1, is centered and located 800 ft from the reactor. Lengths for the five designs are 500, 1000, 2000, 3000, and 4000 ft, respectively. Referring to Figure 7.3-4, this location has hydraulic conductivities of about 1,100 gpd/sq ft, values considerably

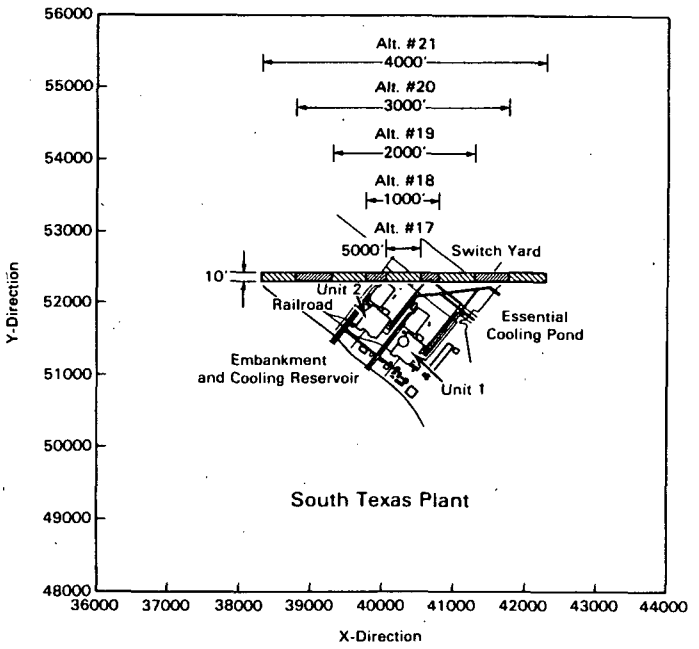

FIGURE 7.5.2-1. Location of Alt. #17 (L=500 ft), Alt. #18 (L=1000 ft), Alt. #19 (L=2000 ft), Alt. #20 (L=3000 ft), and Alt. #21 (L=4000 ft).

higher than where the downgradient cutoffs were located (e.g., 600 gpd/sq ft at y coordinate 50,450 ft). Consequently, the impact of the cutoffs on hydraulic gradients, for a given length, is attenuated relative to the downgradient barriers. The potential surfaces for the 500-ft and 4000-ft cutoffs are shown in Figures 7.5.2-2 and 7.5.2-3 to illustrate the range of effects produced by the five designs. Taking the 500-ft cutoff as an example, it only produces a maximum potential drop of 0.26 ft in contrast to a drop of 0.70 ft for a downgradient cutoff of the same length. Likewise, resultant gradients are higher, 4.5×10^{-4} ft/ft compared to 3.6×10^{-4} ft/ft.

In terms of performance, as with the downgradient cutoffs, flux from the reactor site was actually increased for cutoff lengths less than 1000 ft. Likewise, for longer cutoffs, increased length produces decreased flux (see Figure 7.5.2-4). When compared to the flux rates for downgradient cutoffs in shown Figure 7.5.1-9, it is seen that the upgradient cutoff flux rates are higher for a given length indicating greater downstream migration of the contaminant plume. From this limited analysis it appears that for a given length, downgradient cutoffs are more effective than upgradient cutoffs in reducing contaminant flux from the site. However, with regard to future efforts to remove all contaminated soil, it's noteworthy that because the upgradient barriers do not obstruct the flow (i.e., they simply reduce gradient and velocity), less lateral spreading of contaminant occurs. This is clearly illustrated in Figure 7.5.2-5 which shows the strontium-90 plume at 1000 years

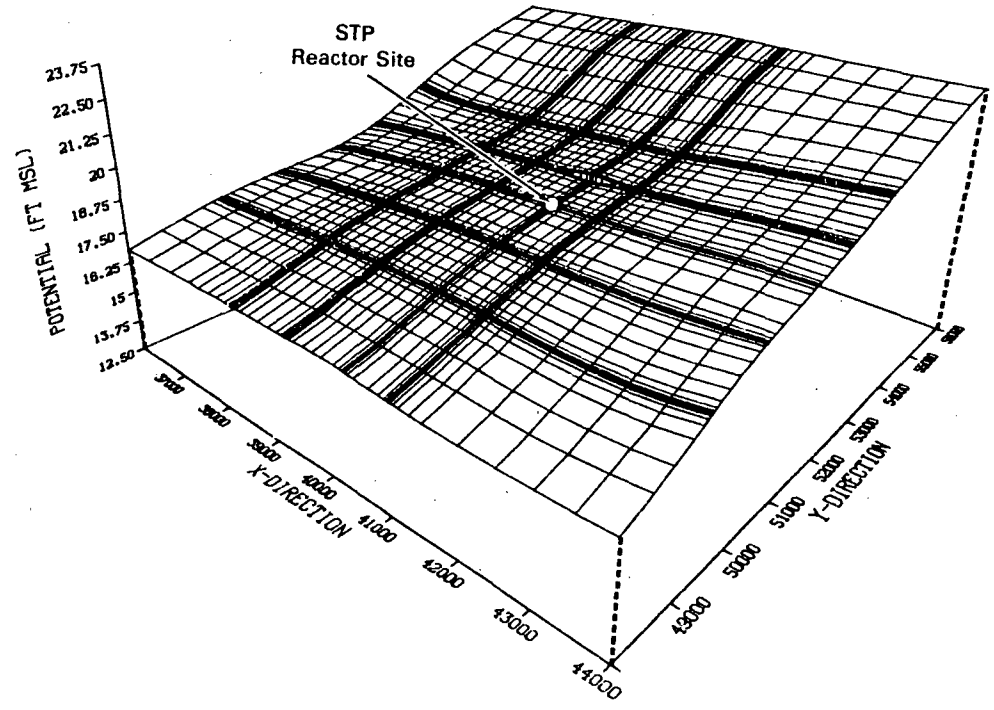

FIGURE 7.5.2-2. Simulated Potential Surface, Alt. #17 (L=500 ft).

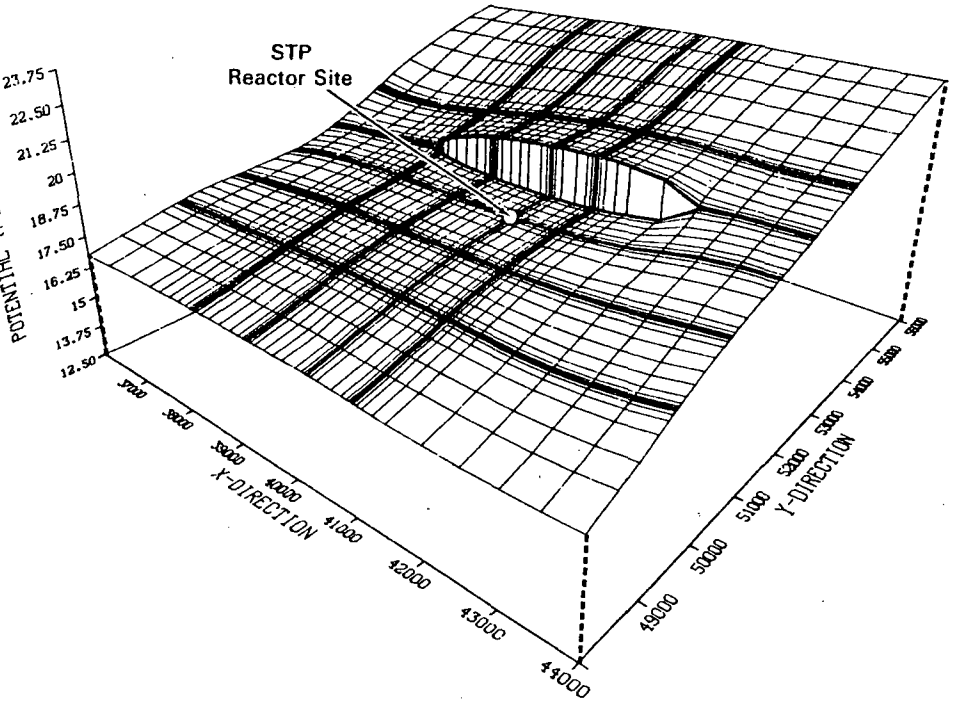

FIGURE 7.5.2-3. Simulated Potential Surface, Alt. #21 (L=4000 ft).

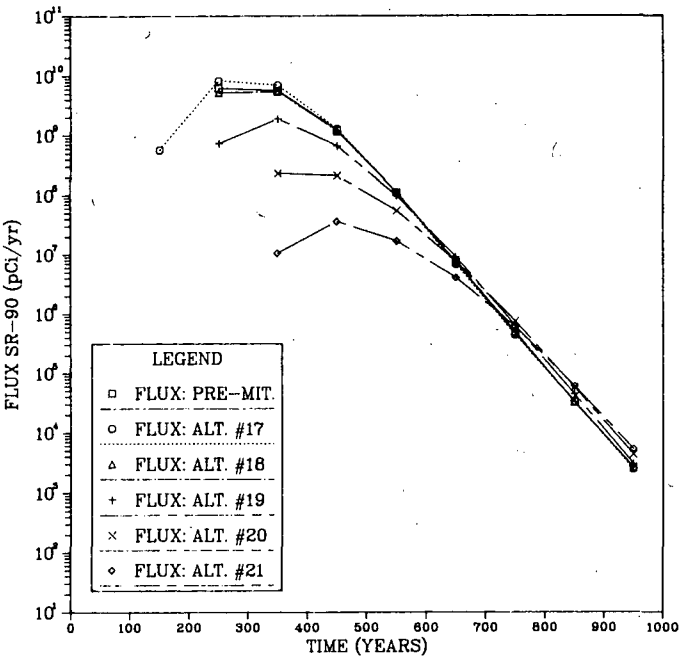

FIGURE 7.5.2-4. Simulated Flux Rates: Alt. #17 (L=500 ft), Alt. #18 (L=1000 ft), Alt. #19 (L=2000 ft), Alt. #20 (L=3000 ft), and Alt. #21 (L=4000 ft).

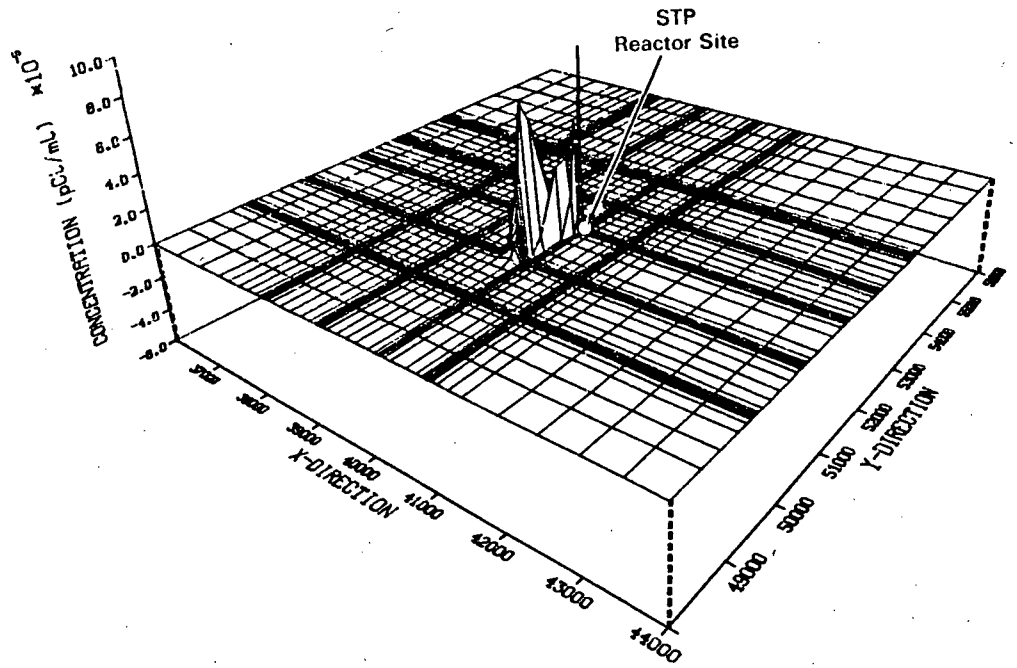

FIGURE 7.5.2-5. Simulated Strontium-90 Concentrations at 1000 years: Alt. #20 (L=3000 ft).

for the 3000-ft cutoff. The plume width is only about 300 ft compared to a width of over 1000 ft for the corresponding downgradient cutoff (see Figure 7.5.1-11).

Alt. #22

The only combination design evaluated consists of a 1500-ft cutoff located 1000 ft downgradient of the reactor and a 1500-ft cutoff placed 800 ft upgradient (see Figure 7.5.2-6). The potential field produced by the two cutoffs is plotted in Figure 7.5.2-7. The two barriers, though the same length, produce different head drops, demonstrating the influence of hydraulic conductivity on design performance. The maximum head drop across the upgradient cutoff is about 0.5 ft. In contrast, the downgradient cutoff, located in the a region with relatively low conductivities, produces a drop of almost 0.9 ft. The combined effect of the two cutoffs is to produce a gradient at the reactor site of 1.5×10^{-4} ft/ft. The resultant flux is compared to the pre-mitigated flux in Figure 7.5.2-8. The first arrival is delayed to between 400 and 500 years and the peak flux rate is reduced over two orders of magnitude. The concentration distribution, plotted in Figure 7.5.2-9, shows that the plume is largely contained to within 1000 ft of the reactor and has spread to a width of about 1000 ft.

A summary of the upgradient alternatives, including those analyzed but not discussed is provided in Table 7.5.2-1.

7.5.3 Sensitivity Analysis: Cutoff Design Parameters

One of the keys to identifying a "best" design, given specific design objectives, is to develop insight into how performance changes with variations in major design characteristics. Mathematical models are ideally suited for accomplishing this in that once a model is developed for a site, any number of designs can be simulated without appreciable additional cost. Though there is no attempt to select an optimum design in this study, for demonstration purposes a limited sensitivity analysis of cutoff design parameters is conducted. The approach used is simply to compare mitigation performance of different alternatives as a function of selected design parameter values. The parameters evaluated include length, distance from the reactor, cutoff permeability, shape and orientation. Performance is measured on the basis of the strontium-90 flux at the breakthrough section 800 ft downgradient of the reactor. In an actual mitigation design situation, many more simulations than are presented here would be conducted, perhaps in conjunction with optimization techniques, to select the most appropriate design.

7.5.3.1 Cutoff Length

The general effect of increasing cutoff length is to decrease velocities in both the upgradient and downgradient directions. It follows that velocities approaching zero could be achieved with a sufficiently long cutoff. However, infinitely long cutoffs are not necessary or practical. As the simulation results have shown (see Figure 7.5.1-10), significant reductions in flux can be achieved with cutoffs of several thousand feet. The question then is how long

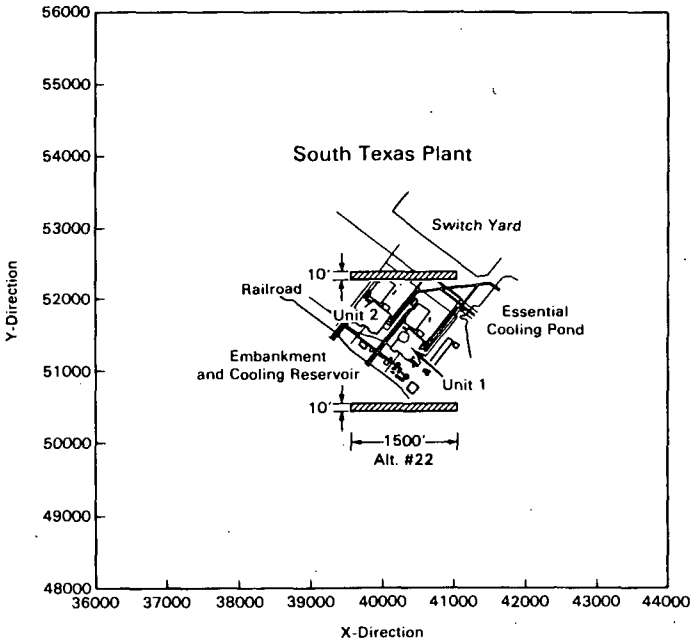

FIGURE 7.5.2-6. Location of Alt. #22 (Combination Design).

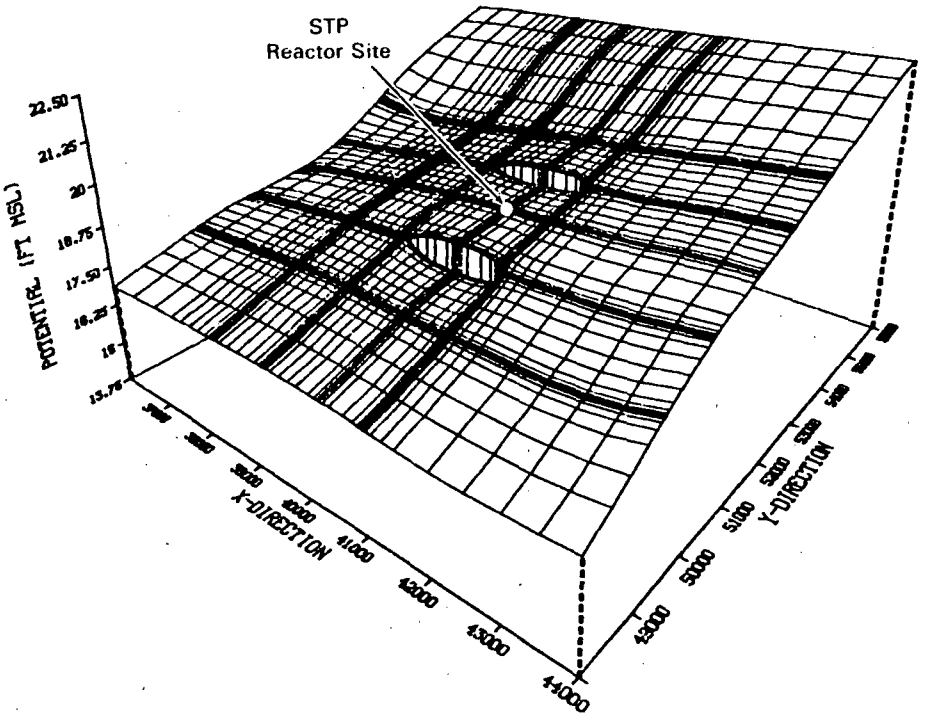

FIGURE 7.5.2-7. Simulated Potential Surface, Alt. #22 (Combination Design).

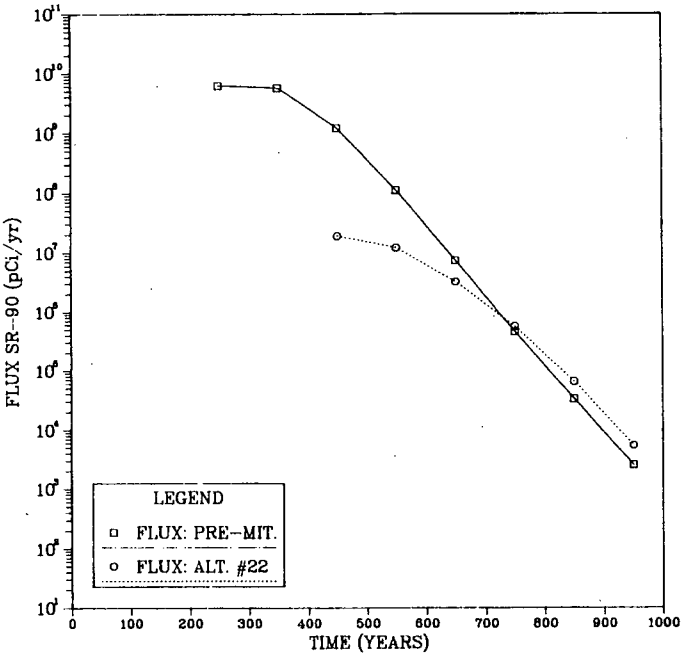

FIGURE 7.5.2-8. Simulated Flux Rates: Alt. #22 (Combination Design).

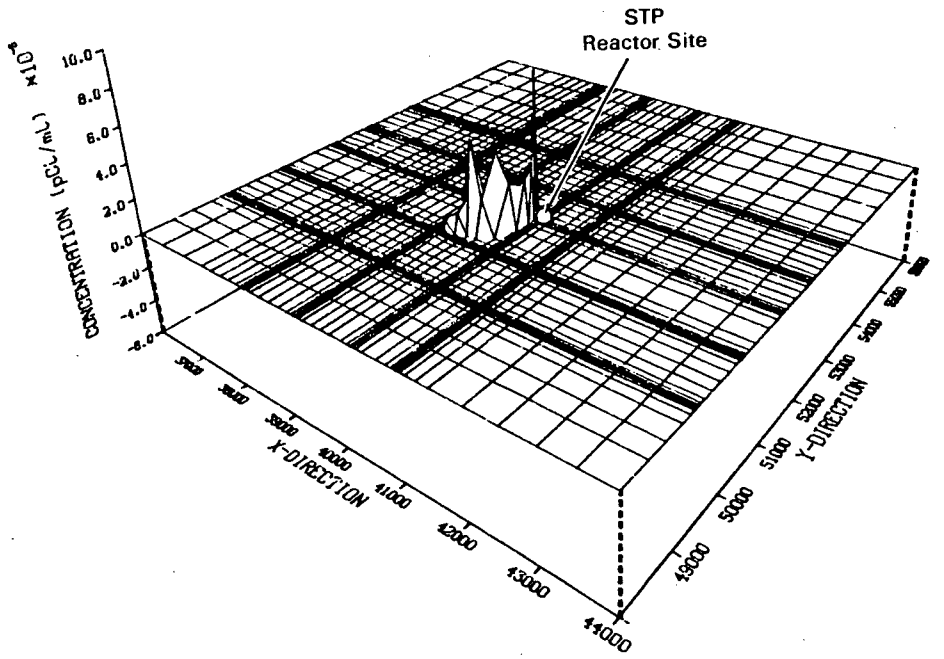

FIGURE 7.5.2-9. Simulated Strontium-90 Concentrations at 1000 years: Alt. #22 (Combination Design).

TABLE 7.5.2-1. Summary: Upgradient Design Parameters and Performance

Alternative	Type/Shape	Distance from STP Reactor (ft)	Length (ft)	Cutoff Permeability (gpd/ft^2)	Maximum Heat Drop (ft)	Potential[a] Gradient at the STP Reactor (ft/ft)	Approximate Strontium-90[b] First Arrival Time (yr)	Maximum Flux Rate[b] of Strontium-90 (pCi/yr)	Total Flux[c] of Strontium-90 (pCi)
#17	Cutoff Linear (Centered)	800	500	0.0	0.3	4.5×10^{-4}	150	8.3×10^{9}	1.7×10^{12}
#18	"	800	1000	0.0	0.4	4.3×10^{-4}	250	5.5×10^{9}	1.2×10^{12}
#19	"	800	2000	0.0	0.9	3.8×10^{-4}	250	1.9×10^{9}	3.4×10^{11}
#20	"	800	3000	0.0	1.4	3.3×10^{-4}	350	2.3×10^{8}	5.1×10^{10}
#21	"	800	4000	0.0	1.9	2.7×10^{-4}	350	3.6×10^{7}	6.8×10^{8}
#22	Cutoff/Combination (Centered)	800	3000	0.0	0.9	1.5×10^{-4}	450	1.9×10^{7}	3.5×10^{9}
#23	Cutoff/Linear (Offset-East)	800	3000	0.0	1.8	3.7×10^{4}	250	1.2×10^{9}	2.1×10^{11}
#24	Cutoff/Linear (Offset-West)	800	3000	0.0	1.5	3.7×10^{-4}	250	8.8×10^{8}	1.5×10^{11}
#25	Cutoff/Linear (Centered)	800	3000	0.0	2.2	2.3×10^{-4}	250	5.0×10^{9}	1.1×10^{12}
#26	"	800	3000	0.001	1.7	3.5×10^{-4}	250	5.5×10^{8}	1.3×10^{11}
#27	"	800	3000	0.01	1.7	3.5×10^{-4}	250	7.7×10^{8}	1.3×10^{11}
#28	"	800	3000	0.1	1.7	3.6×10^{-4}	250	7.7×10^{8}	1.3×10^{11}

(a) Average potential gradient 1000 ft downgradient of the STP reactor site.
(b) At the breakthrough section 800 ft downgradient of the reactor site.
(c) During the 1000 year simulation period.

of a cutoff should be constructed? This question must be answered based on specific performance criteria. As a hypothetical example, it might be determined that site restoration is planned 300 years following a severe accident at the STP; consequently, specific mitigation performance objectives might be to extend the first arrival time at the breakthrough section to greater than 300 years. Figure 7.5.3-1 is a plot of first arrival time as a function of cutoff length for linear, downgradient cutoffs located 1000 ft from the reactor and linear, upgradient cutoffs located at a distance of 800 ft. The plot clearly shows the relationship between cutoff length and travel time. For the pre-mitigation case (cutoff length equal to zero) the first arrival of strontium-90 occurs at approximately 250 years. For both downgradient and upgradient designs, for lengths less than 1000 ft, the arrival time is actually shortened. For downgradient cutoffs with lengths greater than 1000-ft, there is an approximate increase in first arrival time of 150 years for a 1000-ft increase in length. The upgradient designs, which are less effective for the STP, produce an average increase of less than 50 years for each 1000-ft increment over 1000 ft. For a first arrival of 300 years, the minimum acceptable linear cutoff is approximately 1500 ft for an downgradient design and 2500 ft for an upgradient alternative.

In addition to concerns about first arrival of contaminant, there could also be interest in the total flux from the site. For example, site restoration might involve removal and disposal of all contaminated soils. To minimize this future effort, the objective of mitigation would be to contain the contaminant at the site (i.e, reduce flux from the site). A performance measure for this objective is total flux from the site. Figure 7.5.3-2 shows the simulated total flux for the 1000-year simulation period for the same downgradient and upgradient designs discussed above. These curves show the increasing marginal gains in flux reduction for increased cutoff length. Such curves, if properly extended, could be used to determine the design length necessary to totally eliminate flux or to limit flux to a set level.

7.5.3.2 Cutoff Distance from the Reactor

Selection of the exact location for construction of mitigative measures will be determined by a number of factors such as the nature and location of plant facilities, the level and extent of both surface and subsurface contamination, prevailing wind conditions and the type of design. Therefore, in selecting a final design it's important to understand how distance from the contaminant source will effect the performance of designs in question. To begin to address this question, Figure 7.5.3-3 contains plots of simulated flux against time for a 3000-ft cutoff at four different locations: 1000 ft downgradient, 2000 ft downgradient, 800 ft upgradient, and 1800 ft upgradient. For both the downgradient and upgradient designs an increase in distance from the source significantly impacts performance, both in terms of flux rate and first arrival time. For the downgradient designs, an increase in distance from 1000 to 2000 ft reduces the first arrival time by about 200 years while increasing the initial flux rate by approximately three orders of magnitude. The same increase in distance for the upgradient designs produces a 100-year increase in arrival time and an order of magnitude increase in flux rate. Though limited in scope and extent, this brief analysis points out the

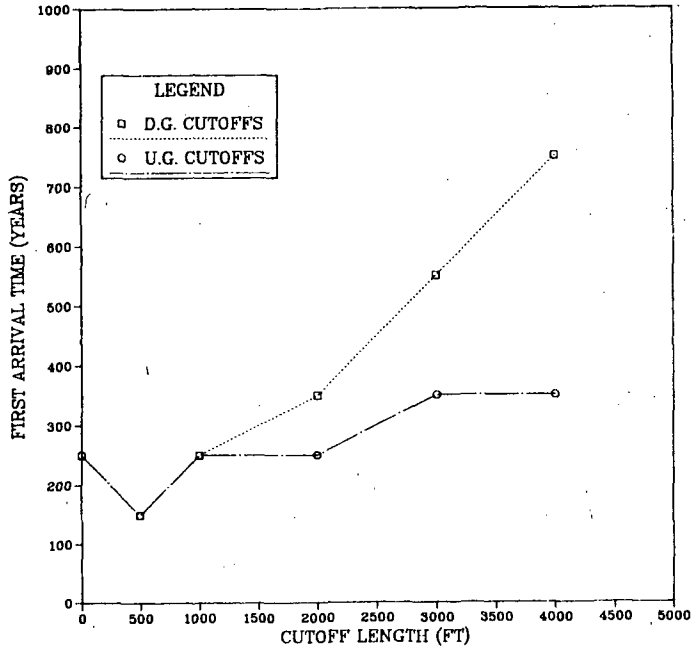

FIGURE 7.5.3-1. First Arrival Times as a Function of Cutoff Length.

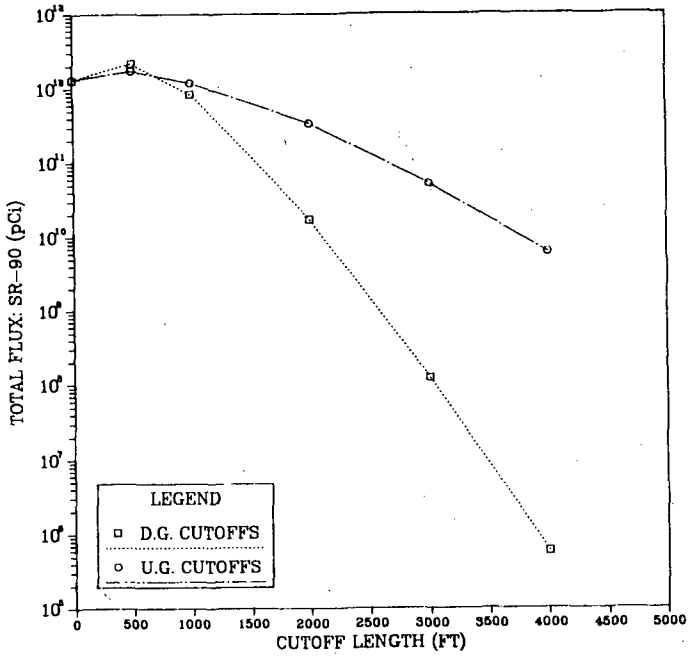

FIGURE 7.5.3-2. Simulated Total Flux as a Function of Cutoff Length.

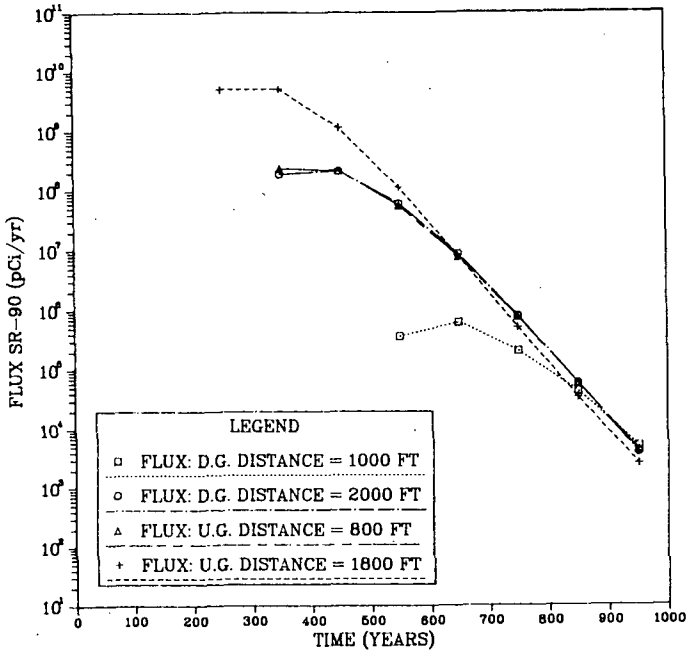

FIGURE 7.5.3-3. Comparison of Flux Rates for Downgradient and Upgradient Designs.

importance of distance from the site to mitigation performance and the potential trade-offs that could be made between distance and cutoff length.

7.5.3.3 Cutoff Permeability

An important aspect of grout cutoff performance as a barrier to groundwater contaminant migration is the grout permeability, in terms of both the "as constructed" condition and the change in permeability with time. For simplicity, all of the grout cutoff flow and transport simulations discussed above assume cutoff permeabilities equal to 0.0 gpd/sq ft. Under actual conditions it's not realistic to expect total permeability reduction. Laboratory tests with silicate-based grouts achieved permeability values averaging approximately 4.8×10^{-7} cm/sec or about 0.01 gpd/sq ft. According to Baker (1982), chemically grouted sands exhibit permeability reductions relative to the host media of three to six orders of magnitude. For the STP site this would indicate possible values on the order of about 0.001 to 0.1 gpd/sq ft. Also, less than ideal performance can be introduced during construction. Littlejohn (1982) identifies three causes of variability in grout curtain properties which affect permeability:

1. inadequate/improper mixing of grout,

2. variations in quantity and quality of grout material, and

3. apparent variations from testing procedures.

Avoiding these types of problems and assuring acceptable quality construction requires rigid engineering supervision of all grouting operations (see Section 4.3.1.6 for further discussion of grout curtain construction considerations).

Another issue for consideration is grout durability. In place, grouts are subject to deterioration due to wet-dry cycles, weathering, exposure to pH extremes, etc. Silicate-based grouts with silicate concentrations greater than 35% are resistant to these effects. Nonetheless, mitigation utilizing grout cutoffs will require continual monitoring to ensure maintenance of permeability reduction. Undoubtedly, with time, repair and/or replacement will be necessary to meet long-term mitigation objectives that span hundreds of years.

To gain insight into how variable or deteriorating cutoff permeability may affect performance, four simulations were conducted varying the cutoff permeability. The analysis is based on the 3000-ft design located 1000 ft downgradient of the reactor with permeability values of 0.001, 0.01, 0.1, and 0.1 gpd/sq ft. The simulated flux rates are presented in Figure 7.5.3-4 and compared to the zero permeability case and the pre-mitigation case (permeability equal to that of the host media). The 0.001 permeability curve, not shown on the plot is practically identical to that for 0.0 case. Similarly, the 0.01 and 0.1 permeability cases show only minor increases in flux. The increase to 1.0, however, results in a dramatic change, increasing the maximum flux rate from about 1×10^6 to almost 6×10^7 pCi/yr. The time of first arrival is also reduced about 200 years. Nonetheless, the simulation results show that even with appreciable deterioration of the grout's permeability reduction properties (i.e., over a couple orders of magnitude) significant reduction in contaminant flux is achieved. Also, over the ranges of achievable permeability reduction (i.e., 0.001 to 0.1 gpd/sq ft) performance is essentially unchanged.

Cutoff Shape

From the discussion of the different-shaped cutoff designs in Section 7.5.1.2, it's quite evident that perhaps the single most important design parameter with regard to reduction of flux is design shape. For the purpose of evaluating relative performance, several designs are compared including a linear or straight line, U-shape, L-shape, and an upgradient/downgradient combination. All four designs consist of a total cutoff length of 3000 ft and are 1000 ft downgradient from the reactor. The L-shape design has the leg section attached to the west end (high conductivity region). The combination design consists of two 1500-ft sections, one located 1000 ft downgradient and the other 800 ft upgradient. The comparison of the 1000-year flux rates for the four designs in Figure 7.5.3-5 shows the dramatic differences in performance. Clearly, the L-shape and U-shape designs are the best evaluated. This is attributable to the leg sections obstructing lateral flow through the high conductivity region of the contaminant flow path. The other two designs obstruct the flow and decrease the potential gradient but do not have the same beneficial effect. Also, the combination design, per unit length, is not as effective as the single linear design. This comparison points out the advantages to accurately determining the hydraulic and

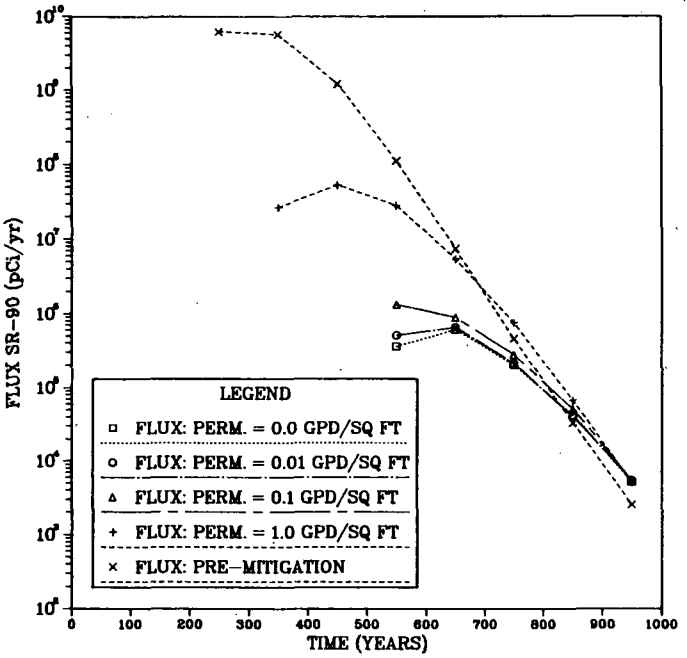

FIGURE 7.5.3-4. Comparison of Flux Rates for Various Cutoff Permeabilities (L=3000 ft, 1000 ft Downgradient).

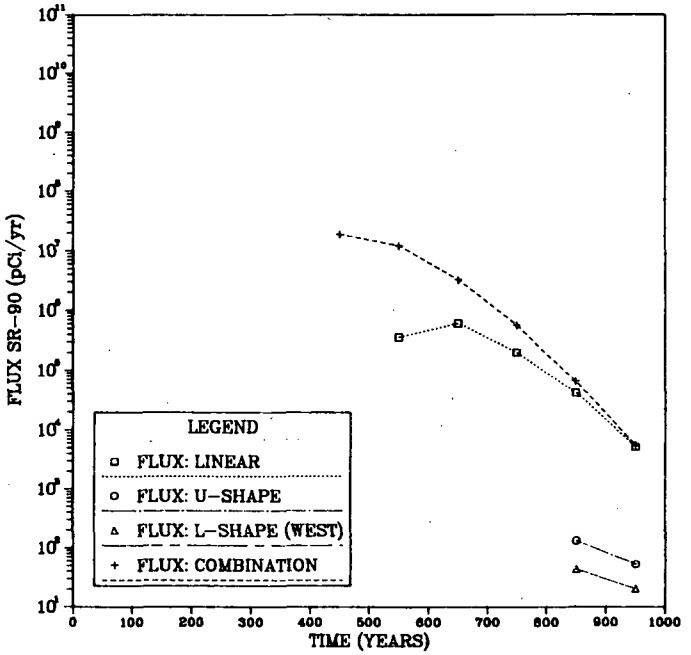

FIGURE 7.5.3-5. Comparison of Performance as a Function of Design Shape (Total Length=3000 ft, 1000 ft Downgradient).